Access to Electronic Thesis

Author:	Ahmad Yusoff
Thesis title:	Optimisation of variable helix end milling tools
Qualification:	PhD
Date awarded:	22/09/10

If this electronic thesis has been edited by the author it will be indicated as such on the title page and in the text.

OPTIMISATION OF VARIABLE HELIX END MILLING TOOLS

by

Ahmad Razlan Yusoff

Submitted for the degree of Doctor of Philosophy

August 2010

Department of Mechanical Engineering

Supervisor: Dr N. D. Sims and Prof K. Ridgway

SUMMARY

High productivity, low cost and high profits are important issues in aerospace, automotive and tool/die metal manufacturing industries. Machining processes are widely used in manufacturing operations for metal manufacturing rather than casting and forming. However, the dynamic deflection of tool and workpiece systems generates unstable cutting forces when machining with high material removal rate. Here, sudden large vibration amplitudes occur when energy input exceeds the energy dissipated from the system, leading to self-excited vibration or chatter. This thesis focuses on the avoidance of milling chatter by using variable helix milling tools.

Since milling chatter is strongly influenced by the frequency response function of the dynamic system, a preliminary study is first presented to assess the feasibility of non-contacting electromagnetic modal analysis for milling tools. It is shown that this approach shows some promise for use in real machining problems where traditional modal hammers have some drawbacks. In particular, the amplitude dependency of the frequency response function could be qualitatively illustrated.

The main focus of this thesis is the optimisation of variable helix tool geometry for improved chatter performance. A semi-discretisation method was combined with Differential Evolution to optimise variable helix end milling tools. The target was to reduce chatter and maximise performance by modifying the variable helix and variable pitch tool geometry. The performance of the optimisation routine was benchmarked against a more traditional approach, namely Sequential Quadratic Programming. Numerical studies indicated that the Differential Evolution optimisation performed much better than Sequential Quadratic Programming due to the nonlinearity of the optimisation problem. The numerical study predicted total mitigation of chatter using the optimised variable helix milling tool at a low radial immersion. However, in practice, a five-fold increase in chatter stability was obtained, compared to traditional milling tools. In addition to this practical contribution, this study has provided new insight into the experimental nonlinear dynamics of variable helix milling tools, which exhibit period-one bifurcations under certain conditions.

There have been very few previous studies that have investigated variable helix milling tools. However, one previous study proposed that the so-called 'process damping' phenomenon is particularly important for variable helix milling tools. Consequently, the final contribution of this thesis is a study of process damped milling and the influence of different tool geometries. Testing was performed for tools with different rake and relief angle, edge radius and variable helix/pitch. It was found that variable helix/pitch had the greatest influence on the process damping phenomenon.

ACKNOWLEDGEMENTS

Praises to Allah and peace be upon the beloved final Prophet Muhammad. Thanks to Allah to be always with me to give guidance and mercy along my life. From His help and blessing to give me strength and teach me patience to complete the thesis.

I would like to express my deepest appreciation to the people who have given their time and support to contribute towards completion of the thesis. Dr Neil D Sims, my supervisor, is on the top of the list, whose strong encouragement, support and ideals, with patience and understanding in supervising, were significant from the first day towards the final effort in pursuing my PhD study. Neil's advice and expertise with his high standards and rich ideas create a meaningful working experience. I would also like to convey my gratitude to my second supervisor, Prof Keith Ridgway.

I would like to give thanks to Dr Chris Taylor for having the opportunity to give help and valuable feedback on my study progress. My thanks also go to Samuel Turner and everyone at Factory of Future, AMRC for their technical support in providing tools, materials and machine in this research. I thank Jamie Booth for his invaluable help with my experimental work, my officemate and departmental staff, Dr Dave, Pauziah, Lizzie, Pae, Mehmet, Khalid and Fatma for their support and friendship in a colourful study environment. To all Malaysian friends, especially to Dr Roshdi, Tarik, Fairusham, Bukhari, Dr Shahruddin, Kamil, Tamreen and Dr Halim, thanks for the pleasant and informative lunch times.

I offer my deepest thanks to my parents and my parents-in-law in Malaysia, who always pray sincerely for my success in study and life. Not to forget, this space and credit to my dearest wife, Fatimah Az-Zahrah, and my three lovely children, Alif, Ainul and Anis, whose love, sacrifice and patience, make 'abi' feel stronger and inspired. There is no greater support and encouragement besides all of you.

TABLE OF CONTENTS

LIST OF FIGURES

LIST OF TABLES

ABBREVIATIONS

1/Rev	One per Revolution
ACO	Ant Colony Optimisation
CAD/CAM	Computer Aided Design/Computer Aided Manufacturing
CM	Characteristic Multiplier or Eigen Value
CNC	Computer Numerical Control
CR	Crossover Factor
CTCR	Cluster treatment of Characteristic roots
DDE	Delay Differential Equation
DE	Differential Evolution
DOE	Design of Experiment
DP	Dynamic Programming
EMA	Electro Mechanical Actuator
ER	Electro Rheology
FEM	Finite Element Method
FFT	Fast Fourier Transform
FRF	Frequency Response Function
GA	Genetic Algorithm
GP	Geometric Programming
KBS	Knowledge Based Systems
LDV	Laser Doppler Velocity
LQR	Linear Quadratic Regulator
MRR	Material Removal Rate
NC	Numerical Control
NG	Number of Generation

NP	Number of Population
PSO	Particle Swarm Optimisation
QP	Quadratic Problem
RMS	Root Mean Square
RP	Real Parameter
RSM	Response Surface Methodology
SA	Simulated Annealing
SDM	Semi Discretisation Method
SF	Scaling factor
SQP	Sequential Quadratic Programming
TFEA	Time Finite Element Analysis
VPA	Virtual Passive Absorber

NOMENCLATURES

$\mathbf{A}_m$	State matrix for the discretised structural dynamics (-)
$\mathbf{A}_s$	State matrix for the structural dynamics (-)
b	Axial depth of cut (m)
b_{cr}	Critical depth of cut (m)
b_{lim}	Limit depth of cut (m)
$\mathbf{B}_m$	Input matrix for the discretised structural dynamics (-)
$\mathbf{B}_s$	State matrix for the structural dynamics (-)
c	Chip load (-)
$\mathbf{C}_s$	Output matrix for the structural dynamics (-)
d	Tool diameter (m)
D	Total number of states, in x and y direction (-)
$\mathbf{D}_d$	Feedthrough matrix for the system delays (-)
E_e	Modulus of elasticity (N/m^2)
f	Frequency (Hz)
f_c	Chatter frequency (Hz)
f_{hopf}	Hopf bifurcation instability frequency (Hz)
f_n	Natural frequency (Hz)
f_{PD}	Period doubling instability frequency (Hz)
f_{PO}	Period one instability frequency (Hz)
fr	Feed rate (m/min)
F	Cutting force (N)
F_n	Normal force (N)
F_s	Friction force (N)
F_t	Tangential force (N)

F_x	Resultant force in x direction (N)
F_y	Resultant force in y direction (N)
$\overline{F}_x$	Average force in x-direction (N)
$\overline{F}_y$	Average force in y-direction (N)
F_{xc}	Gradient for force in x-direction (N)
F_{yc}	Gradient for force in y-direction (N)
F_{xe}	Intersection for force in x-direction at y- axis (N)
F_{ye}	Intersection for force in y-direction at y- axis (N)
G	Step function compensation to flute j at layer l
$G(s)$	Transfer function of structural displacement (m/N)
h	Chip width (m)
Δh_β	Helical angle height difference (m)
h_m	Mean chip thickness (m)
h_{max}	Maximum chip thickness (m)
H_i	Constraint (-)
Im	Imaginary (-)
j	Index denoting tooth number (-)
K_n	Normal cutting coefficient (N/m^2)
K_{ne}	Normal edge cutting force coeffiecient (N/m^2)
K_s	Cutting stiffness (N/m^2)
K_t	Tangential cutting coefficient (N/m^2)
K_{te}	Tangential edge cutting force coeffiecient (N/m^2)
l	Index denoting axial layer number(-)
L	Axial layer discretisation (m)
∇L	Gradient function (-)
$L(f(x))$	First order optimality (-)

m	Number of teeth (-)
m_m	Modal mass (kg)
max	Maximum (-)
MRR_n	Normalised material removal rate (-)
N	Time step per revolution (s/rev)
N	Number of integer (-)
p_k	Directional search (-)
$\mathbf{q}_i$	State vector matrix (-)
r	Radial depth of cut (m)
$\mathbf{R}$	Periodic time matrix(-)
Re	Real (-)
RI	Radial immersion (m)
S	Structural dynamics (-)
T	Sampling time per revolution (s)
$u_{i,g}$	Trial vector (-)
u_x	Vibration in x direction (m)
u_y	Vibration in y direction (m)
v	Cutting velocity (m/s)
$v_{i,g}$	Mutant vector (-)
w	Feed per tooth (m/tooth)
w_k	Hessian matrix (-)
$\mathbf{x}_d$	Relative vibration $\mathbf{u}$ and the delay state relation ship $\varDelta$ (-)
$x_{i,g}$	Parameter vector (-)
$x_{i,l}$	Lower vector limit(-)
$x_{i,u}$	Upper vector limit(-)
x_k	Iteration (-)

$\mathbf{x}_m$	Continues dynamic times with discretisation (-)
y	Current relative vibration (-)
Y	Step unit for time delay (-)
y_p	Previous relative vibration (-)
λ_c	Process damping wavelength (m)
γ	Clearance/relief angle (°)
φ	Cutting parameter (-)
α	Rake angle (°)
ψ	Shear strength of materials
Ω	Spindle speed (rev/min)
τ	Time delayed (s)
ε	Phase angle (°)
θ	Angular position (°)
Δ	Vibration relative vector (-)
β	Helical angle (°)
ϕ	Pitch angle (°)
$\Delta\phi$	Pitch angle different (°)
ξ	Damping ratio (-)
χ	Lagrange multiplier (-)
γ	Lagrange multiplier (-)
σ_{max}	Maximum stress (N/m^2)
ρ	Density (kg/m^3)
θ_{st}	Entry angle of cutter (°)
θ_{ex}	Exit angle of cutter (°)
Φ	Transition matrix (-)

CHAPTER 1
INTRODUCTION

1.1 Background

In the commercial application of advanced materials, almost 90 percent of the materials estimated to be used in 2010 will be metallic [1]. This indicates that despite advances in composite materials attention is still being given to metallic materials. Trends towards monolithic metallic components are enabling efficient cost, weight and strength along with high dimensional accuracy even for complex parts. For example, an aircraft made of 44 parts initially needed 53 die sets; currently the same section can be made with six segments without dies by machining [2]. In addition, machining will also produce a smoother surface finish where a hand finishing process is no longer needed, which will save time and improve the quality. That is why machining processes are widely used in manufacturing operations for metal manufacturing rather than casting and forming. It has been found that milling is a more popular machining process than turning and grinding for production of die cavities, slots, contours and profiles. In the milling process, a milling cutter is held in a rotating spindle, while the workpiece clamped in the table is moved linearly towards the cutter, as shown in Figure 1.1.

In the aerospace, automotive, mould/die and general manufacturing industries, there is great pressure to ensure lower cost, greater productivity and improved quality in order to encourage economic growth. However, machining productivity using a high material removal rate is inhibited by the dynamic deflection of tool and workpiece systems, which generates an unstable cutting force. This causes sudden large vibration amplitudes where energy input exceeds the energy dissipated from the system, producing chatter. Chatter is a self-excited type of vibration that occurs in metal cutting if the chip width is too large with respect to the dynamic stiffness of the system, especially when machining with a high material removal rate. In milling processes, the chip width is the axial depth of cut parameter. This produces a poor surface finish and high tool wear and can even damage machine tools as a result of the regenerative effect, the loss of the contact effect and the mode coupling effect. Regenerative chatter is perhaps the most common form of chatter [3] and will be the focus of this thesis. The

regenerative chatter stability boundary is known as the stability lobe diagram and is a function of depth of cut and spindle speed, as shown schematically in Figure 1.2.

To predict the stability diagram, researchers have created various types of chatter prediction models, particularly time domain simulation [4], analytical solution of delay-differential equations with time periodic coefficients [5], time finite element analysis (TFEA) [6] and semi-discretisation method (SDM) [7]. For chatter suppression, passive and active methods including vibration absorbers, damping, varying spindle speed and others have been applied. Passive methods are often suitable for a wide range of frequencies and machines compared to active methods.

This thesis investigates a passive approach to chatter suppression that disrupts the chatter vibration by modifying the milling tool geometry, in particular the helix or pitch angles. Figure 1.3 illustrates uniform helical end milling tools compared to non-traditional variable helix and variable pitch designs. Variable pitch tools was proposed by Slavicek [8]. Later, Opitz *et al.* [9] studied irregular tooth pitches that produce a higher stable depth of cut. Only Stone [10] applied an irregular *helix* in the early period before the 1970s. Variable pitch tools were re-considered by Altintas *et al.* [5] who used an invariant time constant and a non-uniform multiple regeneration time delay to optimise pitch geometry. Meanwhile, Budak [11] modelled and optimised a non-constant pitch cutter, using an analytical stability model. Recently, Olgac and Sipahi [12] maximised theoretically the material removal rate by applying an irregular pitch cutter that was optimised with the Cluster treatment of Characteristic roots (CTCR) as a mathematical objective function**.**

The above review indicates that current research on chatter suppression methods takes into account variable pitch tools and has overlooked variable helix cutting tools. Besides reducing chatter, the helix angle can also break chip formation and change the line of contact between the tools. Motivated by the success of variable pitch tools, a variable helix tool can be envisaged as an alternative method to suppress chatter and help to disturb the phase between the outer and the inner surface modulation left by previous cutting.

In this thesis, a semi-discretisation method will be combined with Differential Evolution to optimise the variable helix end milling tools. The main target is to reduce chatter and Sequential Quadratic Programming is used to benchmark the simulation results before validating with experiments. Huyanan [13] proposed a semi-discretisation method model for variable helix which was not, however, validated experimentally and also did not consider tool optimisation.

1.2 Aims and Objectives

The main aim for the current research is to design and produce optimised variable helix milling tools. Two secondary aims are (1) to study the importance of amplitude dependency in the FRFs of milling tools, and (2) to investigate the importance of process damping phenomena for variable helix tools.

These can be attained by pursuing the following objectives:

- To investigate an amplitude dependency effect on the cutting tool FRF using non-contacting magnetic force excitation and to evaluate the performance of this method compared to traditional modal testing technique.
- To implement the optimisation of chatter and chatter performance through semi-discretisation method and Differential Evolution algorithm integration for variable helix milling tools.
- To improve the optimised results by refining the Differential Evolution algorithm and objective function and by applying multi-objective optimisation.
- To benchmark the Differential Evolution optimised results using a conventional Sequential Quadratic Programming algorithm, including variable pitch geometry comparison.
- To verify experimentally the optimised variable helix tools in minimising chatter and evaluate the effectiveness of semi-discretisation method in predicting variable helix milling tools.
- To evaluate and rank the effects of relief angle, rake angle, edge radius and variable helix/pitch on the performance of process damping when machining metal at low cutting speed.

1.3 Thesis Overview

The organisation of the rest of thesis is as follows and the thesis structure is shown in the diagram in Figure 1.4.

The next chapter will present a review of the literature, beginning with a historical view of chatter and numerical modelling. Then, literature on the current chatter control technology research is reviewed. The application of optimisation methods in machining and chatter will be emphasised.

Chapter 3 presents a theoretical background for optimising variable helix tools. This chapter describes chatter numerical modelling. The development of optimisation routines from chatter numerical and optimisation algorithms are briefly discussed with an example.

In Chapter 4, a non-contacting electromagnetic FRF measurement is carried out. Experiments on cutting tool with FRF will be measured using non-contacting electromagnet in static condition. The resulting amplitude dependency of the FRF of a cutting tool is discussed and the implications for the remainder of the thesis are explored.

Chapter 5 focuses on the theoretical optimisation algorithms. The formulation of optimisation approaches is described, specifically Differential Evolution, Sequential Quadratic Programming and epsilon constraint multi-objective methods. In Chapter 6, objective functions and optimisation results of variable helix of chatter minimisation and chatter performance maximisation are presented. The Differential Evolution algorithm and objective functions are refined. In Chapter 7, experimental machining is performed to validate the predicted performance. A further experiment is carried out to properly validate the variable helix semi-discretisation method prediction.

The tool geometry effect on process damping is investigated and presented in Chapter 8. The rake and relief angles, edge radius and variable helix/pitch are evaluated experimentally under process damped milling.

In Chapter 9, the research contributions and some suggestions for further work are presented.
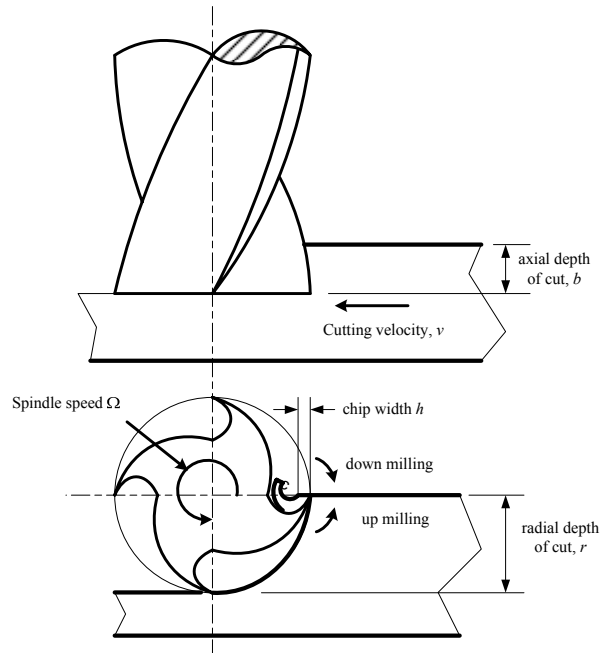
Figure 1.1 Cutting tool process parameters and type of milling operation
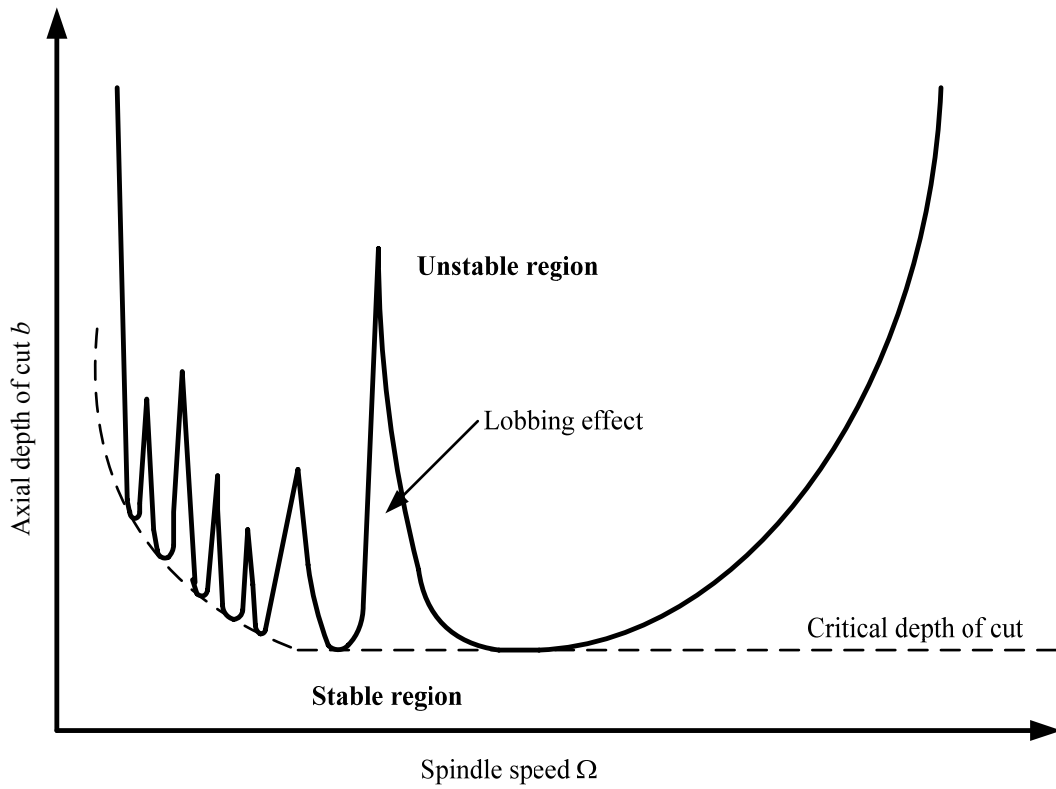
Figure 1.2 Stability lobes diagram.
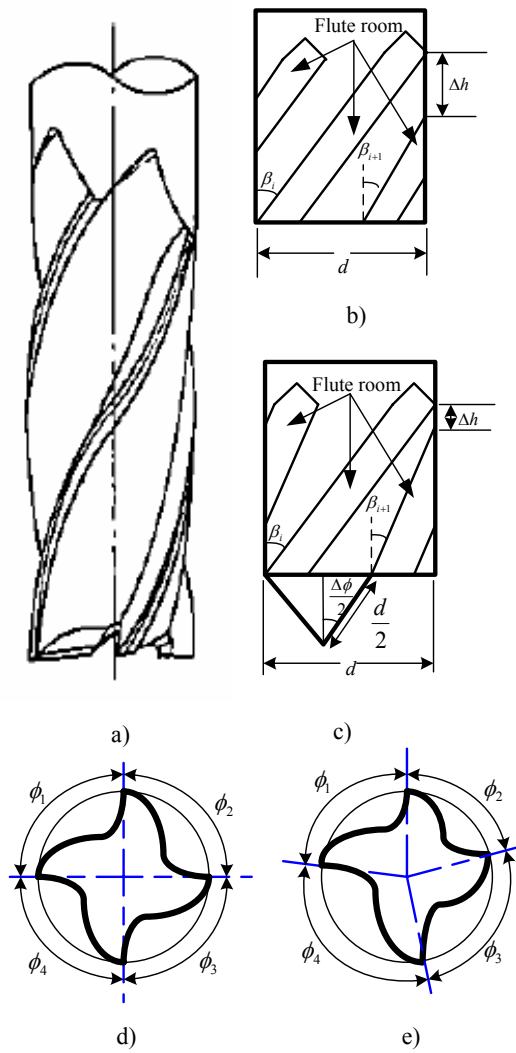
Figure 1.3 Typical cutting helical end milling tools a) 4 flute tool, b) Uniform helix, c) Variable helix, d) Uniform pitch and e) Variable pitch

```
┌─────────────────────────┐
│  Chatter: Analysis,     │
│  mitigation and         │
│  optimisation           │
└─────────────────────────┘
```
Chapter 2
- -

```
┌─────────────────────────┐
│  Theory: Semi-          │
│  discretisation method  │
│  and optimisation       │
│  approach               │
└─────────────────────────┘
```
Chapter 3
- -

```
┌─────────────────────────┐
│  Non-contacting modal   │
│  testing for chatter    │
│  stability prediction   │
└─────────────────────────┘
```
Chapter 4
- -

```
┌─────────────────────────┐
│  Optimisation           │
│  algorithms: Theory     │
│  and examples           │
└─────────────────────────┘
```
Chapter 5
- -

```
┌─────────────────────────┐
│  Optimisation of        │
│  variable helix/pitch   │
│  milling tools using    │
│  DE and SQP             │
└─────────────────────────┘

┌─────────────────────────┐
│  Improved DE algorithm  │
│  and multi-objective    │
│  optimisation           │
└─────────────────────────┘
```
Chapter 6
- -

```
┌─────────────────────────┐
│  Experimental           │
│  validation: optimised  │
│  variable helix milling │
│  tools                  │
└─────────────────────────┘
```
Chapter 7
- -

```
┌─────────────────────────┐
│  Experiment: Effect of  │
│  tool geometry on       │
│  process damped milling │
└─────────────────────────┘
```
Chapter 8
- -

```
┌─────────────────────────┐
│  Conclusion and future  │
│  work                   │
└─────────────────────────┘
```
Chapter 9
- -

Figure 1.4 Overview of thesis

CHAPTER 2
LITERATURE REVIEW

2.1 Chatter History

Almost 100 years ago, Taylor described machine tool chatter as the "most obscure and delicate of all problems facing the machinist" [14]. Merchant [15] presented the kinematics and mechanics of the metal cutting process in orthogonal cutting as represented in Figure 2.1. The relationships between the forces and the cutting parameters (shear angle plane φ, rake angle α), the coefficient of friction F_s between the tool, the chip and the shear strength of the material ψ are derived. However, the relationship is only valid in the steady state cutting process. In fact, metal cutting is a dynamic process where chatter needs to be taken into account as it causes serious problems in machining stability. Furthermore, milling is an interrupted cutting process where the chip thickness changes as the tooth enters and leaves the workpiece.

The development of numerical chatter modelling continued from 1960 till the present. Basic understanding about chatter was provided by Tobias and Fishwick [16] and Tlusty and Polacek [17] who developed an analytical method for predicting stability using a stability diagram. Tobias and Fishwick [16] explored the stiffness increases between workpiece and cutting process which will decrease chatter. They also considered damping, cutting speed, feedrate, tool geometry, workpiece material and machine structure which also play an important role in chatter. Thus, chatter theory was introduced based on velocity or penetration rate and regenerative chatter. Tlusty and Polacek [17] proposed a simple analysis when assuming the proportional relationship between dynamic cutting force and the undeformed chip thickness. From these, the recognition of nonlinearities in machining process, the time domain simulation of the milling process was then developed to explore the additional complexities that occur when milling, compared to simpler turning and boring operations.

Budak and Altintas [18, 19] then proposed the expansion analytical method of the periodic function coefficients to predict the stability diagram. In recent times, a state transition matrix of finite size for passing period of one tooth has been proposed with three methods: Time finite element analysis (TFEA), semi-discretisation method (SDM)

and shifted Chebyshev polynomials. The TFEA and SDM methods were proposed by Bayly *et al.* [6] and Insperger *et al.* [7], respectively. A discrete map can be obtained by using SDM and TFEA, while the third method is presented by Butcher *et al.* [20] who applied shifted Chebyshev polynomials to make an approximation of the delay differential equation (DDE) in the stability analysis.

In this chapter, numerical modelling of chatter in machining is introduced. The chapter also discusses the previous work of other researchers in chatter mitigation methods. The last section focuses on optimisation of milling, in particular avoiding chatter by modifying tool geometry.

2.2 Chatter Stability Prediction

During the regenerative chatter process, variation of cutting force and chip thickness occurs due to surface undulation [21]. Instability of the cutting process or self-excited chatter limits the machine tool performance [22]. Tobias *et al.* [16] proposed a graphical method of stability analysis using the Nyquist plot of the transfer function G(s) for the flexible system. The frequency response at a certain chatter frequency is f_c, which is slightly higher than the natural frequency.

An analytical chatter prediction was presented by Tlusty [3, 21] who formulated the stability lobe diagram that describes the relationship between stability, depth of cut and spindle speed. The analytical prediction was then reproduced based on control system theory [21] when Andrew and Tobias [23] criticised their work on applying only the real value of FRF. From the ignorance between the dynamics of the tool and workpiece system at an early stage, a simplistic model was thus created to prepare the way for more advanced models. The time domain simulations involve milling forces with changing directions (example as modelled by Tlusty and MacNeil [24]) due to a rotating cutter with helical flutes. By using the improved formulation of the dynamic cutting forces, the stability limits showed significant improvement from the previous simple model [25].

Alternative analytical approaches have been proposed. For example, Sridhar *et al.* [26] presented a graphical method for stability analysis of milling. A root locus method with time delays was initiated by Olgac and Hosek [27]. From the point where the locus crosses the imaginary axis, critical stability was determined.

Various authors applied the Floquet theorem which obtained a finite sized state transition matrix for one period. Budak and Altintas [18, 19] developed a delay-differential equation (DDE) with time-periodic coefficients for modelling stability of the milling process. A single frequency solution was created from the tool motion in the x and y directions, along with a truncated Fourier series approximating the periodic coefficients to form a complete frequency domain analysis. Milling modelling with non-linearity in the process was more appropriate than the Tobias's and Tlusty's model that can model only the turning process. However, this model was inaccurate and inappropriate for low radial immersion.

In order to solve the low radial immersion problem, Bayly *et al.* [6] introduced TFEA for complicated interrupted cutting in 2001 after extending work by Davies *et al.* [28]. An exact solution for the tool that is not in contact with the workpiece used the system state transition matrix. The time in the cut is divided into multiple elements and vector position and velocity in a single element when the tool contacts the workpiece. The single element is a linear combination of polynomial trial functions. The current element at the beginning and the previous at the end of the time element position and velocity are matched together. The formula produces a discrete linear map relating coefficients of the solution to coefficients one tooth passage earlier, which is required for the surface regeneration found in milling. The linear map eigen values will determine the stability. Although this TFEA method can be applied to variable pitch [29] and uniform helix [30] tools, this method is still not ready for variable helix milling.

Almost at the same time, Insperger and Stepan [7] proposed a method using the semi-discretisation scheme to obtain discrete maps. The delay term discretises with time coordinates to approximate the DDE. The SDM analyses stability of linear retarded dynamical systems based on discretisation to produce a high dimensional linear discrete system. This method is more effective in time and accuracy than fully discrete methods due to the delayed states and time-dependent coefficient. To date, Sims *et al.* [29] applied SDM in a state space approach to model irregular helix and pitch. DDE with time periodic coefficients, TFEA and SDM, were compared and analysed using experimental results from [30], including capability in predicting the high and low

immersion problem. As well as predicting a low immersion stability, the stability of variable helix and variable pitch tools can be predicted using SDM. As a result, SDM will be combined and integrated with optimisation algorithms for optimising a variable helix milling tool in the current study.

2.3 Chatter Mitigation Technology

Merrit [22] showed that regenerative chatter happens when there is an interaction between the structural dynamics of a machine tool and the dynamics of the cutting process. Based on that interaction, various methods for suppressing chatter have been proposed such as damping, spindle speed manipulation or variation and vibration absorbers. These methods are now described.

2.3.1 Vibration control

In vibration control, the aim is to suppress chatter instability by reducing the relative displacements between the tool and workpiece. Methods can involve active, semi-active or passive control.

An auxiliary mass is added to absorb vibration energy in the absorber as a passive method. For instance, Tobias [31] used a dynamic vibration absorber to improve stability as passive control. He proposed the absorber should demonstrate the largest amplitude of motion with a mass ratio (between absorber and structure) as large as possible. Liu and Rouch [32] proposed an optimal passive dynamic absorber for the milling process. Sims [33] proposed a methodology for optimally tuning an absorber for chatter mitigation. An impact damper proposed by Ema and Marui [34] as a passive method to mitigate the boring process. This was extended by Semercigil and Chen [35] for milling process application. An impact damper located inside a cutter to reduce stiffness, however changes the inertia of the cutting tools to cause instability during machining.

An active control requires external power to counteract the unwanted vibration. Linear Quadratic Regulator control of a boring bar was proposed by Tewani *et al.* [36] to suppress chatter using a piezoelectric actuator for exciting the absorber mass. Tarng *et al.* [37] proposed a tuned vibration absorber to suppress chatter in the turning process that modified FRF of tool structure or specifically at negative real part. In the milling process, Huyanan [38] reduced chatter vibration with an active vibration absorber that

modelled using virtual passive control based on a virtual passive absorber (VPA). VPA was manifested from active feedback control of a mass spring damper in the boring process by Pratt and Nayfeh [39]. Although VPA is suitable for use as it is simple and robust to reduce chatter in milling, it is limited by actuator saturation.

An active damper located at the machine headstock was applied by Chung [40] to reduce the negative part of the FRF of dynamic structure. Ganguli [41] applied an active damping vibrator to dissipate chatter vibration in both milling and turning. Increased stability was illustrated in using a hardware-in-the-loop simulation approach. Zhang and Sims [42] applied a piezoelectric actuator to suppress chatter. A positive position feedback control strategy was used. A pole placement strategy using a state feedback controller, strain gauge sensors and electro-active actuators was proposed by Dohner *et al.* [43]. Glaser and Nachtigal [44] used a feed-forward approach as a controller to control chatter in lathe and boring operations. A complex spindle speed modification was required by integrating active control into the spindle drive system. Also, a high torque spindle speed required a wide range of amplitude and frequency to ramp the spindle speed.

Wang *et al.* [45] and Segalman *et al.* [46] used smart fluids as a semi-active method (electrorheological (ER) or magnetorheological (MR) fluids) for chatter suppression. To tune boring bar stiffness, electrorheology was used by Nigm [47] to control force based on the change of electrorheology properties when electric current was applied to control chatter.

2.3.2 Spindle speed control

The machine's spindle speed can also be used to avoid chatter in cutting either by the spindle speed selection or spindle speed modulation. The spindle speed selection technique is described as offline, while spindle speed modulation is online technique. Spindle speed selection is an offline technique where knowledge of the dynamic system or previous cutting data is used to improve chatter stability by tuning the spindle speed. Spindle speed modulation is manipulated spindle speed or cutting conditions, i.e. axial or radial depth of cut based on chatter detection.

Offline technique can be applied to reduce chatter instability by improving the spindle design. Spindle stiffness and a larger diameter bearing were proposed by Wang and Lee

[48] to stabilise cutters in face milling. This was integrated with chatter vibration stability, cutting process speed and depth of cut of the spindle drive configuration which are required to design and optimise spindle speed for reducing peak response as well as chatter. Besides that, assigned eigenstructure can change model parameters to suppress chatter according to phase change. As proposed by Chiou *et al.* [49], an eigen structure was used to predetermine and modify the parameters. However, this requires extensive computer simulation to change cutting force variation when mode shape changes occur in the machine tools.

Beside offline technique via structural modification, Tlusty [50] proposed cutting at the stable region border by referring to experimental results or numerical prediction. Changing the spindle speed can stabilise an unstable machining operation from unstable to stable in the stability lobe diagram especially the use of lobbing effect when machining with high speed cutting (Figure 1.2). Kurdi *et al*. [51] applied TFEA as an analytical prediction tool to select suitable cutting parameters (spindle speed and depth of cut) when optimising material removal rate and surface location error simultaneously in order to search for stable cutting operation. Relationships between spindle speed and phase angle difference of milling and drilling were studied by Tarng and Lee [52] who suggested 90 degree phase angle for largest stability.   Spindle speed selection is sometimes impractical to apply due to the power, torque, and speed limitations of the machine.

A spindle speed modulation technique is an on-line method for chatter avoidance. This technique manipulates cutting speed or reduces radial or axial depth of cut when chatter is detected. Delio *et al.* [53] detected the dominant chatter frequency by sensing the sound with a microphone, then analysed its frequency. The speed was regulated to search for stable cutting after an audio signal detected the loud noise of an unstable milling process.   By using the same device to detect chatter integrated with a Knowledge Based System of machine tools, cutting tools and machinability data, Sim *et al.* [54] modified spindle speed and feedrate when chatter was detected. However, this method required a directional method to cancel background noise for detecting chatter.

Another popular online technique is using spindle speed variation.   By considering nominal spindle speed and frequency, a spindle servo system was proposed by Lin *et al.*

[55] for controlling variable speed in face milling. Altintas and Chan [56] suggested continuous variable speed to suppress milling chatter. By varying cutting speed, this modulates cutting force and static deflection of the tool when a chatter signal was detected to disturb wave generation. Similar to Liao and Young [57], this variable spindle speed was demonstrated to reduce chatter experimentally by keeping the phase angle at 90 degrees. In application to variable spindle speed, the analytical method is limited because of a variety of dynamics properties and invariant time delay in variable spindle speed chatter stability. As a result, Sridhar *et al.* [58] used Tsao *et al.* [59] analytical stability that considers a variable speed system for face milling. However, the method requires fast computational processor for monitoring of the signal from cutting force and spindle speed simultaneously.

The spindle speed variation technique is costly, requires a high performance of the spindle and the inertia of the rotating parts of the machine is limited. Additionally, speed variation can cause damage to motors and is impractical for the available machines, which have limited power and torque to adjust the spindle speed.

2.3.3 Alternative methods

Alternative methods have been proposed to improve the dynamics of the machine structure. They consist of tool geometry modification and tool path modification, and are now presently used to overcome spindle speed control problems.

The use of special tool geometry to control chatter has been proposed by various authors. Hashimoto *et al.* [60] studied chatter vibration reduction by modifying relief angle and cutting edge radius in milling operation. While in turning operation, Xiao *et al.* [61] and Mei *et al.* [62] studied the effect of rake angle and clearance angle on stability limit, a basic principle of a turning tool with a single cutting point was presented.   Both of them observed that increasing tool rake and decreasing tool clearance angle suppress chatter dynamically. Liu and Liu [63] demonstrated the effect of different rake and clearance angles on dynamic stability and proposed the concept of tool geometry control to suppress chatter vibrations. Nevertheless, a large rake angle and a very small clearance angle cause increase of tool temperature, and flank wear affecting tool life and surface finish.

Instead of modifying rake and relief angles for turning processes, the effects of changing uniform helical angle can be applied for milling processes. Zatarain *et al.* [64] extended a multi-frequency solution with a helix effect and compared the results with the SDM method. The change effect of helical angle at low radial immersion produced unstable island due to period-doubling bifurcation, especially at high spindle speed. Meanwhile, Patel *et al.* [30] applied TFEA to the similar condition as Zatarain *et al.* [64] with complex Fourier series and a three piecewise model to describe force model. The effect of varying helical angle was clearly demonstrated and was useful for low radial immersion applications. They found period-doubling and hopf bifurcation at low radial immersion for both types of milling exist at 30° and 45° helical angle. These two instabilities of period-doubling and hopf-bifurcation, together with period-one bifurcation, will be explained later in the next chapter.

Besides varying the helix in milling, variable pitch and variable helical angles also play an important role in geometry. Variable pitch study was initiated by Slavicek [8] using Tlusty's orthogonal cutting chatter, with the assumption of a rectilinear motion of tool and constant depth of cut, which caused constant vibration amplitude. After that, Opitz [9] studied irregular tooth pitch that shifted towards a wide range with consideration of speed range, natural frequency and number of teeth and pitch ratio. The irregular two pitch angles produced a higher depth of cut when phase angle was shifted to 90°. Irregular pitch angle led to the higher stability zone which was similar to the findings of Slavicek [8] where modulated inner and outer phase angle with nonlinear pitch evolution was used. The application of variable pitch as a mitigation method was reconsidered by Altintas *et. al* [5], Budak [11] and Olgac and Sipahi [12]. Variable pitch milling tools succeeded in its applications, however, the researchers have overlooked the variable helix milling tool for suppressing chatter.

Stone [10] investigated an irregular helix tool in the early period before the 1970s. Besides applying the variable helix cutter, different variable pitch spacing for face milling has been proposed by Varterasian [65]. Then, Tlusty [66] introduced irregular pitch, alternate helix and sinusoidal edge to help suppress chatter. In addition, the variable helix tool increases pitch variation along axial depth of cut to reduce chatter at certain speed ranges.

Elbestawi *et al*. [67] modelled machining dynamics including process damping when tool and workpiece are interfacing but they neglected a runout effect. Helical angle was found to facilitate the material flow past the contact zone and contributed to the reduction of the material recovery effect contributing to process damping in order to improve chatter stability. Recently, Turner *et al*. [68] investigated the variation of the variable helix and variable pitch angles to increase stability. Nonlinear condition or process damping disturbed unstable phase between subsequent teeth, especially at low spindle speed. In certain conditions, the variable helix reacts and behaves similarly to the variable pitch cutter and needs further study and clarification.

Weck *et al.* [69] proposed an automatic chatter-free approach for tool path cutting based on a Computer Aided Design tool. A tool path strategy using Numerical Control is required for adjusting axial or radial depth of cut but is restricted to a specific tool and workpiece. Similar to Weck, Ariffin *et al.* [70] and Smith *et al.* [71] proposed a tool path strategy to avoid regenerative chatter when machining a thin walled workpiece. The workpiece stiffness was increased to reduce the magnitude of the real part of the FRF, to allow cutting at higher depths of cut.   In their work [70], the deflection workpiece was used as a fitness function to be evaluated using Finite Element Method. A Genetic algorithm was defined as a travelling salesman problem to find the tool path that gave the lowest deflection during machining. The Genetic Algorithm was supplied the element sequence as input, and Finite Element Method was calculated the deflection of the machined element where the communication through data exchanged. The processes were repeated until the optimal sequence or tool path was achieved. Although Finite Element Method can be combined with Genetic Algorithm or other optimisation algorithm, this method requires a high performance processor and computational time effort to determine optimum path.

It can be seen for the alternative method that both pitch and helical angles play a significant part in tools' geometry parameter to reduce chatter as well as maximise material removal rate. Research on alternative chatter control for tool modification paid lower attention for modifying the variable helical milling tools with a low radial immersion. Variable helix suitable for a wide range of frequency and machines, and

appropriate for suppressing chatter, as well as overcoming the active method problems, are also applicable for a wide range of spindle speeds, tools and workpiece materials. Consequently, the variable helix should be optimised to search for the appropriate value by considering the maximum material removal rate and minimise the chatter behavior. Next, a suitable optimisation algorithm and problems will be presented and selected for current application in the variable helix milling tools.

2.4   Optimisation in Machining

Since Taylor developed machining techniques, researchers have shown a lot of interest in machining processes [14]. For the milling process, Figure 1.1 shows that process parameters in roughing or finishing operations are the axial depth of cut *b*, radial depth of cut *r*, spindle speed *n*, cutting velocity *v* and chip width *h*. The interactions between the process parameters, machine tools and system cause machining problems such as low productivity, tool life, surface roughness, chatter and others. To solve these problems, global optimum strategy is necessary and important to obtain. All factors relating to each other must be considered at the same time to obtain optimal cutting parameters for producing high productivity, quality and higher profit margins in machining processes. Recent practices based on operator experience and hand books as references were used to optimise process parameters. In this section, optimisation in machining is introduced and the algorithms or methods that have been applied to various problems in machining are summarised with specific focus on optimisation for chatter problems.

2.4.1   Optimisation methods and problems

The development of powerful computer tools has accelerated the optimisation method to solve machining problems. The optimisation problem consists of three basic parameters; like objective function, a set of unknowns or variables and a set of constraints. For the machining problems, these can be solved by optimising the parameters in processes, tools and objective functions. The problem functions consist of constraint parameters and operation conditions based on the problem to be solved. The objective function is called a cost function when its value is to be minimised, fitness function to maximise its value and error function to search its zero value [72].

Computer optimisation methods for metal cutting operations can classified as traditional, modern and intelligent methods. The operational research or traditional

methods are Geometric Programming, Dynamic Programming and Sequential Quadratic Programming. However, the traditional method is based on derivative technique when an objective function is used which cannot be differentiated. In addition, an objective function can also be a computer program or experimental data that are very subjective and the constraint may also consist of differentiation parameters [73]. Therefore, modern technology is introduced to overcome the problems by applying the statistic methods such as the Taguchi Method, Design of Experiment and Response Surface Methodology. Nevertheless, the statistical methods can suffer from problems such as, local optimal, premature population and not generalised due to equations that used obtained from experiment [73]. Thereby, intelligent technique overcome the problem by introducing Hill Climbing, Neural Network, Simulated Annealing, Tabu Search, Genetic Algorithms, Ant Colony Optimisation, Differential Evolution and Particle Swarm Optimisation. Latest technology, optimisation can be applied in a virtual manufacturing environment, as proposed by Merdol and Altintas [74, 75].

Abuelnaga and El-Dardiry [76] reviewed mathematical approaches (Geometric Programming, Dynamic Programming and Sequential Quadratic Programming) to solve optimisation problems in machining, while Aggarwal and Singh [77] only compiled turning machining optimisation problems according to the conventional and latest technology.   Meanwhile, Mukherjee [78] reviewed the advantages and disadvantages of machining optimisation methods used in current research. In contrast, Table 2.1 summarises optimisation of machining problems literature into the problems, technique and parameters. The machining problems can be classified into product quality, productivity, tool life and chatter. In short, Genetic Algorithm and Sequential Quadratic Programming are the dominant methods to solve for most of the problems in machining. It also indicates that machining problems can be faced and solved by either conventional or intelligent methods. Although Genetic Algorithm is more popular than Differential Evolution, for current research, Differential Evolution will be applied to optimise variable helix and variable pitch due to its robustness and its being faster than Genetic Algorithm [79]. For instance, Mayer *et al.* [80] used a small population of Differential Evolution to guarantee efficient, robust and better results than Genetic Algorithm in optimising a beef model. Stochastic methods (Genetic Algorithm, Particle Swarm Optimisation, Differential Evolution, electromagnetic algorithm, stigmergy algorithm) comparison made by Tusar *et al.* [79] in optimising universal motor

geometries strongly agreed that Differential Evolution and stigmergy algorithm improved the loss of power of the motor better than other stochastic methods.

In addition to those advantages, Differential Evolution is the only algorithm which can consistently find the optimal solution with a few function evaluations [81]. By using a small population size, Differential Evolution has the capability to escape from local optima during mutation process. Additionally, Differential Evolution has a better exploration ability and can work with noisy data compared to Genetic Algorithm and Particle Swarm Optimisation to optimise several constraint problems [81]. Differential Evolution also is successfully applied in various applications [82]: digital design, neural network learning, fuzzy decision making and heat exchanger. In machining optimisation, Saikumar and Shunmugan [83] applied Differential Evolution to select best cutting speed, feedrate and depth of cut to achieve optimum surface finish. Additionally, Krishna [84] applied Differential Evolution in grinding to search for a suitable process for minimising surface grinding. Besides that, Sequential Quadratic Programming as a popular conventional method can be used to benchmark the result of Differential Evolution. Kurdi *et al.* [51] applied SQP to optimise multi-objective function using a Pareto front approach where each time a single objective was solved, the second objective was constrained until an optimal front found. Sequential Quadratic Programming can also transform the nonlinear optimisation problem into a quadratic sub-problem around an initial guess, showing a better performance than Particle Swarm Optimisation. Therefore, based on the previous research and experience justfications, Differential Evolution and Sequential Quadratic Programming are used for optimising the current problems.

2.4.2 Optimisation in chatter suppression

Regenerative instability is affected by many factors such as workpiece, tool material, machine stiffness, tool geometry and cutting processes. On the other hand, milling stability is more complex problem than turning and grinding due to rotating, multiple cutting teeth, periodic force, chip load direction and multiple degree of freedom structural dynamics [3]. In order to show the chatter of the system is mitigated, the stability limits should increase from the original dynamics machine tools system. In suppressing chatter, certain methods require optimisation to be taken into consideration.

For example, in spindle design, tool path, cutting process and variable pitch require optimisation algorithm to be applied and are now reviewed.

The chatter problem is directly related to the spindle stiffness. An appropriate spindle design is required, especially in optimising the geometry to produce high productivity machining without chatter. Maeda *et al.* [85] optimised bearing distribution along the spindle shaft using Sequential Quadratic Programming. The Finite Element Method was applied to predict FRF of the spindle speed based on Timoshenko beam theory. Integrated with chatter vibration stability, cutting speed and axial depth of cut, the spindle drive configuration was then designed and optimised. Maximum critical depth of cut was included in the objective function which changes according to the bearing location FRF and the number of flutes. Liu and Rouch [32] proposed an optimal passive dynamic absorber for the milling process. Before carrying out the passive control, dynamic mass was to be connected with the optimised passive elements such as spring and damper. The objective function was chosen as the optimal critical depth of cut that can apply in the wide range of spindle speeds.

Chatter stability is represented by depth of cut in the spindle speed function (Figure 1.2). This involves cutting process parameters that should be optimised in order to minimise chatter. Kurdi *et al.* [51] optimised spindle speed and depth of cut under stability condition of chatter to achieve high material removal rate and minimum surface location error using TFEA method. Particle Swarm Optimisation (PSO) and Sequential Quadratic Programming (SQP) were applied to search for two objective functions under Pareto front approach where each time a single objective was solved, the second objective was constrained until the optimal front was found. Both objective functions used spindle speed and depth of cut as parameters and constraint of dynamic map eigen values. Material removal rate calculation also involved chip width besides depth of cut and spindle speed as constraint. Epsilon constraint was easily applied to solve multi-objective optimisations problem.

On the other hand, Budak and Tekeli [86] maximised the material removal rate while optimising axial and radial depth of cut without sacrificing chatter using analytical method. Maximum material removal rate can be achieved at certain combinations of axial and radial depth of cut while spindle speed and number of cutters are constant, and

is related to FRF of the cutting tool change. From integrating the optimisation with the computer aided design/ computer aided manufacturing (CAD/CAM) system, machining time was reduced when applied to pocket machining They used their own algorithm to optimise the machining process that maximised material removal rate and at the same time minimised chatter and machining time. However, by maximising radial and axial depth of cut, it requires double optimisation approach and takes time to achieve optimum immersion conditions.

Variable geometry can be optimised to reduce chatter in generating a low cutting force, high material removal rate and precise product using several approaches. For example, Altintas *et al*. [5] emphasised to maximise axial depth of cut when the regenerative phase angle shifts to 90°. The phase changes when using different spindle speed, chatter frequency f_c and depth of cut. To optimise variable pitch angles, a manual mathematical calculation was applied by considering specific spindle speed and chatter frequency that minimise chatter. Using variable pitch tools, Shirase and Altintas [87] minimised the force and location error. Not much variable pitch range can be modified due to phase angle constraint to maintain no chatter conditions.

Meanwhile, Budak [11] modelled and optimised a non-constant pitch angle cutter model with an analytical stability model. A simple equation based on Hill Climbing was used to determine optimal pitch angles from stability and pitch variation. A linear pitch variation was used that gives higher stability rather than non-linear variation.   In addition, the non-linear variation also caused difficulties in manufacturing the tools. Thus, the spindle speed and chatter frequency need to be tuned to optimise pitch angles at constant depth of cut. Phase difference and chatter frequency were set as constraints to ensure that higher stability was accomplished.   The variable pitch cutter is appropriate for low speed machining, besides reducing force this also does not increase cost and only needs measurement analysis. On the other hand, at a certain pitch variation, this approach suits only a limited frequency and speed ranges.

Olgac and Sipahi [88] maximised material removal rate in simultaneous machining with an irregular pitch cutter using Cluster treatment of Characteristic roots (CTCR) algorithm. The algorithm has capability to optimise unstable variable pitch at certain axial depth of cut and spindle speed. This is based on the characteristic equation of the

CTCR, at certain axial depth of cut, to represent two time delays in pitch ratio and spindle speed variation. The characteristic equation depends on the number of flutes, spindle speed and different depth of cut to give different optimal value using the time delays. For variable pitch results, the chip evacuation phenomena, which occurs at particularly small angles, as reported by [5], should be considered. And Olgac and Sipahi [12] continued the same approach with a 6-flute cutter. Nevertheless, no experimental implementation results are discussed.

2.5 Summary

The early and latest research on machining dynamics has been reviewed including the analytical and the approach to suppress chatter by either passive or active methods by applying absorber, damping, varied speed and alternatives. The alternatives method of variable helix and variable pitch is highlighted reviewed, especially in suppressing chatter by optimising the tool's geometry. In the literature, it can be observed that the optimisation focuses on spindle design, tool path, cutting process and variable pitch. There are various algorithms which can be applied in optimisation of machining problems. DE is the appropriate candidate that can solve time consuming, local optimal and more robust as compared to GA. To benchmark the simulation results, SQP has widely applications and a famous conventional algorithm will be used.

Stone [10] and Turner *et al.* [68] studied the effect of stability on irregular helical angle milling cutter. Both investigated how chatter stability can be suppressed using irregular helix tools. Currently, the variable pitch optimisation has mostly focused on modifying the milling tool for chatter suppression [5, 11, 12] and the current research related to variable helix and variable pitch milling tool as presented by Sims *et al.* [29]. However, Sims's model only predicted the chatter stability of variable helix and variable pitch tools, and did not optimise the tool design for chatter suppression. It can be seen that variable helix modification has received little attention and interest in the optimisation and mitigation of milling chatter. As a result, an optimisation of variable helix milling tools using DE and SQP will be largely study in this thesis.

A proper understanding of SDM algorithms in predicting a variable helical milling tool is required, so the initial background is studied on how the SDM algorithms solve irregular tool geometry. Theory of DE and SQP algorithm are then presented with the numerical examples. Next, current research tendencies to maximise chatter performance

and minimise chatter are examined. Before being applied to multi-objective problems, the current DE algorithm is refined to improve its performance. The succeed optimisation are finally validated experimentally.

Table 2.1 Summary of problems, techniques and parameters used in optimisation problems in machining

No	Problem	Technique	Parameters commonly used
1	Production cost/time/profits	Genetic Algorithms [89-91] Simulated Annealing [92] Sequential Quadratic Programming [85, 93, 94] Specific algorithms [95] Hill Climbing [89] Memetic Algorithm [89]	Machine power [89-91, 93, 95] Chip width [89, 91-93, 95] Cutting force [89, 95] Surface roughness [89-91] Tool life [92] Cutting speed [90-93, 95] Spindle speed [89, 90] Axial depth of cut [85, 90-94] Radial depth of cut [94]
2	Material removal rate	Dynamic Programming [96] Neural Network [97] Sequential Quadratic Programming [98] Geometric Programming [99] Specific Algorithm [100]	Chip width [96, 97, 99, 100] Cutting speed [97, 99] Axial depth of cut [97] Radial depth of cut [97] Tool life [99] Machine power [99] Surface roughness [98]
3	Surface finish	Genetic Algorithms [101-103] Differential Evolution [83] Taguchi Method [104] Response Surface Methodology [102] Design of Experiment [101, 105] Specific algorithms [106]	Chip width [101-106] Cutting speed [101-105] Spindle speed [103] Axial depth of cut [83, 101-105] Radial depth of cut [102, 104, 105]
4	Tool life	Specific algorithms [107]	Chip width [107] Cutting speed [107] Axial depth of cut [107]
5	Chatter	Genetic Algorithms[70] Hill Climbing [11, 108] Specific algorithms [5, 12, 86, 88, 109, 110]	Material removal rate [86, 110] Spindle speed [5, 11, 12, 86, 88, 108-110] Cutting speed Axial depth of cut [11, 12, 86, 88, 108-110] Radial depth of cut [86, 110] Phase angle [11, 108] Chatter frequency [5, 11, 108] Tool path [70] Pitch angle [5, 11, 12, 88, 108, 109]
6	Combine problems	Particle Swam Optimisation [51, 111] Sequential Quadratic Programming [51, 111-113] Genetic Algorithms [113-117] Specific algorithms [118-122] Taguchi Method [123, 124] Differential Evolution [84] Simulated Annealing [114] Dynamic Programming [114] Tabu Search [115] Geometric Programming [125, 126]	Machine power [113, 114, 117-119, 122, 125, 127] Surface roughness [113, 116, 118, 119, 122, 127] Tool life [113, 116] Cutting speed [112-114, 116-119, 121, 123-127] Spindle speed [51, 111, 119, 120] Axial depth of cut [51, 111-113, 116, 117, 123-125, 127] Chip width [112-114, 116-127] Radial depth of cut [116] Force [117, 119, 120]

24
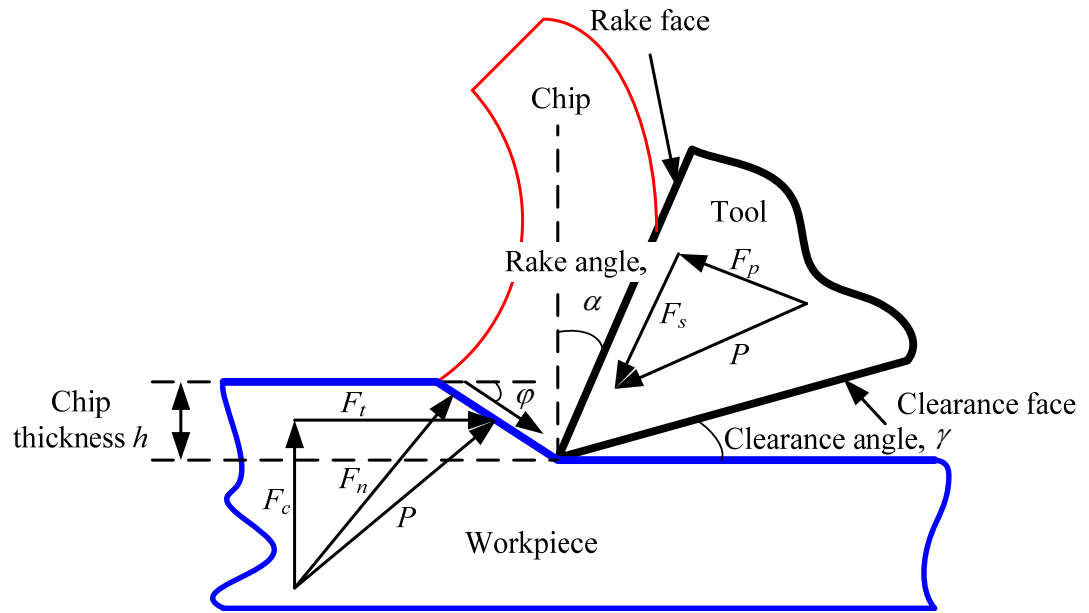
Figure 2.1 Model of metal cutting by Merchant [15]

CHAPTER 3
THEORETICAL BACKGROUND

3.1 Introduction

In Chapters 1 and 2, various chatter mitigation technologies were described and it was argued that variable helix and variable pitch tools can provide an alternative. In this chapter, the theoretical background of numerical chatter prediction and optimisation methods are properly explained.

The semi-discretisation method (SDM) is an appropriate stability algorithm to apply when investigating variable pitch and variable helix tools as discussed in Chapter 2. This approach has the capability to predict stability limits with variable time delays arising due to variable helix and variable pitch conditions. The method is appropriate for low radial immersion and has been verified (experimentally) by Patel *et al.* [30] and (numerically) Sims *et al.* [29]. In Chapter 2, various optimisation methods with different objective functions and constraints were discussed. A single objective approach either maximises or minimises a function in a straightforward fashion, whereas multi-objective methods need other tools to operate with more than one objective function.

This chapter is structured as follows. Initially, basic chatter stability theory is introduced before the SDM algorithm is described in detail for variable helix and variable pitch tool geometry. The SQP optimisation algorithm will be used to benchmark the simulation results from the DE algorithm. As an initial study, an analytical model is then used to optimise depth of cut using DE and SQP algorithms.

3.2 Chatter Numerical Modelling

As discussed in Chapter 1, the sources of chatter in metal cutting include mode coupling, loss of contact and regeneration of waviness [3]. The regenerative effect occurs most in the machining case and is the focus of this thesis. Regenerative chatter will now be described and analytical chatter prediction algorithms discussed.

3.2.1   Regenerative chatter and basic stability lobes

The cutting process affects the dynamics of the flexible cutting tool and the workpiece. During cutting, the tool starts to oscillate when it might face a hard spot on the metal surface, producing waviness on the workpiece surface. The tool then faces the waves left during the previous pass after one full rotation leads to surface waviness, as shown in Figure 3.1. Relative vibration between tool and workpiece results in a time–varying depth of cut h

$$h = h_m + y_p - y \qquad (3.1)$$

where h_m is the mean chip thickness due to workpiece feed and y_p and y are the previous and current relative vibrations of the tool, respectively. The vibration of the previously cut surface can be expressed as a time delayed version of the current vibration:

$$y_p = h(t - \tau) \qquad (3.2)$$

Where τ is the time delay between each tooth pass. y_p also can be represented in the Laplace domain as $y(s)e^{-s\tau}$. Merrit [22] introduced a closed loop feedback diagram to represent regenerative chatter in a control perspective, as shown in Figure 3.2. Therefore the machine tool transfer function between two chip thicknesses can be derived as

$$\frac{h(s)}{h_m(s)} = \frac{1}{1 + K_s b G(s)(1 - e^{-s\tau})} \qquad (3.3)$$

where $G(s)$ is the transfer function, K_s is the cutting stiffness and b is axial depth of cut. In Equation (3.3), the characteristic equation of the closed loop system is $1+K_s b(G(s)(1-e^{-s\tau})=0$ and the time delay between two cutting processes with frequency f results in a phase shift $\varepsilon=\tau f$ which can be represented by the factor $e^{-j\varepsilon}$. The limit of stability for b value can be derived as

$$b = \frac{-1}{K_s G(1 - e^{-j\varepsilon})} \qquad (3.4)$$

The above formula is only satisfied if the term $G(1-e^{-j\varepsilon})$ is a real number. Both imaginary terms, $\text{Im}(G)$ and $\text{Im}(Ge^{-j\varepsilon})$ can be cancelled to present a real number as:

$$G(1 - e^{j\varepsilon}) = 2\,\text{Re}(G) \qquad (3.5)$$

Thus Merrit [22], Tlusty [3], Tobias *et al.* [128] and Altintas [129] have demonstrated that the application of Nyquist's stability criterion leads to an expression for critical depth of cut b_{cr} above which chatter will occur:

$$b_{cr} = \frac{-1}{2K_s \, \mathrm{Re}(G(j\omega))} \qquad (3.6)$$

The critical depth of cut is inversely proportional to K_s and $Re(G)$ according to Equation 3.6. The limited critical depth of cut b_{lim} can be obtained from minimum value of $Re(G)$ as follows:

$$b_{\lim} = \frac{-1}{2K_s \, \mathrm{Re}(G(j\omega))_{\min}} \qquad (3.7)$$

Meanwhile, the frequency f of the self-excited vibration is given by

$$n + \frac{\varepsilon}{2\pi} = \frac{f}{m\Omega} \qquad (3.8)$$

where n is an integer number, Ω is spindle speed and m is number of teeth. The phase ε can be represented as

$$\varepsilon = 2\pi - 2\tan^{-1}\left(\frac{\mathrm{Re}(G(j\omega))}{\mathrm{Im}(G(j\omega))} \right) \qquad (3.9)$$

Different ε can be obtained, as shown in Figure 3.3, from the relationship in Equation 3.9. Using Equations 3.7 and 3.8 from the critical chip width and the spindle speed, the stability limit can be constructed. Combinations of depth of cut and spindle speed can produce a stable or unstable region, as shown in Figure 1.2. More recently, various researchers have extended this model to consider the more complex cases of milling. From knowledge of the frequency response function $G(j\omega)$, the stability limit can be derived as shown by Tlusty and Polacek [17], Merrit [22], Tobias *et al.* [128] and Altintas [129]. Thus, in any case it is apparent that the FRF G is required in order to determine chatter stability. In Chapter 4, experiments are described that obtained this FRF using an electromagnet and the results are compared to those from an impact hammer.

3.2.2 Semi-discretisation method algorithm

SDM is a well known technique in Finite Element Method (FEM) of solid bodies and Computer Fluid Dynamics (CFD). This delay system theory started in the 1950s and has solved many problems in engineering such as wheel shimmy, ship stabilisation, machine tool vibration and neural network model [7]. Compared with a fully discrete method, SDM is more effective in time and accuracy due to the delayed states and time-dependent coefficients applied. The details about SDM can be referred to in [7] and recently Sims *et al.* [29] applied SDM in a state space approach to model irregular helix

and pitch tools. In this section, the summary of the important governing equations in [29] are presented before continuing with optimising the variable helix tools.

In Figure 3.4, the engagement between a discretised axial layer of the milling cutter is considered. Using a discrete time approximation, the sampling time period of one full rotation of the workpiece T equals $2\pi/N\Omega$, where N is the number of discrete time steps per revolution and Ω is the spindle speed in radians per second. It can be assumed that for a circular tool path and a feed per tooth w_o, the chip thickness for tooth j on layer l is given by [29]

$$
\begin{aligned}
h_{l,j} = {}& g\!\left(\theta_{l,j}(nT)\right)\!\left[w_o\sin\!\left(\theta_{l,j}(nT)\right)\right] && k = 1,2,\dots \\
& + \left(u_x(kT)-u_x\!\left(kT-\tau_{l,j}\right)\right)\sin\!\left(\theta_{l,j}(nT)\right) \\
& + \left(u_y(kT)-u_y\!\left(kT-\tau_{l,j}\right)\right)\cos\!\left(\theta_{l,j}(nT)\right) && n = 1,2,\dots,N
\end{aligned}
\tag{3.10}
$$

where the relative vibration between the tool and workpiece is in x-direction u_x and in y-direction u_y. The static component $w_o\sin\!\left(\theta_{l,j}\right)$ is neglected in the stability analysis due to non-contribution to the regenerative effect [129]. θ is the periodic angular position of each axial layer of each flute given by

$$
\theta_{l,j}(nT) = \theta_{l,j}(0T) + \frac{2\pi n}{N} \qquad n = 1,2,\dots,N
\tag{3.11}
$$

g is a unit step function with the value either unity or zero corresponding to flute j at layer l engaged or not in the workpiece.

$$
\begin{aligned}
g\!\left(\theta_{l,j}(nT)\right) = 1 \rightarrow \theta_i < \theta_{l,j}(nT) < \theta_o \\
g\!\left(\theta_{l,j}(nT)\right) = 0 \rightarrow \theta_i < \theta_{l,j}(nT)\cdot or \cdot \theta_{l,j}(nT) > \theta_o
\end{aligned}
\tag{3.12}
$$

For current time delay, τ is given by the time when the axial discrete tool engages with the workpiece, using the following relationship:

$$
\tau_{l,j} = T\cdot round\!\left(N\frac{\delta\theta_{l,j}}{2\pi}\right)
\tag{3.13}
$$

However, the chip thickness relates to current u_x, u_y and past displacement at the same point. For each tooth or axial layer of variable pitch, τ is not steady or constant. Thus an intermediate states variable Δ is valuable to describe the displacement difference for current and previous conditions.

$$
\Delta_{x/yn}(kT) = u_{x/y}(kT) - u_{x/y}(kT - nT)
\tag{3.14}
$$

The vector $\mathbf{\Delta} = \{\Delta_x \Delta_y\}^\mathbf{T}$ describes the vibration relative to a previous sample time in tool revolutions for each element. The chip thickness corresponds to tangential force F_t and normal force F_n at each flute to give

$$F_{t,l,j} = K_t \delta b w_{l,j} \qquad (3.15)$$

$$F_{n,l,j} = K_r F_{t,l,j} \qquad (3.16)$$

where $\delta b = b/L$ refers to the tool in L axial layer discretised into depth. The resultant forces F_x and F_y are summed from all teeth and all axial discretisation layers in x and y directions. By using the variable Δ that relates to matrix formulation can be developed

$$\begin{Bmatrix} F_x(kT) \\ F_y(kT) \end{Bmatrix} = \mathbf{R}(nT) \begin{Bmatrix} \Delta_x(kT) \\ \Delta_y(kT) \end{Bmatrix} \text{ with } n=1,2,...,N \qquad (3.17)$$

$\mathbf{R}$ is the periodic time varying matrix and the populated elements r are as follows

$$r_{1,k}(nT) = \frac{1}{2} \delta b K_t \sum_{j=1}^{N_t} \sum_{l=1}^{L} h(k, \tau_{l,j}) \overline{a}_{xx}(\phi_{l,j}(nT))$$

$$r_{2,k}(nT) = \frac{1}{2} \delta b K_t \sum_{j=1}^{N_t} \sum_{l=1}^{L} h(k, \tau_{l,j}) \overline{a}_{xy}(\phi_{l,j}(nT))$$

$$r_{1,N+k}(nT) = \frac{1}{2} \delta b K_t \sum_{j=1}^{N_t} \sum_{l=1}^{L} h(k, \tau_{l,j}) \overline{a}_{yx}(\phi_{l,j}(nT))$$

$$r_{2,N+k}(nT) = \frac{1}{2} \delta b K_t \sum_{j=1}^{N_t} \sum_{l=1}^{L} h(k, \tau_{l,j}) \overline{a}_{yy}(\phi_{l,j}(nT)) \qquad (3.18)$$

where h is a unit step function that defines the appropriate delay term

$$h(k, \tau_{l,j}) = 1 \rightarrow k = \frac{\tau_{l,j}}{T}$$

$$h(k, \tau_{l,j}) = 0 \rightarrow k \neq \frac{\tau_{l,j}}{T} \qquad (3.19)$$

Referring to Figure 3.4, the equation of motion can be represented as

$$\ddot{x} + 2\xi\omega\dot{x} + \omega^2 x = \frac{F(t)}{m_m} \qquad (3.20)$$

Where m_m is modal mass, ξ is damping ratio, ω is frequency in rad/s and $F(t)$ force function. The first step in the state space approach is to write Equation 3.20 as the following state space equation (where $x_1 = x$ and $x_2 = \dot{x}$):

$$\begin{bmatrix} \dot{x}_1 \\ \dot{x}_2 \end{bmatrix} = \begin{bmatrix} 0 & 1 \\ \frac{-1}{m_m} & -2\xi\omega \end{bmatrix} \begin{bmatrix} x_1 \\ x_2 \end{bmatrix} + \begin{bmatrix} 0 \\ 1 \end{bmatrix} F \qquad (3.21)$$

$$u = \begin{bmatrix} \begin{bmatrix} 1/m_m \end{bmatrix} & 0 \end{bmatrix} x$$

It is straightforward to include additional modes of vibration in this formulation. The tool and workpiece relative motion in the x and y directions are now referred to as u_x and u_y, respectively. These are assumed to be the same for all tool axial layers in the present study. The state space form of relative motion is therefore:

$$\{\dot{\mathbf{x}}_s\}_{[D \times 1]} = \mathbf{A}_s \mathbf{x}_s + \mathbf{B}_s \begin{Bmatrix} F_x \\ F_y \end{Bmatrix}$$

$$\begin{Bmatrix} u_x \\ u_y \end{Bmatrix}_{[2 \times 1]} = \mathbf{C}_s \mathbf{x}_s \qquad (3.22)$$

where the subscript s refers to the structural dynamics and D indicates the total number of states used to model the vibration in the x and y directions. In Equation 3.22, $\mathbf{A}_s$, $\mathbf{B}_s$, $\mathbf{C}_s$ and $\mathbf{x}_s$ define the state matrix, input matrix, output matrix and state variable for structural dynamics, respectively.

The first term Equation (3.22) can be defined as $\dot{\mathbf{x}}_s(t) = \lim\limits_{\Delta t \to 0} \dfrac{\mathbf{x}_s(t + \Delta t) - \mathbf{x}_s(t)}{\Delta t}$. From this derivative definition, t is divided by a small intervals $\Delta t = T$ can be used to determine the value $\mathbf{x}_s(t)$ as approximation of the derivative as

$$\dot{\mathbf{x}}_s = \frac{\mathbf{x}_s(t + T) - \mathbf{x}_s(t)}{T} \qquad (3.23)$$

This equation can be substituted into first term Equation 3.22 to obtain

$$\frac{\mathbf{x}_s(t + T) - \mathbf{x}_s(t)}{T} \cong \mathbf{A}_s \mathbf{x}(t) + \mathbf{B}_s \begin{Bmatrix} F_x(T) \\ F_y(T) \end{Bmatrix}$$

$$\mathbf{x}_s(t + T) \cong \mathbf{A}_s \mathbf{x}(t)T + \mathbf{x}_s(t) + \mathbf{B}_s T \begin{Bmatrix} F_x(T) \\ F_y(T) \end{Bmatrix} \qquad (3.24)$$

where t is divided into intervals of width T as sampling time. Therefore, this t can be written as $t = kT$ ($k = 0, 1, 2, 3, \ldots$). Then Equation 3.24 is written as

$$\mathbf{x}_s[(k+1)T] \cong \mathbf{A}_s T \mathbf{x}(kT) + \mathbf{x}_s(t) + \mathbf{B}_s T \begin{Bmatrix} F_x(kT) \\ F_y(kT) \end{Bmatrix} \qquad (3.25)$$

Note that $\mathbf{A}_s(T)$ and $\mathbf{B}_s(T)$ depend on the sampling period T. However, the second term in Equation 3.22 does not depend on sampling period T. Both terms become

$$\mathbf{x}_s\left(kT+T\right)=\mathbf{A}_s\mathbf{x}_s\left(kT\right)+\mathbf{B}_s\begin{Bmatrix}F_x\left(kT\right)\\F_y\left(kT\right)\end{Bmatrix}$$

$$\begin{Bmatrix}u_x\left(kT\right)\\u_y\left(kT\right)\end{Bmatrix}=\mathbf{C}_s\mathbf{x}_s\left(kT\right) \qquad (3.26)$$

The continuous time dynamics Equation (3.26) is discretised to give

$$\mathbf{x}_m\left(kT+T\right)=\mathbf{A}_m\mathbf{x}_m\left(kT\right)+\mathbf{B}_m\begin{Bmatrix}F_x\left(kT\right)\\F_y\left(kT\right)\end{Bmatrix}$$

$$\begin{Bmatrix}u_x\left(kT\right)\\u_y\left(kT\right)\end{Bmatrix}=\mathbf{C}_s\mathbf{x}_m\left(kT\right) \qquad (3.27)$$

$\mathbf{x}_m$, $\mathbf{A}_m$ and $\mathbf{B}_m$ are the state variable, state matrix and input matrix for the discretised structural dynamics, respectively. Using the Matlab function c2d.m [130], this $\mathbf{A}_m$ and $\mathbf{B}_m$ are given by the matrix exponential:

$$\begin{bmatrix}\left[\mathbf{A}_m\right]_{[D\times D]} & \left[\mathbf{B}_m\right]_{[D\times 2]}\\ \mathbf{X}_{[2\times D]} & \mathbf{W}_{[2\times D]}\end{bmatrix}_{[(D+2)\times(D+2)]}=\exp\left(T\begin{bmatrix}\left[\mathbf{A}_s\right]_{[D\times D]} & \left[\mathbf{B}_s\right]_{[2\times D]}\\ \left[\mathbf{0}\right]_{[2\times D]} & \left[\mathbf{0}\right]_{[2\times 2]}\end{bmatrix}\right) \qquad (3.28)$$

Where $\mathbf{X}$ and $\mathbf{W}$ are unused variable and purpose to introduce is to make balance right with other equations in the same matrix size.

The relationship between the relative vibration $\mathbf{u}$ and the delay state Δ can also be represented state space as

$$\left\{\dot{\mathbf{x}}_s\right\}_{[D\times 1]}=\mathbf{A}_s\mathbf{x}_s+\mathbf{B}_s\begin{Bmatrix}u_x\\u_y\end{Bmatrix}$$

$$\begin{Bmatrix}\Delta_x\\\Delta_y\end{Bmatrix}_{[2x1]}=\mathbf{C}_s\mathbf{x}_s+\mathbf{D}_s\begin{Bmatrix}u_x\\u_y\end{Bmatrix} \qquad (3.29)$$

where $\mathbf{D}_s$ is feedthrough matrix for the system delays. Equation 3.29 can be solved using same method as Equation 3.22 to give in discrete-time state-space form as

$$\mathbf{x}_d\left(kT+T\right)=\mathbf{A}_d\mathbf{x}_d\left(kT\right)+\mathbf{B}_d\begin{Bmatrix}u_x\left(kT\right)\\u_y\left(kT\right)\end{Bmatrix}$$

$$\begin{Bmatrix}\Delta_x\left(kT\right)\\\Delta_y\left(kT\right)\end{Bmatrix}=\mathbf{C}_d\mathbf{x}_d\left(kT\right)+\mathbf{D}_d\begin{Bmatrix}u_x\left(kT\right)\\u_y\left(kT\right)\end{Bmatrix} \qquad (3.30)$$

$\mathbf{x}_d$, $\mathbf{A}_d$, $\mathbf{B}_d$, $\mathbf{C}_d$ and $\mathbf{D}_d$ are the state variable, state matrix, input matrix and feedthrough matrix of the system delays, respectively. This $\mathbf{x}_d$ is used to determine the delay state Δ and other the terms in Equation (3.30) are

$$\mathbf{A}_d = \begin{bmatrix} \begin{bmatrix} \{0 \quad \cdots \quad 0\}_{[N-1]} & 0 \\ [I]_{((N-1)\times(N-1))} & \{0 \quad \cdots \quad 0\}^{\mathbf{T}}_{[N-1]} \end{bmatrix} & [0] \\ [0] & \begin{bmatrix} \{0\cdots0\}_{[N-1]} & 0 \\ [I]_{((N-1)\times(N-1))} & \{0\cdots0\}^{\mathbf{T}}_{[N-1]} \end{bmatrix} \end{bmatrix}$$

$$\mathbf{B}_b = \begin{bmatrix} \{1 & \{0 \quad \cdots \quad 0\}^{\mathbf{T}}_{[N-1]}\} & \{0 \quad \cdots \quad 0\}^{\mathbf{T}}_{[N-1]} \\ \{0 \quad \cdots \quad 0\}^{\mathbf{T}}_{[N]} & \{1 \quad \{0 \quad \cdots \quad 0\}^{\mathbf{T}}_{[N-1]}\} \end{bmatrix}$$

$$\mathbf{C}_d = \begin{bmatrix} -[\mathbf{I}]_{[N\times N]} & [0] \\ [0] & -[\mathbf{I}]_{[N\times N]} \end{bmatrix}$$

$$\mathbf{D}_d = \begin{bmatrix} \{1 \quad \cdots \quad 1\}^{\mathbf{T}}_{[N]} & \{0 \quad \cdots \quad 0\}^{\mathbf{T}}_{[N]} \\ \{0 \quad \cdots \quad 0\}^{\mathbf{T}}_{[N]} & \{1 \quad \cdots \quad 1\}^{\mathbf{T}}_{[N]} \end{bmatrix} \qquad (\ 3.31)$$

The three Equations (3.17), (3.27) and (3.30) are important to represent the time delay terms that arise especially on variable helix and variable pitch tools. These terms can be combined to give

$$\begin{Bmatrix} \mathbf{x}_m(kT+T) \\ \mathbf{x}_d(kT+T) \end{Bmatrix} = \begin{bmatrix} \mathbf{A}_m & [0] \\ \mathbf{B}_d\mathbf{C}_s & \mathbf{A}_d \end{bmatrix} \begin{Bmatrix} \mathbf{x}_m(kT) \\ \mathbf{x}_d(kT) \end{Bmatrix} + \begin{bmatrix} \mathbf{B}_m \\ [0]_{[2N\times2]} \end{bmatrix}$$

$$[\mathbf{R}(nT)\mathbf{D}_d\mathbf{C}_s \quad \mathbf{R}(nT)\mathbf{C}_s] \begin{Bmatrix} u_x(kT) \\ u_y(kT) \end{Bmatrix} \qquad (\ 3.32)$$

The regenerative chatter in milling can be represented as in Figure 3.5. This compiles structural dynamics (Equation 3.27), regenerative effect (Equation 3.30) and dynamic cutting force coefficient (Equation 3.17) that relate to each other and are used for searching optimum variable helix and variable pitch.

Let $\mathbf{Q}(p) = \left(\begin{bmatrix} \mathbf{A}_m & [0] \\ \mathbf{B}_d\mathbf{C}_s & \mathbf{A}_d \end{bmatrix} + \begin{bmatrix} \mathbf{B}_m \\ [0]_{[2N\times2]} \end{bmatrix} [\mathbf{R}(p)\mathbf{D}_d\mathbf{C}_s \quad \mathbf{R}(p)\mathbf{C}_s] \right)$. Then the variation of

states of the system between the revolution of one tool and its next revolution can be presented as follows:

$$\begin{Bmatrix} \mathbf{x}_m(kT+NT) \\ \mathbf{x}_d(kT+NT) \end{Bmatrix} = (\mathbf{Q}(NT)\times\mathbf{Q}(NT-T)\times\ldots\times\mathbf{Q}(1T)) \begin{Bmatrix} \mathbf{x}_m(kT) \\ \mathbf{x}_d(kT) \end{Bmatrix} \qquad (\ 3.33)$$

Thus, the characteristic multiplier (CM) or eigen value of Equation (3.33) that governs the stability of the system. This can be used to obtain the chatter frequency and stability limit for a given set of cutting conditions.

From Floquet theory, $\mathbf{q}_{i+1} = \mathbf{\Phi} \cdot \mathbf{q}_i$ where $\mathbf{q}$ is the state vector matrix and $\mathbf{\Phi}$ is the transition matrix. The eigenvalues of the Floquet transition matrix (Equation 3.33) at the stability limit lie on the unit circle as shown in Figure 3.6. When the characteristic multiplier or eigen value is not located in the unit circles, this indicates self-excitation vibration loss of linear stability with frequency from parametric excitation and characteristic. There are three cases

- Secondary Hopf-bifurcation. This kind of instability is the most common instability in milling, corresponding to the eigenvalue's becoming modulus larger than 1. At intervals of the tooth passing frequency, the chatter frequency exists at multiple values, using Equation 3.27.

$$f_{hopf} = \left\{ \pm f_c + k \frac{2\pi}{T} \right\} rad/s = \left\{ \pm \frac{\omega_c}{2\pi} + k \frac{\Omega}{60} \right\} Hz, \qquad k = \ldots, -1, 0, 1, \ldots \qquad \textbf{(3.34)}$$

  It is associated with structural mode instability and refers to high unstable regions in the stability lobe diagram, as experienced by Davies *et al.* [28] and Gabor *et al.* [131].

- Period doubling or flip bifurcation happens when eigenvalue is less than -1 and the frequencies are

$$f_{PD} = \left\{ \frac{\pi}{T} + k \frac{2\pi}{T} \right\} rad/s = \left\{ \left(\frac{1}{2} + k \right) \frac{\Omega}{60} \right\} Hz, \qquad k = \ldots, -1, 0, 1, \ldots \qquad \textbf{(3.35)}$$

  This kind of instability arises from the chatter frequency at harmonics of odd multiples of one half of the tooth passing frequency. This mostly happens in a low radial immersion for the cutting process [28].

- Period one (Saddle Node Bifurcation or cyclic fold) which can happen in turning is shown by Davies *at al.* [22] and in [29] for milling process. This bifurcation behaviour corresponds to a real eigenvalue higher than 1. The critical frequency becomes zero and the corresponding chatter becomes

$$f_{PO} = \left\{ 0 + k \frac{2\pi}{T} \right\} rad/s = \left\{ 0 + k \frac{\Omega}{60} \right\} Hz, \qquad k = \ldots, -1, 0, 1, \ldots \qquad \textbf{(3.36)}$$

Gabor *et al.* [131] discussed the multiple chatter frequencies which exist in the milling process. For hopf bifurcation, the displacement signal always contains frequencies at multiples of the tooth passing frequencies for both stable and unstable milling operations. However, for period doubling, the chatter frequency exists close to a modal frequency with side bands at the tooth passing frequency intervals.

Both techniques of TFEA and SDM can certainly demonstrate hopf bifurcations and period doubling and are characterised by plots of the eigenvalues in the complex plane. The analytical solution cannot accurately predict the period doubling-bifurcation regions [132]. The milling force with a large immersion milling has continuous and insufficient harmonics in the Fourier spectrum where the use of an average cutting force neglected the harmonic force in an analytical solution. In contrast, an intermittent milling coefficient in a low immersion milling causes the higher harmonics in the Fourier spectrum that contribute to the force signal. A repetitive cutter beating workpiece is modelled as impact where a strong force pulsation was relatively generated by a small and repetitive cutting to produce the vibratory energy in the Fourier spectrum. Additionally, amplitude modulation is also developed by the dynamic force for each of the cutter beating workpiece in the TFEA and SDM numerical modelling.

The present study will use the CM as the target for evaluating an objective function when applying the optimisation algorithm. For the current study, chatter optimisation problems of three-flute variable pitch and helix tools are introduced. Chatter is the main characteristic to be minimised by using the eigenvalues from SDM algorithms as objective functions. The performance at specific spindle speeds and depths of cut can be optimised by modifying the tool's variable helix and variable pitch. A multi-objective approach can be considered if the spindle speed and depth of cut are not constrained and productivity is considered as a second objective problem. These cases of the objective functions and constraints are then presented. Three approaches to this optimisation problem will be presented and explained in Chapter 6.

3.3 Optimisation Procedures

By combining with the analytical method for chatter stability prediction, the process of DE optimisation can be used to optimise tool/helix geometry. Figure 3.7 shows the sequence of operations, namely optimisation setting process, SDM process, objective function evaluation process and DE optimisation process. DE parameters are first set to create an initial population in the optimisation process. To search for the optimum values, DE requires the predicted values from the SDM stability analysis with consideration of the input variables (i.e. helix angles β_i and pitch angles ϕ_i). The fitness of each population member is evaluated in terms of the chatter stability; consequently, the DE process will strive to obtain tool geometry (helix and pitch angles) that

maximises the chatter stability. This process continues until the termination criteria are met.

For the current study, the procedure adopted is as follows:

1. First, DE selects the input parameter value together with optimisation parameters such as strategy, population size, number of generation (NP) crossover factor (CR) and scaling factor (SF).

2. Optimisation setting process parameters are read by the numerical algorithm process through the DE optimisation process as new input parameters.

3. Then analytical chatter stability will predict the output value to evaluate by the objective function evaluation process.

4. The output generated from this prediction is evaluated and compared with the next output.

5. These steps are repeated until the optimal input values of chatter stability are found.

6. This is an iterative process at the end of which the DE arrives at the optimum set of input parameters, i.e. variable helix βi and variable pitch ϕ_i, which generate optimum output.

In order to benchmark the DE optimisation method, a traditional gradient based optimisation method (SQP) was combined with the SDM to minimise chatter and optimise variable helix tool geometry.

3.4 Optimisation Example: Chatter Stability with Analytical Method

An optimisation procedure that combines chatter stability prediction and optimisation algorithm is now presented. The analytical stability algorithm developed by Budak and Altintas [19] is used to predict chatter stability. Details of the algorithm can be found in [19]. However, this example considers only a single degree of freedom dynamic milling model with the condition of milling tool, modal and cutting parameters as described in Table 3.1. The condition for lower radial immersion was taken from [19] that was applied for a uniform pitch and uniform helical angle cutting tool. This work is extended to consider optimising depth of cut. Although this problem is trivial, it serves to demonstrate that the optimisation will work for a simple problem, before extending to complex problem.

For the current optimisation problem, the chatter stability limit using the analytical method is shown in Figure 3.8a. DE and SQP algorithms are applied to optimise depth of cut *b* with chatter-free condition. Single objective functions are carried out based on the maximisation of axial depth of cut with specific range of axial depth of cut *b* and spindle speed Ω. The optimisation processes of the constraint condition of the chatter stability process are as follows:

Objective function

Maximise $$f(b) = b_{max} \tag{3.37}$$

Subject to constraints

Depth of cut $0 \leq b \leq 10$ (mm)

Chatter free $[b,\Omega] \leq b_{min}, \Omega_{min}$

Where the minimum axial depth of cut *b* and spindle speed Ω are given by the algorithm. Figure 3.8b shows the machining conditions for the current case specifically for certain axial depth of cut and spindle speed. This justifies that certain machines have their speed limitation and wide variation in materials' thickness.

The DE optimisation algorithm is used from parameter settings as illustrated in Table 3.2. In the current research, the DE source code written by Markus Buehren, available at Matlab Central [133], was used. The code is based on the DE algorithm of Storn and Price [134]. By combining with analytical method for chatter stability prediction, the processes on DE optimisation and chatter prediction are generated simultaneously. Figure 3.7 shows the sequence of operations to search for optimum evaluation values based on four processes. To search for optimum value, DE requires the predicted value from the numerical algorithm of the analytical method of stability analysis. The numerical method then uses DE to generate a new input in the DE optimisation process to estimate a new output value for objective function evaluation. Consequently, both DE and analytical chatter stability prediction should be linked through function control in the Matlab environment to exchange data with each other.

This is an interactive process, at the end of which the DE arrives at the optimum set of input parameters, i.e. axial depth of cut which generates optimum output. Instead of DE, SQP was used to compare the results. The general method of SQP to solve

constrained optimisation is stated in [72]. In this research, the SQP in the *Matlab Optimisation Toolbox* was used with the constrained minimisation function [135]. In Chapter 5, DE and SQP are described in detail.

A single objective to search for maximum *b* below 10 mm was predicted with DE and SQP. Figure 3.9 shows the performance of the two algorithms in searching for maximum depth of cut. In Figure 3.10, the SQP method shows the same optimal value as DE for maximising axial depth of cut. SQP using gradient-based optimisation method is sensitive to local optimal whereas for the current case the prediction is used just as a constraint and objective function. And SQP is always to search for maximum value of the constraint [72]. DE is a population-based algorithm needed to search for optimum values of the parameters within the design constraints. Therefore, both methods can be applied and succeed in searching for the same optimum value and they can be used for optimising the variable helical end milling tools as complex problem.

3.5 Summary

In this chapter, the theoretical background was presented for optimising variable helix and variable pitch milling tools. Using SDM for chatter stability prediction, the multiple time delays for variable helix and variable pitch tools can obviously be taken into account to calculate and evaluate CM as eigenvalue for the specific range of spindle speed and depth of cut.

Feasibility of the optimisation procedure was applied where DE and SQP were tested to search for depth of cut by an analytical method with periodic coefficient. Since a current optimisation methodology can be implemented for a simple case, further simulation to search for optimum variable helical/pitch tool geometry can be confidently applied. The problem is regarded towards designing an optimum variable helix/pitch tools for a specific machining condition with chatter suppression target.

In summary, this chapter has made an important initial step to exhibit the feasibility of the optimisation procedure for optimising depth of cut. Nevertheless, DE and SQP algorithms need to be described in detail to understand their theory for optimisation in Chapter 5. In addition, the optimum results were based on an analytical method with a periodic coefficient that limited uniform helix and uniform pitch. Therefore, the SDM chatter stability prediction will be integrated and combined with optimisation algorithms

to optimise variable helix and variable pitch and this will be concentrated on in Chapter 6.

From this chapter, it can be seen that the FRF or $G(j\omega)$ is a critical input parameters to the prediction or optimisation the chatter stability problem. In practice, this FRF can be influenced heavily by tool/machine operating conditions. Consequently, the next chapter assesses the feasibility of FRF measurement using non-contacting electromagnetic techniques.

Table 3.1 Modal and tool parameters for optimisation

Tool and cutting parameters	
Tool diameter d (mm)	19.05
Radial immersion RI (mm)	1.00
Tangential cutting coefficient K_t (MPa)	550
Normal cutting coefficient K_n (MPa)	200

Modal property in x-direction mode	
Natural frequency f_n (Hz)	169.3
Modal effective mass. m_m (kg)	6.5363
Damping Ratio ξ	0.0056

Table 3.2 DE parameters settings for example study

Parameter	Value
Strategy	7- DE/rand/1/bin
Number of Generation (NG)	50
Population (NP)	10*RP
Crossover factor (CR)	0.7
Scaling factor (SF)	0.6

Table 3.3 Optimum chatter stability optimisation results for single objective of maximum axial depth of cut

Method	DE	SQP
Spindle speed Ω (rev/min)	2200	2200
Axial depth of cut b (mm)	10	10
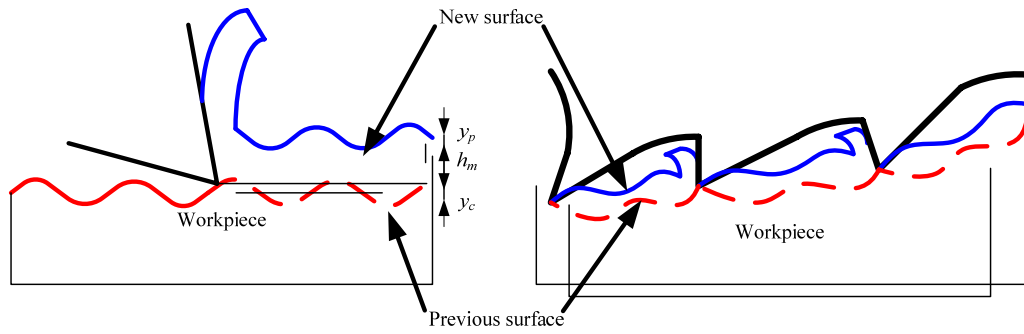
a) Turning b) Milling

Figure 3.1 Regeneration process during metal cutting
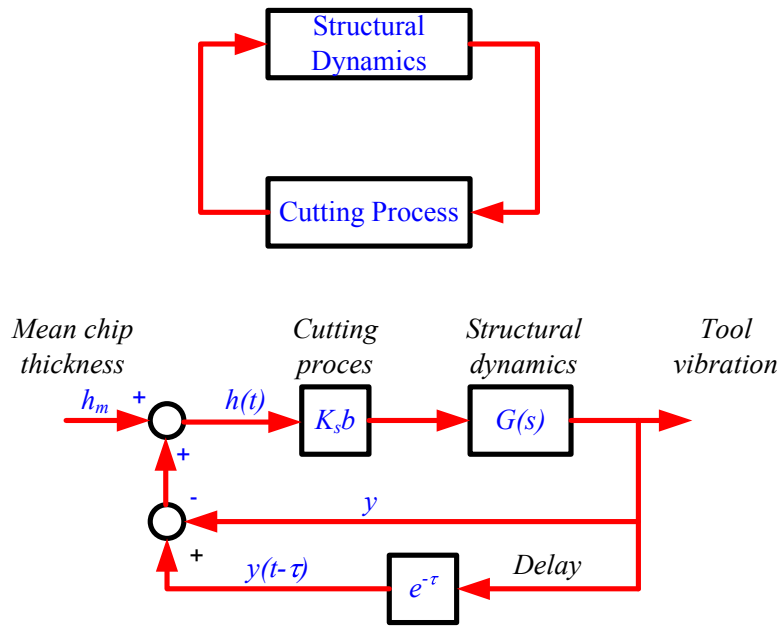
Figure 3.2 Chatter in closed loop by Merrit [22]
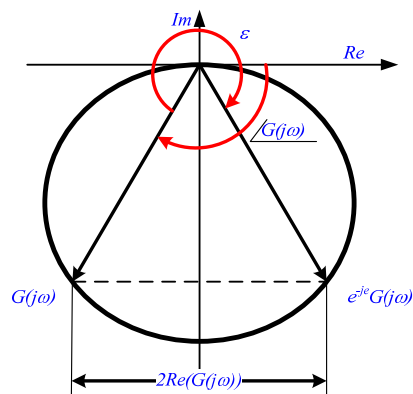
Figure 3.3 Transfer function of the system using Nyquist plot
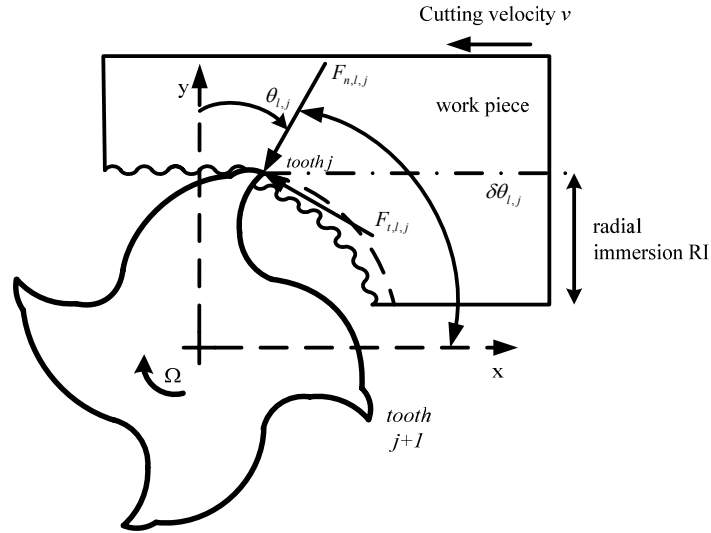
Figure 3.4 Forces on axial slice of a milling tool
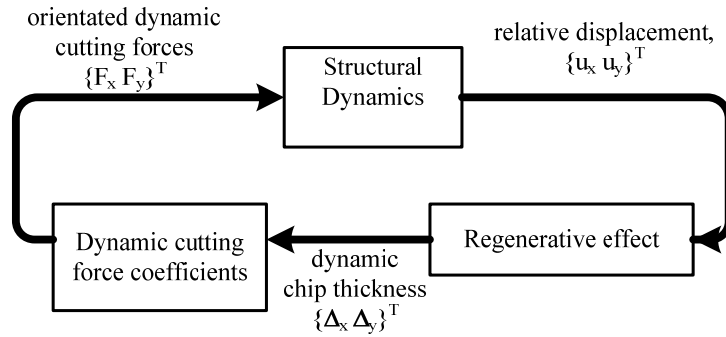
Figure 3.5 Schematic block diagram in state space form for regenerative chatter
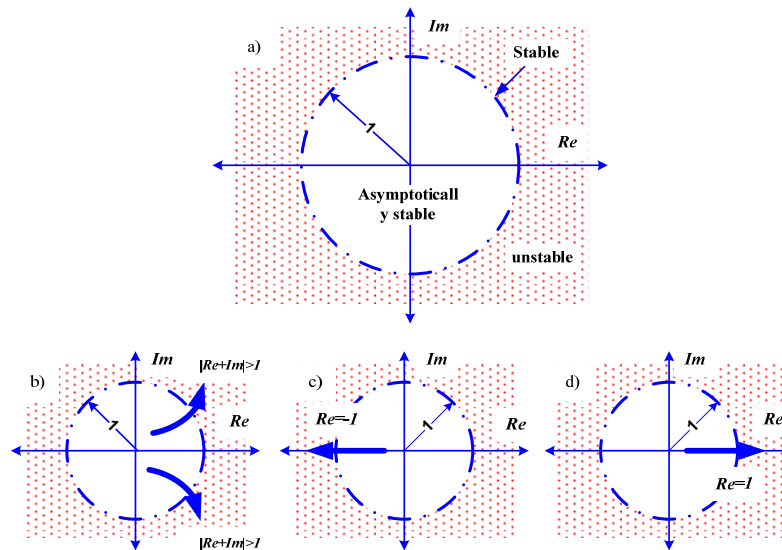
Figure 3.6 Stable and unstable behaviour in a) Stability of discrete map and unstable behaviour b) Hopf-bifurcation c) Period doubling d) Period-one
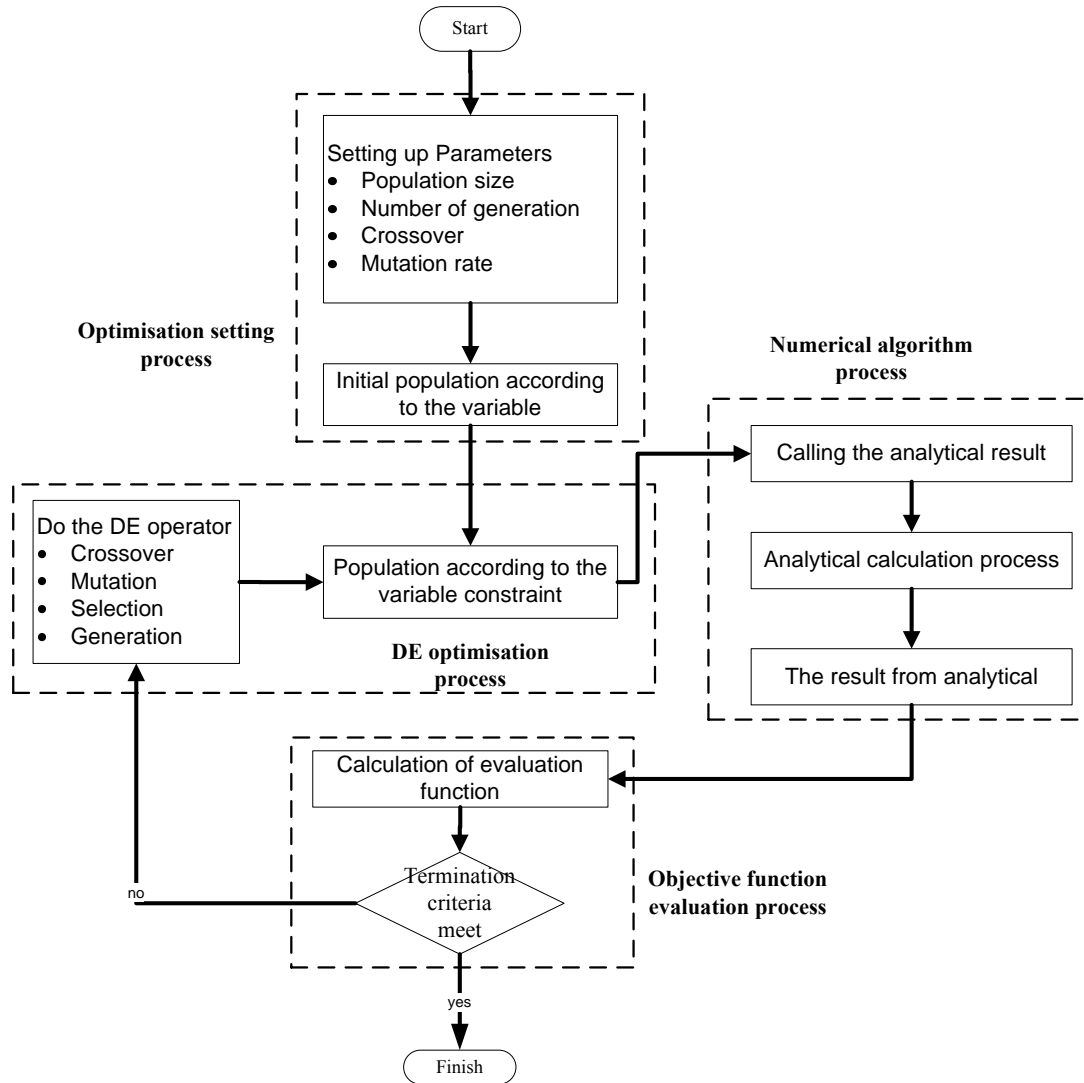
Figure 3.7 The sequence operation of optimisation with Differential Evolution

a) **Spindle speed (2000-8000 rev/min) and depth of cut (0-35 mm)**

b) **Spindle speed (2200-3200 rev/min) and depth of cut (0-10 mm)**
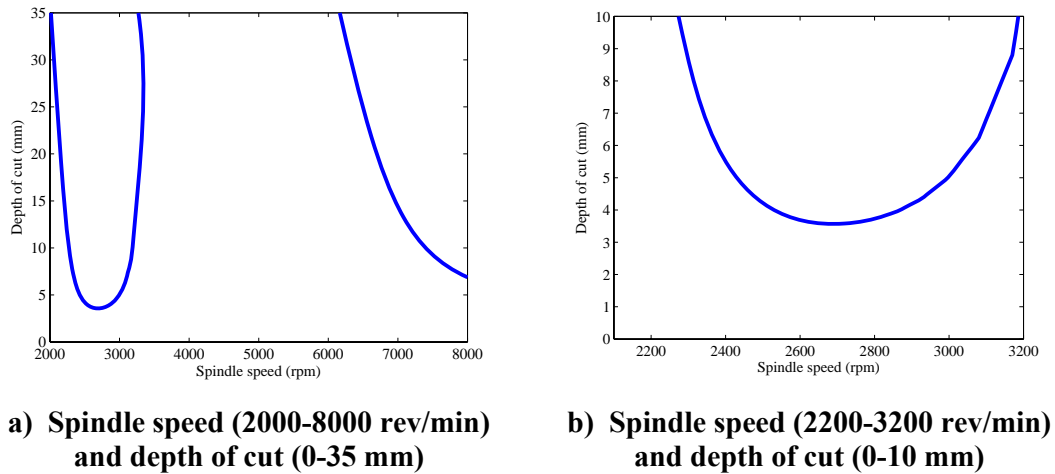
Figure 3.8 Stability lobes diagram using analytical with periodic coefficient method
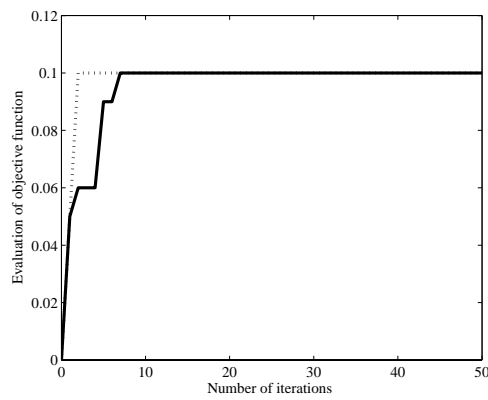
Figure 3.9 Performance of optimization between DE (——) and SQP (---) in maximising depth of cut.
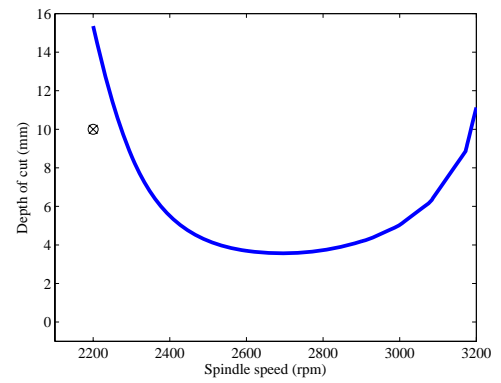
Figure 3.10 Optimal depth of cut result of analytical with periodic coefficient method using DE ('o') and SQP ('×').Stability limit is indicated by (——).

CHAPTER 4

PRELIMINARY EXPERIMENTS ON NON-CONTACTING FRF ESTIMATION

4.1 Introduction

In general, the frequency response function (FRF) of the structurally compliant system is needed in order to determine chatter-stability as discussed in Chapter 3. Traditionally, an impact hammer is used to excite the system at the tool tip and the response is measured with a co-located accelerometer. However, this configuration has a number of disadvantages, such as:

- The cutting edge of the tool can easily be damaged by the hammer strike.

- On large machines, the test engineer must work inside the machine itself, which can entail exposure to a health and safety hazard.

- The tool cannot rotate during the test. The FRF during rotation could differ due to gyroscopic forces and bearing loads [136]. Furthermore, some computer numerical control (CNC) machines automatically modify the tool drawbar force as a function of spindle speed, which may influence the tool's FRF.

- In practice, the mechanical interfaces in the system lead to some nonlinearity in the FRF. During machining, the tool load differs substantially from the forces induced by an impact hammer, so these nonlinearities cannot be considered.

To date, non-contact excitation systems have been developed by Snyder *et al.* [137], Esterling *et al.* [133], Kiefer [138], Tatar *et al.* [139], Rantatalo *et al.* [140] and Sodano [141]. Snyder *et al.* [137] initially created a device for stable speed prediction, using a fixed electromagnetic field. Esterling *et al.* [142] obtained FRF data using a compact electromagnet. Tatar *et al.* [139] and Rantatalo *et al.* [140] used laser Doppler vibrometry (LDV), an active magnetic bearing and capacitive sensors to measure dynamic vibration of the cutting with an optically smooth surface at different cutting speeds. The mass loading and added stiffness in a traditional impact hammer can be eliminated by introducing a non-contact eddy current excitation method to preserve the structure mode shape from magnetic actuation [141]. Keifer [138] integrated the electromagnet with a receptance coupling substructure to predict chatter. The

electromagnet demonstrated easy and accurate dynamic characteristic of cutting tool or FRF.

However, this earlier work has in general not considered the amplitude dependency of the tool FRF. Using a non-contacting electromagnet allows this amplitude-dependency to be investigated experimentally. This will be the focus of the present chapter. The chapter is organised as follows. The experimental method is first described. The results of cutting tool FRF from the impact hammer are shown and compared to non-contacting excitation systems. Following a discussion of the amplitude dependent excitation behaviour, conclusions are drawn concerning the suitability of the device to measure milling tool chatter stability. This chapter formed a conference paper and an abstract is given in Appendix A.I.

4.2   Experimental Method

The experimental approach involved three steps. First, impact hammer testing was applied to measure cutting tool FRF. Then, the magnetic force excitation was applied to measure the cutting tool in static condition. Signal processing was used to observe the FRF response of velocity and force. Finally, the electromagnetic excitation was applied with various excitation amplitudes.

The experimental apparatus consisted of a Siglab 20-22A two channel data acquisition system. For impact testing, a normal force was applied at the tool tip using a PCB 086C01 hammer with vinyl tip. The acceleration response was captured by a PCB 352C16 accelerometer placed opposite the hammer impact point.

The force excitation by the impact hammer can be replaced by a magnetic force generation system. A coil of length 205 mm was used with 224 turns surrounding an E type laminated ferromagnetic core, as shown in Figure 4.1a. This can maintain a maximum current of 20 A at frequencies up to 1000 Hz and generate 100 N peak force for 1 A r.m.s. current supplied. The electromagnet was driven by a Techron 7700 series power supply amplifier which could deliver instantaneous peak currents at 180 A and voltages up to 146 V. Figure 4.1b shows an experimental configuration with a 6- flute

high speed steel ball nose cutting tool. The SigLab system supplied a voltage signal to the Techtron amplifier configured in current-control mode to generate the magnetic field. The current with a burst chirp signal from 0 to 1000 Hz is suitable to excite the structure. The FRF was obtained using a minimum of five averages.

Two signal processing configurations were initially investigated. In the first case, the current in the electromagnet was measured and the FRF estimated between this current and the resulting tool motion was obtained. In the second case, the electromagnetic force was measured using the dynamometer (force transducer) so the FRF G($j\omega$) could be estimated.

4.3   FRF Amplitude Dependent Measurement Results

To begin, the FRF of the tool was obtained using a modal hammer and co-located accelerometer. This is shown in Figure 4.2. The tool is expected to have a closed pair of dominant bending modes occurring at 635 and 655 Hz. In Figure 4.3, the mobility FRF is shown, where the system input was the measured current in the electromagnet, whilst the system output was the velocity measured by the laser vibrometer. Two dominant frequencies can be observed in the FRF, which agree with the response obtained using the modal hammer. It should be noted that the electromagnet applies a distributed load to the tool, rather than a point load on the tool tip. Consequently, the point FRF at the tool tip can not be directly determined but the natural frequencies of the structure can at least be observed.

This result is now repeated using the electromagnet and laser vibrometer under various excitation amplitudes. The results shown in Figure 4.4 were obtained by applying a chirp signal of a given rms amplitude with a dc offset. This dc offset ensured that the current signal was always positive. As the amplitude of the dc offset voltage is reduced (shown by the arrows in Figure 4.4), the FRF decreases in magnitude. Furthermore, the location of the resonant frequencies is seen to increase. This trend is observed for all four values of the chirp signal's rms amplitude (Figure 4.4a-d). However, at low chirp r.m.s. amplitudes (Figure 4.4a) the influence of signal noise can be more clearly observed.

The amplitude-dependency observed in Figure 4.4 can be attributed to two factors: the nonlinear relationship between electromagnetic current and excitation force and the nonlinear relationship between excitation force and resulting tool motion. This latter scenario is of greater interest, since this nonlinearity can not normally be observed using a modal hammer.

In Figure 4.5, this experiment is repeated for the case where the force measurement from the dynamometer was considered to be the system input. These FRFs clearly include resonant frequencies (particularly above 700 Hz) that were not present in the impact hammer FRF (Figure 4.5a,b) or in the current-velocity FRF. The additional resonant frequencies can be attributed to the force measurement substructure, i.e. the mass of the electromagnet mounted on the slightly compliant force measurement platform. Strong amplitude dependency can be observed in these additional resonances. However, the natural frequency of the tool can still be observed in the region of 625 Hz (Figure 4.5b-d). As for the current-velocity FRF, the resonant frequency increases with decreasing excitation amplitude and the FRF magnitude decreases.

To further illustrate that the electromagnet can be used to induce amplitude-dependent behaviour, a series of step-response tests were made. The electromagnetic current was switched between high and low constant currents, as indicated by the current-time measurement shown in Figure 4.6a. The resulting tool velocity is shown in Figure 4.6b-e and it can be seen that the vibration decay depends strongly on the magnitude of the electromagnetic current or preload on the tool.

Some preliminary experiments on a rotating structure are shown in Figure 4.7. Here, a steel rod was mounted in a non-CNC milling machine and rotated at 2000 rev/min. The rod was chosen because it had a lower natural frequency than the tool, well below the natural frequencies of the force measurement substructure.   The same amplitude dependent behaviour can be observed. The poor quality of the frequency response function can be attributed to tool runout effects (i.e. eccentricity) and slack in the machine bearings. Although the laser vibrometer signal was degraded by the tool rotation, it is felt that better data would be obtained on a modern CNC milling machine with a better quality spindle system. Furthermore, these tests did not use a dc offset for

the chirp excitation. Since the electromagnet can only induce attractive forces, the resulting measurement force would not have been a smooth chirp signal, which would also degrade the FRF estimate.

To demonstrate how FRF estimation affects the sensitivity of chatter stability when amplitude dependency is applied for certain cutting tools, Figures 4.7 and 4.8 show the stability prediction of regular and optimal tools with 5 percent changing of the natural frequency. It can be seen that when the natural frequency of the tools increased within 5 percent, the chatter stability was also modified from a lower to a higher spindle speed. This is true for both the regular and optimum tools where the stability lobes also slightly increase in the function of depth of cut. Consequently, the FRF measurement is generally significant to predict the stable, unstable or optimal cutting region when predicting the chatter stability. Moreover, FRF estimation is more complex when considering amplitude dependency and spindle speed dependency to predict theoretical chatter stability.

In practice, it is therefore important to obtain an accurate estimate of the FRF of the machining structure. This can be difficult due to amplitude dependency and other effects, as shown in preliminary test results presented in this chapter. A further complication that arises for variable helix tools is that the tool helix angle (which in being optimised) will influence the tool FRF. This makes the optimisation problem considerably more complex.

In order to circumvent these issues, the reminder of this thesis will focus on scenarios where the FRF of the tool/workpiece structure is assumed to be tune and amplitude independent, and independent of the tool helix angle. Practically, this occurs with a single-degree of freedom flexible workpiece that is considerably more compliant than the tool, spindle, or machine structure.

4.4 Summary

This chapter has focused on alternative techniques for extracting the frequency response function of rotating milling tools for the purpose of regenerative chatter prediction. It has been argued that the traditional approach (i.e. a modal impact hammer and

accelerometer) suffers from a number of drawbacks. Although previous researchers have suggested electromagnetic techniques as an alternative, this research has not normally used the electromagnet to investigate amplitude dependent behaviour in the system. This is probably because a high electromagnetic force requires a large amplifier and results in a heavy actuator, making it difficult to measure the electromagnetic force accurately.

In the present chapter, a high performance amplifier was used so that amplitude dependency of the structure could be investigated. However, it was found that the difficulties in measuring the resulting electromagnetic force meant that high quality frequency response function measurements were difficult to achieve. Despite this, it was shown that the device could be used to investigate qualitatively the changes in resonant frequencies with excitation magnitude for both stationary and rotating systems. From a milling chatter perspective, this means that the influence of tool preload during milling can be considered when predicting the chatter stability boundary.

Up to now, the study has explored the effect of FRF to predict chatter stability for variable helix and variable pitch (optimum tool) in flexible tool condition. It can be seen that the modal parameters of flexible tool are more complex and easily change when optimising the variable helix and variable pitch geometry. However, the current case will consider flexible workpiece not flexible tool to avoid this problem. Consequently, the chatter stability is not affected by modal parameters' change when optimising a variable helix and variable pitch tool using a combination of semi-discretisation method and optimisation algorithms (DE and SQP). In the next chapter, the optimisation algorithms of DE and SQP with their numerical examples' solutions are discussed. Then, Chapter 6 presents and discusses the results of optimisation of variable helix for milling tools.
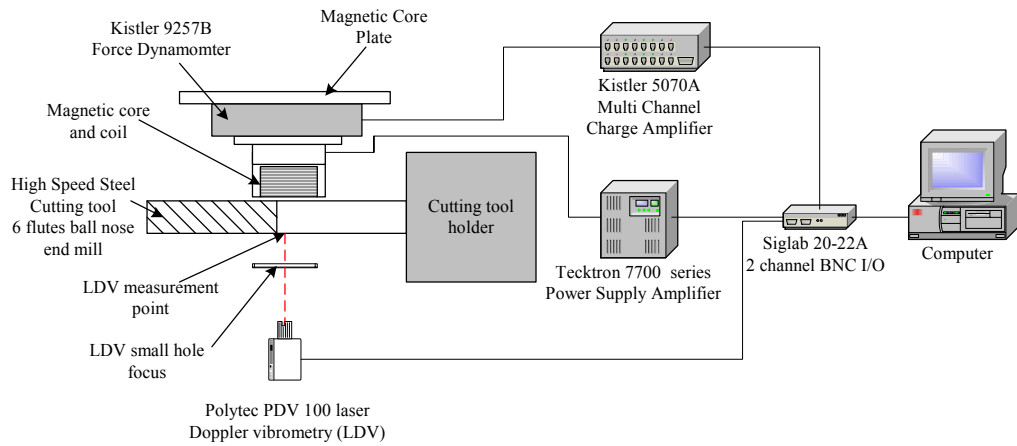
a) Schematic diagram
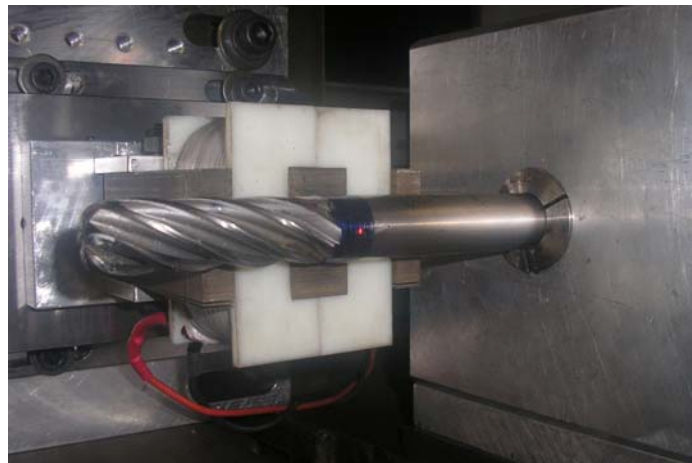
b) Electromagnet and LDV beam

Figure 4.1 Experimental setting
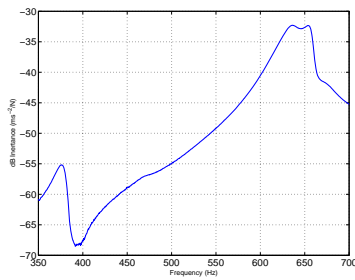
Figure 4.2 FRF inertance (impact hammer - accelerometer)
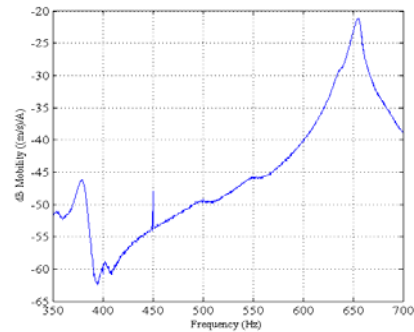
Figure 4.3 FRF mobility (electromagnet - laser vibrometer)

a) 2 A

b) 6 A
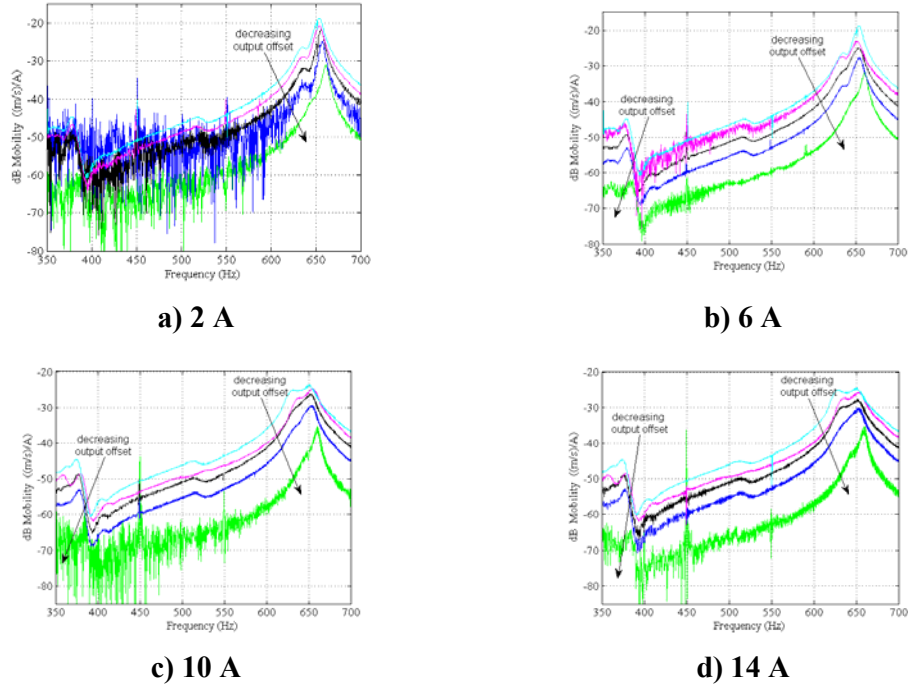
c) 10 A

d) 14 A

Figure 4.4 Current FRF with output offset increasing at range 0 V to 8 V a) 2 A b) 6 A, c) 10 A, d) 14 A

a) 2 A

b) 6 A
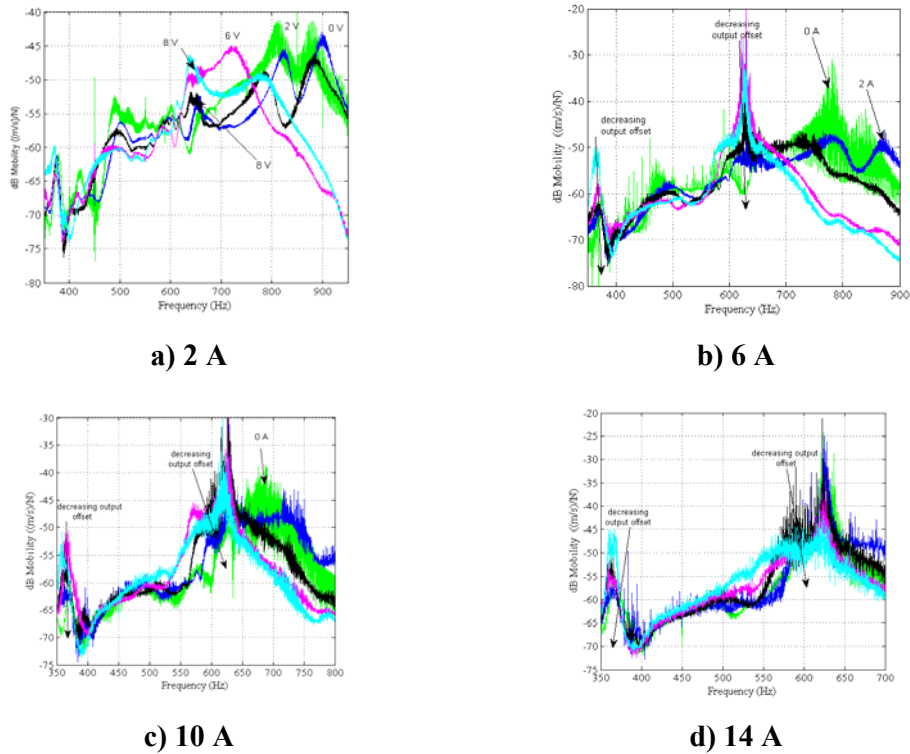
c) 10 A

d) 14 A

Figure 4.5 Force dynamometer FRF with output offset increasing at range 0 V to 8 V a) 2 A, b) 6 A, c) 10 A, d) 14 A
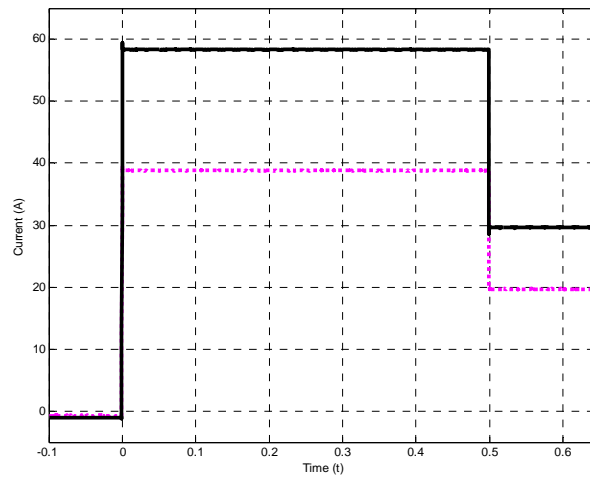
a) Current excitation signal
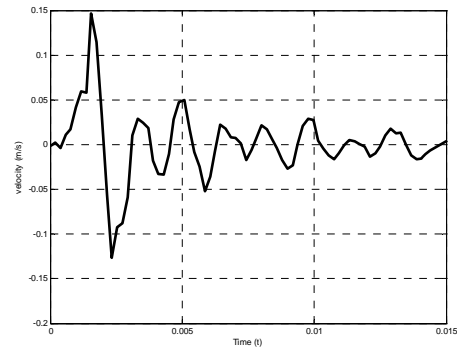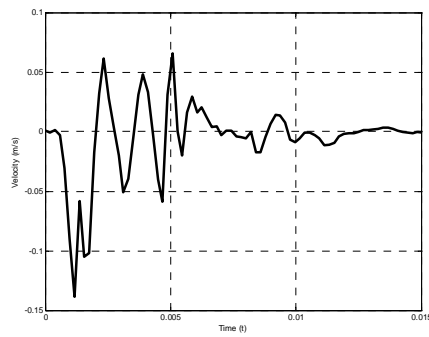
b) step response, 0 A to 38 A excitation

c) step response, 38 A to 20 A excitation
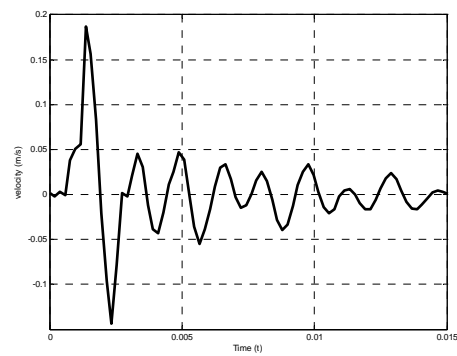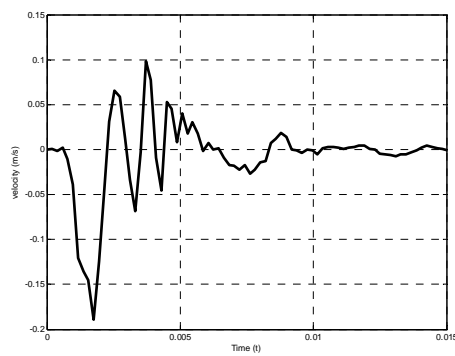
d) step response, 0 A to 58 A excitation

e) step response, 58 A to 30 A excitation

Figure 4.6 Square wave current excitation and velocity response from LDV
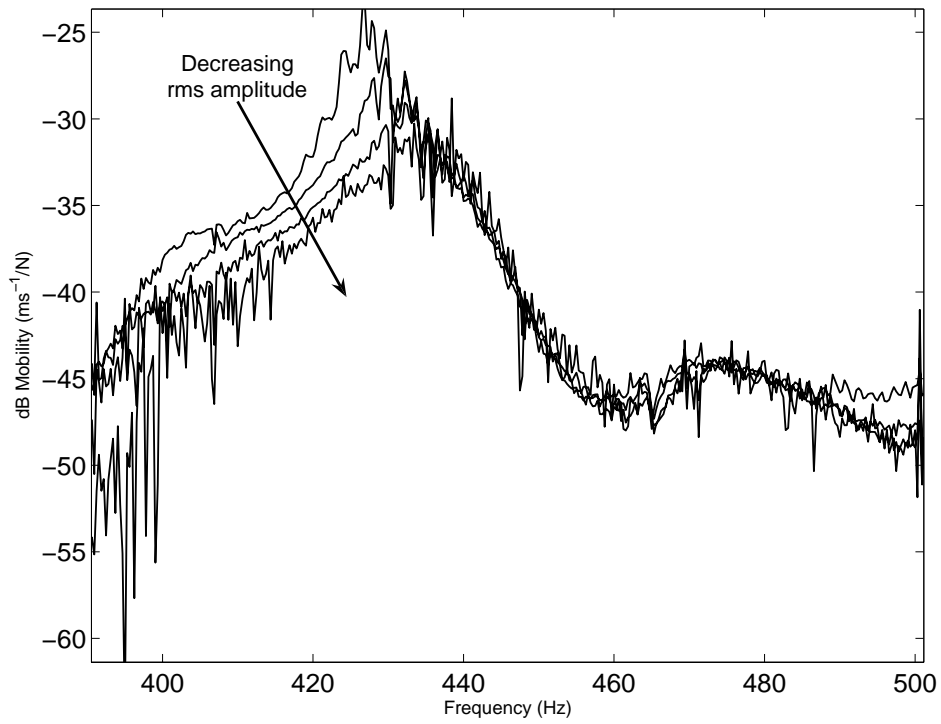
Figure 4.7 FRF data (dynamometer force measurement, electromagnetic excitation) from rotating bar in milling machine running at 2000 rev/min. Electromagnetic current excitation-chirp signal with r.m.s. magnitude 4, 6, 8 and 10 A r.m.s.
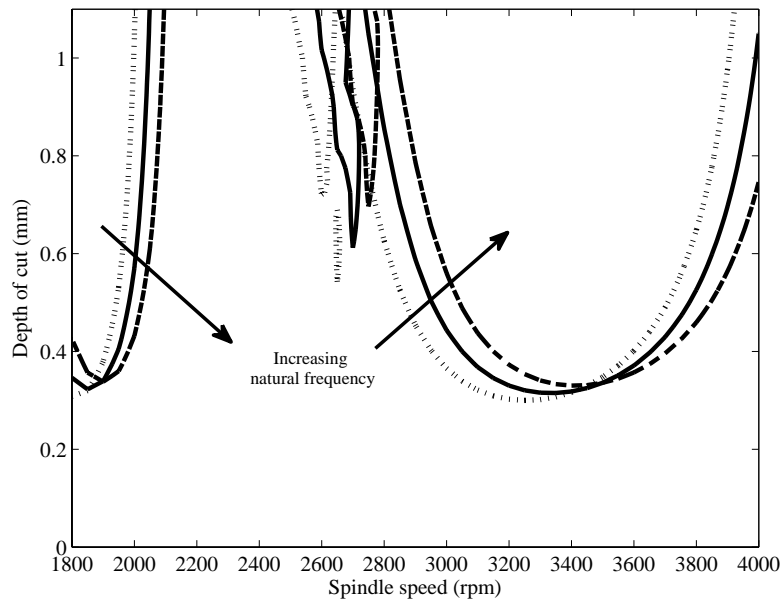
Figure 4.8 Stability diagram with natural frequency increasing for regular tool
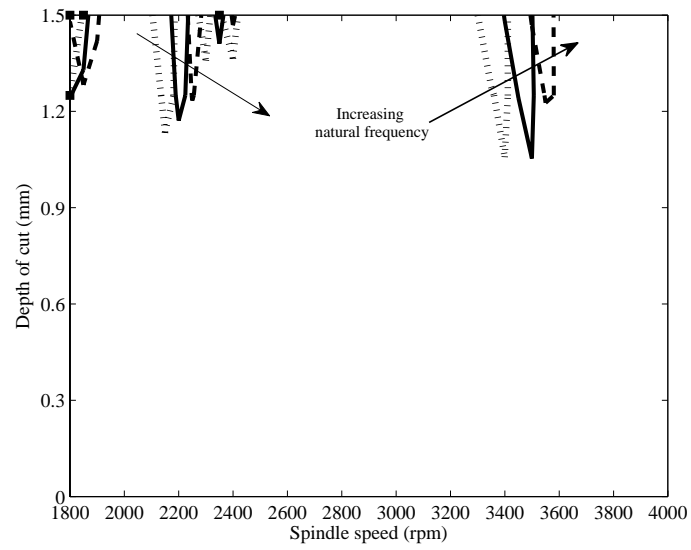
Figure 4.9 Stability diagram with natural frequency increasing for optimum (variable helix/pitch) tool

CHAPTER 5

NUMERICAL OPTIMISATION: THEORY

5.1 Introduction

As discussed in Chapters 2 and 3, Differential Evolution (DE) and Sequential Quadratic Programming (SQP) algorithms can be used to mitigate chatter by optimising variable helix and variable pitch angles of the tools. A theoretical background of the SDM algorithm was explained in detail in Chapter 3. However, the DE and SQP algorithms were not combined with SDM numerical chatter stability. Before combining with SDM, theoretical backgrounds of both optimisation algorithms are properly explained in this chapter.

The optimisation approach focuses on modifying the milling tool's geometry, namely variable helix and variable pitch angles, through optimisation. This is unlike previous research [5, 11, 12] where only the pitch angle was optimised and modified. To execute the optimisation procedures, two algorithms are used: DE and SQP. The DE algorithm is based upon that developed by Markus [133] and SQP used a minmax function as in the Matlab Optimisation Toolbox [135]. Both DE and SQP algorithms are used to allow verification and benchmarks of the results. Before application to chatter problems, DE and SQP are applied to famous mathematical functions, involving both single and multi-objective optimisation. The Epsilon constraint method is applied for multi-objective optimisation because it is appropriate for both DE and SQP algorithms. Selected DE examples for single and multi-objective optimisation are used to explain the methodology.

This chapter covers the methods used to optimise variable helix end milling tools. First, the DE and SQP as optimisation algorithms are described with examples for solving mathematical problems for single objective optimisation. Second, applications in multi-objective using current DE and SQP are discussed. Mathematical functions are used to verify the capability of two algorithms to solve multi-objective optimisation with the epsilon-constraint method.

5.2   Differential Evolution

Various Evaluation Algorithm strategies have been developed, such as Genetic Algorithm, Evolutionary Programming and Evolution Strategy. Differential Evolution was introduced by Storn and Price in 1996 [134]. Differential Evolution based on stochastic or non-deterministic approaches for solving polynomial fitting problems. Differential Evolution is developed from an improved Genetic Algorithm with different strategies for faster optimisation. This is similar to other Evaluation Algorithm in which mutation plays the key role with real valued parameters to search for the global optimum. A basic idea in Differential Evolution is that of adapting the search during the evolution process. Differential Evolution advantages are simple structure, ease of use, speed and robustness. In addition, Differential Evolution has been successfully applied in various optimisation applications [82] such as heat exchangers, robotic manipulator design, neural network training, turbo machinery design, production and scheduling, electric motor design, engine and wheel mount identification, diesel engine combustion and machining optimisation. In machining applications, Saikumar and Shunmugan [134] applied Differential Evolution to select the best cutting speed, feedrate and depth of cut to achieve optimum surface finish, while Krishna [84] applied Differential Evolution in a grinding process to search for suitable parameters in minimising surface grinding. Before Differential Evolution can be applied in machining problems, the Differential Evolution algorithms will be described and used to solve numerical case studies.

Differential Evolution can solve objective functions that are non-differentiable, non-linear, noisy, flat and multi-dimension, with multi-local minima. Such functions are difficult to solve analytically. This algorithm begins by using initial samples at multiple random chosen initial points. With simple algorithms, Differential Evolution can search for the optimal condition very fast with minimal control parameters such as mutation, crossover, selection and population. The concept is evolved from Genetic Algorithm with a layer population and a special evolutionary strategy of self-adaptive mutation. Instead of a binary encoded population as for a Genetic Algorithm, Differential Evolution deals with a real coded population with its own processes of mutation and crossover. The mutation process is created from three randomly selected population members, using the vector difference between individuals [51]. Although it uses the same evaluation as other Evaluation Algorithm during the crossover process,

Differential Evolution applied crossover between any individual population member. Moreover, the population has an equal opportunity to survive in the next generation based on its fitness value.

Differential Evolution can be started by specifying algorithm real parameters (RP), population size (NP), number of generation (NG) and parameters vector x_i which can be set as follows:

$$x_{i,g} = \left[x_{1,g}, x_{2,g}, x_{3,g}, \cdots x_{NG-1,g} \right] \quad g = 0,1,\ldots,NG \tag{5.1}$$

The population will be initialised and will then continue assessing the objective function before the termination criteria will be considered. It is suggested that the range of NP is between 5 and 10 but the minimum is 4, due to the crossover process to be described later. At termination criteria stage, the algorithm decides either to accept or reject the population. This process must proceed to the next process if the objective function value is rejected for improvement of the next population. Figure 5.1 shows the population improvement processes, including mutation, crossover, objective function assessment and selection. This takes several generations before the global optimal solution is achieved.

5.2.1 Initialisation

The limits of search parameters are always specified before the population is initialised. For instance, the lowest point can be defined as lower bound $x_{i,l}$, while the highest point is known as upper bound $x_{i,u}$. After that, a randomised generator $rand_i$ and H as a factor assign an initialisation value for every vector with the prescribed range in the limit as follows:

$$x_{i,g} = x_{i,l} + H.rand_j(0,1)(x_{i,l} - x_{i,u}) \tag{5.2}$$

The initialisation of the random number generator produces real values as DE treats all variables as floating values in the range (0,1), not considering their type internally. Randomisation of the vectors in DE is greatly affected to overcome a premature population that converged when using a low population [82].

5.2.2 Mutation

Mutation is a process to mutate and recombine the initialised population to create a donor vector with the same size as the initial population. This concept borrowed from

Neader and Mead's idea to use information from the vector to change search space [82]. The donor vector is produced from the initialisation vector and mutant vector $v_{i,g}$ that expands the search space $x_{i,g}$ into three vectors as $x_{r1,g}$, $x_{r2,g}$ and $x_{r3,g}$ to be

$$v_{i,g} = x_{r1,g} + SF\left(x_{r2,g} - x_{r3,g}\right) \tag{5.3}$$

Each of the vectors is randomly selected per mutant. Figure 5.2 describes how to produce the mutation vector. Scaling factor $(SF) \in (0,1+)$ is a positive real number to control the rate at which the population evolves. It is suggested that SF effective value is 0.5 as initial start with effective range 0.4 to 1 [82].

5.2.3 Crossover

Trial vector $u_{i,g}$, known as child vector, is a result of its parent vectors, either mutation vector $v_{i,g}$ or target vector $x_{i,g}$. Uniform crossover will inherit equal probability parameter values from parents while non-uniform crossover often takes parameters from one parent rather than the other. Particularly, uniform crossover will decide which chromosome will be given to $u_{i,g}$ either from $v_{i,g}$ or $x_{i,g}$ to crossover. A random number is used to generate $u_{i,g}$ and crossover factor (CR) definition will control the chromosomes. In Figure 5.3, by evaluating CR to the output of the randomly generated number, uniform crossover decides the two parent vectors to contribute to each chromosome of $u_{i,g}$. $u_{i,g}$ is directly received from the $x_{i,g}$ if the random number is greater than CR or else the parameter is taken from $v_{i,g}$. This can be illustrated as

$$x_{i,g} = \left(x_{1,g}, x_{2,g}, x_{3,g}, \cdots x_{Np,g-1}\right) \tag{5.4}$$

$$v_{i,g} = \left(v_{1,g}, v_{2,g}, v_{3,g}, \cdots v_{Np,g}\right) \tag{5.5}$$

$$u_{i,g} = \begin{cases} v_{i,g} \cdot if \cdot rand_i \leq CR \cdot or \cdot i = I_{rand} \\ x_{i,g} \cdot if \cdot rand_i > CR \cdot or \cdot i \neq I_{rand} \end{cases} \tag{5.6}$$

$$u_{i,g} = \left(x_{1,g}, v_{2,g}, x_{3,g}, , \cdots u_{Np,g}\right) \tag{5.7}$$

Crossover factor, CR $\in$ [0, 1], is a positive real number that controlled the crossover process. The CR value 0.5 is recommended for adequate choice, while 0.1 is too slow and very risky [82]. This gives an offer to both parent and child to compete in the selection process. However, for a quick solution, value 0.9 to 1 is suitable CR .

5.2.4 Selection

Selection is a process to select a point of reference between $x_{i,g}$ and $u_{i,g}$. This will determine whether either $x_{i,g}$ or $u_{i,g}$ will be preferred, depending on objective function value that needs to proceed to the next generation. DE integrates more tightly crossover and selection by comparing between each $u_{i,g}$ and $x_{i,g}$ that takes over parameters. In both processes of crossover and selection, the parents as $x_{i,g}$ can always compete with their own offspring as $u_{i,g}$ for the next generation. As compared to GA, competition only happens during evaluation before mutation and crossover, to produce a new population. The children replace the parents with some probability regardless of their fitness [143]. However, in DE, there is an equal opportunity for children and parents which depends on their fitness value as follows:

$$x_{i,g+1} = \begin{cases} u_{i,g} \cdot if \cdot f(u_{i,g}) \le (x_{i,g}) \\ x_{i,g} \cdot otherwise \end{cases} \tag{5.8}$$

5.2.5 Generation

The process of evolving mutation, crossover and selection through generations or new population is repeated until the optimum solution is achieved. Similarly, when the population converged with only a few function solutions evaluated, the criterion is fully satisfied. Figure 5.4 explains diagrammatically the whole process of generating from the old population to the new population. A large population number could reach global optimum but increase the complexity and computation time [82, 143].

5.2.6 DE Strategies and algorithm

The crucial idea behind DE is a scheme for generating $u_{i,g}$ by adding the weighted difference between two population vectors into a third vector. This is known as the DE strategy. The key parameters in controlling DE are the NP, CR and SF. Price *et al.* [82] initially suggested a single strategy, then six strategies and recently added another four strategies. They also suggest that the robustness of DE depends on SF and CR values. There are 10 suggested strategies with the nomenclature *DE/x/y/z*.

- Here the first column refers to DE as an optimisation algorithm

- The second refers to the vector to be perturbed, either random *rand,* the best *best* or rand and the best, *rand-best*

- The third is the difference in vectors considered for perturbation of x in the mutation process

- The last is type of crossover, either exponential *exp* or binomial *bin*.

Strategy-1 has been explained earlier during the mutation process and all 10 strategies are as follows:

1c DE/rand/1/exp, $\qquad$ $v_{i,g} = x_{r1,g} + SF\left(x_{r2,g} - x_{r3,g}\right)$ $\qquad\qquad$ **(5.9)**

2 DE/best/1/exp, $\qquad$ $v_{i,g} = x_{best,g} + SF\left(x_{r2,g} - x_{r3,g}\right)$ $\qquad\qquad$ **(5.10)**

3 DE/rand-to-best/1/exp, $\quad$ $v_{i,g} = x_{i,g} + \vartheta\left(x_{best,g} - x_{i,g}\right) + SF\left(x_{r1,g} - x_{r2,g}\right)$ $\quad$ **(5.11)**

4 DE/best/2/exp, $\qquad$ $v_{i,g} = x_{best,g} + SF\left(x_{r1,g} + x_{r2,g} - x_{r3,g} - x_{r4,g}\right)$ $\quad$ **(5.12)**

5 DE/rand/2/exp, $\qquad$ $v_{i,g} = x_{r5,g} + SF\left(x_{r1,g} + x_{r2,g} - x_{r3,g} - x_{r4,g}\right)$ $\quad$ **(5.13)**

6 DE/best/1/bin, $\qquad$ $v_{i,g} = x_{best,g} + SF\left(x_{r2,g} - x_{r3,g}\right)$ $\qquad\qquad$ **(5.14)**

7 DE/rand/1/bin, $\qquad$ $v_{i,g} = x_{r1,g} + SF\left(x_{r2,g} - x_{r3,g}\right)$ $\qquad\qquad$ **(5.15)**

8 DE/rand-to-best/2/bin, $\quad$ $v_{i,g} = x_{i,g} + \vartheta\left(x_{best,g} - x_{i,g}\right) + SF\left(x_{r1,g} - x_{r2,g}\right)$ $\quad$ **(5.16)**

9 DE/best/2/bin, $\qquad$ $v_{i,g} = x_{best,g} + SF\left(x_{r1,g} + x_{r2,g} - x_{r3,g} - x_{r4,g}\right)$ $\quad$ **(5.17)**

10 DE/rand/2/bin, $\qquad$ $v_{i,g} = x_{r5,g} + SF\left(x_{r1,g} + x_{r2,g} - x_{r3,g} - x_{r4,g}\right)$ $\quad$ **(5.18)**

The exponential and binomial crossovers are described as follows. The Exponential crossover performs single loop on the real parameter variable until crossover factor bound. At first time, this will randomly pick up between 0 and 1 beyond the crossover factor value, so there is no crossover and the current real parameter variables remain. In binomial crossover, however, the crossover randomly picked between 0 and 1 within the crossover factor value is performed on each of the real parameter variables. The last variable always comes from the noisy vector to ensure different $x_{i,g}$. Therefore, both the exponential and binomial crossovers yield similar results for very high crossover factor value.

A strategy is selected by trial and error and depends on the problems. A strategy that works successfully for a specific problem may not work well when applied to a different problem [82, 143]. However, strategy 7 (DE/rand/1/bin) is the most successful and widely used in many applications [83, 84, 134]. In the current research, the DE source code written by Markus Buehren and available at Matlab Central [133] was used. The code is based on the DE algorithm of Storn and Price [134].

The algorithm of DE is given as follows:

1. Choose strategy.
2. Initialise the independent parameters' number of dimension, NP, CR, SF and maximum generation.
3. Initialise randomly all the dimension with the given upper and lower bound ($x_{j,L}$ and $x_{j,u}$).
4. Evaluate each vector for its function value.
5. Determine the vector with the optimum function value.
6. For each $x_{i,g}$, select three vectors randomly from the current population from other than $x_{i,g}$ to perform mutation.
7. Create $u_{i,g}$ for each $x_{i,g}$ by the crossover with its noisy vector.
8. After the mutation and crossover, the vectors are checked to ensure they are in the bound range. This process will terminate if the vectors are out of bounds.
9. Make selection for each $x_{i,g}$ by comparing its function evaluation with $u_{i,g}$ produced from crossover process. Selected and random $x_{i,g}$ from current population compete with $u_{i,g}$ based on evaluation value. For the next generation, select optimal function value for next generation $x_{i,g+1}$.
10. Repeat 4-9 if termination criteria not met.
11. Print results.

The flow process of DE is presented in Figure 5.1 and the detailed processes are shown in Figure 5.4.

5.3 Sequential Quadratic Programming

In order to verify the DE result, SQP will be applied. SQP is widely used in machining applications [93, 94, 112, 144] and can solve nonlinear problems and search for local

optima. The method has been successful in various fields such as structures, dynamics, materials, robotics, heat exchangers control systems and manufacturing processes, production and design. In machining problems, Kurdi *et al.* [144] compared SQP with Particle Swarm Optimisation for optimising the surface location error and material removal rate (MRR). SQP results showed as better than Particle Swarm Optimisation. In addition, SQP has been applied by Yeo *et al.* [112] in optimising a machinability data system, while Chua *et al.* [93] minimised the production time of the multipass turning process and Stori *et al.* [94] optimised process parameters to maximise material removal rate.

The main idea of SQP is to obtain a search direction from a quadratic program solution, together with its constraints. Consider the problem:

$$\text{Minimise} \quad f(x) \tag{5.19}$$

$$\text{Subject to} \quad \begin{aligned} H_1(x) &= 0 \\ H_2 &\geq 0 \\ x_l &\leq x \leq x_u \end{aligned} \tag{5.20}$$

where *f(x)* is a function to be minimised, H_1 and H_2 are equality constraint and inequality constraint, respectively.

The Equations 5.19 and 5.20 are converted to Lagrange equation as follows:

$$L(x,\chi,\gamma) = f(x) + \chi^T H_1(x) + \gamma^T H_2(x) \tag{5.21}$$

where $L(x,\chi,\gamma)$ is the first order optimality condition that is to be zero, χ and γ are Lagrange multipliers. p^T is a positive approximation of the Hessian matrix of the Lagrangian function used to develop Quadratic Programming objective function from Equation (5.21) to be:

$$\text{Minimise } f(x) = \frac{1}{2} p^T \nabla_{xx}^2 L(x_k,\chi_k,\gamma_k) p + p^T \nabla_x L(x_k,\chi_k,\gamma_k) \tag{5.22}$$

Subject to constraint

$$H_1(x_k) + \nabla H_1(x_k)^T p_k = 0$$
$$x_l \leq x_k + p_k \leq x_u \qquad \qquad \textbf{(5.23)}$$
$$H_2(x_k) + \nabla H_2(x_k)^T p_k \geq 0$$

The SQP algorithm generates search direction p_k of the problem at x_k iteration k for solving Equation 5.22. In each line search of $x_{k+1} = x_k + \delta_k p_k$, the modified Broyden-Flecher-Goldfarb-Sanno (BFGS) formula is used to update matrix Equation 5.21 . The general method to solve constrained optimisation is stated in [72].

The algorithm starts as follows:

1. Initialise starting value of the parameters as an initial guess and use the Hessian matrix from the previous step to update it.

2. Solve the QP problem as in Equation (5.21), using the modified BFGS formula, at the same time linearise with constraints.

3. At each iteration, solve the objective function value by linearised $x_{k+1} = x_k + \delta_k p_k$ with initial value p_k and δ_k together with x_k .

4. Achieve optimal or repeat the iteration.

The SQP efficiency, accuracy and changes of solution are fully tested against other standard algorithms in [145]. In this research, the SQP in *Matlab Optimization Toolbox* was used, employing the constrained minimisation function [135].

5.4 Numerical Case Study for Single Objective

To illustrate the applicability of DE in optimisation problems, four test problems proposed by different authors are solved. Problems 1 and 2 minimise a single variable and two variables, respectively. For maximising function, Problem 3 uses a single variable and Problem 4 deals with two. Problem 5 was used for testing local minima behaviour of DE and SQP. All problems incorporated equal constraints.

5.4.1 Single objective case study

Problem 1

The sphere function (Equation (5.24)) is considered to be a very simple case for the minimisation method [82]. This function has a smooth, unimodal, strongly convex and

symmetric function and there should be no difficulty to find minimum value of $f(0) = 0$.

$$f_1(x) = \sum_{i=1}^{2} x_i^2 \qquad x_{1,2} \in [-5.12, 5.12] \qquad \textbf{(5.24)}$$

Problem 2

The Himmelblau function (Equation (5.25)) is another minimisation function to search two variables with wide constraints [143]. To find the global minimum is easy, due to the flat-shaped profile of the function.

$$f_1(x) = (x_1^2 + x_2 - 11)^2 + (x_1 + x_2^2 - 7)^2 \qquad x_{1,2} \in [-30, 30] \qquad \textbf{(5.25)}$$

Problem 3

The initialisation bound is specified as (-5.12,5.12), as given in Price and Storn [82]. Hyper ellipsoid (Equation (5.26)) will take the same bound to find the minimum point.

$$f_1(x) = \sum_{i=1}^{2} 2x_i^2 \qquad x_{1,2} \in [-5.12, 5.12] \qquad \textbf{(5.26)}$$

Problem 4

The famous Rosenbrock function [82] in Equation 5.27 is minimised in two dimensions, with bounds (-30,30). This is a classical optimisation function known as the Banana function. The global optimum is located inside a long, narrow, parabolic-shaped flat valley.

$$f_1(x) = 100(x_2 - x_1^2)^2 + (x_1 - 1)^2 \qquad x_{1,2} \in [-30, 30] \qquad \textbf{(5.27)}$$

Problem 5

To test the local minima problem, a function that has 4 local minima, named *Six Hump Camel* (Equation (5.28), is used as suggested by Storn and Price [134]. Two variables are used with the constraint (-1.9, 1.9) and (-1.1, 1.1).

$$f_1(x) = \left(4 - 2.1x_1^2 + \frac{x_1^4}{3}\right)x_1^2 + x_1 x_2 + \left(-4 + 4x_2^2\right)x_2^2$$

$$x_1 \in [-1.9, 1.9]; x_2 \in [-1.1, 1.1]$$

(5.28)

Next, to demonstrate the DE procedures, *Problem 2* was used with simplicity to give an understanding of how DE solves the optimisation problem and the solutions for current problems are also presented.

5.4.2 DE with single objective example and solutions

For example, the Himmelblau function (Figure 5.5a) is used to describe in detail how DE procedure works to optimise the function. In order to make a simple and easy illustration, the constraint of Himmeblau function is [-6,6], as shown in the contour plot of the function in Figure 5.5b, and DE population is set as 4 and produces only for 10 generations. The other mutation factors and crossover values are the same as in the previous examples using DE strategy 1.

An initialisation process which starts with four populations generated using Equation (5.2) is represented in Figure 5.5c. Then, four sets of mutated vectors $x_{r1,g}$, $x_{r2,g}$, $x_{r3,g}$ and $x_{r4,g}$ are randomly selected from the population in initialisation. In using Equation 5.3, the mutated vectors are introduced and, for example in Figure 5.5d, $x_{r1,g}$, $x_{r2,g}$ and $x_{r3,g}$ are shown by '×', '×' and 'o', respectively. In this case, $x_{r1,g}$ and $x_{r3,g}$ are located at the same vector and $v_{i,g}$ '*' is out of boundary. Consequently, in the crossover process of Figure 5.5e, the crossover selects '×' as $u_{i,g}$ from randomised selection of the population as compared to $v_{i,g}$, 'o' according to Equation 5.6 to produce a trial population '*' from combination of two $u_{i,g}$ ('×' and 'o'). After that, a $u_{i,g}$ is needed to compete with other randomised vectors to be selected as a new population in the selection process (Figure 5.5f).

This new vector is introduced into the current generation and each four populations of generation are evaluated, as shown in Figure 5.5g. The processes in Figure 5.4, as illustrated before (mutation, recombination and selection), are continued until the criteria meet either maximum population or the fitness value. Figures 5.5h, 5.5i and 5.5j show generations 1, 5 and 10, respectively. Due to the small number of population size and number of generations used, the final value is not achieved, as the purpose of the current example is only to illustrate how DE works.

For all the above problems, DE parameters are shown in Table 5.1 and Strategy 7 is selected. In Table 5.2, the solutions of all functions from (5.24) to (5.28) are shown with their optimum parameter and function values. For sphere function, both DE and SQP can search for minimum value. However, SQP is sensitive to the initial value and can be easily trapped in local minima. For example, the optimal value (zero) changes to 7.45e-9 when an initial value of one is used instead of zero. It can be seen from results that to minimise sphere function is much easier than Himelblau function for both algorithms. To sum up, DE shows better accuracy than SQP but requires large computational time.

Similar cases occurred for minimising Hyper Ellipsoid and Rosenbrock. Hyper Ellipsoid is simple compared to Rosenbrock. The bound range also plays an important role for the optimisation for DE and SQP algorithms. Both can handle the local minima occurring in the *Six Hump Camel* problems, although with different optimum value, the evaluation value is not much different.

5.5 Multi-Objective Study

Problems in engineering design, scientific experiments and business decision-making are introduced to find optimal solutions in practical applications. However, most problems consist of several objectives which always conflict with each other. As a result, in many cases, the multiple objectives are then conducted with one optimal objective. The result strongly depends on how the conversion is made and causes difficulty in exploring a broad set of optimal solutions. Pareto optimal concept was created by Vilfredo Pareto to trade off between the objectives [146]. For example, Abburi and Dixit [113], Sardinas *et al.* [147], Karpat and Ozel [148] and Wang [149] applied multi-objective optimisation in the turning process and Kurdi *et al.* [144] optimised the milling process under the chatter problem. Before the multi-objective approach can be applied to the current problems, the concept of the approach and the choice of methods will be discussed.

5.5.1 Definition

Optimisation problems with $f(x): R^n \to R$ as a scalar vector objective function, $H(x): R^n \to R^m$ as equality constraints, inequality constraints and x_l and x_u are described in the general form, the same as Equations 5.19 and 5.20.

However, in a multi-objective problem, instead of a single objective *f(x)*, there is a vector of objectives as follows:

$$f(x) = \{f_1(x), f_2(x), \ldots f_n(x)\} \tag{5.29}$$

Because $f(x)$ is a vector, there is no unique solution to this problem when any component in Equation (5.29) competes with each other. Thus, the concept of non-inferiority or Pareto optimal can be used to represent the objectives' characteristic. Therefore, the non-inferior solution improves one objective by degradation of the other objectives.

An important concept in multi-objective optimisation is that of convex and non-convex problems. Deb [146] defined the convex problem for multi-objective if all objective functions are convex and the feasible region is also convex. However, a solution is trapped in the Pareto local optima if the method cannot handle the non-convex problem. Figures 5.6a-d show the Pareto front solution for all possible cases of minimisation *min* and maximisation *max*. A utopian objective is an ideal objective but represents a non-existent solution. Figure 5.6a shows a Pareto front when minimising two objective functions f_1 and f_2. Figures 5.6b, 5.6c and 5.6d show the Pareto front for *max-f₁* and *max-f₂*, *min-f₁* and *max-f₂* and *max-f₁* and *min-f₂*, respectively. In addition, the concavity and continuity problems of non-Evaluation Algorithm function cause the introduction of multi-objective optimisation for Evaluation Algorithm algorithm [146].

5.5.2 Methods

In solving multiple objective problems, there are several methods that can be classified into traditional and modern methods. Traditional methods or *a priori* articulation methods [146] include weighted sum method, goal programming method, epsilon-constraint method (ε-constraint), goal attainment method, value function method and Benson's method. For modern methods, the updated Evaluation Algorithm algorithms

are [146] Non-Dominated Sorting Genetic Algorithms, Multi-Objective Struggle Genetic Algorithm, Niched Pareto Genetic Algorithm, Vector Evaluated Genetic Algorithm, Strength Pareto Evolutionary Algorithm, Multi-Objective Differential Evolution, Multi-Objective Genetic Algorithm and Neural Network.

The ε-constraint as a non-dominated solution is easy to implement for a bi-objective problem which is suitable for the current study. Additionally, the advantage of this method is its ability for both convex and non-convex problems. Furthermore, this is simple to express, preference can be retained and easily controlled [146]. Particularly, in this research, both DE and SQP will be applied to create and solve multi-objective problems. However, this method is capable to analyse only one optimum point and the disretisation has to be fine enough to prevent losing the Pareto solution. So the constraint limits set should lie with the minimum and maximum limits of the considered objective function. The successful applications of ε-constraint method have been reported in specific projects [146] such as brake-forming processes, multi-reservoir water supply systems, space heating and especially in machining processes [144] that also deal with the chatter problem. The method has also been successfully applied with various optimisation algorithms such as DE [146], SQP [146] and Particle Swam Optimisation (PSO) [144].

5.5.3 ε-constraint algorithm

The ε-constraint method was proposed by Haimes *et al.* [150] for generating a Pareto optimal solution by solving a sequence of constrained single objective problems. With this method, one objective function is chosen while the remaining objective functions act as constraints. The different elements of the Pareto front can be obtained from a systematic and equal frequent variation of the constraint bounds. The multi-objective problem can be transformed into several single objectives with constraints, using the following procedure:

$$\text{Minimise} \qquad f_n(x) \qquad\qquad\qquad \textbf{(5.30)}$$

$$\text{Subject to} \qquad f_j(x) \le \varepsilon_j \qquad\qquad\qquad \textbf{(5.31)}$$

$$\text{for all } \ j = 1, 2, \ldots, m, \cdot j \ne n,$$

where $n \in \{1,2,\ldots,m\}$ and x is in the feasible region, which can be defined by any equality and inequality constraint. $\varepsilon = \varepsilon_1, \varepsilon_2, \ldots, m$ is defined as the vector of the upper bounds the maximum value of each objective can have. In Figure 5.7, the different points of Pareto are generated using different values of upper bound. In order to obtain the entire set of the Pareto optimal solutions, the vector of upper bounds must vary along the Pareto front for each objective and make a new optimisation for each new vector.

For application with the ε-constraint method, the previous SQP and DE sources were used. Additionally, the objective function was converted into inequality constraint to optimise a single objective function. For DE parameters, these are similar to the single objective problem.

5.6   Numerical Case Studies for Multi-Objective Optimisation

Investigation of the performance of the DE and SQP used benchmark test problems from Deb [146]. Problems 6-8 deal with two minimisation objective functions and the second problem needs to solve the maximisation multi-objective functions. All solutions will be presented and the mechanism of applying the ε-constraint method to current algorithms (DE and SQP) is also described with an example.

5.6.1   Case study

Problem 6

The first *Problem 6* used simple functions with two variables that need to be minimised. For applying the ε-constraint method, $f_2(x)$ was used as a single objective function, while $f_1(x)$ was used as inequality constraint in the upper bound.

$$\text{Minimise} \qquad f_1(x) = x_1 \qquad (5.32)$$

$$\text{Minimise} \qquad f_2(x) = \frac{1+x_2}{x_1} \qquad (5.33)$$

$$x_1 \in [0.1, 1.0]; x_2 \in [0,5]$$

Problem 7

Equations (5.34) and (5.35) were used to maximise a problem with two variables. The single objective function used $f_2(x)$ and for the inequality constraint $f_1(x)$ was used and applied as lower bound instead of upper bound for minimising the problem.

Maximise $\qquad\qquad f_1(x) = 1.1 - x_1$ **(5.34)**

Maximise $\qquad\qquad f_2(x) = 60 - \dfrac{1 + x_2}{x_1}$ **(5.35)**

$$x_1 \in [0.1, 1.0]; x_2 \in [0, 5]$$

Problem 8

Problem 8 needs to minimise the cantilever beam weight f_1 and deflection behaviour f_2 that conflict with each other. The two design variables are diameter *d* and length *l*. Beside that, the inequality constraints (5.38) and (5.39) also need to be considered. The maximum stress σ_{max} must be less than the allowable strength ψ_y and the end deflection δ is smaller than a specific limit of δ_{max}. For DE and SQP algorithms, the ε-constraint method was applied by setting the inequality constraint for $f_1(x)$ to be the lower bound and the single objective function used $f_2(x)$.

Minimise $\qquad\qquad f_2(d, l) = \delta = \dfrac{64Pl}{3E\pi d^4}$ **(5.36)**

$$\sigma_{max} \leq S_y$$ **(5.37)**

$$\sigma_{max} = \dfrac{32Pl}{\pi d^3}$$ **(5.38)**

$$d \in [10, 50]; l \in [200, 1000]$$

where density ρ = 7800 kg/m3, force P = 1 kN, modulus of elasticity E = 207 G N/m2, allowable strength ψ = 300 MN/m2 and deflection δ = 5 mm.

5.6.2 ε-constraint method with DE and SQP example and solutions

To demonstrate how ε-Constraint method is applied to solve multiple-objective optimisation, *Problem 7* was used as an example. In Equation 5.34, f_1 was functioned as an inequality constraint in lower bound because this problem dealing with maximisation becomes:

$$1.1 - x_1 \geq \varepsilon_j$$ **(5.39)**

In order to calculate ε_j, the limit or range of f_1 should be considered from bound constraints (x_1 and x_2). This depends on the user to define how many discretisations are to be obtained. For instance, in this problem, j = 11, and ε_j can be calculated using Equation 5.41.

$$\varepsilon_j = \frac{f_{1\max} - f_{1\min}}{j-1} \tag{5.40}$$

This equation was used as objective function to maximise the problem within the bounds, including the inequality constraint of Equation 5.40. The problem then used a DE algorithm or SQP in a similar fashion as single objective problems. This was repeated with a different value of ε_j as a constraint to obtain the Pareto front, for instance as shown in Figure 5.7. In Table 5.3, the second problem was solved to obtain the Pareto front by repeating use of ε_{10} 10 times to solve multi-objective for both f_1 and f_2 maximisation problems.

Solutions for *Problems 6-8* are now presented. In Figure 5.8a, the solution for *Problem 6* obtained using DE is plotted compared with SQP, both using the ε-constraint method. The results show as similar for both methods to solve the multi-objective function problem. A simple minimisation problem follows the same pattern of optimal Pareto, as shown in Figure 5.8a. Figure 5.7b shows the solution for *Problem 7* using DE and SQP which also duplicate each other at the same point and follow the Pareto optima for maximisation problem. Thus, both methods can handle the maximisation problem using ε-constraint method. The simulation results are applied for an engineering problem, as shown in Figure 5.8c. This shows trade-off between the two objectives at the same point for both algorithms. Both minimisations of *Problems 6* and *8* illustrate the Pareto front as similar to Figure 5.6a. Consequently, both methods with ε-constraint method can be applied for multi-objective optimisation in machining. It is proved that ε-constraint can give the same results as modern approaches.

5.7 Summary

The basic theory of the DE algorithm was reviewed and the SQP algorithm was also introduced. After that, five well known problems were solved using DE and validated with SQP in the present work. A single and double variable problem can be minimised or maximised for convergence to the global optimum. Parameter numbers, upper and lower limits as bounds, are the factors affecting algorithm performance in searching for optimum values. Both methods excelled in capturing and solving global optimal on the mathematical function.

As an alternative to single-objective optimisation that cannot solve two objectives simultaneously, the introduction of multi-objective optimisation has provided a way to overcome the problem, using the ε-constraint approach. In theory, two objectives can be solved by assigning one of the objectives as a constraint. By setting and changing constraint values, the Pareto front solution can be achieved by using either DE or SQP. The use of the ε-constraint method with DE and SQP was explored to solve three famous problems in multi-objective optimisation. The results of ε-constraint of DE are similar to SQP to demonstrate the capability and ability of both methods to produce Pareto optimal point for the current case study. Both methods, either DE or SQP, can be continued to solve optimised single and multiple objective functions for machining problems.

Since the DE and SQP algorithms discussed above were applied with numerical problems, analytical stability will be considered in the following chapter. In Chapter 3, SDM as a numerical algorithm is initially introduced and discussed on how to apply it in optimisation algorithms. In the next chapter, DE and SQP optimisation algorithms are combined with SDM as chatter numerical modelling in Chapter 3 to search an optimal variable helix tools for chatter suppression.

Table 5.1 Typical DE parameter setting

Parameter	Value
Strategy	7- DE/rand/1/bin
Number of generation (NP)	60
Crossover factor (CR)	0.7
Scaling factor (SF)	0.8

Table 5.2 Optimum numerical simulation results

Function	Optimum parameter value			Optimum evaluation		
	Actual	DE	SQP	Actual	DE	SQP
Sphere	0,0	0,0	$7.45e^{-9}$, $7.45e^{-9}$	0	0	$5.51e^{-9}$
Himelblau	3, 2	2.95, 2.05	3, 2	0	0.084	0.051
Hyper Ellipsoid	0, 0	0,0	$0.44e^{-15}$, $0.89e^{-15}$	0	0	$-1.97e^{-31}$
Rosenbrock	1, 1	1, 1	1, 1	0	0	0
Six Hump Camel	-0.089, 0.713	-0.814, 0.707	-0.897, 0.713	-1.031	-1.031	-1.032

Table 5.3 ε-constraint method combined with DE to search for Pareto front of multi-objective of problem 7

J	ε_j	f_2	x_1	x_2
1	0.1	50.00	0.1	0
2	0.2	55.00	0.9	4.0
3	0.3	56.66	0.8	3.5
4	0.4	57.50	0.7	3.0
5	0.5	58.00	0.6	2.5
6	0.6	58.33	0.5	2.0
7	0.7	58.57	0.4	1.5
8	0.8	58.75	0.3	1.0
9	0.9	58.75	0.2	0.5
10	1.0	59.00	0.1	0
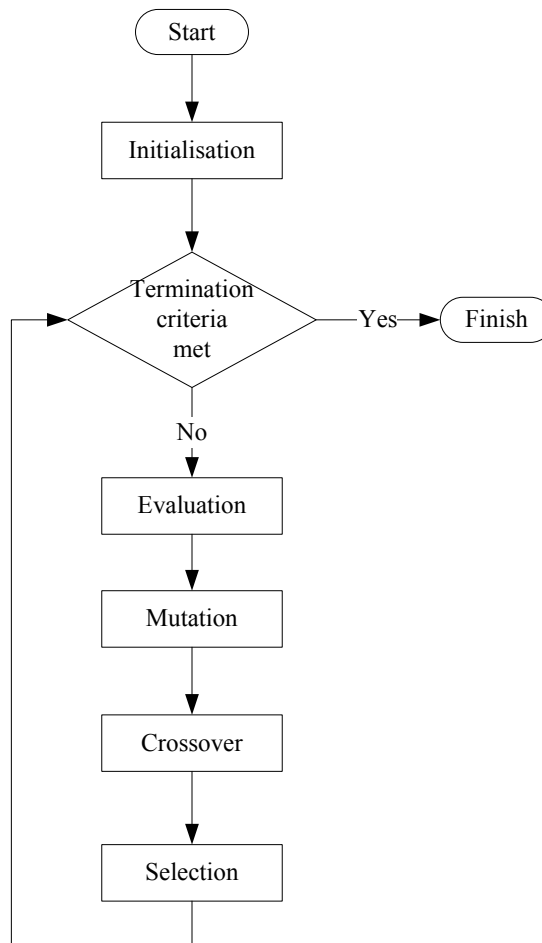
Figure 5.1 Flow process of DE optimisation
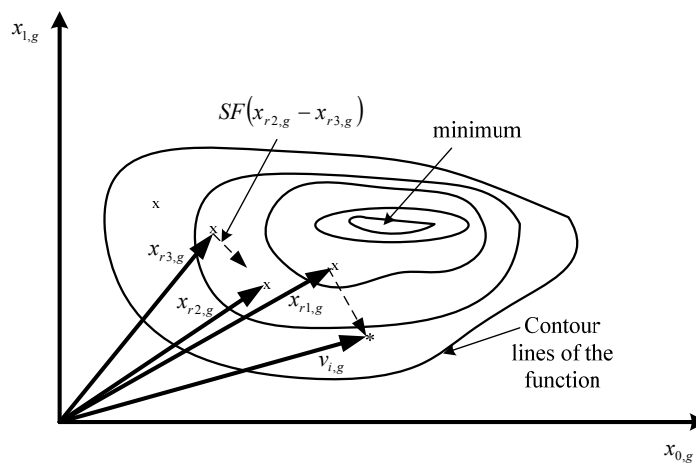
Figure 5.2 Process of mutation where *x* is Number of Population parameter vector from current
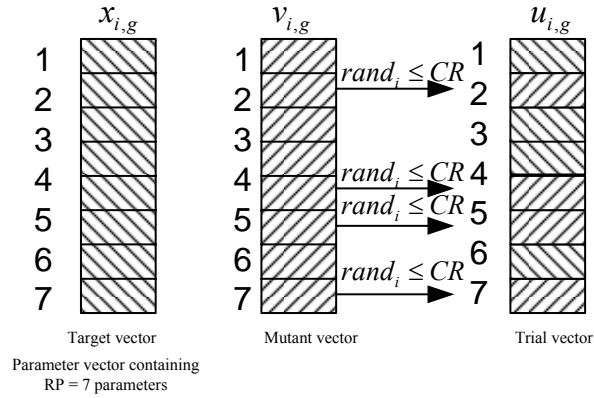
Figure 5.3 Process of crossover in recombination
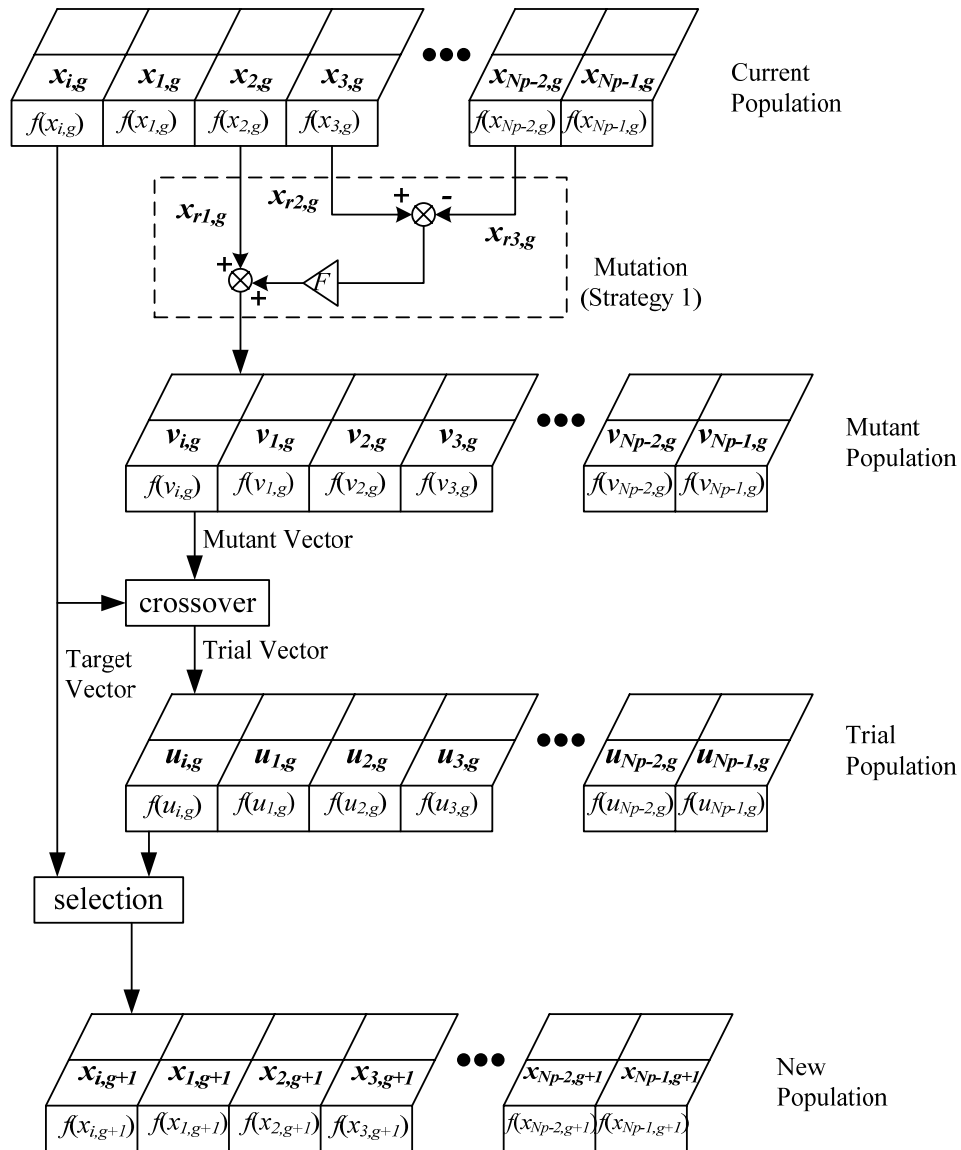
Figure 5.4 Process of generating one population to next
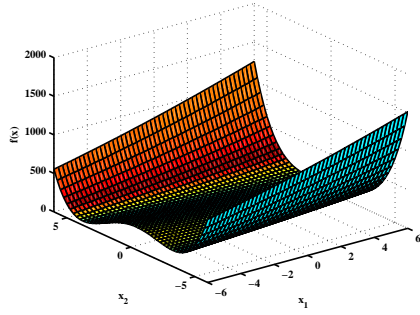
a) Himmelblau surface
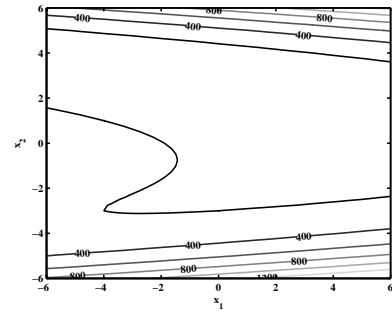
b) Himmelblau contour
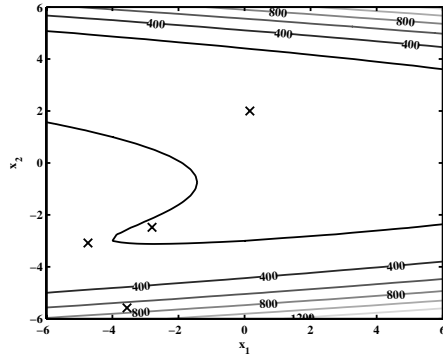
c) Initialisation
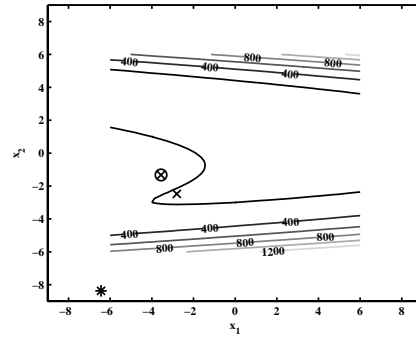
d) Mutation
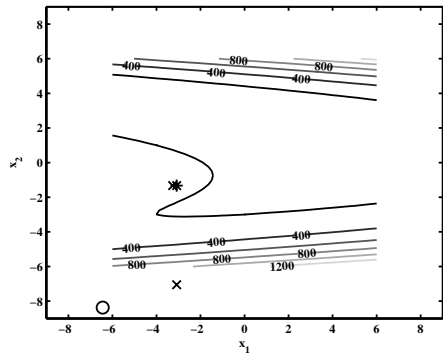
e) Crossover
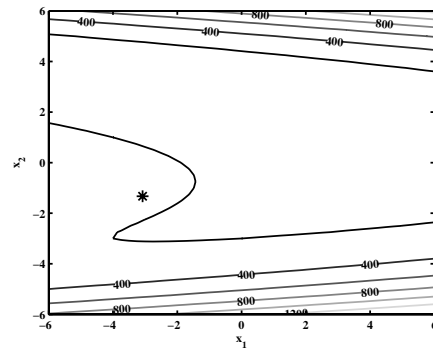
f) Selection
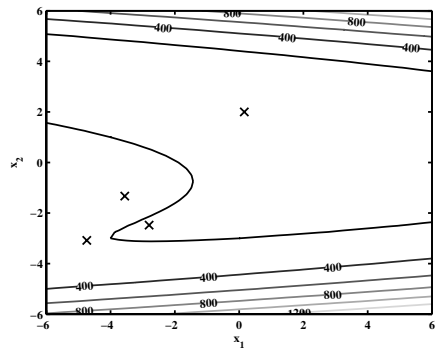
g) Generation 1

h) Generation 2
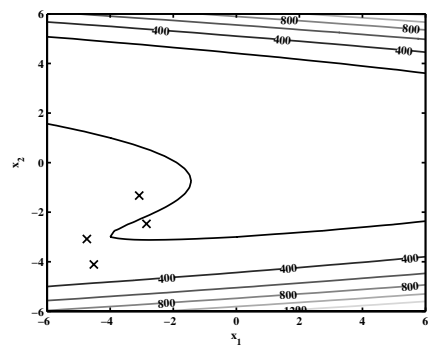
i) **Generation 5**   j) **Generation 10**
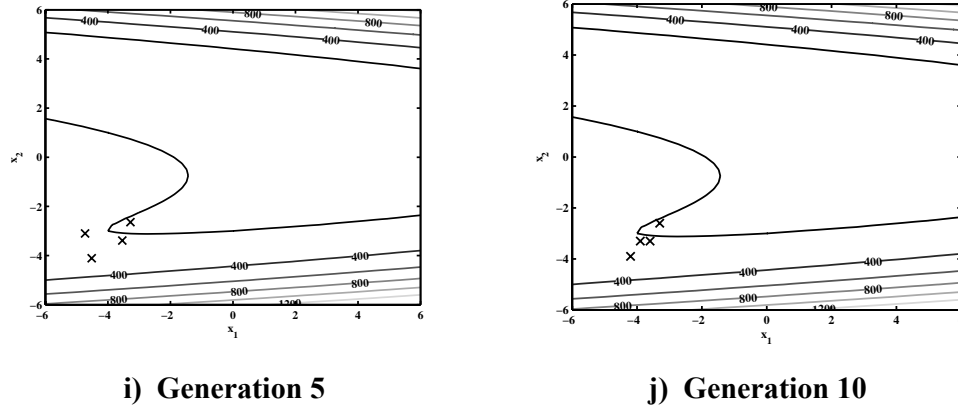
Figure 5.5 Typical Differential Evolution processes using Himmelblau function

a) **Min-f_1 and Min-f_2**   b) **Max-f_1 and Max-f_2**

c) **Min-f_1 and Max-f_2**   d) **Max-f_1 and Min-f_2**
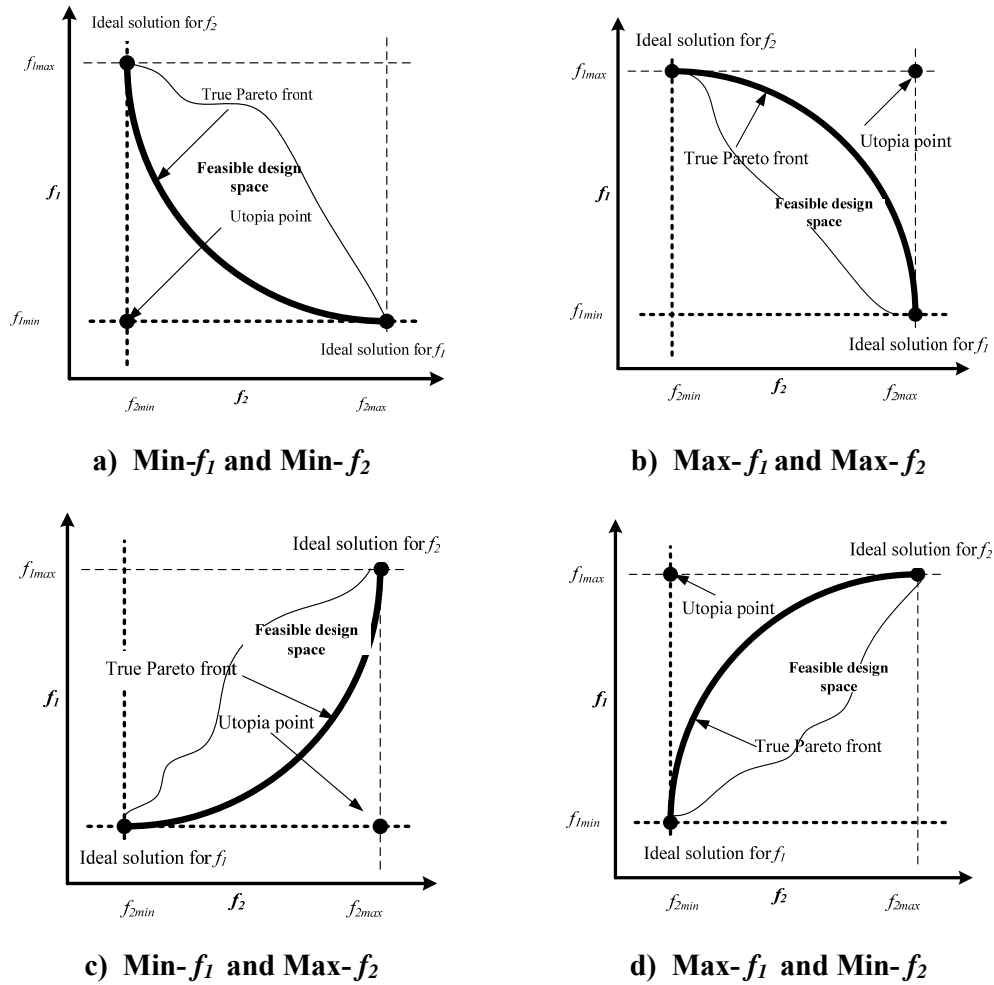
Figure 5.6 Pareto front solution for two-dimensional problem with two objectives
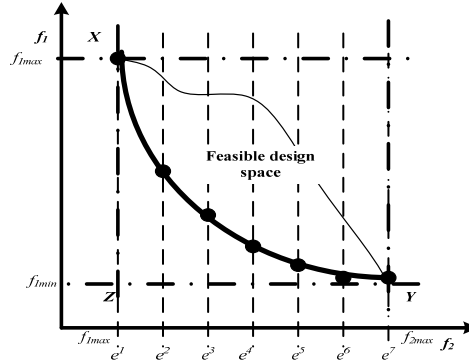
Figure 5.7 Generating different solution of Pareto front with ε-constraint method
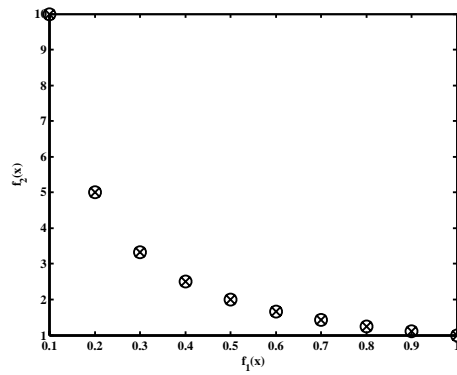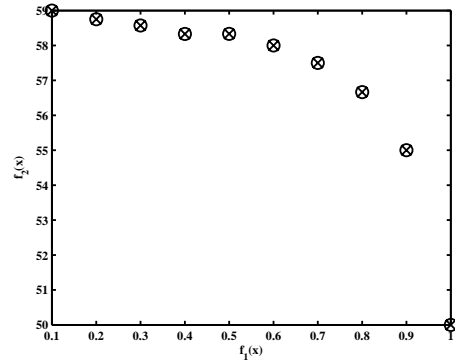
a) **Problem 6**   b) **Problem 7**
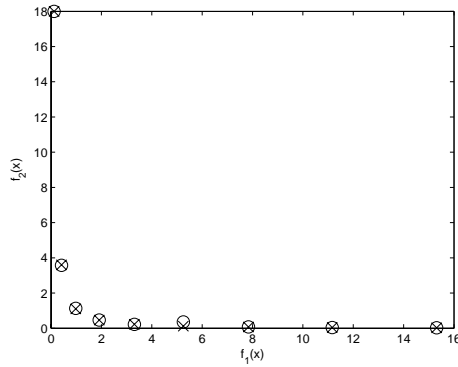
c) **Problem 8**

Figure 5.8 Performance of DE ('o') and SQP ('×') in ε-constraint multi-objective optimisation for numerical tests.

CHAPTER 6
NUMERICAL OPTIMISATION: RESULTS

6.1 Introduction

The aim of this chapter is to present the results for optimising variable helix milling tools. Based on the optimisation approach described in Chapter 5 and objective functions (minimise chatter, maximise chatter performance, and combined chatter reduction and maximised material removal rate), the tools' geometry is modified.

Before the results from integration of DE/SQP and SDM are presented, three objectives are properly explained. Parametric study is then carried out to search for optimal parameters in DE, such as crossover, scaling factor, number of population and number of generations for minimisation of the chatter problem. Using these optimum parameters, the results of the minimisation of chatter and the maximisation of chatter performance for three-flute cutter results are presented. After that, two approaches are applied to improve the current results: mixed population during population process and bounce back approach in mutation and crossover processes. Besides the modified algorithm, objective functions are also modified for both problems. The multi-objective problem of minimisation of chatter and maximisation of material removal rate is then considered to achieve Pareto front results. Finally, the best results will be compared with the variable pitch tools approach. The overall results' structure is shown in Figure 6.1. The research results for chatter minimisation for this chapter formed a published conference paper [151] and an abstract for this work is given in Appendix A.II.

6.2 Objective Function

A SDM can be applied to calculate and optimise variable helix angle. Optimal variable helix is suitable for a wide range of spindle speed, workpiece material and frequencies. Based on the optimisation of suppression chatter, objective function and variable included and constraints will be proposed. For the current case, there are three problems which will be optimised, consisting of minimising chatter, maximising chatter performance and combining minimising chatter and simultaneously maximising material removal rate (MRR). Before that, the constraint to variable helix and variable pitch are now discussed.

6.2.1 Constraints for variable helix and variable pitch tools

Machine speed limits and workpiece thickness are two factors which need to be considered from a practical viewpoint. A constrained spindle speed should be considered for a specific range of machine speed limits, while the workpiece thickness limits the axial depth of cut. MRR varies when different radial depth of cut r, chip width h and number of teeth m were used, which affects the chatter frequency. MRR is determined using following relationship:

$$MRR = b * r * h * \Omega * m \qquad\qquad (6.1)$$

As stated before, variable helix and variable pitch were considered for the current study. Refer back to Figure 1.3 that illustrates the helix angle β_i and pitch angle ϕ_i and other constraints variables in the optimisation. The helical angle purpose is actually to break chip formation, change line of contact between tool and workpiece and reduce chatter [152]. By adjusting the helix randomly, the optimisation process will be more generalised, besides avoiding premature population and preventing local optimal problem in the optimisation processes. β_i is the helical angle value range from low helix (25°) to high helix (55°) conditions. For variable pitch, the chip evacuation should be prevented when high chip removal is used [11, 12], particularly when higher value pitch angles are selected for the finishing process. Without chatter frequency and phase angle as constraint, as suggested by Budak [11] and Altintas *et al.* [5], the selection of the appropriate helical and pitch angles will be randomised. During the optimisation process, however, the candidate values of tooth helix β_i and pitch ϕ_i may result in milling cutters whose flutes intersect with each other. This is clearly inadmissible from a practical viewpoint. To prevent helical angles intersecting, the helical angle height different Δh_β is introduced as a constraint in the DE optimisation. Δh_β calculations for variable helix and variable helix with variable pitch at its end are as follows:

$$\Delta h_\beta = \frac{d - d(2m)^{-1}}{\tan \beta_i} - \frac{d - 2d(m)^{-1}}{\tan \beta_{i+1}} \qquad \text{(variable helix)} \qquad (6.2)$$

$$\Delta h_\beta = \frac{d - d(2m)^{-1}}{\tan \beta_i} - \frac{\left(d - 2d(m)^{-1}\right)\sin\left(2^{-1}\Delta\phi\right)}{\tan \beta_{i+1}} \qquad \begin{array}{c} \text{(variable helix and} \\ \text{variable pitch)} \end{array} \qquad (6.3)$$

Here, Equation (6.2) relates to optimisation problems where the free end of the milling cutter has teeth uniformly spaced, but the variable helix of each flute means that the teeth are irregularly spaced along the rest of the cutter's axial length. Equation (6.3) relates to cutters with both variable helix and variable pitch at the free end. The Δh_β

value is based on the parameters illustrated in Figure 1.3c, along with the number of cutter teeth m and cutter diameter d and pitch difference $\Delta\phi$.

6.2.2 Chatter minimisation

For a single objective function that considers minimised chatter as target, where chatter relates to absolute characteristic multiplier or iegen values CM that must be less than one to fully eliminate chatter. In the current case, the worst chatter indicated by eigen value is minimised by optimisation algorithms. This occurs within a specific region of spindle speed and axial depth of cut. The final optimisation problem can be specified as follows:

Objective function: Minimise $f(\beta_i,\phi_i) = \max|CM|$ **(6.4)**

Subject to constraints:

Helical angle $\begin{aligned}25 \le \beta_i \le 55 \\ i = 1,2,3 \ldots n\end{aligned}$ (°)

Pitch angle $\begin{aligned}\phi + 22.5 \le \phi_i \le \phi + 22.5 \\ i = 1,2,3 \ldots n\end{aligned}$ (°)

Helical height difference $\Delta h_\beta \ge 5$ (mm)

During optimisation, each point of specific spindle speed and axial depth of cut was evaluated on characteristic multiplier value to produce a matrix of characteristic multiplier. A single value of characteristic multiplier is calculated after two determinations of maximum characteristic multiplier matrix. The constraint on pitch angle ϕ_i (55°) is to ensure good chip evacuation as suggested by previous work [11, 12]. The DE needs to search for the suitable values of variable helix β_i and variable pitch ϕ_i that produce minimum chatter across the chosen spindle speed and depth of cut range (along with the additional constraints). Helical angle height difference Δh_β is constraint greater than 5 to prevent intersection.

6.2.3 Performance maximisation

Performance is defined by maximum of material removal rate divided by absolute value of character multiplier. The worst performance with specific regions of depth of cut and spindle speed is maximised using DE and SQP algorithms. The same as for the previous objective function, each point of spindle speed and depth of cut is evaluated but for this case is based on Equation 6.5 and constraint as follows:

Objective function   Maximise $f(\beta_i,\phi_i) = \max\left(\dfrac{MRR}{|CM|}\right)$ **(6.5)**

Subject to constraints

Pitch angle
$$22.5 + \phi_{\min} \leq \phi_i \leq 22.5 + \phi_{\max}$$
$$i = 1,2,3\ldots n \qquad (°)$$

Helical angle
$$25 \leq \beta_i \leq 55$$
$$i = 1,2,3\ldots n \qquad (°)$$

Helical height difference $\Delta h_\beta \geq 5$ (mm)

A single value of Equation 6.5 is calculated after the maximum value. A combination of spindle speed and axial depth of cut will be used to calculate material removal rate according to Equation 6.1. At the same time, structural dynamics from the variable helix will be changed through characteristic multiplier evaluation either in stable or unstable condition at optimum performance. The iteration will finish when the optimal variable helical angles have achieved the maximum performance.

6.2.4 Multi-objective optimisation

In the third case, multi-objective function is applied by considering maximisation of normalised MRR ($MRR_n = \dfrac{MRR}{MRR_{\max}}$) and minimisation of chatter. MRR_n is an important objective function by considering spindle speed and axial depth of cut to generate optimum productivity and easily compare with other specific spindle speed and axial depth of cut range. A stable cutting generates a good quality surface roughness and a longer tool life to produce from a lower tool wear and cutting force were applied to the workpiece.   This unstable condition can be suppressed by minimised characteristic multiplier at the same time maximise normalised material removal rate MRR_n. The following is the objective function and constraints for the multi-objective problem:

Multi-objective function

Minimise $f(\beta_i, \phi_i) = \max(CM), -f(b, \Omega) = MRR_n$ **(6.6)**

Subject to constraints

Pitch angle
$$22.5 + \phi_{\min} \leq \phi_i \leq 22.5 + \phi_{\max}$$
$$i = 1,2,3\ldots n \qquad (°)$$

Helical angle
$$25 \leq \beta_i \leq 55$$
$$i = 1,2,3\ldots n \qquad (°)$$

Helical height difference $\Delta h_\beta \geq 5$ (mm)

To compromise two or more objectives, multi-objective function is considered a Pareto front concept. In Figure 5.7, the Pareto front that connects a line *X* to *Y* is comprised of

a set of optimal points or nondominated points. All possible values of the objectives for feasible design points consist in the function space. The Pareto front is part of the feasible function space boundary where in that space one point relates to another in the set [146]. Any improvement in one of the objective functions comes to use at least one of the other objective functions. According to definition, point *Z* is not on the Pareto front as compared to points *X* and *Y* that belong to the Pareto optimal set. Thereby, the front will define a limit for the objectives that cannot be further improved simultaneously.

In order to address the multi-objective problem, the epsilon constraint method is used as discussed in Chapter 5. The two-objective problem is changed into a single objective problem by minimising one objective with a set of different limits on the second objective. The second objective is constrained to a specific value until sufficient optimum points are found to produce the two objectives Pareto front [146]. At each time the single objective problem is solved, so the constrained form of the problem for specific spindle speed and axial depth of cut becomes:

Minimise $$f(\beta_i, \phi_i) = \max(CM) \qquad\qquad \textbf{(6.7)}$$

Subject to constraints

Normalise material removal rate	$f(b, \Omega) = \varepsilon_i$ $i = 1, \dots, k$
Helical Angle	$25 \le \beta_i \le 55$ $i = 1,2,3 \dots n$ (°)
Pitch angle	$22.5 + \phi_{\min} \le \phi_i \le 22.5 + \phi_{m\epsilon}$ $i = 1,2,3 \dots n$ (°)
Helical height different	$\Delta h_\beta \ge 5$ (mm)

Equation 6.7 applied to calculate MRR_n is more straightforward than characteristic multiplier. The reason to use a number of initial guesses for MRR_n along the characteristic multiplier is because the characteristic multiplier needs to be found explicitly in the objective function. Figure 6.2 illustrates the constraint in multi-objective problem. Instead of using a specific matrix of spindle speed and axial depth of cut for the previous problem, the current approach will apply an array of spindle speed and axial depth of cut from indicated maximum MRR_n. First, an array of combination of spindle speed and axial depth of cut is set for searching for the first

maximum MRR_n. Then, these sets of spindle speed and axial depth of cut values will be considered to search for minimum worst chatter by modifying the variable helix β_i and variable pitch ϕ_i. Next, the second optimal point can be calculated from the second maximum value of MRR_n to produce an array of spindle speed and axial depth of cut values in order to minimise other worst chatter conditions. The process is repeated until all value limits of constraints are used and should be similar to the theoretical result in Figure 5.6c. Besides using maximum value of characteristic multiplier for calculation of the objective function, the second trial will use the average of characteristic multiplier values as objective function.

6.3 Results for Chatter Minimisation and Chatter Performance Maximisation

In this study, a single degree of freedom dynamic milling model with conditions of milling tool, modal and cutting parameters the same as in Table 6.1 is used, but the helical and pitch angles and other constraints need to be set before using DE and SQP as optimiser. Each case is solved for variable helix tools and variable helix and variable pitch tools to investigate the influence on chatter stability limit. Parametric study of DE parameters was made before analysis for chatter minimisation and chatter performance.

6.3.1 Parametric Study of DE

Before DE is applied, DE parameters, such as crossover (CR), scaling factor (SF), number of population (NP) and number of generation (NG) for each 'strategy 7', need to be determined. For this purpose, the problem to minimise chatter (objective function in Equation 6.1) of three-flute variable helix and variable pitch was selected. The parameter settings were evaluated based on the effects on DE performance.

An initial study was made for different CR (0.2, 0.4, 0.5, 0.9), with other parameters kept constant, as shown in Table 6.2: 50 NG, 0.7 CR, 0.6 SF and 70 NP (10 multiplied by number of real parameter (7)). The second attempt was for SF of 0.5, 0.6, 0.7, 0.8 and 0.9, with other parameters kept constant. The DE was executed for 50 generations, 0.6 CR and 70 NP. A similar setting of the DE parameter was used to examine the effect of population size or NP. Various population sizes (4, 35, 40, 70 and 105) based on minimum NP, 5, 8, 10 and 15 times, respectively, with other parameters kept constant. The fourth study used a maximum number of generations of 10, 50, 75, 100 and 150, other parameters kept constant.

The optimum values of DE parameters summarised in the present work are given in Table 6.3. Crossover rate CR is 0.9, scaling factor SF is 0.9 and the number of population NP is 10 times the real parameter (10*RP) and 70 generations are employed in DE optimisation.   A 'strategy-7' (DE/rand/1/bin) methodology [82-84] was implemented in view of its wide application in the literature. This methodology involves random perturbation of a population vector ('/rand'), perturbation of a difference vector for the mutation process ('/1') and binomial crossover ('/bin'), as discussed in the previous chapter.

6.3.2   Chatter minimisation results

The result from a three-flute variable helix tool from Sims *et al*. [29] is presented initially. Milling cutter helix geometry is then optimised, based on variable helix and variable pitch modifications, to reduce chatter based on objective function in Equation 6.1. This considered only a single degree of freedom dynamic milling model with the condition of milling tool, modal and cutting parameters the same as in Table 6.1. The numerical optimisation is based on the optimum settings in Table 6.4. Stability lobes and characteristic multiplier results of optimum cutting tools are illustrated and compared with the original design chosen arbitrarily.

The original tool geometry consisted of a three-flute variable helix (25°, 30°, 35°) cutter with variable pitch (120°, 100°, 140°) at its free end. In Figure 6.3, a large unstable region can be observed at a high depth of cut. For this low radial immersion scenario three instability conditions are seen: period-one, hopf and period doubling bifurcations. The optimisation routines were used to adjust the tool helix to obtain the most stable chatter performance across the illustrated spindle speed range. Two scenarios were considered: a variable helix with a uniform pitch at the tool's free end (variable helix and uniform pitch) and a variable helix with a variable pitch at the tool's free end (variable helix and variable pitch).

The performance of the DE and SQP algorithms is summarised in Figure 6.4. Note that the objective function is a maximum characteristic multiplier (CM) value, so a value less than unity represents complete stability over the chosen spindle speeds and depths of cut.

The DE algorithm achieved complete stability (maximum CM= 0.897) by the second generation. The corresponding variable helix (52°, 52°, 41°) and variable pitch (107°, 169°, 90°) stability diagram is shown in Figure 6.5. Since the maximum CM is less than unity, no chatter is observed. In comparison, the SQP algorithm achieved a maximum CM of 0.952 after 25 iterations.   The corresponding best-case stability diagram is shown in Figure 6.6. Although this system is also completely stable, the CM are considerably greater than those obtained with the DE algorithm. This indicates a lower margin of stability.

For the scenario where the tool's free-end pitch angle was uniform, Figure 6.4 shows that a poorer performance was obtained for both optimisation methods.   The DE algorithm converged at 50 generations with 1.005 evaluation value. This refers to a variable helix geometry (53°, 27°, 54°). The resulting stability prediction and CMs are given in Figure 6.7. Meanwhile, for the SQP result, the maximum CM value is higher (1.071) and converges at 5 iterations, as shown in Figure 6.4.   The corresponding stability prediction is shown in Figure 6.8, indicating a very large unstable island in contrast to the DE (Figure 6.7) and the original (Figure 6.3b) results.

6.3.3   Performance maximisation results

To maximise chatter performance, similar settings in minimising chatter of variable helix tools were applied. The performance is the objective function in Equation 6.2 to be evaluated and measured during the optimisation process.

In Figure 6.9, the performance of the DE and SQP algorithms is summarised. Note that the objective function is chatter performance, so a value cannot represent complete stability over the chosen spindle speeds and depths of cut as a minimisation problem.

By generation 37, the DE algorithm achieved a maximum CM= 0.292. In Figure 6.10, the corresponding variable helix (27°, 25°, 26°) and variable pitch (83°, 194°, 83°) stability diagram are shown where no chatter is observed. In comparison to the SQP algorithm, the DE achieved a maximum CM of 0.174 after 4 iterations. Unfortunately, it corresponds to a stability diagram the same as the original (Figure 6.3b).

For the case where the tool's free-end pitch angle was uniform, Figure 6.9 shows that a poorer performance was obtained for both optimisation methods. The DE algorithm

converged at 34 generations with 0.74 evaluation value and refers to a variable helix geometry (43°, 25°, 55°). The stability prediction is shown in Figure 6.11 where a large unstable island was predicted. This is poorer than the original (Figure 6.3b) results. However, for the SQP result, the maximum CM value is larger (0.118) and converges at 4 iterations, as shown in Figure 6.9. This corresponds to a stability diagram the same as the original.

Consequently, the performance maximisation approach is unsatisfactory, whilst the minimisation approach shows some promise.   However, the performance of the minimisation problem showed a very fast convergence at the second iteration. This indicates that the performance converged to a premature population where the population can not be improved. In the next section, the algorithm is refined to improve its performance.

6.4   Refined DE Algorithm

During the population process, it is desirable to produce a robust feature and a high convergence rate to create a population with high probability. To achieve trade-off between convergence and robustness, a few attempts have been made by researchers by introducing modified DE, hybrid DE and combined with Particle Swarm Optimisation and Ant Colony Optimisation.

In modified DE, instead of one array on population update, Babu and Angira [153] applied two population updates during the mutation and crossover process and the original population to ensure each population had equal opportunity. To relocate the violated bound vector to the interior bound, a penalty function was used for avoiding local optimal. A different approach was used by Lee *et al.* [84] to reduce search space, by applying the modified constraint and the local search approach to improve the population. Meanwhile Nearchou and Omirou [154] and Zhang and Xu [155] used random keys encoding to handle discrete variables to produce high performance of the modified DE. By adjusting of minimum space distance, a population's being located in the same area was prevented, as proposed by Hendershot [156]. To accelerate the mutation process and exploration region, Kaelo and Ali [68] recommended a random uniform mutation factor and localisation around best vectors, respectively.

Migration and acceleration strategies were mainly added to the original DE to perform hybrid DE by Chiou and Wang [157] and Pedchote and Purdy [158]. Migration strategy is used to diversify a population that failed in certain tolerance besides escaping from local optimal and preventing premature convergence. Acceleration reacts to generate fast convergence to improve fitness with population diversity. However, fast convergence leads to obtaining a local optimal and a large population region that causes large computational time.

To overcome convergence and robustness, Particle Swarm Optimisation was applied by Hendtlass [159] as a main rule for each individual, while DE reacts to search for a better individual. Meanwhile, Ant Colony Optimisation was applied in combination with DE to accelerate search in the mutation process. Besides that, Tasoulis *et al.* [160] and Chiou *et al.* [161] applied parallel processing to make computational time faster without compromising its performance. In applying acceleration and migration region in hybrid DE [160], a local optimal and large population region obtained cause a large computational time. When a violated vectors are modified to inside bound [161], this can solve a local optimal problem and a new population has a wide diversity of searching of the global optimal.

For the current case, DE algorithm really needs to be changed and modified based on poor performance in minimising chatter. Particularly for a case of a three-flute variable helix and variable pitch where the iteration converges at second generation and does not improve for the next 68 generations. Additionally, a mutation process causes a current algorithm to reject or remove the population vector when producing a violated vector of the boundary. This was shown in the previous Himmelblau function example (Section 5.4.2). To overcome the problems, mixed population update and bounce back strategy are applied to modify and improve the current DE algorithm.

6.4.1 Mixed population

The initialisation process consists of uniform distribution, randomisation range between (0,1), Gaussian distribution with mean and standard deviation with 0.5 and random without restrictions [82]. Although randomised initialisation was used, the population for every generation is not guaranteed to be updated or changed as shown by previous result (chatter minimisation of variable helix and variable pitch tools' population). As a result, it is suggested that the current population be interrupted by a small amount of

random noise population to improve DE process for every generation by encouraging more search space to search for the global optimal and exploring to accelerate the convergence rate. The other population is the best population from the previous generation. This mixed population has a feature of diversity and guarantees to produce a high probability of the global optimal from the introduction of some noise population to the current population as a mixed population.

In every new generation, the next population will consist of 75 percent of the best current population and 25 percent from a randomised population. This randomised population reacts as noise to improve the next population. The pseudo algorithm for the current approach is shown in Figure 6.12. In every generation, a 25 percent population with additional noise will improve DE performance to overcome premature problem of the population during the optimisation process.

6.4.2   Bounce back boundary

In constraint optimisation, several methods [82] have been proposed to solve the problem, such as penalty function, random initialisation, bounce back method and rejection of the vectors . Previously, the rejection of the vector was applied; however, the point outside bounds may have a better solution but unfortunately not in the feasible region. A bounce back method function can be used to modify an out of bounds trial parameter with one located on the boundary. Besides escaping from the local optimal, especially at the boundary, this replaces out of bounds vectors to have a highly diverse population.

Figure 6.13 illustrates the bounce back strategy in a two-dimensional search space. When the population moves outside the bounds, this strategy allows the generation of vectors close to bounds. The pseudocode of the strategy is shown in Figure 6.14. The violated vector at the upper and lower boundaries is relocated with a trial vector to the each of them, respectively.

6.4.3   Himmelblau function example

As in the example in Section 5.4.2, a Himmelblau function was used to demonstrate how a modified DE improves in optimising the function. For simplicity, the constraint, DE population, number of generation, mutation factor, crossover and strategy are set as

in the previous example.   The mechanism of bounce back and randomised noise population approaches are now described for a Himmelblau function.

An initialisation process of generating four populations was started similarly to Figure 5.5c. In the mutation process of Figure 6.15a, the three mutated vectors are introduced, such as $x_{r1,g}$, $x_{r2,g}$ and $x_{r3,g}$ indicated by '×', '×' and 'o', respectively .   Due to '∗''s having violated the boundary, the bounce back strategy takes action to propose '+' as a substitute with the violated vector. In Section 5.4.2, this violated vector was previously terminated. A bounce back reacted to the violated boundary vector during the crossover process to substitute '•' with '+' (Figure 6.15b). In the previous example, the violated boundary vectors had also been terminated. Again, bounce back boundary approach made an action to replace the violated vector with the nearest boundary vector. These mutation and crossover processes strongly represented how bounce back improved the DE algorithm for the Himmelblau example. Figures 6.15b and 6.15c show the selection and generation process with substitution vectors during mutation and crossover processes.

The mechanism of a random noise population approach is now presented. Initially, a generation of four vectors is produced, as shown in Figure 6.15d. Using a random noise, '+' and 75 percent best population are introduced to update generation (Figure 6.15e). The 25 percent noise of the new vector is introduced into the current generation to improve optimisation as discussed before. Previously, the generation is taken as proposed by the algorithm without any updating of a new random vector and best vector in the population. Figures 6.15f, g and h show generations 2, 5 and 10, respectively. Despite a small population size and number of generations, the result of the current population is the 10th generation towards minimum coordinates at 3, 2 location (minimum value vectors). The final value is better than the result in Section 5.4.2. This example is only needed to show how bounce back and randomised noise population approaches improved the Himmelblau function when compared to previous example. Next, this refined DE algorithm is applied to the chatter minimisation problem.

6.4.4 Chatter minimisation example

The main problem which occurred was illustrated in the three-flute variable helix and variable pitch tool. During the optimisation shown (Figure 6.4), the generation cannot be improved and performed after the second iteration.   In order to indicate that the

refined DE performs well and overcomes the previous problem, minimisation of chatter is reconsidered with the same DE settings and machining parameters.

In Figure 6.16, the original DE and refined DE were compared in their performance in optimising chatter of three-flute variable helix and variable pitch tool. It shows that the refined DE is significantly better than the original where generation improved during iterations although the population of refined DE showed improved maximum eigen value at the 63th generation converged at 0.8. Characteristic multiplier *CM* value is 6-fold greater than the previous optimisation. This corresponds to a variable helix (41°, 43°, 40°) and variable pitch (68°, 283°, 36°) that showed stable or unchattered behaviour (Figure 6.17). By comparing with Figure 6.5, the refined DE is better than the original DE results, indicated by a larger gap in the stable border line in the CM diagram. Moreover, the magnitude of the absolute eigen value contour for the refined DE is between 0.6 and 0.85 and for the original DE is between 0.8 and 0.9. This not only represents that the CM value of the refined DE has a lower value or better than the original result, but also more damping behaviour from the original DE.   This clearly indicates the bounce back and mixed population can improve the DE result. Next, the refined DE algorithm is reconsidered for previous problems.

6.5 Modification of Current Objective Function

Before considering the refined DE algorithm for the previous problem, the current objective functions are now modified to improve their performance. The current objective refers to the maximum value of the objective function either for chatter minimisation or chatter performance maximisation.   The objective function was calculated from the matrix of spindle speed and depth of cut cutting range. However, the current objective function did not represent the overall system as it evaluated the maximum value and, as a result, it is modified.

It can be seen that average characteristic multiplier values in the characteristic multiplier diagrams of previous optimisations were plotted and scattered at higher eigen value. Even though the characteristic multiplier represents the stable condition, other higher values of characteristic multiplier can be minimised to ensure that the whole system as minimum as geometry can be modified. To represent all eigen values, the maximum value is changed to an average value for representing average objective function in the matrix, as shown in Figure 6.1 (in minimise chatter box). For the chatter minimisation

problem, maximum characteristic multiplier (Equation 6.3) is changed to average characteristic multiplier, while for chatter performance maximisation, maximum value changes to average value of Equation 6.4 , as shown in Figure 6.1 (in maximise chatter performance box).

The performance maximisation results for the previous objective function showed all SQP solutions were trapped in local optima.   To solve this problem, a random initialisation is used in the next solution. During optimisation, the objective function of Equation 6.2 was optimised by considering depth of cut and spindle speed as main process variables, so this cannot be compared with other operating processes.   To represent and compare with other systems, the normalisation of MRR (MRR_n) is introduced. Thus, by combining with the average objective function and normalising with average of Equation 6.3, the equation becomes the modified objective function as follows:

$$f_{MRR}(\beta_i, \phi_i) = mean\left(\frac{MRR_n}{CM}\right) \qquad (6.8)$$

The function of MRR_n is to ensure the optimum MRR as unity within the maximum of the spindle speed and depth of cut. If the MRR_n searches the maximum value, it represents 1/CM for Equation 6.8. Each point is evaluated based on the average of MRR_n and eigen value. The average objective value is calculated to achieve a greater value by modified variable helical and variable pitch angles.   Current modified objective functions and refined DE algorithm are now used for previous problems.

6.5.1 Improved chatter minimisation results

The performance improved chatter minimisation of the DE and SQP algorithms is summarised in Figure 6.18. Note that the objective function is the average value for a characteristic multiplier, so a value less than unity cannot represent complete stability.

The DE algorithm achieved an average CM = 0.76 at 67 generations. The corresponding variable helix (46°, 35°, 43°) with variable pitch (67°, 233°, 60°) stability diagram is shown in Figure 6.19. Since the system is completely stable, the contour for values lower than unity is used here. This indicates the CM range of 0.55 to 0.9, which is better than previous optimisation. In comparison, the SQP algorithm achieved a mean CM of 0.82 after 4 iterations. The corresponding stability diagram is shown in Figure 6.20. This system shows lower CM where stability contour is between 0.75 and 0.9

than previous optimisation, as shown in Figure 6.6.   This indicates larger damping behaviour in the stability contour.

For the scenario where the tool's free-end pitch angle was uniform, Figure 6.18 shows that a poorer performance was obtained for both optimisation methods.   The DE algorithm converged at 65 generations with 0.98 evaluation value, corresponding to a variable helix of (55°, 25°, 55°), as shown in Figure 6.21.   The resulting stability prediction and characteristic multipliers are given in Figure 6.21.   It can be observed that the stable area is better than the previous result (Figure 6.7).   Meanwhile, for the SQP result, the mean CM value is (0.99) and converges at 4 iterations (Figure 6.18). The corresponding stability prediction of variable helix (55°, 53°, 29°) is shown in Figure 6.22.   This shows a larger unstable island than DE, but better than the previous result (Figure 6.8) that was trapped in local optimality when random initialisation was used.

6.5.2   Improved performance results

The performance of improved chatter performance maximisation with the DE and SQP algorithms is summarised in Figure 6.23.   Note that the objective function is the average value for Equation 6.8, so a value less than unity cannot represent complete stability.

The DE algorithm achieved complete stability (average MRR/CM= 0.77) by the 50th generation.   The corresponding variable helix (29°, 34°, 33°) and variable pitch (66°, 228°, 66°) stability diagram is shown in Figure 6.24.   The characteristic multiplier CM contour for less than unity is plotted with range 0.5 to 0.95.   In Figure 6.10, although the original DE result used a different objective function, the stable contour is plotted with a range 0.65 to 0.95.   Not only is there a lower range of stable contour, but also the currently optimised cutter showed larger gap toward the unit circle (CM diagram).   In comparison, the SQP algorithm achieved an objective function of Equation 6.8 of 0.58 after 18 iterations.   Although the value is lower than DE, stability of systems (Figure 6.25) is better than in the previous case (Figure 6.3b).   Again, this shows how random initialisation can escape local optimal for SQP optimisation.

For the case where the tool's free-end pitch angle was uniform, Figure 6.23 shows that a poorer performance was obtained for both optimisation methods.   The DE algorithm converged at 54 generations with evaluation value 0.54, corresponding to variable helix

(50°, 25°, 55°).   The resulting stability prediction and characteristic multipliers are given in Figure 6.26.   It can be seen that better stability is achieved since there is a lower unstable region than in the previous result (Figure 6.11).   On the other hand, for the SQP result, objective function value is 0.55 and converges at 7 iterations, as shown in Figure 6.23.   The corresponding tool geometry of the variable helix is 25°, 55°, 42° (Figure 6.27).   Randomised initial parameters can escape from the local optimal problem but the result is still poorer than DE and almost similar to Figure 6.21.

In the present study, numerical optimisations are made to optimise the chatter stability with the original and the improved strategy (algorithm and objective function) for different tool geometries (variable helix tools and variable pitch and variable helix tools), algorithms (DE and SQP).   The results can be summarised and ranked based on chatter stability, as shown in Table 6.4.   A refined DE algorithm and variable helix/pitch for chatter minimisation is most significantly followed by chatter performance maximisation.   In addition, variable helix and variable pitch tools geometry to moderately improve chatter performance for both algorithms and objective functions.   A smaller effect caused by variable helix tools (refined algorithm and modified objective function) for improving chatter performance.

6.6   Multi-Objective Optimisation

A main key issue is robustness to minimise chatter and performance to maximise MRR. To solve these, a Pareto front concept was introduced to overcome and fulfil the two objectives or problems by combining chatter minimisation and performance maximisation.   Epsilon constraints, as described in Chapter 5, are suitable for both DE and SQP algorithms and are now presented to solve the multi-objective optimisation problem.

6.6.1   Current approach

Minimised chatter and maximised MRR were stated and introduced as a single objective function for modifying variable helix and variable pitch tool geometry.   Both objectives are important for the machining process and need to be combined and referred to as multi-objective.   To manage both objectives, multi-objective optimisation was applied to solve and overcome the problem.   Pareto front optimal makes trades off between robustness of chatter and performance of material removal rate.   For the multi-objective problem, epsilon constraint method as conventional was applied due to its applicability

to convex and non-convex problems and easy to implement and suit both DE and SQP as optimisation algorithms. Using DE and SQP, the ε-constraint method was used to modify variable helix and variable pitch of three-flute milling tools.

Objective function offers multi-objective optimisation as stated in Equation 6.7. For ε-constraint value, MRR_n relates to normalised MRR (0.1, 0.2, 0.3, …, 1) which refers to ε value (1, 2, 3, …, 10), as shown in Figure 5.7. In each ε-constraint applied, chatter or CM is minimised by modified variable helix and variable pitch geometry. Figure 5.6c also indicates robustness as CM and performance as MRR_n in vertical and horizontal axis. Theoretically, the robustness always increases with increase in performance. CM is not indicated as stable when the eigen value is less than unity and both end points represent the maximum and minimum extreme solutions.

The results for variable helix tool, variable helix and variable pitch tool will be illustrated in a Pareto front solution and angle distribution for DE and SQP. Pareto front solution shows the convergence value at each of MRR_n for both algorithms in maximum and average CM. The distribution of helical angles and pitch angles corresponds to the convergence and CM diagram. For example, in optimising a three-flute variable helix and variable pitch, $MRR_n = 0.5$ converges at 0.67 average CM value, as shown in Figure 6.28a. This was evaluated and calculated from intersecting of $MRR_n = 0.5$ line and average CM value. In the intersection line, CM values varied from 0.65 to 1 to give 0.67 average CM value. Similarly, for $MRR_n = 0.9$ that converges at 0.73. In Figure 6.28b, MRR_n line intersected with contour range from 0.7 to 1. Due to the CM contour being located at an unstable region, a higher average CM was evaluated. To conclude, the CM converged value depends on the intersection between MRR_n and the CM contour.

6.6.2 Results

A variable helix and variable pitch cutter was optimised based on a multi-objective approach to perform a Pareto solution of DE and SQP, as shown in Figure 6.29. It can be clearly seen that DE results for average and maximum give comparable solutions. However, both SQP (mean and max) converge towards poorer results with a fluctuating pattern. Moreover, SQP(max) follows the same pattern as the theory in Figure 5.6c. At $MRR_n = 0.5$, DE shows minimum CM value of 0.67. In comparison to SQP, DE

converges at 0.59 as the lowest CM value which is almost double the SQP convergence at maximum performance. This Pareto front solution corresponds to the variable helix and variable pitch angles showed by Figure 6.30. In variable helix angle, as performance increases the geometrical value is more highly modified than variable pitch. This clearly indicates the greater robustness of DE than SQP and separates DE and SQP into global and local convergence curves, respectively.

For the scenario where a variable helix is considered, the multi-objective approach using ε-constraint produces a Pareto front solution of DE and SQP, as shown in Figure 6.31. It can be clearly seen that both algorithms give comparable solutions at MRR_n between 0.1 and 0.4. When performance increases, the large difference happens at $MRR_n = 0.6$ and 0.7. At $MRR_n = 1$, DE can search for minimum CM value 0.92 which is lower than the SQP results. This Pareto front solution corresponds to the variable helix and variable pitch angles showed by Figure 6.32. The minimum CM for MRR_n 0.6 and 0.7 relates to β_1, β_2 and β_3 values. This clearly indicates the robustness of the DE algorithm although the results used only the variable helix as modified geometry. Theoretically, chatter behaviour is proportionate to the material removal rate. However, it can be observed that the chatter area can be located at any place of spindle speed and depth of cut that causes high CM value to be produced.

6.7 Comparison of Variable Pitch and Uniform Helix Tool

Previous approaches as discussed in Chapter 2 that optimised uniform helix and variable pitch [29, 151] should be considered and compared with the current approach. Therefore, current approach with objective function to minimise chatter, maximise chatter performance and combine both single objectives are now presented to optimise uniform helix and variable pitch tools. These results are then compared with current optimised tools.

For minimising chatter, the performance of the variable helix and variable pitch tool and uniform helix and variable pitch tool using refined DE algorithms and average value of objective function of Equation 6.4 is shown in Figure 6.33. The uniform helix and variable pitch cutter achieved complete stability (average CM = 0.77) by the 57th generation. This corresponds to uniform helix (30°, 30°, 30°) and variable pitch (69°, 146°, 145°). It can be seen that the variable helix and variable pitch perform better than the variable pitch tool. This system is not completely stable where the characteristic

multipliers are considerably higher than those obtained for variable helix and variable pitch tools.

For the case with the objective function that maximises performance, the tool's variable pitch angle shows result in Figure 6.34. The uniform helix and variable pitch tool converged at 26 generations with 0.75 evaluation value, corresponding to a uniform helix (30°, 30°, 30°) and variable pitch (68°, 147°, 145°). This is poorer than variable helix and variable pitch and almost similar to variable pitch geometry for chatter minimisation result.

A uniform helix and variable pitch tool is optimised based on ε-constraint of multi-objective to perform the Pareto front solution DE, as shown in Figure 6.35. As performance value or normalised material removal rate increases, both results showed decreased robustness. It is clearly seen that the uniform helix and variable pitch tool result shows a similar pattern to the variable helix and variable pitch tool. Similar results clearly occur particularly at $MRR_n = 0.1$ and 0.9. However, at $MRR_n = 0.5$ and 1, variable helix and variable pitch tool performs better than uniform helix and variable pitch tool. The largest difference happens at maximum performance. Overall, it can be clearly seen that the variable helix and variable pitch Pareto front solution is better than uniform helix and variable pitch cutter. The corresponding pitch angle for both approaches is shown in Figure 6.36. It can be seen that the influence of helical angle contributes to minimise chatter for variable helix and variable pitch tool.

6.8 Discussion

To recap, the DE algorithm was able to design a variable helix tool (with variable pitch at its free end) that showed a great improvement in chatter stability. However, the importance of also allowing a variable pitch at the free end of the tool has been highlighted. Without this variable pitch at the free end, the variable helix geometry is much less effective because there is less potential to 'disrupt' the time-delay parameters in the governing stability equations, for both single and multi-objective problem. For multi-objective problems, variable helix angle values proportionately change when chatter performance increases, as shown in Figures 6.30 and 6.32.

Both the DE and SQP algorithms were able to improve the chatter stability. However, by referring to the maximum objective function value, the optimisation results for the

DE algorithm are consistently better than for the SQP algorithm. For the variable helix tool with a uniform helix at the free end, the SQP algorithm is clearly trapped in a local optimum. Furthermore, the performance strongly depends on the chosen initial value that uses gradient-based optimisation where randomised initialisation improved the SQP results. In multi-objective optimisation, both the DE (max and mean) and SQP (mean) algorithms were able to improve the chatter stability when increasing material removal rate. DE algorithm converges to global Pareto front, while the SQP algorithm clearly converges in local Pareto front. The comparison between theoretical and multi-objective solution showed that different pattern except for SQP (max). With decreasing performance, the robustness or eigen value should increase, however the nonlinearities of unstable region of robustness (CM) contour causes this to happen. In Figure 6.28a, b, at certain performance (MRR_n) can be seen to intersect with the high robustness contour (CM) resulting higher chatter performance.

In comparison with the original objective function, modified objective function performed better when the objective function applied average objective function and normalised material removal rate. Table 6.4 shows a lower range of stable contour and a large unstable region reduced to be a small region for both single objective functions. Similar results were obtained for chatter performance maximisation problem. Additionally, SQP using random initialisation can escape local optima particularly for improved chatter performance maximisation results but not for chatter minimisation results.

Different objective functions can search for different optimal geometry values. From current results, improved chatter minimisation (Figures 6.19) is the most significant compared to chatter performance maximisation (Figures 6.24). Therefore, this objective function (average (CM)) is applied for optimising variable helix and variable pitch tool in experimental validation in the next chapter. When comprised with lower material removal rate, lower stability can be achieved for multi-objective problems. At optimum material removal rate, DE performed better convergence than SQP the same as single objective function due to its global and evolution-based optimisation algorithm.

Optimum uniform helix and variable pitch stability performed poorer than the current approach (variable helix and variable pitch) for the problems of chatter minimisation

and performance maximisation. Although showing the same Pareto front solution pattern, the convergence values for variable helix and variable pitch are a better and more robust solution when increasing performance (multi-objective optimisation). It can be observed that the convergence of both results actually depends on unstable behaviour at high depth of cut. In comparison with the previous method used by the researchers that applied only variable pitch, outstanding performance can be achieved after using variable and variable pitch. Use of a variable helix and variable pitch tool is suggested for a great performance for chatter suppression.

An optimised variable helix and variable pitch tool can suppress chatter and all nonlinear instability (secondary hopf bifurcation, period doubling bifurcation and cyclic fold bifurcation) in the original condition becomes extinct. However, cyclic fold and period doubling bifurcation still occur for the variable helix tool due to use of low radial immersion conditions.

6.9 Summary

It can be observed that optimised variable helix and pitch milling tools can totally eliminate chatter for both algorithms, but DE outperformed SQP when compared with the CM diagram where a larger gap to unity indicates higher damping properties. In other cases, implementing variable helix cannot beat the variable helix and variable pitch results.

The maximisation of performance has exhibited poor results compared to chatter minimisation. SQP offers a poor solution for all the cases, where the solutions became trapped in local optimal near the original tool geometry. Better maximisation results can be achieved using randomised initialisation. From the results, DE that optimised variable helix and variable pitch milling tools using chatter minimisation that demonstrated a larger damping behaviour and a larger margin of stability is considered for experimental validation.

The introduction of mixed population and bounce back approach improved the current DE algorithm. A refined DE algorithm and modified objective function can solve and improve the results of chatter minimisation and performance maximisation. Multi-objective optimisation of minimisation of chatter and maximisation material removal rate simultaneously is considered to achieve a Pareto front solution. All optimisation

results showed DE is better than SQP in a single and multi-objective strategy. When compared to uniform helix with variable helix as in the previous approach, a better solution is for variable helix and variable pitch tool in all types of objective function, both single and multi-objective optimisation.

In this chapter, three problems in minimising chatter, maximising chatter performance and multi-objective optimisation have been demonstrated and optimised. DE and SQP algorithms have been considered in optimising variable helix and variable pitch milling tools, with cases for in [29]. In the next chapter, experimental validation of optimised the variable helix and variable pitch milling will be used for chatter minimisation objective function (average CM).

Table 6.1 Cutting, modal and tool parameters for optimisation

Tool and cutting parameters	
Tool diameter d (mm)	19.05
Radial immersion RI (mm)	1.00
Tangential cutting stiffness K_t (MN/m^2)	550
Tangential cutting stiffness K_n (MN/m^2)	200
Modal property in x-direction mode	
Natural frequency f_n (Hz)	169.3
Modal effective mass m_m (kg)	6.5363
Damping Ratio ξ	0.0056

Table 6.2 DE parameter settings for machining optimisation

Parameter	Initial value	Optimum
Strategy	7- DE/rand/1/bin	
Number of Generation (NG)	50	70
Number of Population (NP)	10*RP	10*RP
Crossover factor (CR)	0.7	0.9
Scaling factor (SF)	0.6	0.9

Table 6.3 Parametric study of DE to optimise variable helix for 'strategy 7'

Performance of DE	DE parameters				
	Crossover rate (CR)				
	0.2	**0.4**	**0.5**	**0.7**	**0.9**
Minimum CM	0.7533	0.7481	0.7489	0.7487	0.7481
	Scaling factor (SF)				
	0.5	**0.6**	**0.7**	**0.8**	**0.9**
Minimum CM	0.7543	0.7490	0.7532	0.7487	0.7486
	Number of Population (NP)				
	4* RP	**5* RP**	**8* RP**	**10*RP**	**15* RP**
Minimum CM	0.7711	0.7489	0.7491	0.7487	0.7487
	Maximum Number of Generation (NG)				
	10	**50**	**70**	**100**	**150**
Minimum CM	0.7514	0.7487	0.7470	0.7470	0.7470

Table 6.4 Chatter stability summary and ranking during numerical optimisations

Figure	Algorithm		Modification of Algorithm		Objective Function		Tool geometry		Chatter Stability Result		Rank
	DE	SQP	Original	Improved	Chatter minimisation	Chatter performance maximisation	Variable helix and variable pitch	Variable helix	Unstable area (%)	Stable contour range (CM)	
6.6	×		×		×		×		0	0.80-0.90	**5**
6.7		×	×		×		×		0	0.90-0.95	**6**
6.8	×		×		×			×	15	-	**11**
6.9		×	×		×			×	50	-	**16**
6.11	×		×			×	×		0	0.65-0.95	**3**
6.12		×	×			×	×		25	-	**14**
6.4b	×		×			×		×	10	-	**9**
6.4b		×	×			×		×	10	-	**9**
6.20	×			×	×		×		0	0.55-0.90	**1**
6.21		×		×	×		×		0	0.75-0.95	**4**
6.22	×			×	×			×	1	-	**7**
6.23		×		×	×			×	15	-	**11**
6.25	×			×		×	×		0	0.50-0.95	**2**
6.26		×		×		×	×		17	-	**13**
6.27	×			×		×		×	1	-	**7**
6.28		×		×		×		×	25	-	**14**

Figure 6.1 Structure of numerical optimisation results
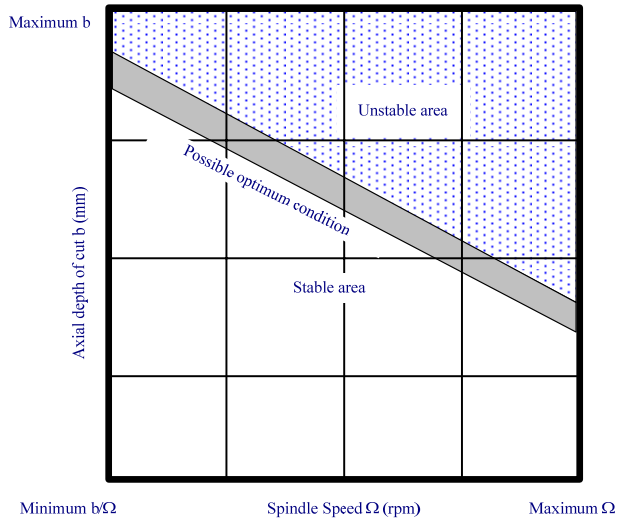
Figure 6.2 Constraint arrangement for multi-objective optimisation

a) **Depth of cut (0-45 mm)**
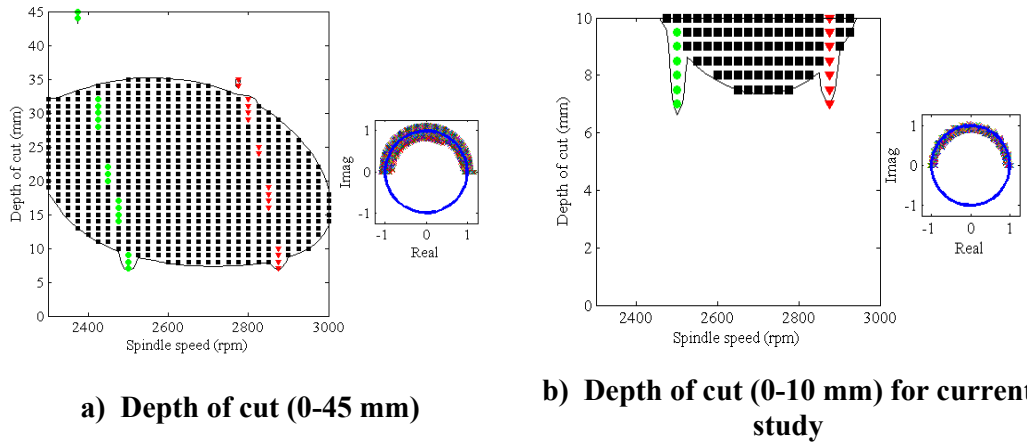
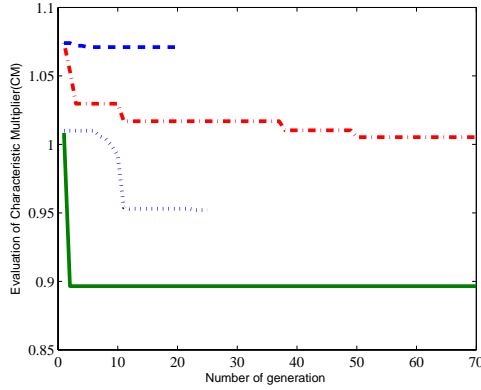b) **Depth of cut (0-10 mm) for current study**

Figure 6.3 Original stability prediction for three-flute variable helix (25°,30°,35°) and variable pitch (120°, 100°, 140°) [29]. (■) hopf bifurcation (▼) period doubling bifurcation (●)period one bifurcation
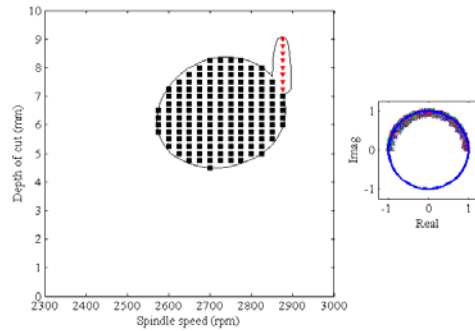
Figure 6.4 Performance of DE and SQP in chatter minimisation. (—) DE variable helix and variable pitch, (-.-)DE variable helix, (---) SQP variable helix and (…) SQP variable helix and variable pitch
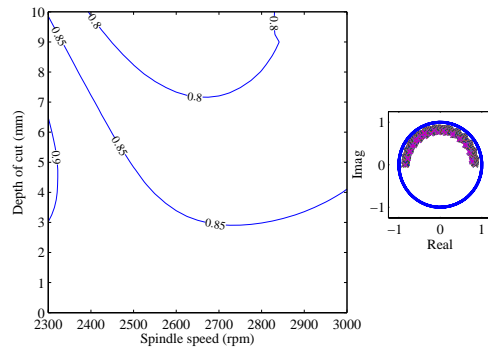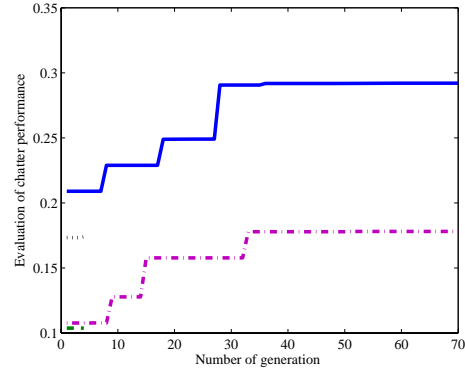

Figure 6.5 Optimised stability prediction for chatter minimisation of three-flute variable helix (52°, 52°, 41°) and variable pitch (107°, 163°, 90°) using DE. (⬭) stability contour
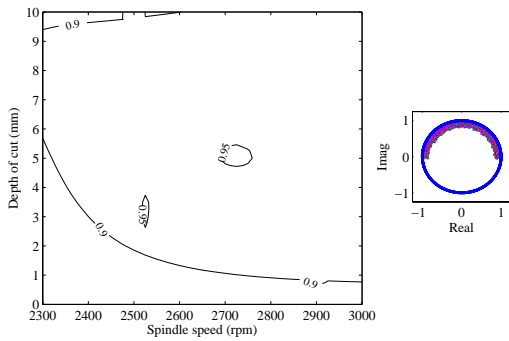
Figure 6.6 Optimised stability prediction for chatter minimisation of three-flute variable helix (25°, 38°, 55°) and variable pitch (120°, 105°, 135°) using SQP. (⬭) stability contour

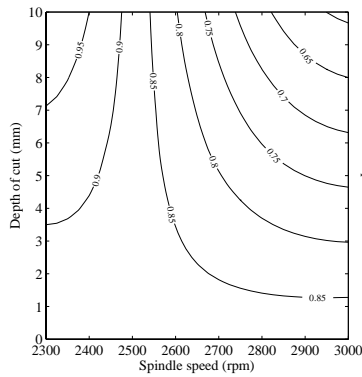**Figure 6.7 Optimised stability prediction for chatter minimisation of three-flute variable helix (53°, 27°, 54°) using DE. (■) hopf bifurcation (▼) period doubling bifurcation**

106
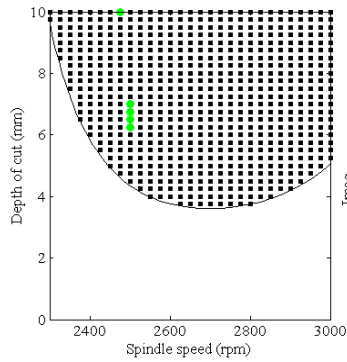
Figure 6.8　Optimised stability prediction for chatter minimisation of three-flute variable helix (28°, 32°, 37°) using SQP. (■)hopf bifurcation (●)period one bifurcation

Figure 6.9　Performance of DE and SQP for maximising performance of three-flute variable helix. (━) DE variable helix and variable pitch, (-.-)DE variable helix, (---) SQP variable helix and (…) SQP variable helix and variable pitch

Figure 6.10　Optimised stability prediction for maximising chatter performance of three-flute variable helix (27°, 25°, 26°) and variable pitch (83°, 194°, 83°) using DE. (◎) stability contour
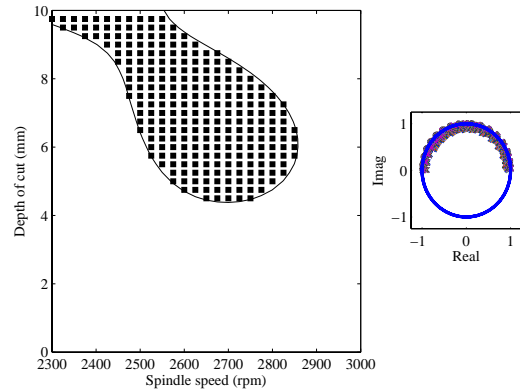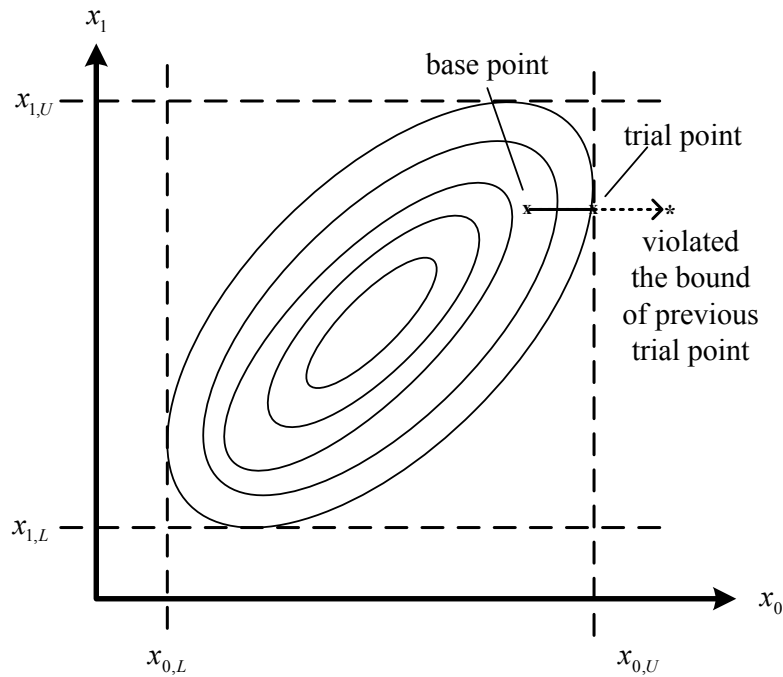

Figure 6.11　Optimised stability prediction for maximising chatter performance of three-flute variable helix (43°, 25°, 55°) using DE. (■)hopf bifurcation

D = size (pop,2);

For n = memIndex;

Pop(n,:) = 0.75 * baseMem + 0.25 *rand (1,D) * (XVmax-XVmin);

**Figure 6.12 Introduction of random noise of population to next generation**

Figure 6.13 Bounce back strategy of trial vector to replace out of bounds trial from base vector and violated bound trial point

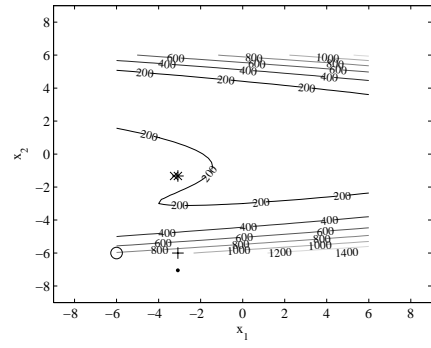For k = 1 : I_NP % population filled with best member of last generation

For j =1:I_D

If (u(j,i) < XVmin) % if parameter exceeds lower bound

u(j,i) = Xvmin;

End

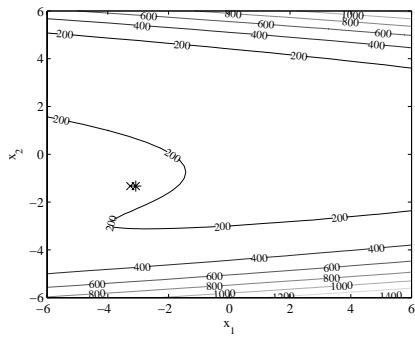If (u(j,i) > XVmax) % if parameter exceeds upper bound

u(j,i) = XVmax;

End

End

Figure 6.14 Pseudocode for bounce back strategy
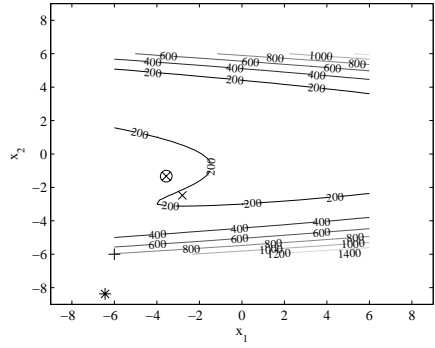
a) **Mutation**

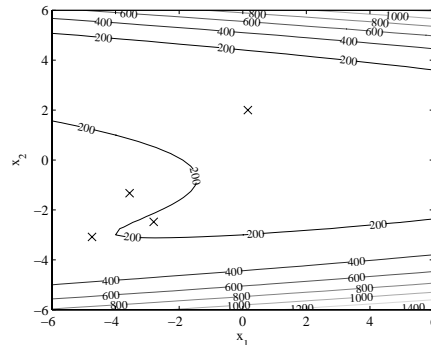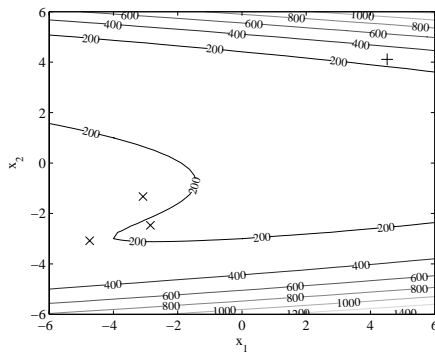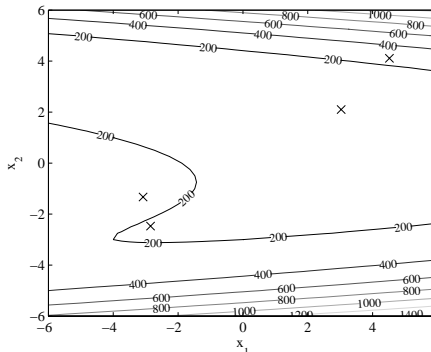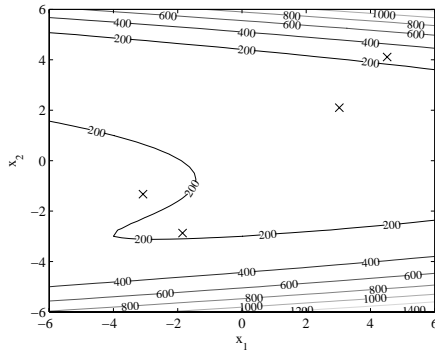

b) **Crossover**

c) **Selection**

d) **Generation**

e) **New generation with noise**

f) **Generation 2**

g) **Generation 5**
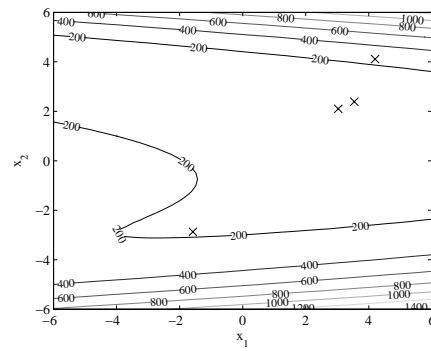
h) **Generation 10**

Figure 6.15 Typical example of how improved DE works on Himmelblau function
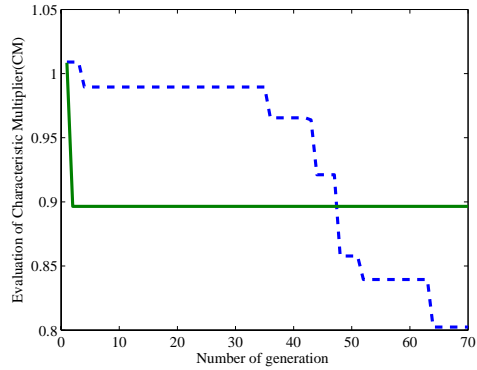
Figure 6.16 Performance of DE and improved DE on optimising three-flute variable helix and variable pitch. (━) DE and (---) refined DE variable helix with variable pitch at end
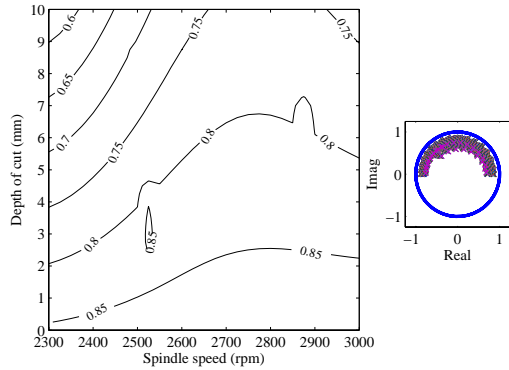
Figure 6.17 Optimised stability prediction for improved chatter minimisation of three-flute variable helix (41°, 43°, 40°) and variable pitch (68°, 225°, 87°) using DE. (◎) stability contour
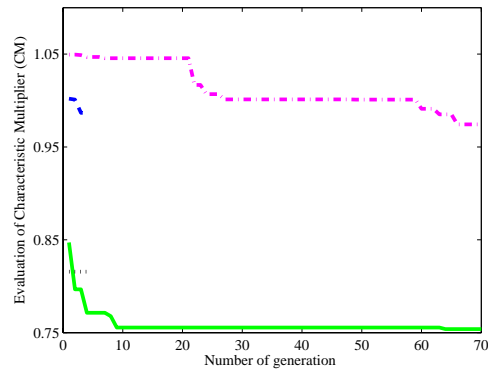
Figure 6.18 Performance of three-flute of DE and SQP using improved chatter minimisation. (━) DE variable helix with variable pitch, (-.-)DE variable helix, (---) SQP variable helix and (…) SQP variable helix with variable pitch
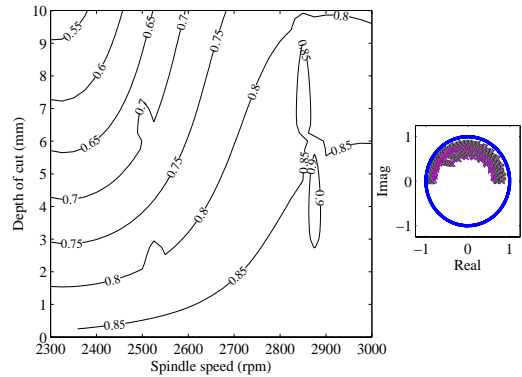
Figure 6.19 Optimised stability prediction for improved chatter minimisation of three-flute variable helix (46°, 35°, 43°) and variable helix (67°, 233°, 60°) using DE. (◎) stability contour

110

Figure 6.20 Optimised stability prediction for improved chatter minimisation of three-flute variable helix (54°, 40°, 49°) and variable pitch (142°, 143°, 85°) using SQP. (◎) stability contour

Figure 6.21 Optimised stability prediction for improved chatter minimisation of three-flute variable helix (55°, 25°, 55°) using DE. (▼) period doubling bifurcation
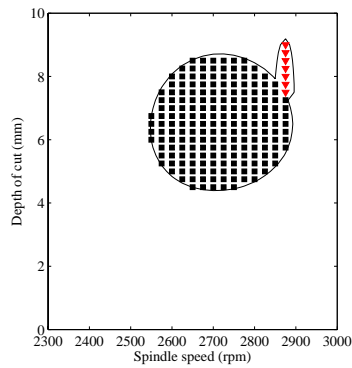
Figure 6.22 Optimised stability prediction for improved chatter minimisation of three-flute variable helix (55°, 53°, 29°) using SQP. (■)hopf bifurcation (▼) period doubling bifurcation
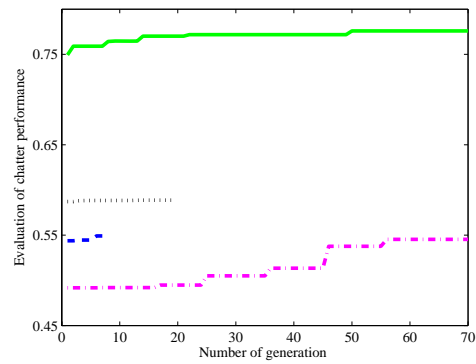
Figure 6.23 Performance of DE and SQP of improved performance of three-flute milling tools. (━) DE variable helix and variable pitch, (-.-)DE variable helix, (---) SQP variable helix and (…) SQP variable helix and variable pitch
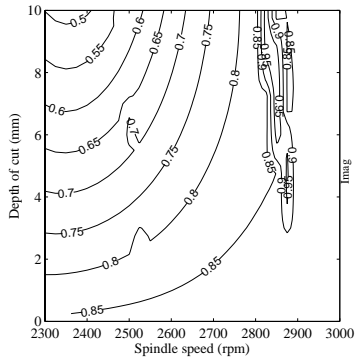
Figure 6.24 Optimised stability prediction for improved chatter performance of three-flute variable helix (29°, 34°, 33°) and variable pitch (66°,228°, 66°) using DE. (◉) stability contour
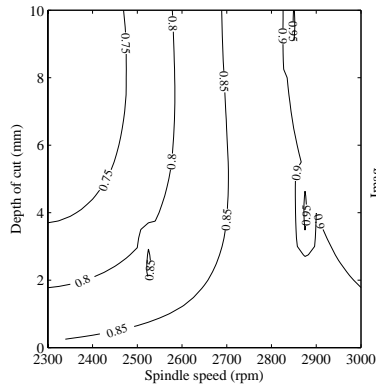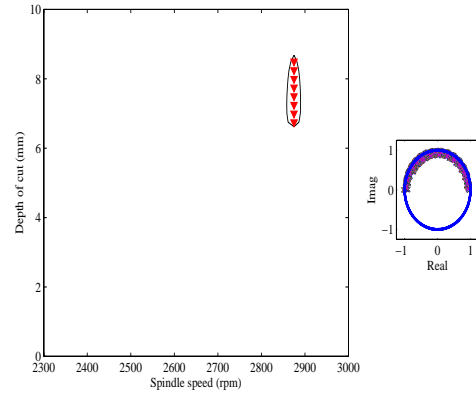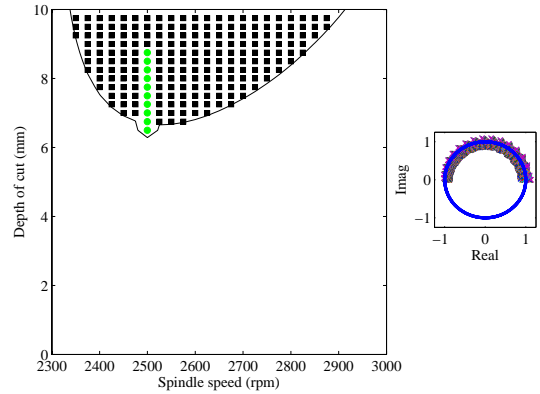
Figure 6.25 Optimised stability prediction for improved chatter performance of three-flute variable helix (25°, 53°, 29°) and variable pitch (121°, 178°, 61°) using SQP. (■)hopf bifurcation (●)period one bifurcation
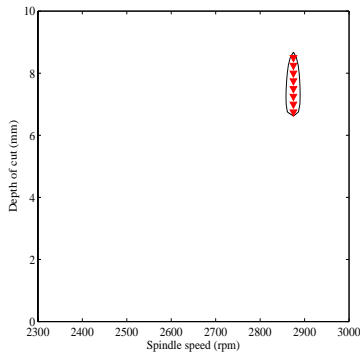
Figure 6.26 Optimised stability prediction for improved chatter performance of three-flute variable helix (55°, 25°, 55°) using DE. (▼) period doubling bifurcation.
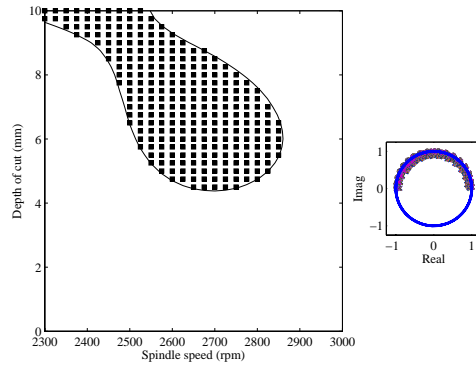
Figure 6.27 Optimised stability prediction for three-flute variable helix (25°, 55°, 42°) using improved chatter performance of SQP. (■)hopf bifurcation.

a) MRR$_n$ = 0.5   **b) MRR$_n$ = 0.9**
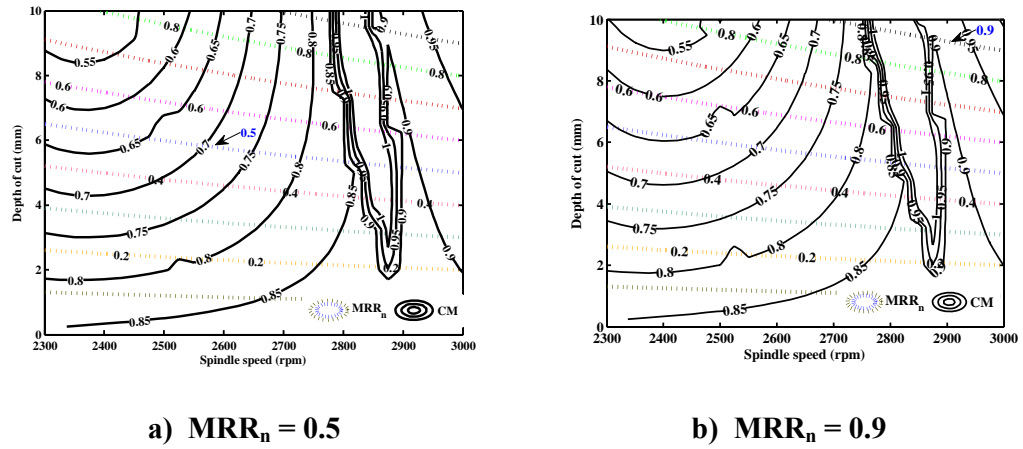
Figure 6.28 Typical stability limit of DE multi-objective optimisation of ε-constraint for optimising three flute variable helix and variable pitch. ( ) normalised material removal rate ( ) stability contour.
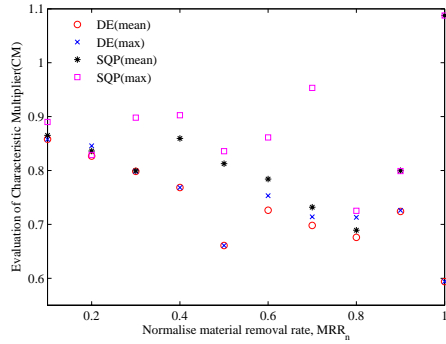
Figure 6.29 Pareto front solutions of DE and SQP multi-objective optimisation of ε-constraint for optimising three flute variable helix and variable pitch.
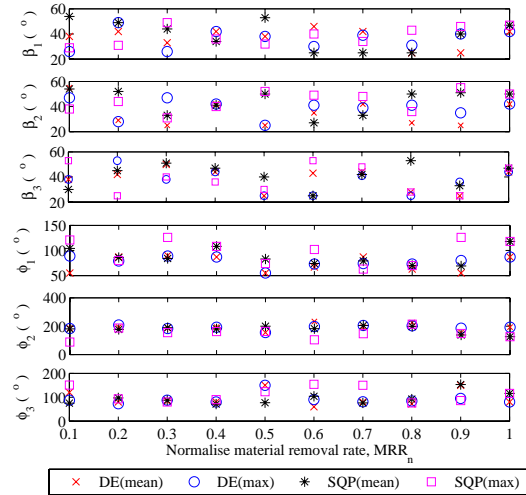
Figure 6.30 Distribution of optimised helical angle for three-flute variable helix and variable pitch from multi-objective optimisation.
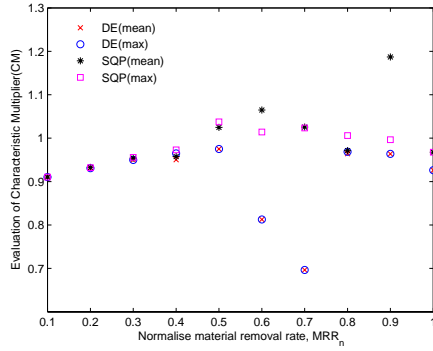
Figure 6.31 Pareto front solutions of DE and SQP multi-objective optimisation of ε-constraint for optimising a variable helix for multiple objective
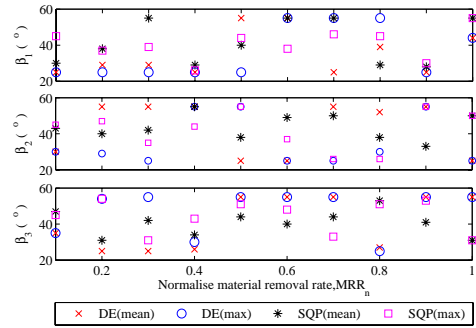
Figure 6.32 Distribution of optimised helical/pitch angle for three-flute variable helix from multi-objective optimisation.
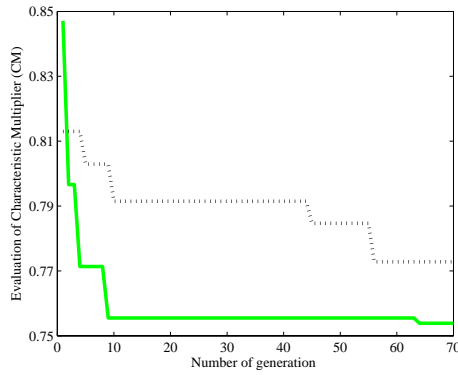
Figure 6.33 Performance of DE for optimising three-flute variable pitch and variable helix/pitch by minimisation of CM. (▬▬) uniform helix and variable pitch (——) variable helix and variable pitch.
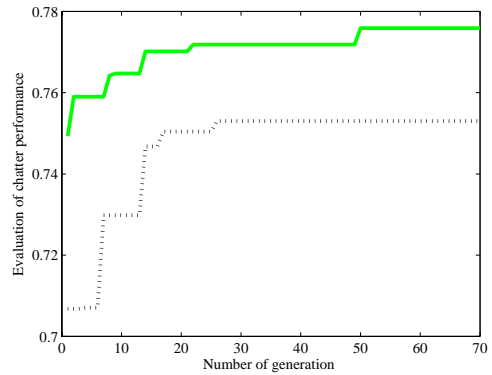
Figure 6.34 Performance of DE for optimising three-flute variable pitch and variable helix/pitch by maximisation of performance...(▬▬) uniform helix and variable pitch (——) variable helix and variable pitch

114
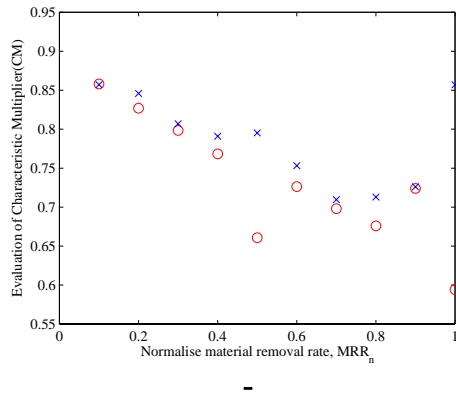
Figure 6.35 Pareto front solutions of DE multi-objective optimisation of ε-constraint comparison between three-flute uniform helix and variable pitch (×) and variable helix and variable pitch (○).
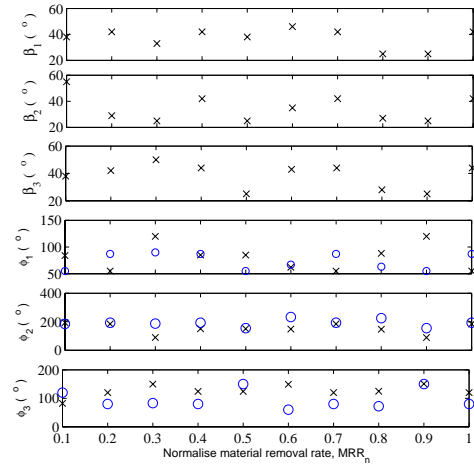
Figure 6.36 Distribution of optimised variable pitch angle for three-flute between uniform helix and variable pitch (×) and variable helix and variable pitch (○) from multi-objective optimization.

CHAPTER 7

EXPERIMENTAL VALIDATION: OPTIMISED AND VARIABLE HELIX MILLING TOOLS

7.1 Introduction

The objective of this chapter is to demonstrate experimental validation of optimised variable helix and variable pitch milling tools based on Differential Evolution (DE) minimisation of self excited vibration or chatter as described in [151]. The focus of the current application is to suppress unwanted chatter vibrations during milling operations using a flexible workpiece. Chapter 6 optimised the helix and pitch angles by combining the SDM and DE algorithms. The present chapter will describe experimental work to demonstrate the performance improvements of the optimum tool. In addition to validation experiment of the optimisation procedure, a further experimental study is performed to better validate the modelling procedure of variable helix tools.

The chapter is structured as follows. The optimisation and modelling procedure is first summarised for the sake of completeness. An experimental procedure and results for optimised tool are then described. Further experiments are carried out for variable helix tools to validate the current SDM modelling. Following results on overall discussion is then presented.

7.2 Experimental Validation for Optimised Tool

The present section will investigate the performance of such an optimised tool in machining experiments. Both tools of regular helix/pitch geometry and optimised geometry using the procedure outlined in next section were used. An experimental procedure is then described where a highly flexible workpiece is used to induce severe chatter instability, and an optimally designed variable helix tool is used to avoid chatter. Current experimental results formed a conference paper [162] and the abstract in Appendix A.III.

7.2.1 Optimisation method

A brief overview of the chatter modelling and optimisation of variable helix and variable pitch milling tools is now described. A more detailed account is given in [151] and previous chapter.

Chatter stability modelling was implemented using SDM as proposed by Insperger and Stepan [7] and implemented by Sims *et al.* [29]. This approach involves discretisation of the structural dynamics so that the time delay effect, that arises from the tool rotation, can be represented as a discrete delay. This leads to an eigenvalue problem that defines the stability for a given set of cutting conditions.

In Chapter 6 and [151], a DE optimisation procedure was combined with SDM to modify and optimise the variable helix/pitch tool geometry. Constraints of helix/pitch must be taken into account to ensure a realistic cutter geometry is produced for fabrication. This optimisation process is summarised schematically in Figure 7.1, while DE parameter settings, as shown in Table 6.2. The objective function of average value of Equation 6.4 and its constraints are used for chatter minimisation of three-flute milling tool.

7.2.2 Experimental procedure

In Figure 7.2, an experimental flexure is illustrated that was designed to behave with compliance in a single dominant mode of vibration. Cutting, modal and tool parameters are summarised in Table 7.1. This was used for cutting experiments on a 5-axis CNC vertical milling machine, the Haas VF6. The flexure consists of a flexible steel base that was machined from a rectangular cross-section beam welded to a rigid steel bases and cutting specimen mounted on top as used by Huyanan and Sims [38, 163]. A 50.0 x 50.8 x 25.5 mm^3 aluminium (7075-T6) cutting specimen was mounted on the flexure. This was to be down-milled at 10 percent radial immersion using a 16 mm diameter 3 flute end mill cutter. The tool was either of regular helix/pitch geometry, or optimised geometry using the procedure outlined previously. To maintain static milling force magnitudes and to prevent large free vibration amplitude because of the interrupted cutting that was applied on the workpiece, a nominal chip thickness of 0.04 mm per tooth was used. A set of spindle speeds and axial depths of cut were tested to determine if the cutting was stable or unstable. At the end of each cutting test, it was necessary to perform a clean-up pass to ensure a sufficient free surface for a later test.

During each cutting test, the flexure acceleration was measured the occurrence of chatter, using a piezoelectric accelerometer (PCB 352C68) connected to a DSPT Siglab 20-22A and laptop as shown in Figure 7.3. To capture a periodic pulse signal matching the tool revolution, a Hall-effect probe triggered by 2-equally space slots on the rotating tool holder was used.   This allowed once per revolution samples (1/Rev) of the accelerometer signal for post-processing. Then, using 1/Rev acceleration samples and its cycle delay, two-dimensional Poincaré maps were constructed [164]. In addition, a Fast-Fourier Transform (FFT) method in Matlab was applied to the acceleration time samples to illustrate the acceleration spectra, using a Hanning window to reduce signal leakage.

The cutting tests were evaluated as either stable or unstable based on the acceleration signal, 1/Rev samples and spectrum analysis. If 1/Rev samples approached a fixed point with a variance less 10^{-3} m/s^2 and the FFT-amplitude was dominated by tooth passing harmonics, the test was declared stable. Not clear or unstable cutting was indicated from the 1/Rev variant between 10^{-3} to 10^{-2} m/s^2 or cutting runout harmonics dominating the FFT-amplitude.   Secondary hopf-bifurcations and period-doubling bifurcations were indicators of unstable cutting.   Hopf-bifurcation instability was indicated by the unstable orbit on the 2-D Poincaré map and period-doubling bifurcation instability was specified from two fixed points of 1/Rev and 2-D Poincaré map.

7.3   Optimised Tool Results

The results for regular and optimised tool will be now presented to measure the effectiveness of current method to mitigate chatter.   Optimised tool results from numerical optimisation are first presented. The identification for vibration signals of workpiece are then presented before the cutting experiment for stability results are then performed.

7.3.1   Optimised tool geometry

The corresponding three flute of regular cutter with uniform helix (30°,30°,30°) and uniform pitch (120°,120°,120°) is shown in Figure 7.5a,c. A variable helix and variable pitch milling cutter was first designed using the optimisation procedure described in Section 7.2.1 and an average value of Equation 6.3 was used as objective function.

From numerical optimisation in Figure 7.4, the performance achieved an average CM =0.923 at 47 generations. This corresponds to the optimised tools of variable helix (43°,44°,48°) and variable pitch (84°,221°,55°), as shown in Figure 7.5b,d. Both cutters were ensured to have 10-times stiffness when compared with the dominant frequency of the flexure to test chatter vibration behaviour under specific spindle speeds and depths of cut.

7.3.2 Acceleration signal identification

For the down-milling operation of the regular 3-flute end mill, the acceleration signals were measured for regular and optimised tools performance. Figure 7.6 shows the cutting tests were carried out in 5 cases for regular tool: A (2000 rev/min, 0.8 mm), B (2700 rev/min, 0.8 mm), C (3000 rev/min, 0.5 mm), D (3300 rev/min, 0.2 mm) and E (3900 rev/min, 0.8 mm). For the optimised tool where variable helix and variable pitch were used, Figure 7.7 shows the results for 4 cases: F (2000 rev/min, 1.0 mm), G (2800 rev/min, 0.6 mm), H (3600 rev/min, 0.9 mm) and I (3300 rev/min, 0.9 mm).

Stable or chatter free cutting is demonstrated in cases D and F, as shown in Figures 7.6 and 7.7, respectively. A small acceleration variance is shown with the Poincaré section approaching a fixed point. The FFT spectrum shows the frequency is dominated by tooth passing frequencies. These frequencies are lower than the flexure frequency, which related to cutting forces for each tooth beating the workpiece.

In cases A, C and I in Figures 7.6 and 7.7, unstable Hopf-bifurcation instability was determined in theory is capable to analyse the chatter frequencies. For example of FFT spectrum in Figure 7.6(cases A and C), the chatter frequency was closed to the flexure natural frequency. For this instability behaviour, the 1/Rev acceleration samples are interacting with the spindle frequency to clearly produce an unstable circular orbit on the Poincaré section.

Unstable period-doubling behaviour is confirmed by the 1/Rev samples and the Poincaré section approached two fixed points as shown case B in Figure 7.6. According to the FFT spectrum, the chatter frequency was closed to the flexure natural frequency as previously described for Hopf-bifurcation.

The resonance corresponds to chatter frequency and the tooth passing frequency located closed each other, where the tooth passing frequency beats the raising of chatter frequency, as shown on cases E, G and H of Figures 7.6 and 7.7. A large vibration signal dominated in FFT spectrum and 1/Rev samples. This unstable period-one behaviour is confirmed by the 1/Rev samples and the Poincaré section approached single fixed points outside stable boundary.

7.3.3 Chatter stability results

From identification of acceleration signal, cutting condition during experiment for each case is then obtained. Both theoretical prediction and experimental results were compared for both tools and their chatter stability diagrams are now presented.

Using SDM, the original cutter chatter stability was predicted and superimposed with experimental stability results at 10 percent radial immersion, as shown in Figure 7.8a. It can be clearly seen that there is an unstable area at high depth of cut, with critical depth of cut 0.3 mm, mostly at high spindle speed (2800-4000 rev/min).

For the down-milling operation of the regular 3-flute end mill, the result indicates a good agreement between predicted stability and experiment, as shown in Figure 7.8b. Stable or chatter free cutting conditions were shown outside the boundary of unstable regions. There are three unstable regions with hopf-bifurcation, period-one bifurcation and period-doubling bifurcation based on acceleration identification approach. The unstable behaviours were observed either by hopf-bifurcation or period-doubling which were located inside instability region, whilst not clearly stable condition happened around stability lobes. However, at high spindle speed, resonance occurred due to similarities of the chatter and spindle frequencies. Theses cutting test disagree with the theoretically stability predictions as indicated by 'Δ' and other 5 cases occurred in Figure 7.8b. It can be seen that the critical depth of cut for regular or original cutter was experimentally confirmed to be less than 0.3 mm.

Figure 7.9a illustrates the effectiveness of modeling and optimisation algorithm for the variable helix and variable pitch tool. The optimised cutter is predicted to totally suppress chatter at three unstable regions in the regular cutter. The critical depth of cut increases 8-fold when compared with the regular cutter. In simulation, the optimised

cutter has the capability to cut the workpiece with 1800 to 4000 rev/min without facing any chatter vibrations.

In Figure 7.9b, experimental work shows the stability results for the optimised cutter. In comparison to the regular cutter, at least 5-fold increase in stable cutting with critical depth of cut of 0.8 mm to enhanced high material removal rate. On the other hand, not clearly stable cuttings were significantly observed at the critical depth of cut. The unstable hopf-bifurcation and period-one bifurcation are observed at high depth of cut and spindle speeds.

The surface finish for regular cutter and optimised tool is shown in Figure 7.10. This has clearly seen that the improvement when optimised variable helix and variable pitch compare with original cutter at 3400 rev/min. The chatter mark on workpiece existed when machining at unstable condition of original cutter.

7.4 Further Experimental Validation for Variable Helix Tool

From previous experiment results, it can be clearly seen a good agreement between prediction and experiment for regular tool, but only moderate agreement for optimised or variable helix and variable pitch tools. Although the optimised tool can increase material removal rate compare to regular tools, further experiments are really important to have a proper validation of the SDM modelling procedure for variable helix tools. In addition to that, the transition between vibration conditions between stable to unstable behaviour as marginal stable are not clearly identified. To identify the marginal stability in milling process, a displacement sensor will be used to replace accelerometer. Before continue with theoretical prediction and cutting experiment validation of the chatter stability, cutting force of four flute variable helix/pitch coefficients should be initially determined by cutting force tests. The results for this experiment formed a conference paper, and abstract is given in appendix A.IV.

7.4.1 Experimental procedure

The cutting force coefficient tests were conducted on a Mori Seiki SV500 3 axis CNC vertical milling machine. A 12 mm 4 flute end milling variable helix (37° ,40° ,37° ,40°) and variable pitch (78.4° ,80.4° , 78.4° ,80.4°) tool, as shown in Figure 7.11 was cut 6061-T6 aluminium workpiece, the force responses data were acquired using a

Kistler 3-component dynamometer (9257B). Cutting condition of 2 mm axial depth of cut and fully radial immersion were used from 0.02 to 0.16 mm/tooth in steps of 0.02 mm/tooth with spindle speeds of 2500 rev/min.

Photograph of variable helix validation experimental on same milling machine for cutting force tests is shown in Figures 7.12. Figure 7.13 shows the corresponding diagram of experimental arrangement where an aluminium (7075-T6) cutting specimen block (50.0 mm, 50.8 mm and 25.8 mm) mounted on the highly flexible workpiece condition. This was 5 percent radial immersion down-milled using above milling cutter to reduce static deflection when applying high axial depth of cut than previous experiment. In order to maintain the static milling force magnitude, the chip load of 0.04 mm per tooth was maintained at any spindle speed. At each set of spindle speed and axial depth of cut, the tests were conducted to examine either the cutting stable or unstable. It was essential to have a clean-up pass to guarantee a clean free surface for a previous test at the end of each cutting test.

In Figure 7.12, the eddy-current displacement (ECL 100 series) sensor signal was used to measure the onset of chatter vibrations of the flexure while acceleration was used only to verify the signal. To measure the vibration signal from stable to marginal stable, then toward unstable condition, displacement vibration signal was used with anti-alias filter at a sampling rate 5.12 kHz using a DSPT Siglab 20-22A connected to a laptop computer. As discussed in previous section, the stability in milling test experiment was examined based on the 1/Rev samples, the Poincare section and frequency spectra. A pulse signal was produced from a Hall-effect probe triggers the slots on the rotating tool holder to produce the 1/Rev samples and the displacement Poincare section versus its half-cycle delay [164]. At the similar time, the displacement frequency spectral was obtained from the raw displacement signal Fast-Fourier transform using a Hanning window.

The cutting experiment was analysed as either stable or unstable by referring to the displacement sensor, 1/Rev samples and spectrum analysis. The test can be declared as stable behaviour when root mean square (RMS) displacement signal approached less than 5 μm toward a fixed point and the FFT-amplitude was dominated by tooth passing

harmonics. For marginal stable cutting, this was declared when the RMS displacement signal range between 5 to 15 μm or cutting force harmonics dominates in the FFT-spectrum. If displacement 1/Rev higher than 15 μm, the unstable cutting behaviour was indicated either secondary hopf-bifurcations or period-doubling bifurcations or period-one. Hopf-bifurcation instability was represented by the unstable orbit on the 2-D Poincaré map, period-doubling bifurcation instability was determined from two fixed points of 2-D Poincaré map and two lines of 1/Rev during cutting, while period-one bifurcation instability was specified from single fixed points of 2-D Poincaré map and single lines of 1/Rev during cutting period outside stable boundary.

7.4.2 Cutting force coefficient determination

It is necessary to identify the relationship between the cutting forces and uncut chip area that can be expressed as a product of the axial depth of cut and feed per tooth in order to predict cutting behaviour. During one tooth period, the average milling force in *x* and *y* direction [129] as follows.

$$\overline{F}_x = \left\{ \frac{Nbc}{8\pi} \left[K_t \cos(2\theta) - K_n [2\theta - \sin(2\theta)] \right] + \frac{Nb}{2\pi} \left[-K_{te} \sin\theta - K_{ne} \cos\theta \right] \right\}_{\phi_{st}}^{\phi_{ex}}$$

$$\overline{F}_y = \left\{ \frac{Nbc}{8\pi} \left[K_n [2\theta - \sin(2\theta)] + K_t \cos(2\theta) \right] - \frac{Nb}{2\pi} \left[K_{te} \cos\theta - K_{ne} \sin\theta \right] \right\}_{\phi_{st}}^{\phi_{ex}}$$

(7.1)

where K_{te} and K_{ne} represent the tangential and normal edge cutting force coefficient, while K_t and K_n represent the tangential and normal cutting force coefficient, respectively. The entry and exit angles of the cutter are $\theta_{st} = 0$ and $\theta_{ex} = \pi$, respectively. These cutting coefficients can be determined through cutting measurement with a force dynamometer and cutting certain conditions. Therefore, the average force per tooth period to be found

$$\overline{F}_x = -\frac{mb}{4} K_n c - \frac{mb}{\pi} K_{ne}$$

$$\overline{F}_y = \frac{mb}{4} K_t c + \frac{mb}{\pi} K_{te}$$

(7.2)

In function of chip load *c,* Equation 7.2 can be written as

$$\overline{F}_q = \overline{F}_{qc} c + \overline{F}_{qe} \ (q = x, y, z) \qquad\qquad (7.3)$$

The experiment completes for a multiple cutting test with a range of chip loads to recorded the cutting force values in *x* and *y* direction. A linear regression was then performed on the mean force values to determine cutting coefficient in Equations 7.1 and 7.2 as given:

$$K_t = \frac{4\overline{F}_{yc}}{Nb}, \qquad K_n = \frac{4\overline{F}_{xc}}{Nb}, \qquad K_{te} = -\frac{\pi\overline{F}_{ye}}{Nb}, \qquad K_{ne} = -\frac{\pi\overline{F}_{xe}}{Nb}, \qquad (7.4)$$

F_{ye} and F_{xe} are determined from intersection at force axis for *x* and *y*-force data direction, while F_{yc} and F_{xc} are determined from the gradient at force axis for *x* and *y*-force data directions.

7.5 Further Variable Helix Validation Results

The results for variable helix tools experimental validation are now presented.

7.5.1 Cutting force results and experimental condition

From cutting force procedure, the average cutting forces in *x* dan *y*-direction were plotted to obtain the linear regression, as shown in Figure 7.14. The average force corresponds to a particular feed rate for each point. Using relation in Equation 7.4 and linear regression, the cutting force coefficient results can be calculated and summarised in Table 7.2. The result shows the tangential cutting force coefficient K_t more than twice normal cutting force coefficient K_n. This trend indicates different cutting force stiffness for previous experimental validation due to different tools was used here. However, these values can be used for current stability prediction in the experiment.

The specific cutting coefficients were above estimated to be K_n =283.2 MN/m^2 and K_t =143 MN/m^2. The following flexure dynamic properties were obtained from impact hammer: the modal mass of 1.41 kg, the natural frequency of 200 Hz and the damping ratio 0.0078. Theoretical stability diagram of variable helix (37°,40°,37°,40°) and variable pitch (78.4°,80.4°, 78.4°,80.4°) was then predicted using these parameters and compared with uniform helix (40°,40°,40°,40°) and variable pitch (78.4°,80.4°,78.4°,80.4°).

Figure 7.15 shows the theoretical stability diagram of variable helix and variable pitch with uniform helix and variable pitch superimposed onto diagram. It can observed in Figure 7.15a that the variable helix and variable pitch tools has almost similar stability to uniform helix and variable pitch for the specific range of spindle speed (1500-7500 rev/min) and depth of cut (0-10 mm) used. However, an unstable island has been observed for variable helix and variable pitch tool clearly in Figure 7.15b. Beside an isolated island in the specific range, it can clearly been seen the variable helix and variable pitch tool lobe is smaller than uniform helix and variable pitch tool. Based on the dissimilarities, current spindle speed (1800-3900 rev/min) and depth of cut (0-5 mm) conditions is used to conduct the experimental validation for variable helix with higher depth of cut than previous experiment. This is practically to ensure that the variable helix has an engagement between tool and workpiece.

7.5.2 Displacement sensor identification

During milling operation of the variable helix/pitch of 4-flute end mill, the vibration signals from displacement sensor are evaluated and used to identify the cutting behaviour as either stable, marginally stable or unstable. The cutting experiment were identified in 4 cases for increasing depth of cut: J (1975 rev/min, 1.5 mm), K (1975 rev/min, 2.0 mm), L (1975 rev/min, 3.0 mm) and M (1975 rev/min, 4.0 mm), as shown in Figure 7.16. Figure 7.17 represents the results for increasing spindle speed indicating by 3 cases: N (2050 rev/min, 2.5 mm), O (2100 rev/min, 2.5 mm) and P (2200 rev/min, 2.5 mm).

In Figures 7.16 and 7.17, cases J, M and N indicate stable or chatter free cutting. A small displacement variance is shown by raw RMS vibration signal less than 5 μm and displacement 1/Rev, including a fixed point was approached on Poincaré section. In the FFT spectrum, the frequency was shown dominating by tooth passing frequencies, which are lower than dominant frequency of the flexure structure. These frequencies referred to cutting forces for each tooth was beat by workpiece.

A marginal stable in case K and O is shown by Figures 7.16 and 7.17, respectively. These were indicated by a moderate RMS displacement variance in vibration signal (between 6 to 15 μm) and 1/rev displacement samples, while a Poincaré section

approached not as a fixed point as case J. Frequency spectrum is dominated by tooth passing frequencies at the beginning, as shown by Figures 7.16K.i and 7.17O.i. However, at end of the cutting, Figures 7.16K.ii and 7.17O.ii shows the chatter frequency was grown and closed to the flexure natural frequency.   Certainly, this indicates the transition behaviour from stable to unstable cutting named marginal stable cutting. This behaviour can be identified using FFT-spectrum and 1/Rev results for two cases: increasing depth of cut and increasing spindle speed. A raw displacement signal cannot distinguish the transition for increasing depth of cut case, but not for increasing spindle speed. For a case where spindle speed increased (case o), a raw displacement signals suddenly was increased at the end of cutting, resulting larger displacement variance in 1/Rev displacement sample and 2-D Poincaré section was noticed. Further explanation about this case related to either higher spindle speed or depth of cut for that particular cutting condition. Both higher depth of cut and higher spindle speed indicates to hopf-bifurcation instability as indicating by its Poincaré section, as shown in Figure 7.17o. It can be seen the Poincaré section consist of a combined of fixed point and circular orbit where hopf-bifurcation caused a larger vibration displacement.

Unstable period-one behaviour is confirmed by the 1/Rev samples and the Poincaré section approached a single fixed point outside stable region as shown case L in Figure 7.16. The chatter frequency was close to the flexure natural frequency as shown by FFT spectrum.   In FFT-spectrum, the resonance happens when chatter frequency located closed to the tooth passing frequency. A large vibration signal dominated in FFT spectrum.

In case P in Figure 7.17, unstable Hopf-bifurcation instability was determined which can be referred according to the chatter frequencies. FFT spectrum shows the chatter frequency was closed to the flexure natural frequency. For this instability behaviour, the spindle frequencies in the 1/Rev displacement samples intersected chatter frequency to produce an unstable circular orbit on the Poincaré section as similar to previous experiment for optimised tool. Nevertheless, the orbit pattern is not as clear as regular tool in Figure 7.6 (case C). This is due to 1/Rev analysis for variable geometry tool analysis that capture one tooth per revolution. Moreover, this unstable orbit has been earlier detected during a marginal stable cutting in case O. To have a clear orbit, it is suggest to have longer cutting period to produce more data captured data.

7.5.3   Displacement and stability results

In Figure 7.18a, the variable helix/pitch tool chatter stability contour was predicted from values of eigen value (CM) less than one. There is range between 0.8 to 1 where the contour higher than one indicating unstable area. When closed to this unstable island, it is bordered by contour values or CM of 0.95. The purpose for introducing contour stability is to compare with the displacement vibration signal measurement during cutting experiment.

The vibration signals can identify its cutting behavior: Stable (less than 5 μm), marginal stable (larger than 6 μm and less than 15 μm) and unstable (larger than 16 μm). For the down-milling operation of the variable helix/pitch 4-flute end mill, the result indicates a good agreement between predicted stability contour and RMS displacement measurement, as shown in Figure 7.18b. Stable or chatter free cutting conditions were observed outside the boundary of CM = 1. The unstable behaviours were observed when RMS displacement larger than 16 which were located inside instability region, whilst marginal stable condition (6 μm<RMS displacement<15 μm*)* happened around stability lobes (CM = 1). It can be seen that the unstable chatter island for variable helix was experimentally confirmed when increasing depth of cut for 1975 rev/min in the identification approach.

The scattered instability of hopf-bifurcation, period doubling bifurcation and period-one bifurcation were theoretical predicted in Figure 7.19a. This illustrates the different types of instability when modeling SDM algorithm for the variable helix/pitch. These instabilities are predicted at two unstable regions. It can be seen these instabilities associated with RMS displacement larger than 16 μm.

Experimental work shows the stability results for the variable helix/pitch based on the identification of displacement signal, as shown in Figure 7.19b. The results indicate a good agreement when superimposed with theoretical prediction where the tool stability representing variable helix and not uniform helix. The unstable hopf-bifurcation are predicted and observed at larger lobe. However, at high spindle speed, resonance occurred due to similarities of the chatter and spindle frequencies and tool runout effect. Theses cutting test disagree with the theoretically stability predictions as indicated by '∆'. Besides validation with larger lobe, the important instability border for isolated

period-one island is proven experimentally at 1975 rev/min spindle speed. In comparison to theoretical prediction, all cases exhibit period-one behavior for a case where the largest magnitude eigenvalues are positive and with real parts of magnitude larger than one. The stable cutting behaviors in between that isolated unstable island also ensure the effectiveness of current SDM in modeling variable helix tool. Overall, the experimental of variable helix compares well with the theoretical prediction and can be used for optimising variable helix and variable pitch tools.

7.6 Discussion

It can be seen that the optimised tool experimental stability results have been accurately predicted by SDM algorithm. In Figure 7.8, unstable Hopf-bifurcation and period-doubling instabilities were determined in theory which can be referred according to the chatter frequencies. These frequencies are lower than the flexure frequency, which related to cutting forces for each teeth beating workpiece. The resonance corresponds to chatter frequency and the tooth passing frequency located close to each other.

The optimised variable helix and variable pitch cutter has clearly demonstrated experimentally as effective suppression of the chatter vibration of the workpiece during milling. The SDM prediction underestimates the experiment, however, better than variable pitch cutter prediction, as shown in Figure 7.9. Additionally, low radial and axial immersion cutting with variable pitch also create an inconsistently cutting force of each tooth hitting the workpiece.

A further experiment was carried out with high depth cut condition to validate variable helix tools chatter stability prediction. Unstable cutting tests around chatter island show a good agreement with theoretical prediction. This undoubtedly demonstrates that the current SDM modeling procedure matches with experiment. In addition to the instability condition identification, there is a large region of that is associated with hopf-bifurcation also captured, as found in classical machining chatter.

It is visibly observed that the marginal stability identified by RMS displacement and FFT spectrum and quantity by 1/Rev displacement signal. With a small increasing depth of cut or spindle speed, both conditions can change stability results to unstable cutting condition either hopf-bifurcation or period-one bifurcation for this variable helix

tool. Previous work [30, 64] on regular helix milling tools has identified regions of period doubling instability, but the existence of period-one bifurcations has previously only been associated with tool runout [165]. The present contribution predicts that period-one bifurcation can also arise for variable helix tools.

7.7 Summary

Practical implementation of an optimised cutter with variable helix and variable pitch has been shown to improve milling stability of a flexible workpiece. It has been indicated that for a uniform helix and uniform pitch (regular cutter), the stability limit of the milling process was verified experimentally with a very good agreement with SDM simulation. Using an optimised variable helix and variable pitch, stability margin can be gained by at least a factor of 5 in suppressing chatter. Optimum material removal rate can be easily applied using current optimised cutter.

The variable helix and variable pitch tool was performed for cutting at higher depths of cut and validate the modelling procedure. From series of very low down-milling cutting experiment, theoretical predictions are validated to confirm the occurrence of isolated chatter island and other hopf-bifurcation instability in a large unstable lobe. SDM modelling can used to optimise variable helix and variable pitch as discussed in this chapter and previous chapter. This contribution has confirmed experimentally that period-one bifurcations can occur for variable helix milling tools. However, the identification of this behavior is not straightforward, since the vibration characteristics are similar to those for stable forced vibrations. Moreover, the transition between stable to unstable or marginally stable zone that almost border to unstable island and lobe were also observed by using displacement sensor.

There have been very few previous studies that have investigated variable helix milling tools as described in Chapter 2. However, Turner *et al.* [68] proposed that the so-called 'process damping' phenomenon is particularly important for variable helix milling tools. Consequently, the following chapter presents the effect of tool geometry in process damped milling for chatter suppression chatter experimentally, including variable helix/pitch influence to process damping performance.

Table 7.1 Cutting, modal and tool parameters for optimisation

Tool and cutting parameters	
Tool diameter d (mm)	16
Radial immersion RI (mm)	1.60
Tangential cutting stiffness K_t (MN/m^2)	1250
Radial cutting stiffness K_r	0.15

Modal property in x-direction mode	
Natural frequency f (Hz)	200
Modal effective mass m_s (kg)	1.41
Damping Ratio ξ	0.0078

Table 7.2 Cutting and tool parameters for variable helix/pitch verification

Tool and cutting parameters	
Tool diameter, mm	12
Radial immersion, mm	0.6
Tangential cutting stiffness K_t (MN/m^2)	283.2
Normal cutting stiffness K_n (MN/m^2)	143.0
Tangential edge cutting stiffness K_{te} (MN/m^2)	0.398
Normal edge cutting stiffness K_{ne} (MN/m^2)	2.325
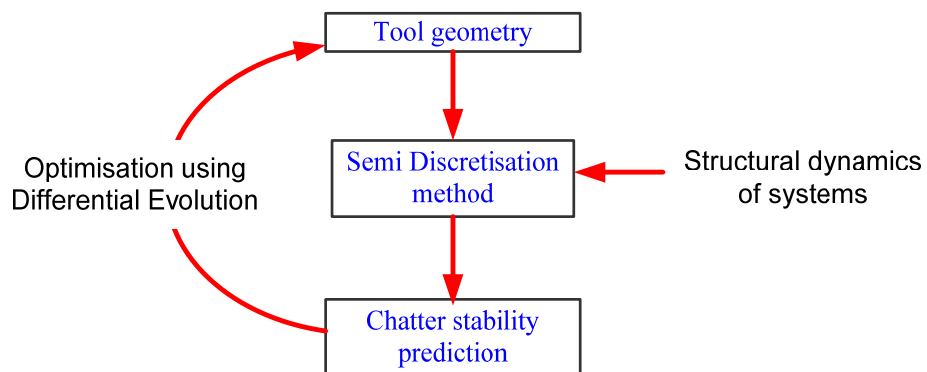
Figure 7.1 Design of tool geometry
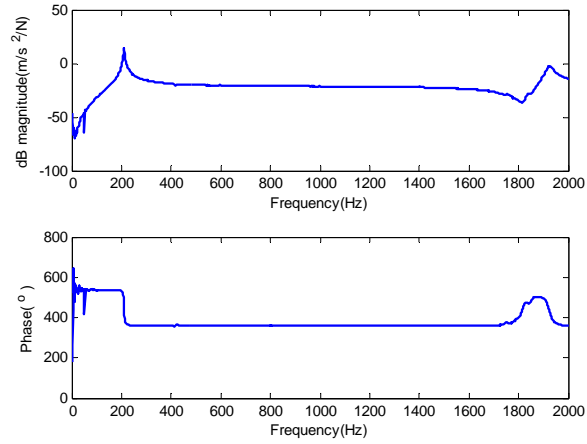
Figure 7.2 Frequency response function for flexure
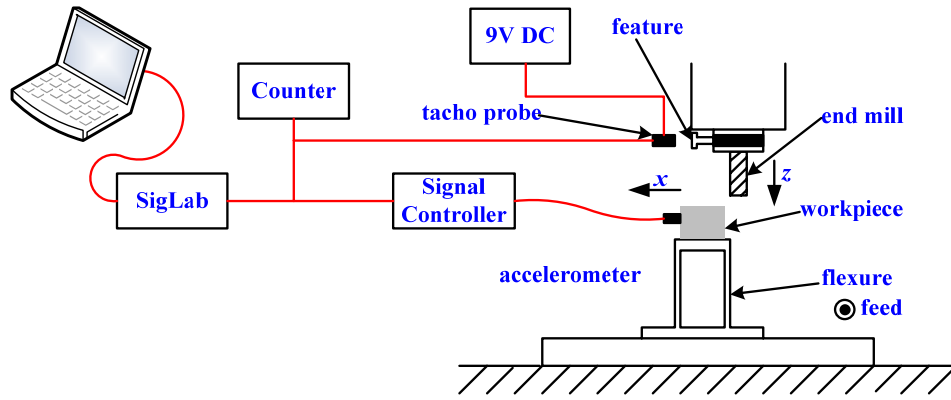
a) Schematic diagram
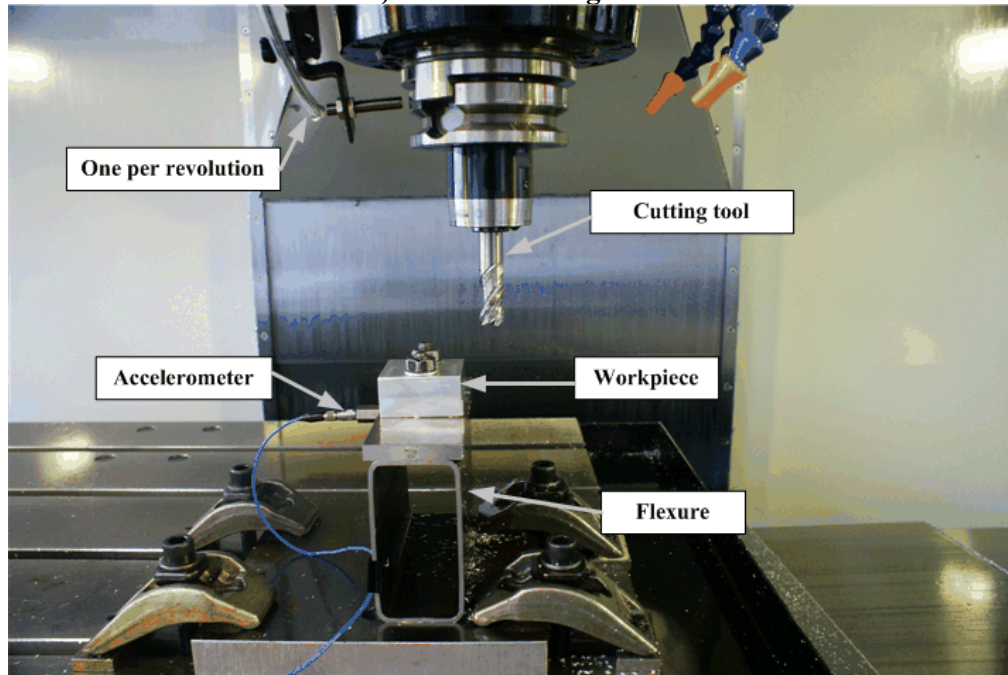
b) Sensor location

Figure 7.3 Arrangement for optimised tool experimental validation
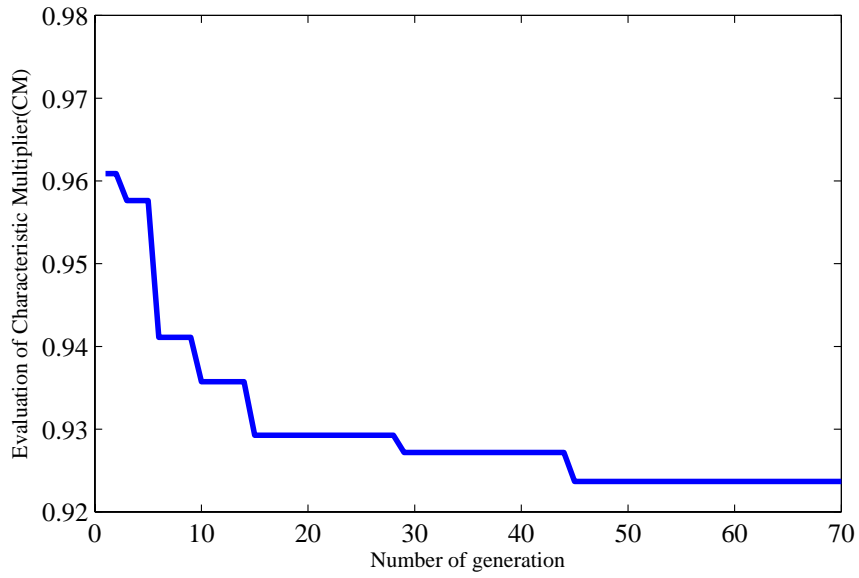
Figure 7.4 Performance of Differential Evolution for optimising a three flute variable helix and variable pitch

a) Uniform helix   b) Variable helix

c) Uniform pitch

d) Variable pitch
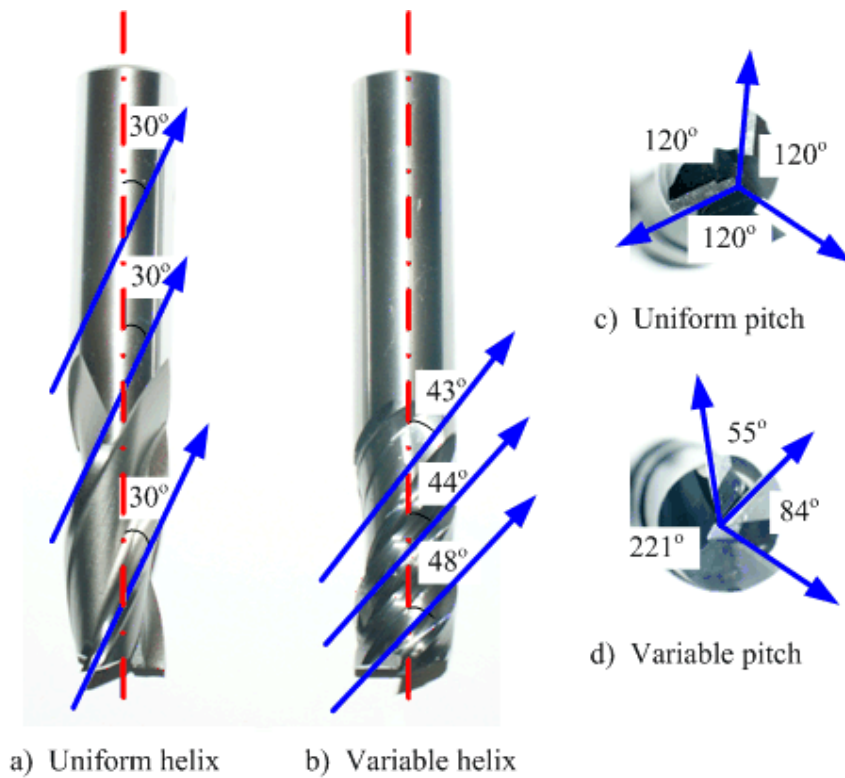
Figure 7.5 Tool geometry for experimental validation

132
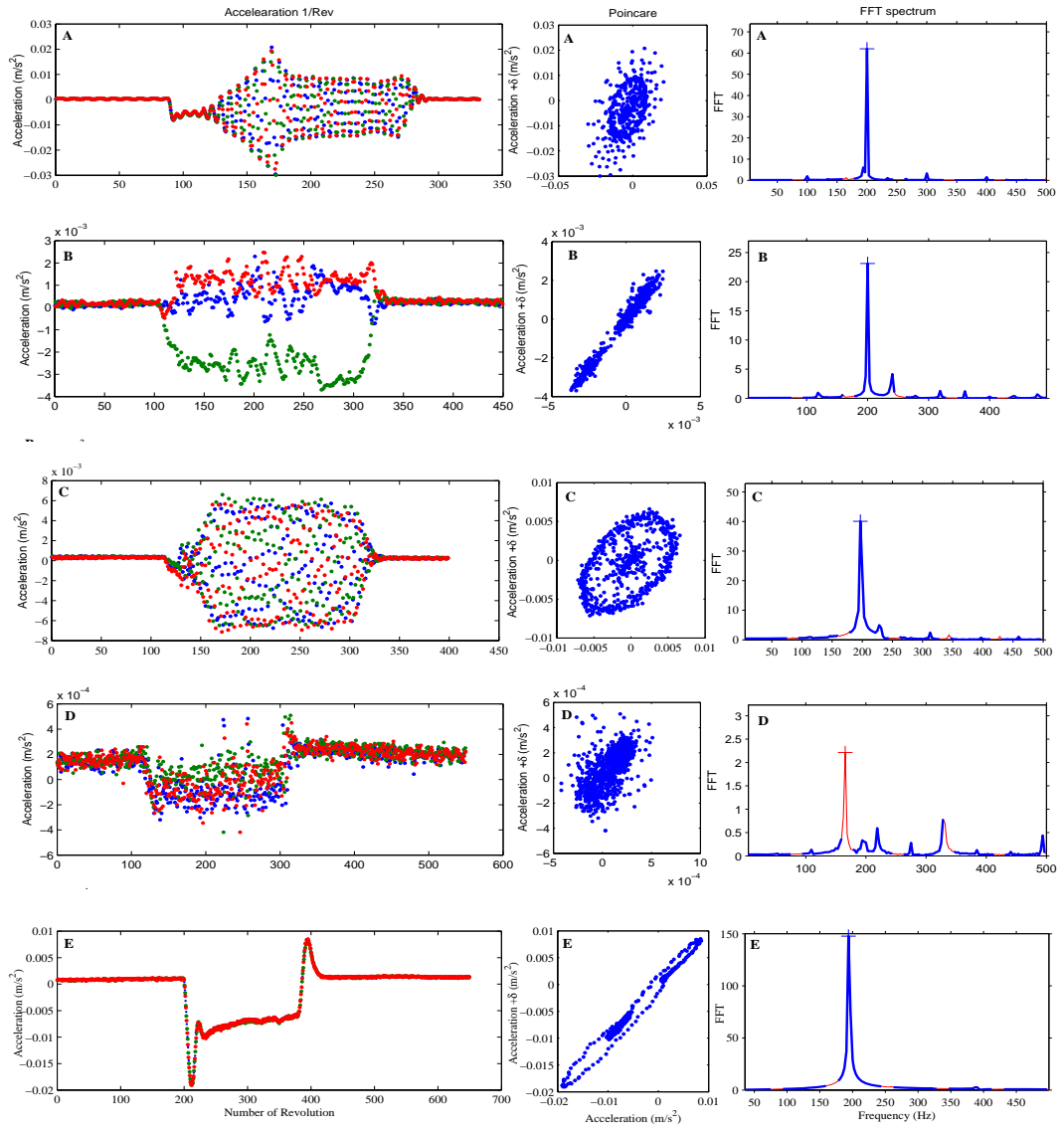
Figure 7.6 1/Rev, Poincare sections and FFT-spectrums for points A, B, C, D and E

Figure 7.7 1/Rev, Poincare sections and FFT-spectrums for points F, G, H and I
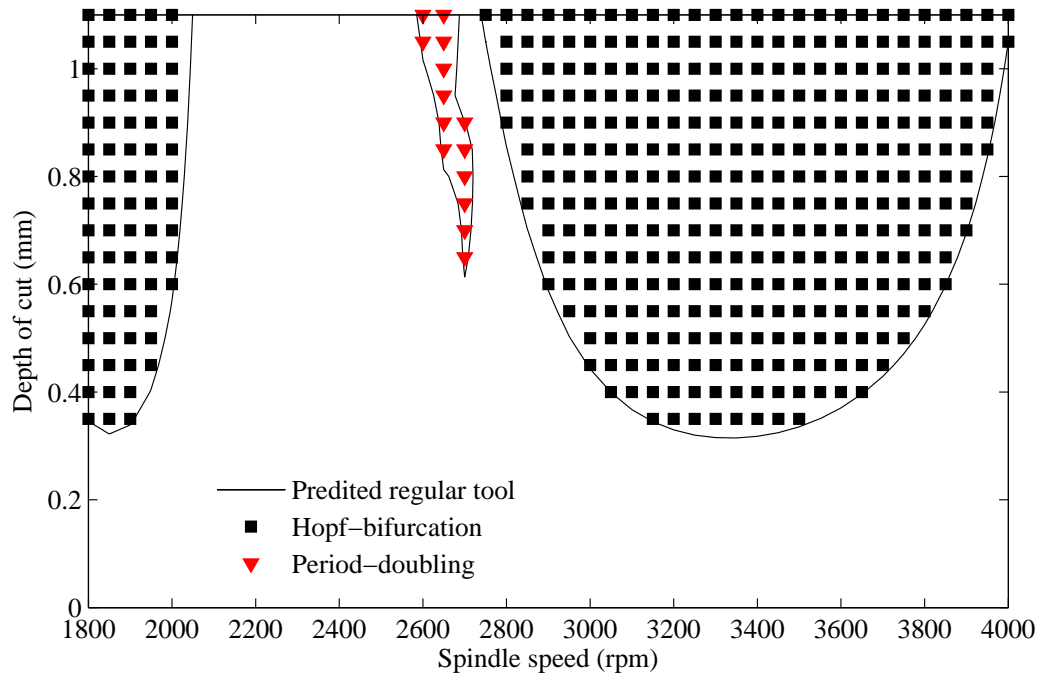
a) Stability diagram of 1800 to 4000 rev/min. (—) stability region, (■) secondary hopf bifurcation (∇) period doubling bifurcation
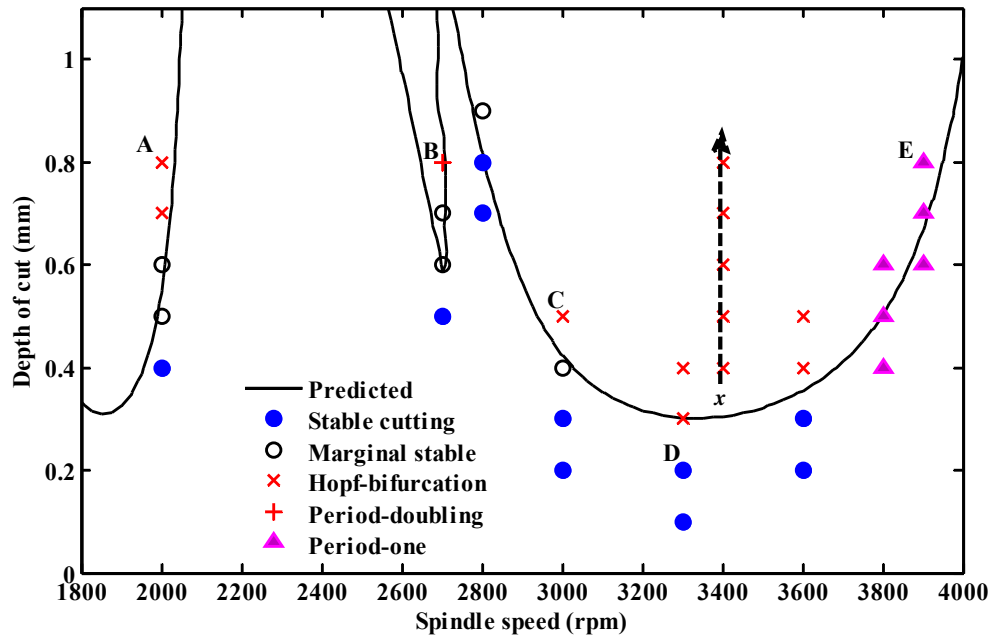
b) Experimental results for original cutter

Figure 7.8 Regular tool predicted stability and experimental results

a) Stability diagram 1800 to 4000 rev/min

b) Experimental results for optimised cutter

Figure 7.9 Optimised tool stability prediction for a three flute variable helix (43°,44°,48°) and.variable pitch (84°,221°,55°)

a) **Original cutter for line** *x*   b) **optimised cutter for line** *y*
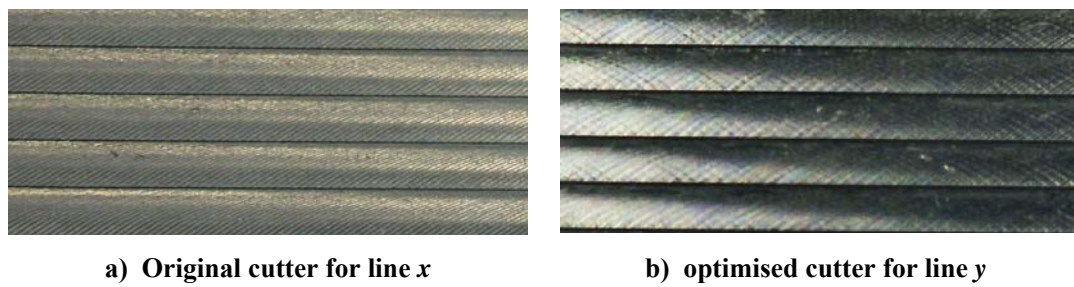
Figure 7.10 Workpiece surface difference between original cutter and optimised cutter at spindle speed 3400 rev/min and depth of cut 0.4 to 0.8 mm(bottom to up)
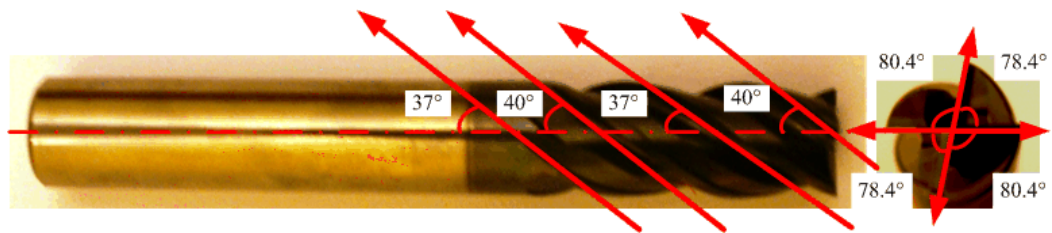
Figure 7.11 Tool geometry for variable helix/pitch milling tool validation
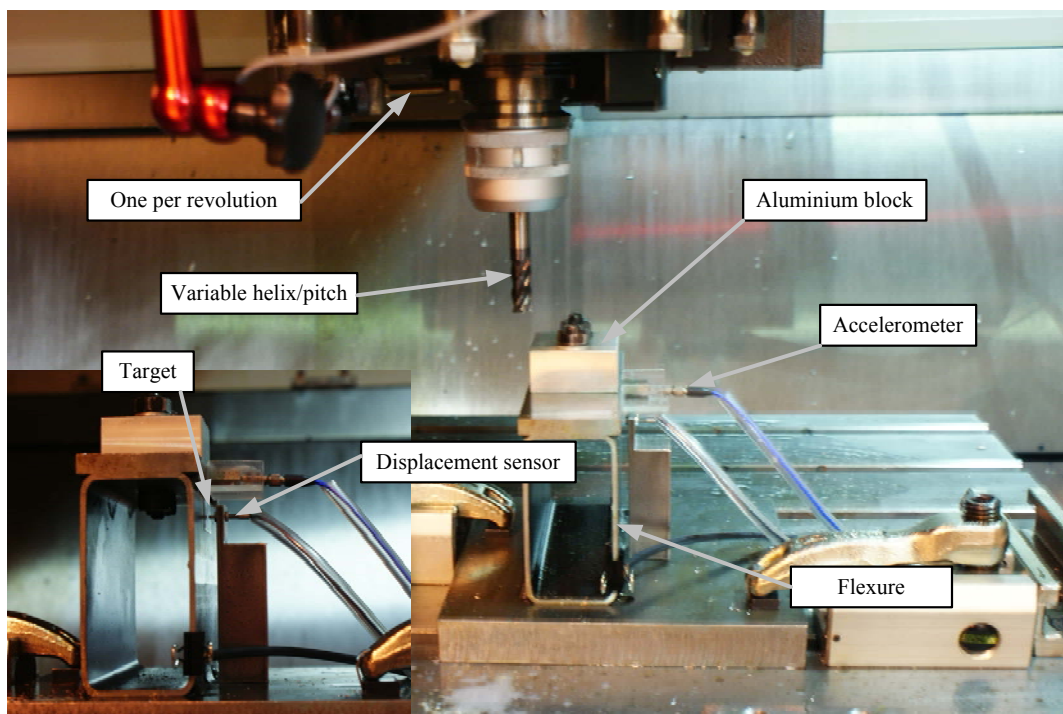
Figure 7.12 Configuration of displacement sensor for variable helix experimental validation
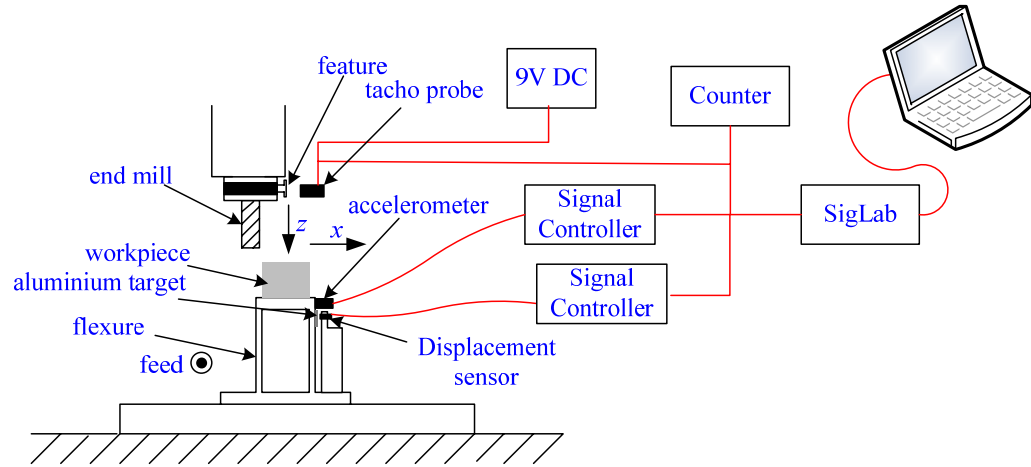
Figure 7.13 Experimental arrangement for variable helix experimental validation
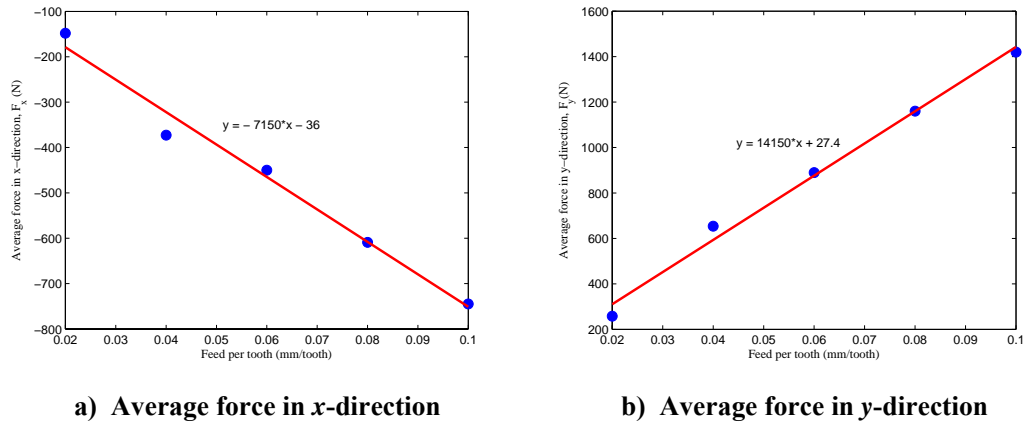
| a) Average force in *x*-direction | b) Average force in *y*-direction |

Figure 7.14 Cutting force stiffness determination
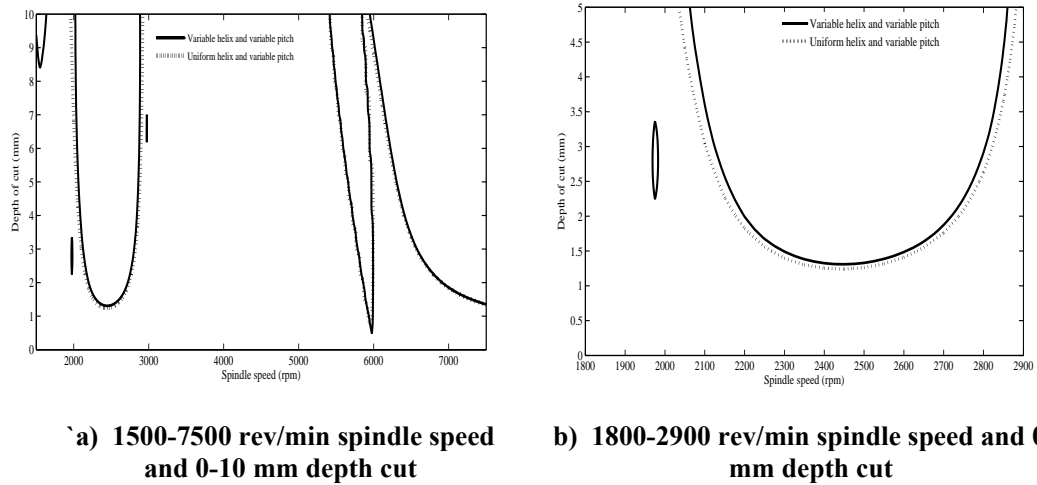
| `a) 1500-7500 rev/min spindle speed and 0-10 mm depth cut | b) 1800-2900 rev/min spindle speed and 0-5 mm depth cut |

Figure 7.15 Stability diagram comparison of 5 percent radial immersion for variable helix (37°,40°,37°,40°) and variable pitch (78.4°,80.4°,78.4°, 80.4°) and uniform helix (40°,40°,40°,40°) and variable pitch (78.4°,80.4°,78.4°, 80.4°)
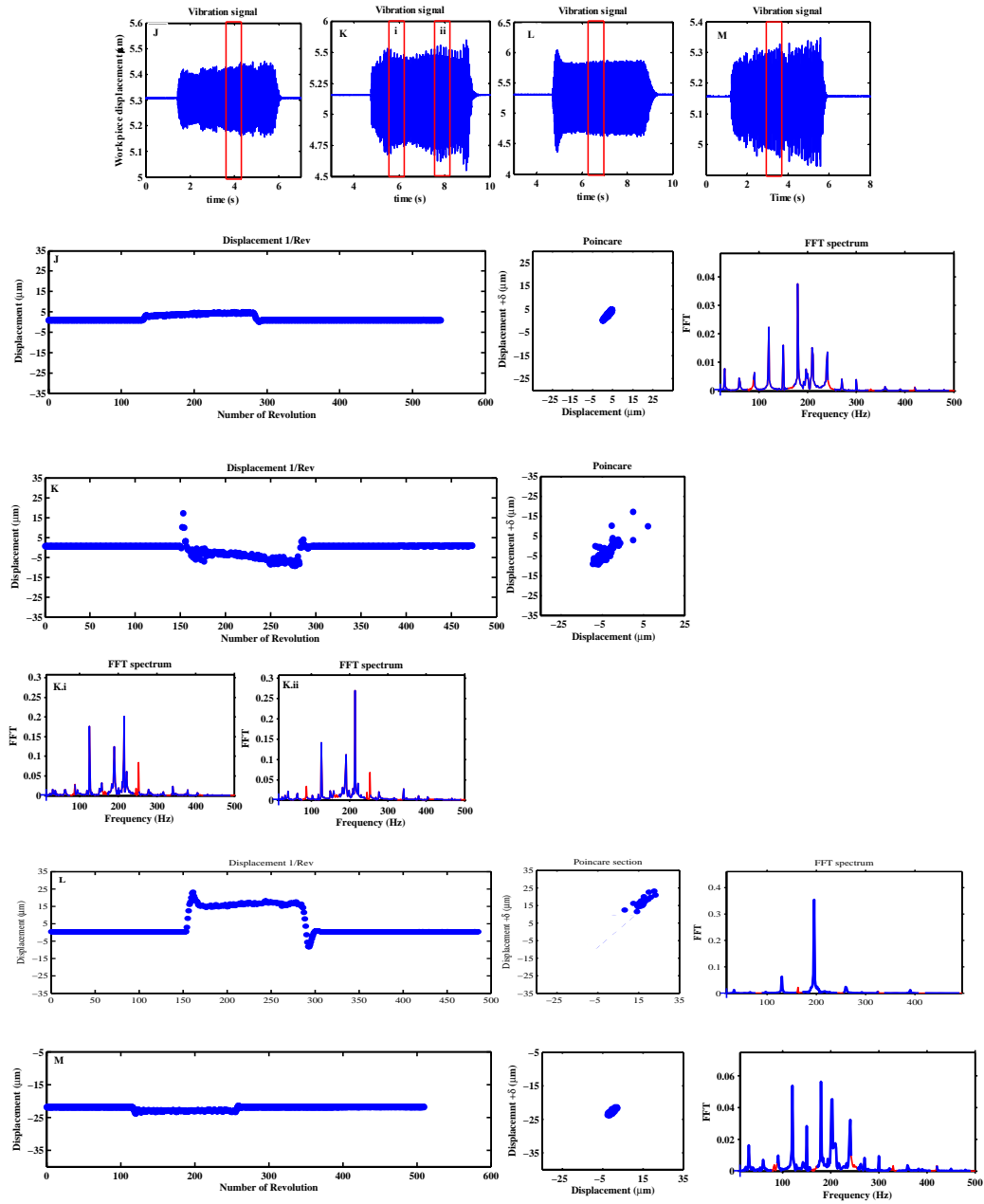
Figure 7.16 1/Rev, Poincare sections and FFT-spectrums for points J (stable), K (marginal stable), L (unstable) and M (stable) when increasing depth of cut
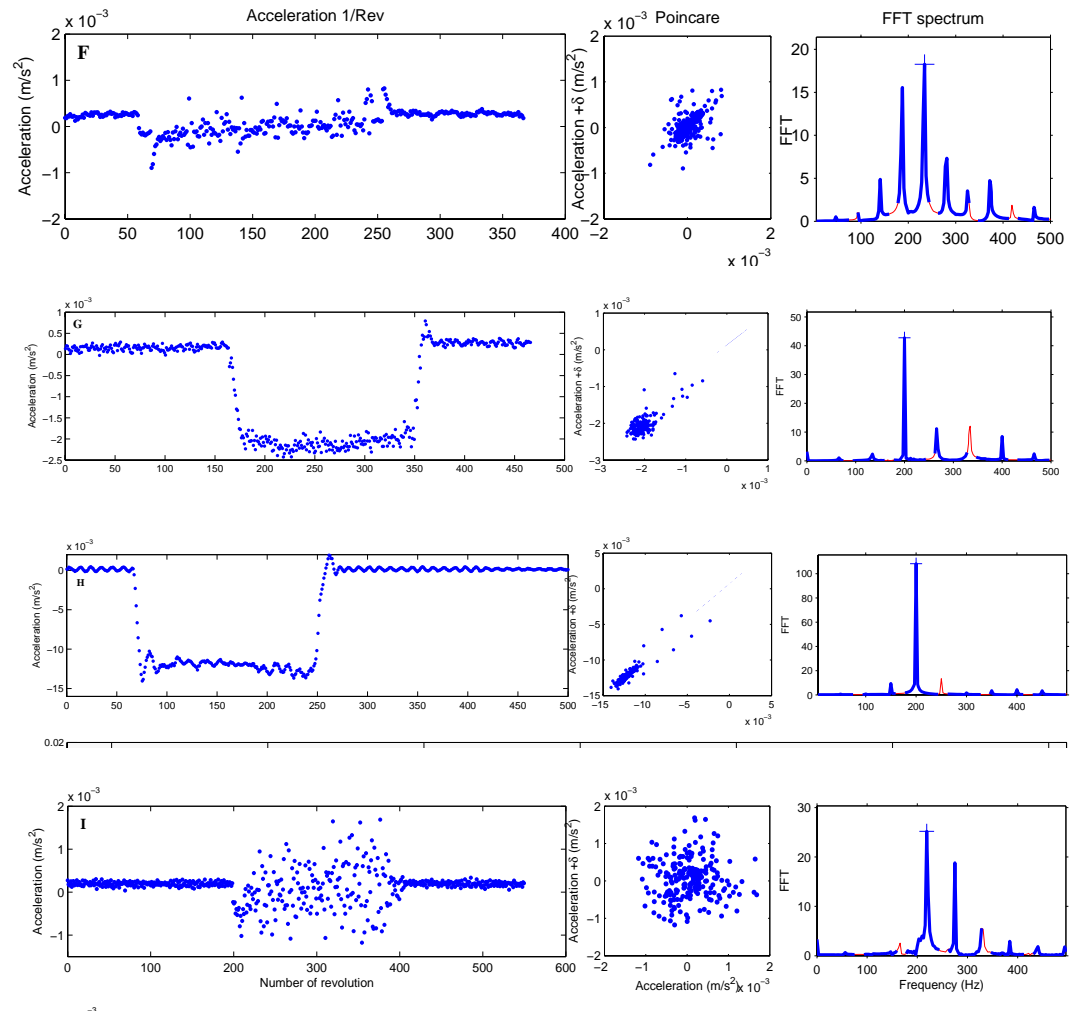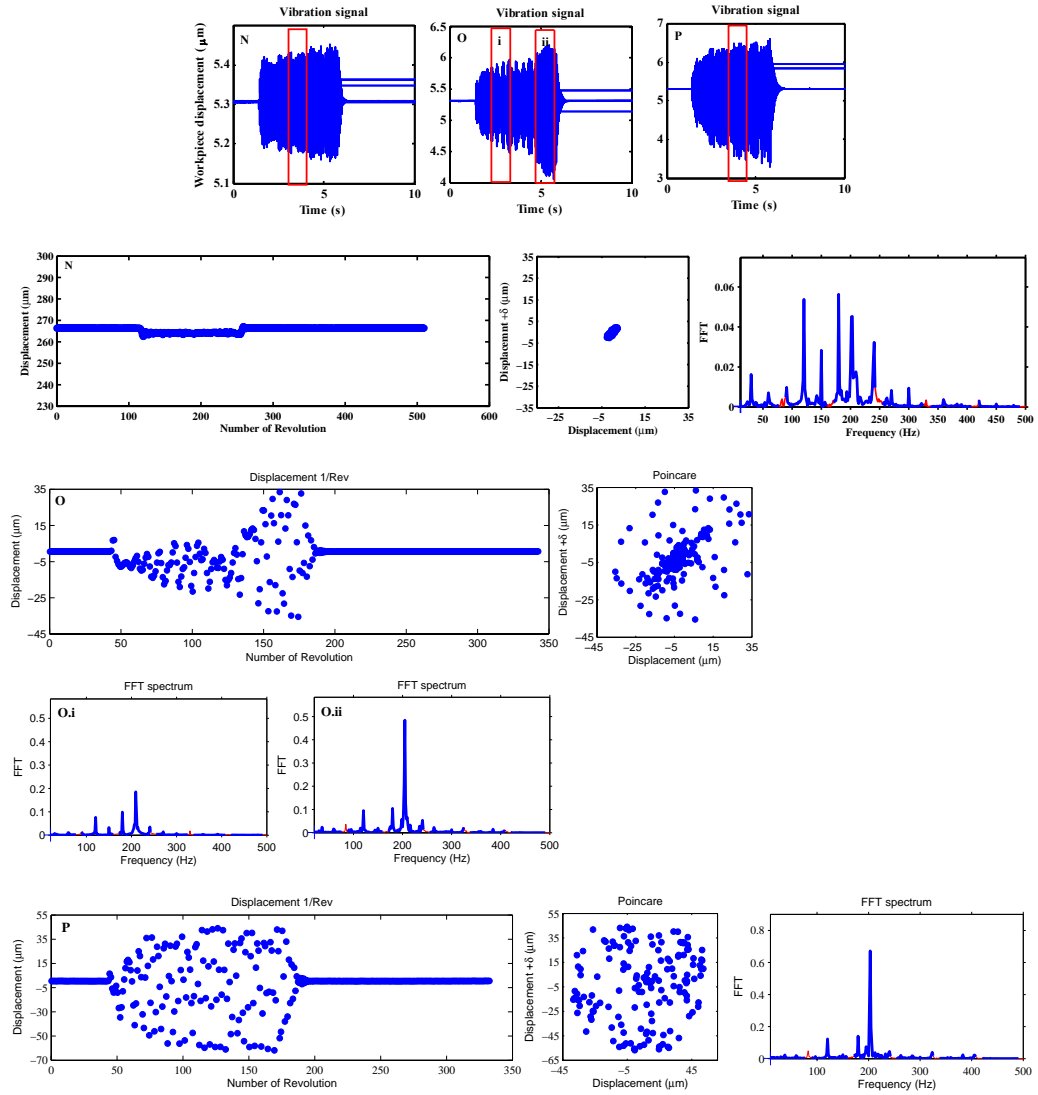
Figure 7.17 1/Rev, Poincare sections and FFT-spectrums for points N (stable), O(marginal stable) and P (unstable) when increasing spindle speeds.
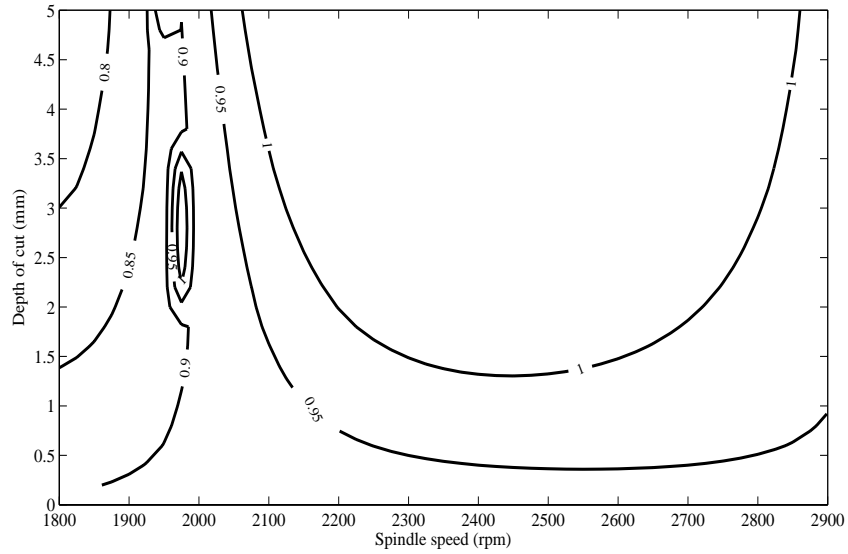
a) Contour stability prediction
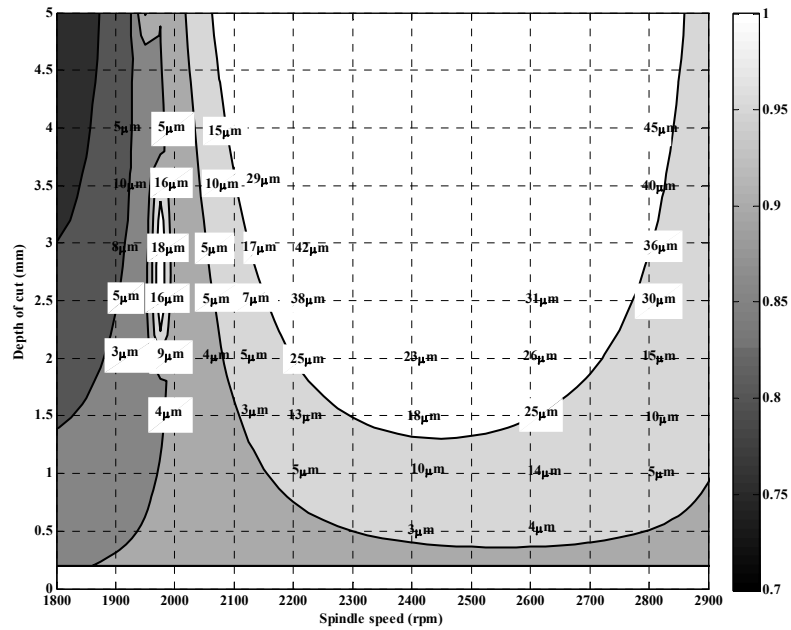
b) Experimental results for RMS displacement and contour prediction

Figure 7.18 Contour stability and RMS displacement comparison of 5 percent radial immersion for variable helix (37°,40°,37°,40°) and variable pitch (78.4°,80.4°,78.4°, 80.4°.)
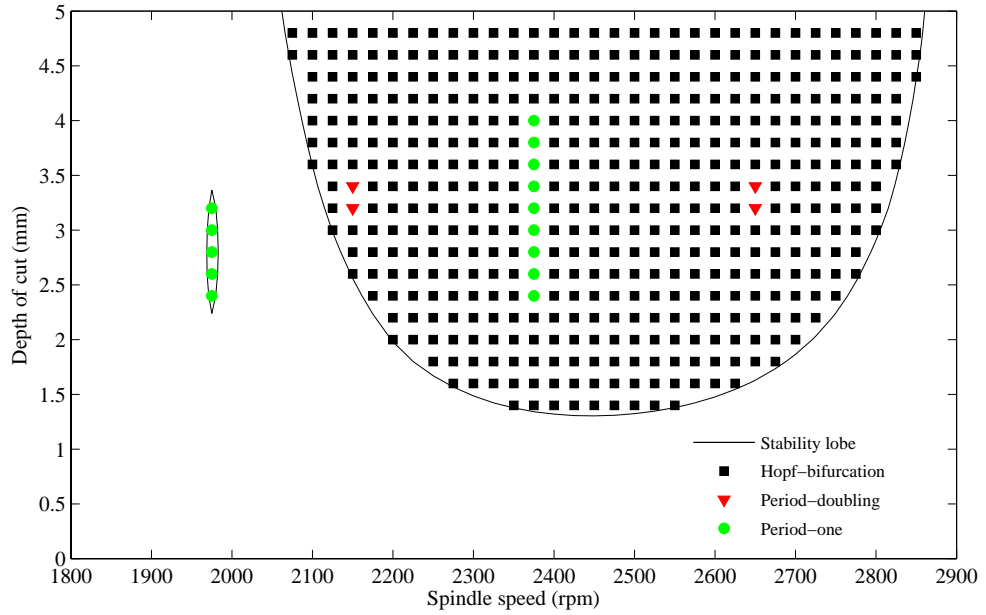
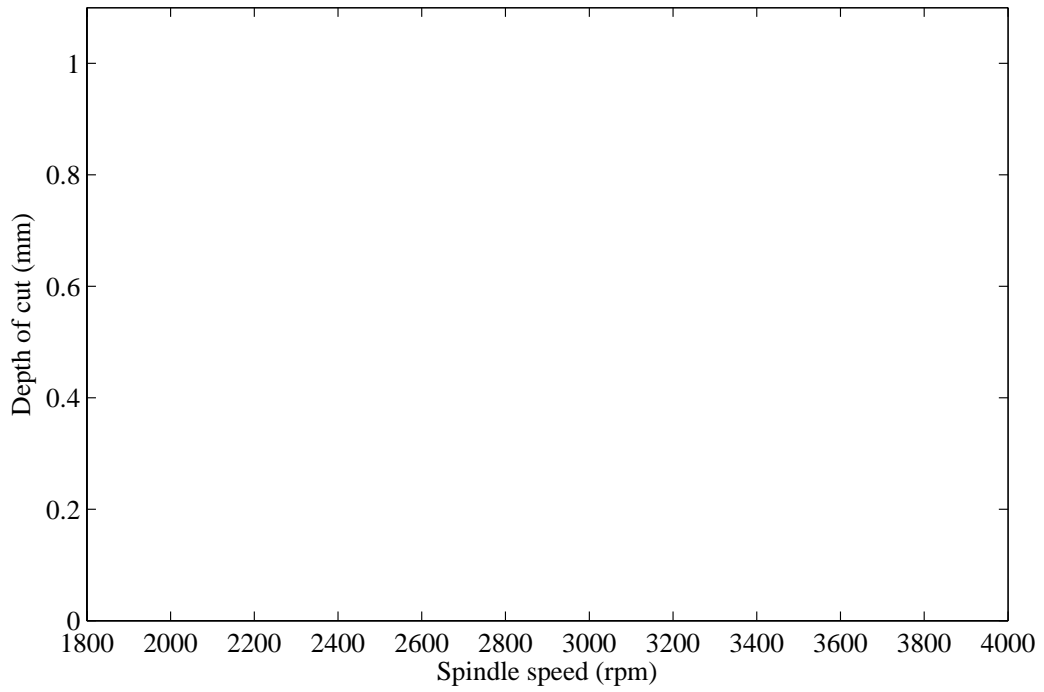a) **Stability diagram of 1800 to 2900 rev/min. (—) stability region, (■) secondary hopf bifurcation (∇) period doubling bifurcation (○) cyclic fold bifurcation**
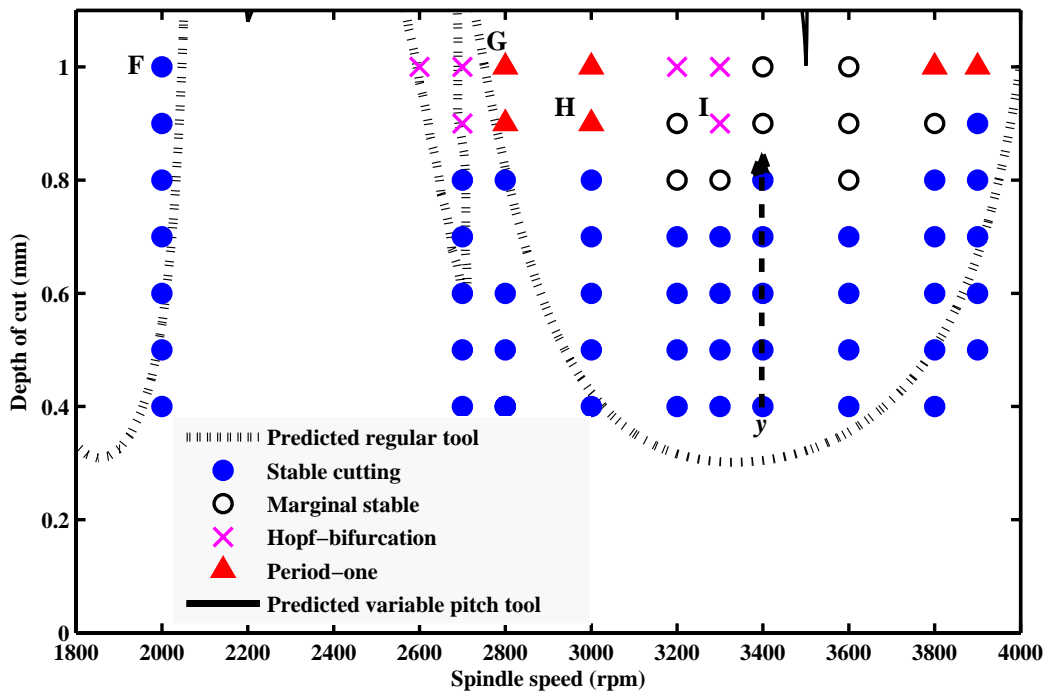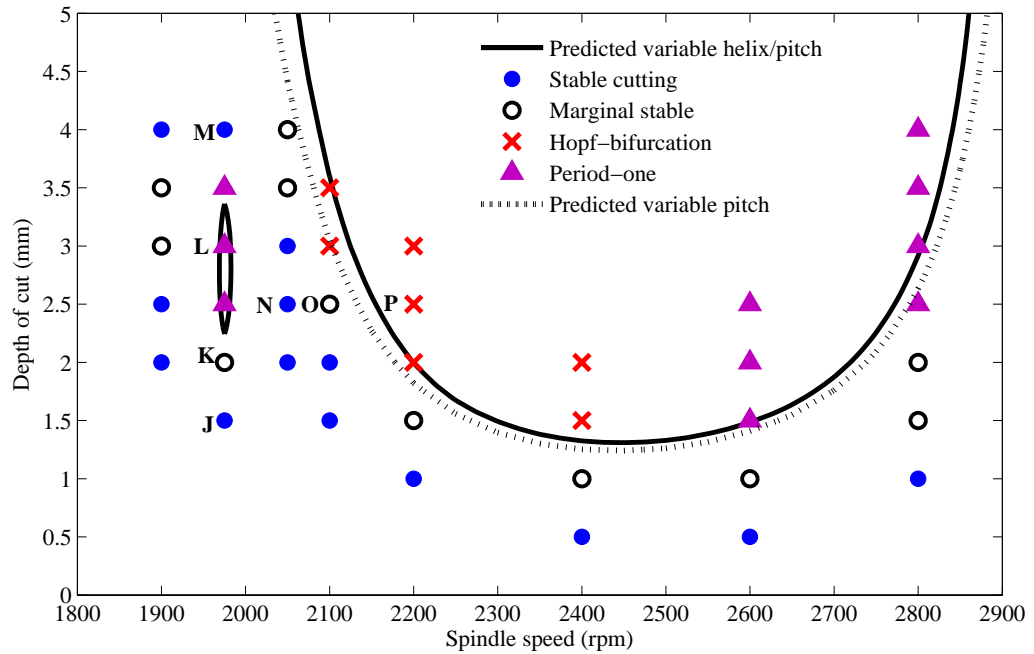

b) **Experimental results for variable helix and variable pitch**

Figure 7.19 Stability diagram of 5 percent radial immersion for variable helix (37°,40°,37°,40°) and variable pitch (78.4°,80.4°,78.4°, 80.4°).

CHAPTER 8
EFFECT OF TOOL GEOMETRY ON PROCESS DAMPING IN MILLING

8.1 Introduction

Besides the damping produced from the structure of machine tools, as shown in Chapters 6 and 7, the machining process itself can add damping to the system through a phenomenon known as process damping. The term process damping or resistance force was introduced by Tobias and Fishwick [16]. They proposed that such force occurs when the tool flank face or rake angle rubs against the wavy workpiece surface at low spindle speeds. The stability diagram shown in Figure 8.1 illustrates the relationship between spindle speeds, depth of cut and chatter stability. At high spindle speeds, stability lobes can be observed, and this allows high productivity cutting to be performed on easy-to-machine materials such as aluminium alloys. Unfortunately, the resulting high surface speeds are incompatible with more difficult-to-machine materials such as titanium and nickel-based alloys. In this case, the practitioner is limited to low spindle speeds, where the chatter stability is strongly influenced by the process damping phenomenon. However, the understanding of process damping remains an unsolved problem in chatter research [166].

There have been many attempts to study process damping in turning operations, using simulation or experimental methods (or both). Recent examples include [167] and [168]. However, there have been fewer studies that have investigated milling processes. For example, Montgomery and Altintas [169] used a model-based approach to investigate ploughing forces. Delio *et al.* [170] considered the wavelength of chatter vibration and the loss of process damping behaviour at higher spindle speeds. Elbestawi *et al.* [67] modelled process damping effects when cutting aluminium and showed that the model could produce additional damping forces due to the tool flank / workpiece interference. Ranganath *et al.* [171] also developed a time-domain model of process-damped milling and compared the results to experimental data from an aluminium alloy workpiece. Huang and Wang [172] proposed a model that considered the consequences of chatter vibration on the effective rake and relief angles. They included additional

empirical parameters in their model so that the cutting stiffness became a function of these effective angles and thereby produced a process damping effect.

Despite this previous work on process damping in milling, there is limited experimental activity that has considered the effect of milling tool geometry when cutting difficult-to-machine materials such as titanium alloys. From a practical and industrial perspective, understanding the effect of these tool parameters on process damping is clearly of great importance, because it allows the practitioner to choose better tooling for specific machining problems. Consequently, the aim of the present chapter is to perform experimental milling experiments so that different tool geometries (edge radius, rake and relief angles and variable helix/pitch angles) can be ranked in terms of their positive influence on process damping in milling.

The remainder of the chapter is organised as follows. The process damping theory is first described, followed by the experimental procedure. Then, the results for the experiments are presented and parameters are ranked in terms of their influence on process damping performance. Finally, conclusions are drawn and recommendations are made for further work. This chapter formed a journal paper and an abstract is given in Appendix A.V.

8.2 Theory of Process Damping

Chatter is produced from self-excited vibration during cutting, resulting in a high amplitude unstable motion. The amplitude of this motion is limited by nonlinearities such as tool loss of contact, nonlinear cutting force coefficients and nonlinear stiffness of the machine tool structure. The chatter frequency is very close to a natural frequency of the system but differs from the tooth passing frequency to produce waves that are longer and deeper on the machined surface. At low speeds, the wavelength λ of these surface waves is much smaller, since the wavelength is proportional to surface velocity v and inversely proportional to regenerative vibration frequency f_c, as follows:

$$\lambda = \frac{v}{f_c}$$

(8.1)

As the spindle speed (and hence surface velocity) is reduced, the process damping phenomenon becomes sufficient for the regenerative chatter to be stabilised or

suppressed. This situation is shown by the asterisk (for particular depth of cut) in Figure 8.1. The corresponding surface vibration wavelength is given by Equation (8.1) and is referred to as the process damping wavelength λ_c.

The commonly proposed mechanism of process damping is shown schematically in Figure 8.2. As each tooth removes the chip from the wavy surface, process damping forces are generated that excite the structure. The damping force corresponds to inference between tool flank face and wavy surface, where more damping force occurs at point 'B'. A ploughing force can be produced from the workpiece's being deformed by the tool, while the surface angle changes the tool's effective shear angle. Interference is minimised when the tool travels upwards on the wave (position 'D' in Figure 8.2) due to the positive slope of the machined surface.

According to this concept, low relief angles should produce high ploughing forces from the interference between tool and workpiece. Consequently, different rake and relief angles should be considered in the evaluation of process damping. Furthermore, Figure 8.2 assumes a perfectly sharp tool, which is unrealistic in practice. Consequently the bluntness of the tool tip, which can be characterised as an edge radius, should also be considered.

In the stability of high speed milling, axial depth of cut b is the most influential factor, since the cutting forces are often considered to be given by the relationship

$$F = k_s b (y_p - y) \qquad\qquad \textbf{(8.2)}$$

where F is the cutting force and $(y_p\text{-}y)$ is the surface thickness difference between current and previous cuts. In theory, the stability boundary is then independant of the feedrate despite the influence of the feed rate on the mean chip thickness. However, under process-damped cutting conditions, the effect of feed rate has been observed to be more significant [173].

It is useful to express the feedrate in terms of the maximum chip thickness h_{max}:

$$h_{max} = w\sqrt{\frac{4r}{d} - \left(\frac{2r}{d}\right)^2} \qquad (8.3)$$

Here, r is the radial depth of cut of the tool and d is the tool diameter. The feed per tooth w is related to the machining feed rate fr, number of teeth m and spindle speed Ω by:

$$fr = m \times w \times \Omega \qquad (8.4)$$

Using a high depth of cut at low cutting speed is a very effective way to encourage process damping, as shown on the left side of the stability diagram in Figure 8.1. Meanwhile, using a low radial depth of cut helps to reduce the total machining forces and improve tool life. This approach will be employed in the present chapter in order to determine the process damping wavelength λ_c under different tool geometry and feed rate conditions.

8.3   Experimental Setup

Two experimental configurations were used in this chapter, and these will now be introduced. It should be pointed out that the majority of experiments were performed on difficult-to-machine titanium alloy, where process damping is frequently encountered. These tests involved a four-flute tool that was considered to be the flexible component in the machine-tool system. However, this configuration does not allow quantitative acceleration data to be collected because the flexible component is the rotating cutting tool. Consequently, one set of data, using three-flute regular helix and variable helix tools, was collected using a workpiece mounted on a flexure. This also ensured that the tool helix angle did not influence the relevant modal parameters of the system. However, the extreme flexibility of the flexure configuration meant that an easier-to-machine workpiece material (aluminium alloy) was needed for this set of tests.

8.3.1   Flexible tool condition

For the flexible tool setup, 16 mm 4-flute solid carbide tools were used to cut titanium $Ti_6 Al_4V$ to evaluate the influence of feed rate, tool edge radius, rake angle and relief angle on process damping. Before the machining test, each tool was measured to determine the average edge radius, using a Mahr Perthometer with a stylus tip. One edge from four was selected to measure the cutting edge radius. With reference to Figure 8.3, the cutting edge radius was measured at 3 mm from the bottom and the middle of the axial depth of cut b. The measurement was repeated three times and then

repeated at the same location for the second, third and fourth flutes (Figure 8.3b) counted clockwise from the bottom.

The experiment was started by determining the frequency response function (FRF) of the tool to recognise the expected dominant chatter frequency for initially selecting the spindle speed Ω and feedrate *fr*. A normal force was applied at the tool tip using a PCB 086C01 modal hammer with steel tip. The acceleration response was captured by a PCB 352C16 accelerometer opposite to the hammer impact point. A Siglab 20-22A two-channel data acquisition system was connected to the hammer and accelerometer to determine the FRF.

From the FRF, the resonant frequency was used to choose a starting value for spindle speed based so that the expected wavelength of vibrations was $\lambda = 0.1$ mm. This was achieved using Equation (8.1) and the relationship between tool diameter, spindle speed and surface speed. Based on previous experience [174], this initial wavelength was expected to be below the process damping wavelength λ_c. For the desired maximum chip thickness, the feed per tooth and hence the initial feed rate were then determined using Equations (8.3) and (8.4). A low radial width of cut ($r = 1$ mm) and large axial depth of cut ($b = 30$ mm) were used to minimise forced vibration, reduce tool wear and prevent damage to the tool if severe chatter occurred.

Machining was done on a Haas *VF6* vertical milling machine, as shown in Figure 8.4a,b. During cutting, the vibration signal was recorded using an accelerometer (PCB Piezotronics 352C68). The spindle speed Ω and feed rate *fr* were increased simultaneously to maintain constant *w* and h_{max}, until chatter was detected. Process damping performance was then evaluated in terms of λ_c from Equation (8.1). Here, the chatter frequency was obtained from Fourier analysis of the vibration signal and the surface speed *v* was determined based upon the spindle speed at which chatter occurred. The procedure was repeated for four h_{max} values between 0.03mm and 0.1mm and for each tool.

8.3.2   Flexible workpiece condition

A separate sequence of experiments evaluated the influence of variable pitch and helix angles on process damping performance. Here, a block of aluminium (7075-T6) was mounted on a flexible structure as used by Huyanan and Sims [38, 163] (Figure 8.4c,d). Two 16 mm 3-flute cutters were used: one with a regular pitch (120°, 120°, 120°)and uniform helix (30°, 30°, 30°), and one with a variable pitch (84°, 221°, 55°) and variable helix (43°, 44°, 48°). These are similar cutters and experiment configuration to those in Chapter 7.

A similar procedure was repeated to determine the initial Ω and f based on the FRF of the flexure. Again, n was gradually increased whilst maintaining the w until chatter was detected. The process damping wavelength λ_c was then evaluated as before. Both regular and variable helix/pitch milling tools were used for down-milling at 1 mm radial and 2 mm axial depth of cut. The low stiffness of the flexure ensured process damped cutting conditions despite the low axial depth of cut. Due to the aluminium being easier to machine than the titanium workpiece, four values of maximum chip thickness h_{max} from 0.04 mm to 0.12 mm were used. Flexure acceleration was detected with an accelerometer as before. In addition, a Hall-effect probe triggered by 2-equally spaced slots on the tool holder was used (Figure 8.3c,d) to measure the spindle rotation. This allowed once per revolution samples (1/Rev) and two-dimensional Poincaré maps to be constructed [164] so as to illustrate the nonlinear response. Stable behaviour was detected from 1/Rev accelerometer samples approaching a fixed point with a variance less 10^{-3} m/s^2. The procedure was repeated for each of the h_{max} values for regular and variable helix/pitch tools.

8.4   Results

The results of both experimental configurations are now presented to investigate the influence of tool geometry on process damping performance. First, edge radius measurements and FRFs of tool and workpiece are presented. Repeatability tests are then shown in order to include a basic error analysis in the main experimental results.

8.4.1   Preliminary tests

The measurements of the cutting edge radius of the tools are first presented in Table 8.1. The relatively high standard deviations indicate that the edge radius varied somewhat between the measurements on individual tools. Nevertheless, there is a significant variation in edge radius between one tool and the next. This allows the process damping performance to be characterised in terms of the tool's average edge radius.

As previously mentioned, the FRF of the tools was used to select initial values for the spindle speed and hence feedrate. The FRF measurement is shown in Figure 8.5, where 2358 Hz is the major resonant frequency of the tool. The FRF was found to be very similar for all the tools used in the flexible tool experiments, so only one set of data is included here. Using the procedure previously described, the required initial feed rate and spindle speed was determined. This led to an initial spindle speed of $\Omega = 281$ rpm, and at $h_{max} = 0.03$ mm and initial feedrate $fr = 70$ mm. A similar procedure was repeated for other h_{max} and tools.

Figure 7.2 (Chapter 7) shows the frequency response function for the flexible aluminium workpiece used in the second experimental configuration. Here, a single resonant frequency is observed at 200 Hz. For these tests, the use of a flexible workpiece has avoided the issue of the tool helix angle's influence on the dominant modal parameters of the system.

In the machining experiments, the spindle speed was increased smoothly and continuously under constant feed per tooth until chatter was found. A typical result to demonstrate this method is shown in Figure 8.6. Here, the accelerometer signal is plotted for different analysis regions from the duration of the cut. Near the beginning of the cut (Figure 8.6a), the vibration level is very low. As the spindle speed is increased (Figure 8.6b, c), the vibration magnitude starts to grow and a Fourier analysis indicates that the peak frequency is close to the natural frequency of the tool. Eventually, the vibration magnitude at the chatter frequency is deemed unacceptable (Figure 8.6d). Based on this result, the corresponding process damping wavelength can then be determined. A corresponding image of the workpiece surface is shown in Figure 8.6e.

This procedure was repeated for each cutter, for four different values of maximum chip thickness.

Clearly, the procedure outlined above is somewhat subjective because it involves an arbitrary threshold for determining the onset of chatter vibrations of unaccepted amplitude. Furthermore, small variations in the setup from one experiment to the next could have an influence on the observed behaviour. Consequently, at the end of the experiments, a selection of tests was repeated to assess the influence of process variability and also to confirm that the threshold-based analysis approach gave consistent results. Making the repeated tests after the other experiments also meant that there would be a slight amount of tool wear, so its influence could be compared to the influence of the other process parameters. Some repeatability tests are presented in Figure 8.7. It can be seen that all tools indicate a repeatability error of less than +/-5 percent between the original test/analysis and the repeated test/analysis. It is clear that even considering this repeatability error, the maximum chip thickness (and consequently the feed per tooth) has a very significant effect on the process damping wavelength.

A further check on the accuracy of the data involved a comparison with previous tests [173] performed using the same tool and workpiece specifications. In these earlier experiments, tool edge measurement facilities were not available and the process damping wavelength was determined only for h_{max} = 0.03 mm. Nevertheless, there was reasonable agreement between the two sets of data. Consequently, in the following sections, the role of tool geometry will be considered, using error margins of +/- 5 percent on the experimental data.

8.4.2 Cutting edge radius

Figure 8.8 show the process damping performance results for all tools. It can be seen that tools with identical rake and relief geometries have different process damping performance due to the edge radius of the tool. In all cases, the process damping performance improves when the cutting edge radius is increased. In some cases, this variation was as significant as that obtained due to change in the maximum chip thickness. However, for some tools, particularly PD8, the change in edge radius has a

marginal effect compared to the magnitude of the experimental error. Closer inspection reveals that tool PD8 had similar edge radii for all three tools and the standard deviation for individual tools was also high. Consequently, the fact that all three PD8 tools had similar performance is less surprising.

8.4.3 Rake and relief angles

In comparison to Section 8.4.2, the task of assessing the influence of tool rake and relief angle becomes more complex. In order to isolate the effect of tool rake and relief angle from the tool edge radius, the tools were first re-classified in terms of their edge radius. Three groups were formed based on a low (5-10 μm), medium (11-15 μm) and high (16-20 μm) edge radius. These groupings are shown in Table 8.2. It can be seen that only two tools, PD5(2) and PD11(4), were classified as having a high edge radius. Nevertheless, based on this classification, it is possible to compare tools that have a similar edge radius but different rake and relief angles.

In Figure 8.9, a comparison of λ_c is made according to the average cutting edge radius classification, and a clear pattern can be seen. Figures 8.9a,c,e show that process damping performance decreased when the rake angle was increased for a relief angle of 6 degrees. In contrast, process damping performance increased when the rake angle was increased for a relief angle of 12 degrees (Figures 8.9b,d). Again, this variation was more significant than the 5 percent repeatability error of the experiment. To summarise, a low relief angle gave better process damping performance with smaller rake angles, while at high relief angles, better performance was obtained with higher rake angles. This was true for all the available edge radius classifications.

8.4.4 Variable helix/pitch angles

Regular and variable helix/pitch cutters were evaluated and their process damping performance compared, as shown in Figure 8.10. It should be reiterated that this experiment concerned the machining of an aluminium alloy block on a very flexible workpiece. Consequently, the measured process damping wavelengths were markedly different to those of the previous experiment (involving a titanium workpiece). In fact, the process damping wavelength for this study was an order of greater. This could be attributed to the different workpiece material or the considerably lower axial depth of cut used in these experiments. Despite this, Figure 8.10 shows the variable helix/pitch

tool has a very high process damping wavelength compared to the standard tool. In fact, the process damping wavelength is almost doubled, which is a far more significant effect than that of the tool geometries considered in the previous experiment.

It is worth pointing out that the measurements from the flexible workpiece experiments allow a more detailed and less subjective analysis of the vibrations, based on once-per-revolution samples of the accelerometer signal. However, this advantage is at the expense of requiring easy-to-machine workpiece material (aluminium rather than titanium alloy) and a very low depth of cut.

8.5 Discussion

The results have demonstrated some interesting and useful relationships between tool geometry and processing damping performance. A number of points are worthy of further discussion.

The experimental data shown in Figure 8.6 indicate that the vibration during machining grew quite steadily as the spindle speed was increased. This makes it difficult to identify a discrete transition from stable cutting to unstable cutting (i.e. chatter). Conversely, previous experiments [170] and models [175] usually suggest a swift transition from stable to unstable cutting. The gradual increase in vibration amplitude observed in the experiments has two implications. First, that the process damping phenomenon has a more complex nonlinear influence on the chatter stability boundary since there is no clearly definable transition from stable machining (with low vibration amplitude) to unstable machining (with excessively high vibration amplitude). This is in constrast to early work on 'dynamic cutting force coefficients' [16] which implies that there is a clearly defined stability boundary even under process damping cutting conditions. Second, the gradual growth in vibrations makes it more difficult to determine reliably the boundary between acceptable and unacceptable cutting indicated by the process damping wavelength. In the first set of experiments, this was addressed by repeatability tests. In the second set of experiments, the use of a flexible workpiece enabled a more quantitative analysis of the machining vibrations based on the variance of the once-per-revolution acceleration samples. Clearly, the quantification and classification of process damped milling performance remains an issue for further research.

Also for discussion are the possible mechanisms that have given rise to the behaviour observed in these experiments. Considering the influence of feedrate, it is clear that increasing the maximum chip thickness has increased the tool's penetration into the workpiece. It could be argued that such changes in chip thickness could exacerbate any nonlinearity in the cutting force coefficients. However, a related set of experiments [173] suggests that this was not the case here. Consequently, alternative explanations are needed to explain the significant increase in process damping performance obtained by increasing the feedrate.

Meanwhile, the influence of tool edge radius is more readily explained by returning to the conceptual explanation illustrated in Figure 8.2. If this figure were redrawn to include a tool radius, then flank/workpiece interference and tool/workpiece ploughing would clearly be increased. However, the complex interaction between rake and relief angle, along with their smaller influence on process damping performance cannot be explained by the Figure 8.2. Likewise, the dramatic influence of variable pitch/helix angles cannot be easily explained. To summarise, the focus of this study has been to illustrate experimental observations of process damped milling. Further work is needed to explain some of these findings using realistic models of milling dynamics and chip mechanics.

The present study has focused on the role of the tool's angular geometry in process damping but the maximum chip thickness has also been considered and this was varied by increasing the machining feed rate. In practice, the chip thickness is also a function of tool diameter and machining radial depth of cut, as shown in Equation 8.3. Further work could investigate whether varying the tool radial depth of cut/diameter ratio has an equivalent effect to varying the machining feed rate. However, in practice, other factors may influence the chosen radial depth of cut. For example, tool life is a critical factor under process damped conditions and for a given material removal rate, tool wear can be spread across more of the tool's length by using a large axial and low radial depths of cut.

It is useful to briefly compare the findings of this study with some of the previous literature on process damped turning and milling that has considered tool geometry. Much of the earlier research has considered easy-to-cut-materials (steel and aluminium), whereas the present study used titanium alloy when considering the tool rake, relief and edge radius. Additionally, previous studies concerning increased edge radius have often focused on turning operations. In turning experiments, Budak and Tunc [167] identified similar results concerning the edge radius, along with increased performance from a low relief angle and smaller rake angles. However, the present study has also indicated that high relief angles coupled with higher rake angles can contribute to better performance. Furthermore, to the author's knowledge, previous studies have not considered the role of variable helix/pitch angles in process damping behaviour.

Finally, as with any experimental investigation of machining chatter and process damping, experimental accuracy and repeatability needs to be properly considered before drawing conclusions from the collected data. In the present study, these experimental errors were addressed as follows. First, measurement and classification of tool edge radius involved an average of 12 measurements for each tool. Second, of the 18 tools tested, five were subjected to a repeat test as described in Section 8.4.1. The repeatability tests showed variations of less than 5 percent and so appropriate error bars were included in the subsequent analysis. Third, a subset of experiments involved a repetition of previous tests reported in Turner [173]. There was close agreement between the data sets, despite the use of different experimental equipment and different operating personnel. Consequently, the authors have sufficient confidence in the present results to draw general and industrially relevant conclusions from the data. Nevertheless, future efforts to provide a more statistically detailed analysis would be of value, particularly from a modelling and model calibration perspective.

8.6 Summary

This chapter has presented experimental results demonstrating the influence of edge radius, rake and relief angles and variable helix/pitch angles on process damping performance in low speed milling. It has revealed variable helix/pitch angles played a more significant role in increasing performance compared to cutting edge, rake and relief angles and feed rate. Increasing the edge radius also tended to increase the process damping performance to a significant extent. This has important implications

because of the difficulties in controlling edge radius during tool manufacture and the inevitable influence of tool wear on the tool edge geometry.

The effect of rake and relief angles was less significant and more complex. A low relief angle tool increased process damping performance when the rake angle was also low. However, for high relief angles, better performance was achieved with high rake angles. Both of these parameters were less significant than the variations in maximum chip thickness used in the present study.

From a practitioner's standpoint, these conclusions can be used to make informed decisions regarding tool choices, when other constraints require low-speed milling. In particular, variable helix/ pitch tooling should be considered, as well as using a high feedrate. Inconsistent behaviour between nominally identical tools could be attributed to poor control of the tool's edge geometry, due to either manufacturing variability or tool wear.

Table 8.1 Milling tools' geometry

Tool	Rake angle, γ (°)	Relief angle, α (°)	Average cutting edge radius, μm (standard deviation)		
			Tool 1	Tool 2	Tool 3
PD5	0	6	16.9(7.8)	9.9(2.6)	8.3(3.1)
PD6	0	12	11.4(5.4)	12.8(3.7)	13.5(3.3)
PD8	6	6	9.7(4.6)	12.8(3.6)	12.4(5.2)
PD9	6	12	9.3(2.5)	7.1(1.9)	8.2(2.0)
PD11	12	6	8.0(1.5)	11.4(3.4)	17.0(8.3)

Table 8.2 Classification of milling tools' average edge radius

Class	Low	Medium	High
Range (µm)	6-10	11-15	16-20
PD5	Tool 2, 3		Tool 1
PD6		Tool 1, 2, 3	
PD8	Tool 1	Tool 2, 3	
PD9	Tool 1, 2, 3		
PD11	Tool 1	Tool 2	Tool 3
PD12	Tool 2	Tool 1, 3	
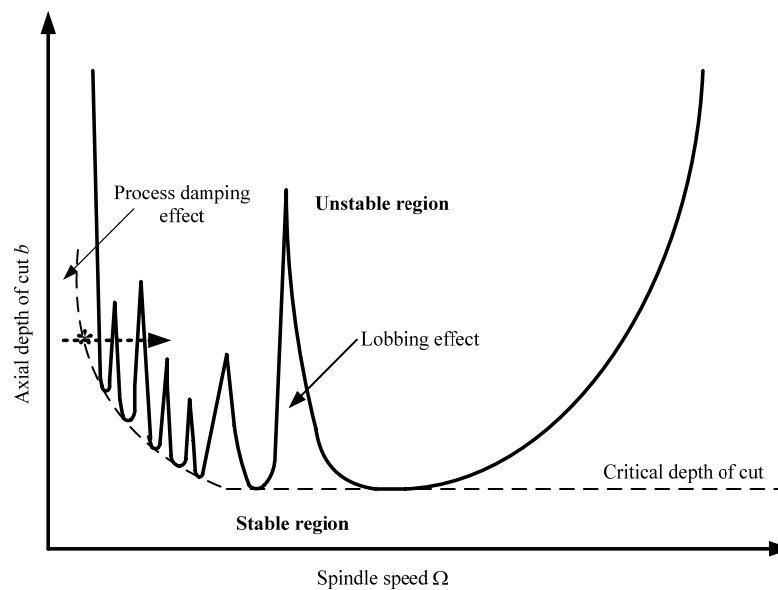
Figure 8.1 Stability lobes for process damping. * shows the spindle speed and ---→cutting test configuration
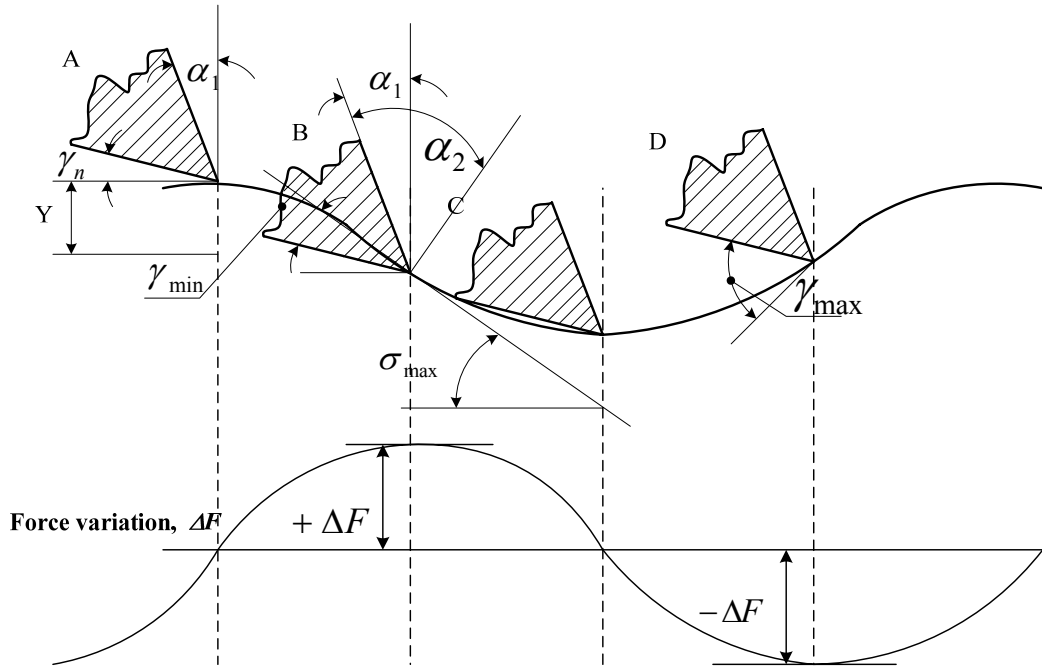
Figure 8.2 Process damping mechanism

a) Edge location   b) Flute location
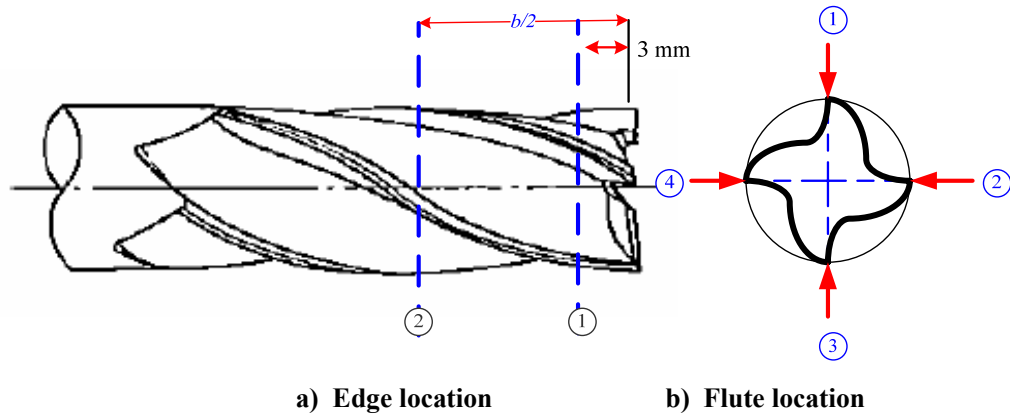
Figure 8.3 Milling tool measurement location

a) Schematic diagram of flexible tool

b) Sensor location of flexible tool

c) Schematic diagram of flexible workpiece

d) Sensor location of flexible workpiece
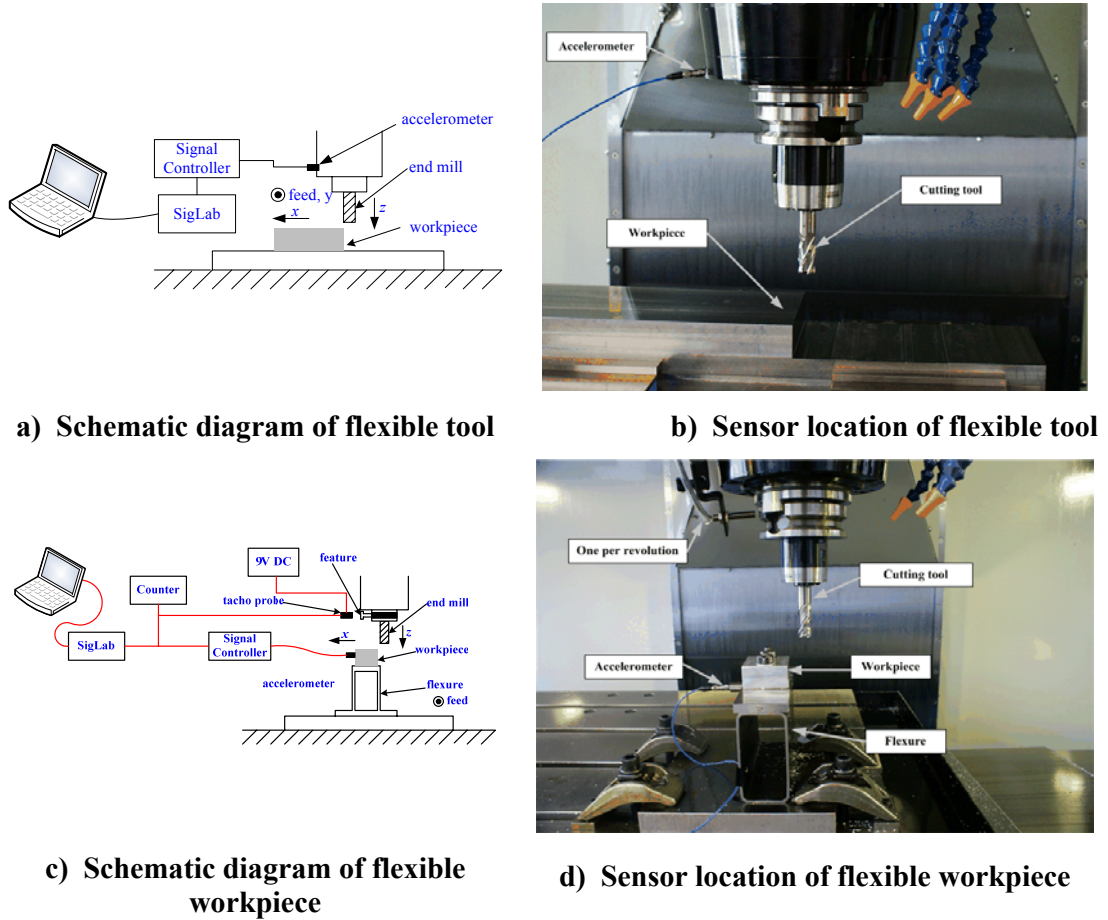
Figure 8.4 Experimental process damping arrangement
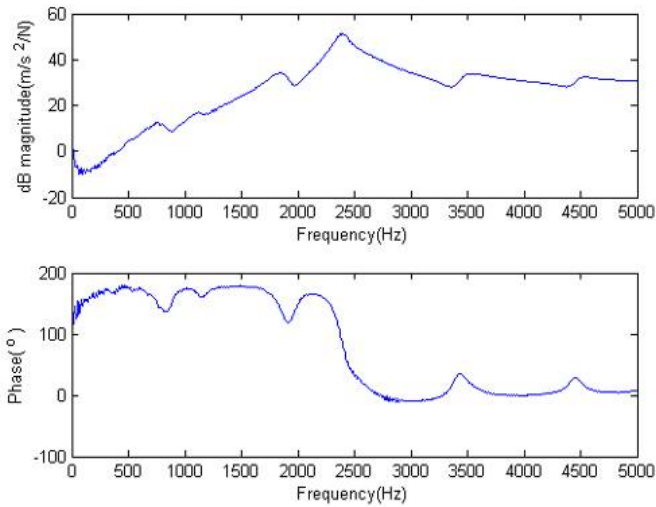
Figure 8.5 Frequency response function for PD5(1) tool in *x*-direction
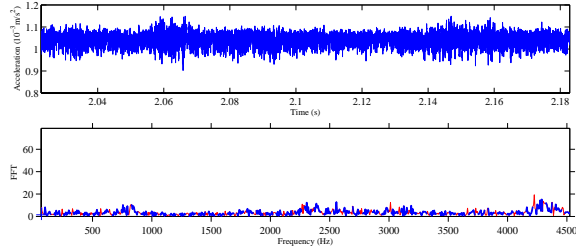
a) Stable condition with Ω = 281 rev/min and *fr* = 174 mm/min.
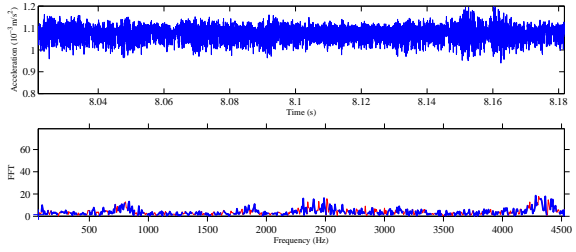
b) Stable condition with Ω = 309 rev/min and *fr* = 262 mm/min.
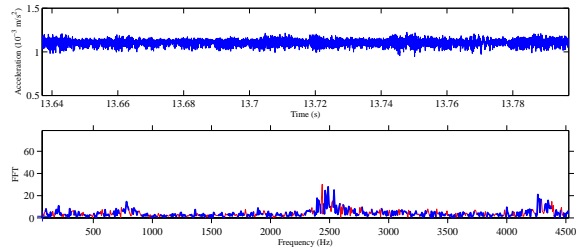
c) Stable condition with Ω = 340 rev/min and *fr* = 289 mm/min.
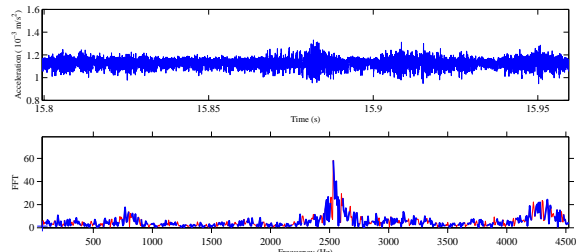
d) Chatter detection with Ω = 374 rev/min and *fr* = 317 mm/min
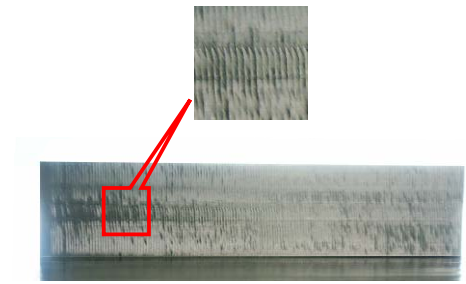
e) Workpiece surface at condition d).

Figure 8.6 FFT level and workpiece surface for PD11(3) at h_{max}= 0.075mm
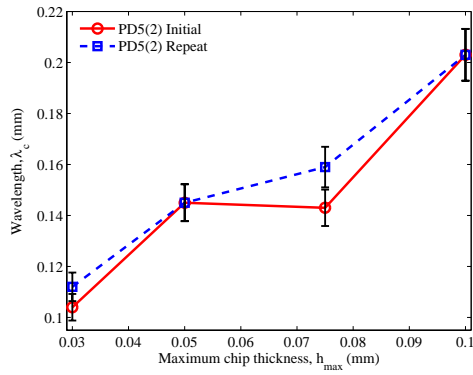
a) **PD5(2)**
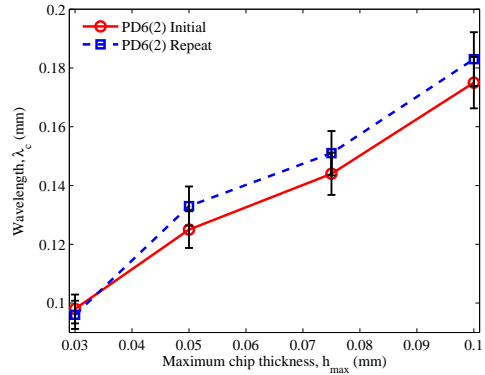
b) **PD6(2)**
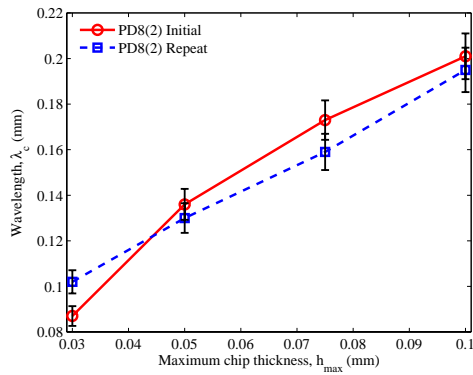
c) **PD8(2)**
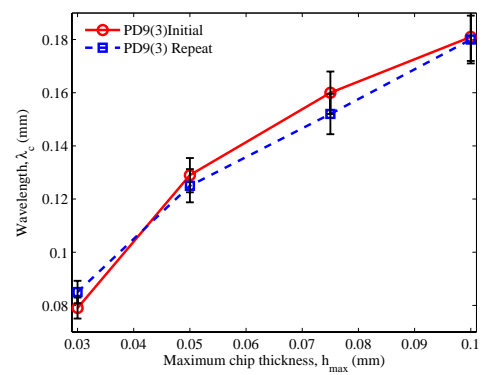
d) **PD9(3)**
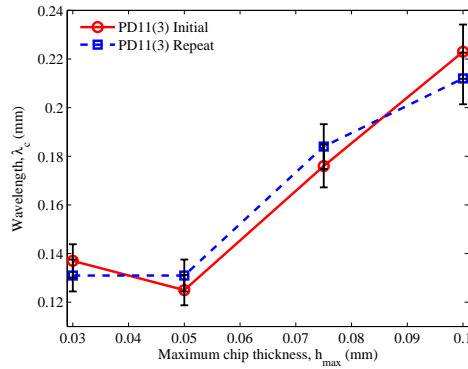
e) **PD11(3)**

Figure 8.7 Repeatability of selected tools
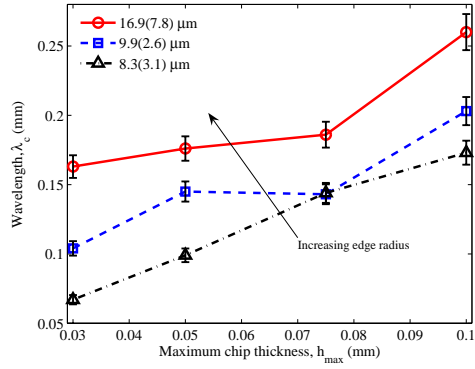
a) PD5
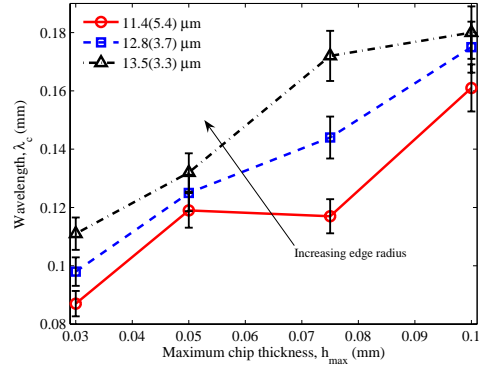
b) PD6
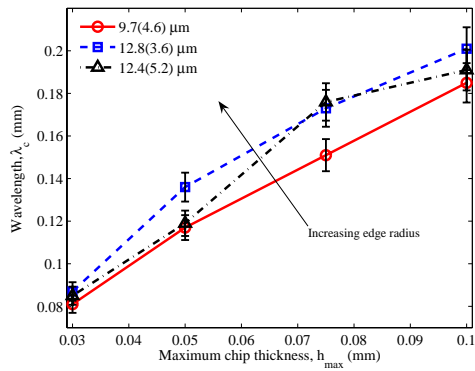
c) PD8
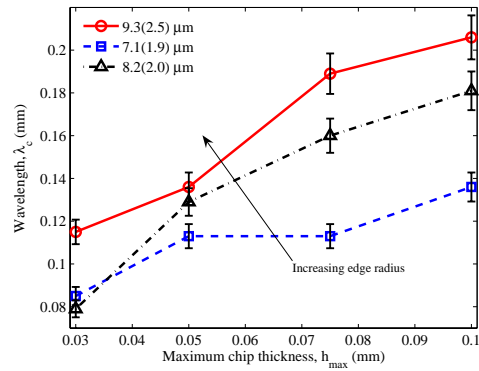
d) PD9
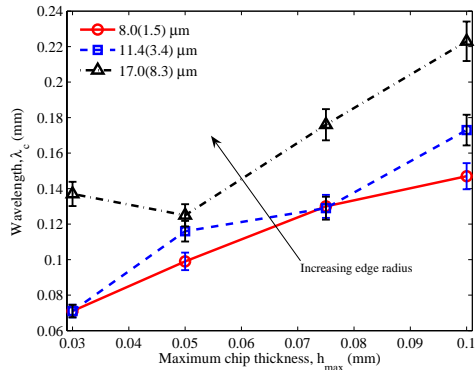
e) PD11
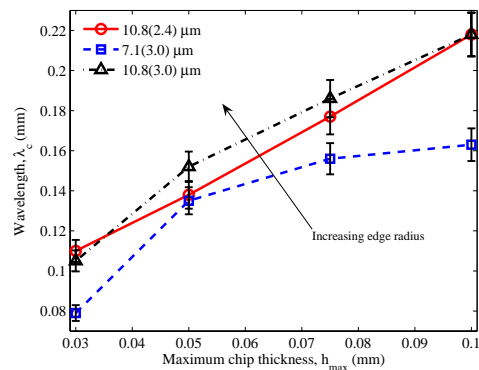
f) PD12

Figure 8.8 Effect of tool edge radius on process damping wavelength
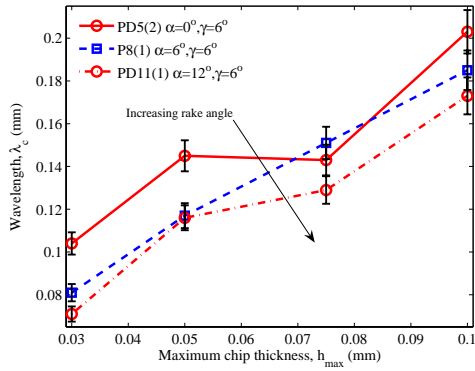
a) Low edge radius at γ **= 6 °**
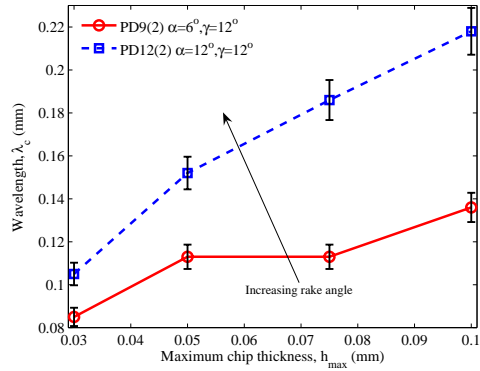
b) Low edge radius at γ **= 12 °**
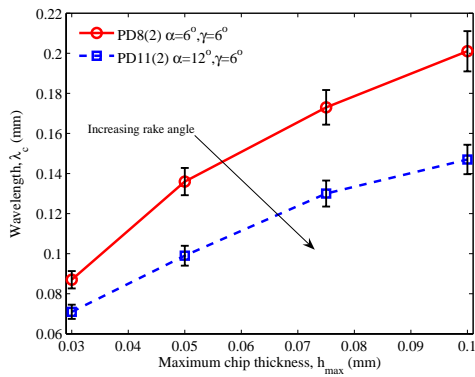
c) Medium edge radius at γ **= 6 °**
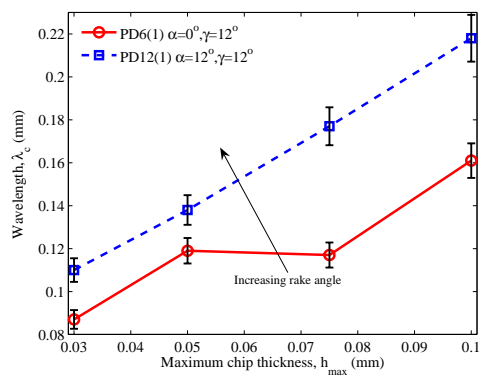
d) Medium edge radius at γ **= 12 °**
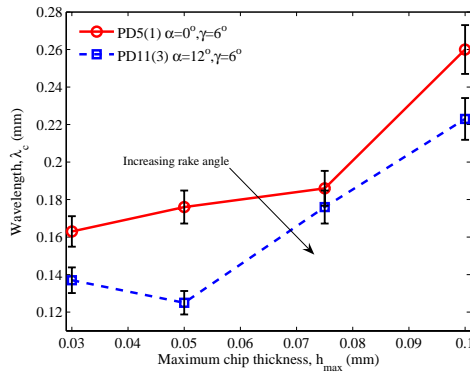
e) High edge radius at γ **= 6 °**

Figure 8.9 Effect of rake and relief angles on process damping wavelength.
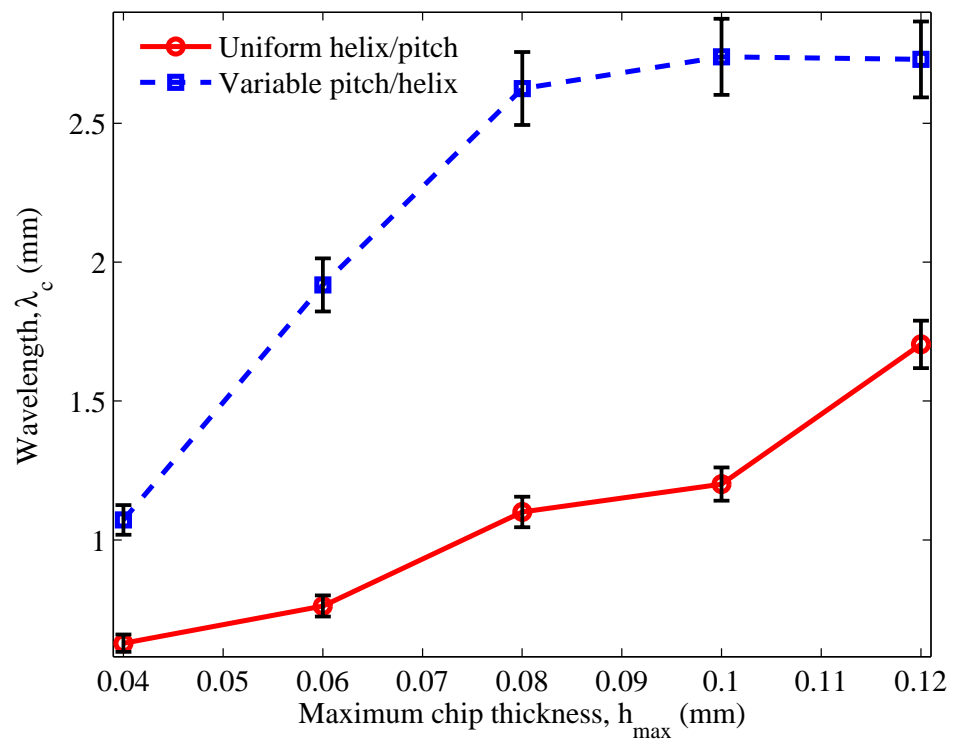
Figure 8.10 Effect of variable helix and variable pitch angles on process damping wavelength

CHAPTER 9
CONCLUSIONS

9.1 Summary of Thesis

Chapter 1 introduced the background, motivation and objectives of the current study. The chatter stability prediction, chatter suppression technologies and chatter optimisation algorithms which have been used in machining are comprehensively reviewed in Chapter 2. In Chapter 3, a semi-discretisation method for analytical chatter stability was mathematically formulated and an optimisation scheme briefly introduced.

In Chapter 4, preliminary experiments were made of amplitude dependence in determining frequency response functions (FRF). Experimental modal analysis using a non-contacting actuator was compared to the results from impact hammer testing. The force and current were used as excitation input to estimate FRFs of cutting tools with amplitude dependent conditions. This FRF amplitude dependency analysis was then extended to study the time response when applying a square wave of different excitation magnitudes. The amplitude dependency of milling tools was shown to be a potential problem for the optimisation of milling tools from a chatter perspective.

Optimisation algorithms of Differential Evolution (DE) and Sequential Quadratic Programming (SQP) were theoretically described in Chapter 5. In Chapter 6, an optimisation approach of the semi-discretisation method (as described in Chapter 3) and optimisation algorithms (in Chapter 5) were combined by the targeting of chatter minimisation and chatter performance maximisation. The DE algorithm was then refined by introducing the bounce back and mixed population approach, including modified objective functions. Chatter minimisation and material removal rate maximisation were then combined to introduce a multi-objective optimisation using the Pareto trade approach of epsilon constraint. The numerical optimisation solutions were benchmarked by the SQP algorithm and compared to variable pitch tool optimisation.

Chapter 7 presented the practical application of optimisation of variable helix and variable pitch to minimise chatter using the DE algorithm. Although the cutting tests were successful in validating and improving the stability margin during the cutting operation with an optimised variable helix and variable pitch tool, its performance has

been limited by low engagement of variable helix geometry. This issue was resolved by using higher depth of cut to properly validate the SDM chatter stability modelling for variable helix tools.

In Chapter 8, experimental testing was conducted for process damped milling. Process damping performance was compared and considered with different milling tool geometry such as edge radius, rake and relief angles and variable pitch.   There were two experimental configurations used. A flexible tool condition was first study for edge radius and rake and relief angles effects. For variable helix/pitch (Chapter 7) geometry effect, a flexible workpiece condition was used to compare the process damping performance to that for regular tool.

The conclusions and contributions will now be listed and recommendations for future works suggested.

9.2   Conclusions

From the thesis summary, the conclusions for this research are as follows:

- Variable helix tools can be optimised to avoid chatter and improve productivity.
- This has been both theoretically predicted and experimentally validated.
- Differential Evolution algorithms find better solutions than Sequential Quadratic Programming especially when refined to include bounce back and mixed population approaches.
- For all the cases considered, tools with variable helix and variable pitch always performed better than those with only a variable pitch, or only a variable helix.
- Variable helix tools can exhibit period-one instability.   This has been observed experimentally for the first time.
- Optimisation of tool helix angle has been shown to be sensitive to the FRF of the system. Unfortunately it has been shown that tools exhibit small changes in FRF dependency upon excitation amplitude. This nonlinearity is not presently considered in stability analysis and remains a topic for further work.
- Finally, under certain conditions, variable helix/pitch tool has a very significant role in increasing process damping performance, compared to cutting edge, rake and relief angles and feedrate.

9.3 Contributions from Current Work

The aims of the current study were to design and produce optimised variable helix milling tools. In addition to this chatter suppression method, the current research also studied the importance of amplitude dependency in the FRF estimation, and investigated the importance of process damped milling for variable helix tools. The following summarises the original contributions for this research:

- Combined the semi-discretisation method with Differential Evolution (DE) algorithm for optimising variable helix tools using chatter minimisation and chatter performance maximisation objective functions.

- Introduced refined (mixed population and bounce back approach) Differential Evolution algorithm and modified objective functions to improve optimisation results.

- Implemented variable helix and variable pitch at its end tools geometry to completely mitigate chatter compared to other tool geometries.

- Compared optimised variable helix and variable pitch tools with previous research of variable pitch tools geometry based on current methodology.

- Applied multi-objective optimisation based on ε-constraints Pareto front optimal solution to optimise chatter performance and material removal rate simultaneously.

- Experimentally validated the optimised variable helix and variable pitch tools based on Differential Evolution optimisation solution to suppress chatter with a 5-fold increase under low radial immersion and flexible workpiece condition.

- Experimentally verified variable helix tools chatter stability prediction based on the semi-discretisation method using higher axial depth of cut condition.

- Identified period-one chatter instability islands experimentally for variable helix tools.

- Experimentally verified nonlinear response behaviours when exciting the cutting tools with an electromagnetic actuation system.

- Ranked the influence of tool geometry (variable helix/pitch, edge radius and rake and relief angles) to improve process damped milling.

9.4 Suggestions for Future Work

The following suggestions can be made for future research:

- A non-contacting electro-magnetic actuator is proposed to be applied under conditions of spindle speed dependency and amplitude dependency. Then investigating FRF and stability lobe effects due to spindle speed and amplitude dependency before can be applied in optimising variable helix and variable pitch for flexible tools condition.

- Applying the current optimisation procedure by considering uncertainty and sensitivity of variable helix and variable pitch. Another candidate which can be proposed for multi-objective problem is non-sorted Genetic Algorithms instead of using ε-constraint multi-objective optimisation.

- Experimental validation for other objective functions such as performance maximisation and multi-objective problems to validate the optimisation procedure. Instead of the flexible workpiece applied for the study, future work on the current method needs to be based upon the flexible tool condition in order to make real industrial applications.

- Further work in process damping is needed to explain these trends with physically realistic models of process damped milling. It should be suggested to be re-iterated that the present study benchmarked variable helix/pitch tools using a flexible aluminium workpiece rather than a rigid titanium workpiece. Experiments are proposed to investigate the performance of these tools when cutting titanium and other difficult-to-cut materials.

REFERENCES

1   **Alcoa**. *Aerospace market dynamics: Metal is the key component*. 2008 [cited 2008 2nd May 2008]; Available from: www.alcoa.com/aerospace/en/metal.asp.

2   **Aronson, R.B.** Machine tool 101:Part 7, machine tools of the future. *Society of Manufacturing Engineering.* July 1994, 1994.

3   **Tlusty, J.** *Manufacturing process and equipment* (Prentice Hall, New Jersey, 2000).

4   **Tlusty, J. and Ismail, F.** Special aspects of chatter in milling. *Journal of vibration, acoustic, stress and reliability in design, Transactions of the ASME*, 1983, **157**, 24-32.

5   **Altintas, Y., Engin, S. and Budak, E.** Analytical stability prediction and design of variable pitch cutters. *Journal of Manufacturing Science and Engineering, Transactions of the ASME*, 1999, **121**(2), 173-178.

6   **Bayly, P.V., Halley, J.E., Mann, B.P. and Davies, M.A.** Stability of interrupted cutting by temporal finite element analysis. *Journal of Manufacturing Science and Engineering*, 2003, **125**, 220-225.

7   **Insperger, T. and Stepan, G.** Semi discretization method for delayed system. *International Journal for Numerical Methods in Engineering*, 2002, **55**, 503-518.

8   **Slavicek, J.** The effect of irregular tooth pitch on stability of milling. *Proceedings of the 6th MTDR Conference*, 1965, 15-22.

9   **Opitz, H., Dregger, E.U. and Rose, H.** Improvement of the dynamics stability of the milling process by irregular tooth pitch. *Advances in Machine Tool Design and Research, Proc. of MTDR Conference* 1966, **7**, 213-227.

10   **Stone, B.J.** The effect on the chatter behaviour of cutters with different helix angles on adjacent teeth. *Advances in Machine Tool Design and Research, Proc. of 11th International MTDR Conference University of Birmingham*, 1970, **A**, 169-180.

11   **Budak, E.** An analytical design method for milling cutters with non-constant pitch to increase stability, part 1: Theory and part 2: Application. *Journal of Manufacturing Science and Engineering* 2003, **125**, 29-38.

12   **Olgac, N. and Sipahi, R.** Dynamic and stability of variable pitch milling. *Journal of Vibration and Control*, 2007, **13**(7), 1031-1043.

13   **Huyanan, S.** An active vibration absorbers for chatter reduction in machining. *PhD Thesis*. Depertmental of Mechanical Engineering, The University of Sheffield, 2007.

14   **Stephenson, D.A. and Agapiou, J.S.** *Metal cutting: Theory and practice*. (Taylor & Francis Group, Boca Raton, 2006).

15   **Merchant, M.E.** Mechanics of the metal cutting process. *ASME J. of Applied Physics*, 1945, **16**(5), 318-324.

16   **Tobias, S.A. and Fishwick, W.** Theory of regenerative machine tool chatter. *The Engineer*, 1958, **205**, 199-203.

17   **Tlusty, J. and Polacek, M.** The stability of machine tool against self-excited vibration in machining. *Proc of International Production Engineering Research Conference*, 1963, 465-471.

18   **Altintas, Y. and Budak, E.** Analytical prediction of stability lobes in milling. *CIRP Annals - Manufacturing Technology*, 1995, **44**(1), 357-362.

19   **Budak, E. and Altintas, Y.** Analytical prediction of chatter stability in milling - part i: General formulation & part ii:Application of the general formulation to common milling systems. *Journal of Dynamic Systems, Measurement and Control, Transactions of the ASME*, 1998, **120**(1), 22-36.

20   **Butcher, E.A., Ma, H., Beuler, E., Averia, V. and Zsolt, S.** Stability of linear time-periodic delay-differential equations via chebyshev polynomials. *International Journal for Numerical Methods in Engineering*, 2004, **59**, 895-922.

21   **Tlusty, J.** A method of analysis of machine tool stability. *Proc 6th MTDR Conference*, 1965, 5-14.

22   **Merritt, H.E.** Theory of self-excited machine tool chatter, contribution to machine-tool chatter research-i. *Transaction ASME Journal of Engineering Industry*, 1965, **87**(4), 447-454.

23   **Andrew, C. and Tobias, S.A.** A critical comparison of two current theories of machine tool chatter. *International Journal of Machine Tool Design and Research*, 1961, **1**(4), 325-335.

24   **Tlusty, J. and MacNeil, P.** Dynamics of cutting forces in end milling. *Ann CIRP*, 1975, **24**(1), 21-25.

25   **Tlusty, J., Ismail, F. and Zaton, W.** Use of special milling cutters against chatter. *SME Manufacturing Engineering Transactions*, 1983, 408-415.

26   **Sridhar, R., Hohn, R.E. and W., L.G.** A general fomulation of the milling process equation, contribution to machine-tool chatter research-v. *Transaction ASME Journal of Engineering Industry*, 1968, **90**(2), 317-324.

27   **Olgac, N. and Hosek, M.** A new perspective and analysis for regenerative machine tool chatter. *International Journal of Machine Tools and Manufacture*, 1998, **38**(7), 783-798.

28   **Davies, M.A., Pratt, J.R., Dutterer and Burns, T.J.** Stability prediction for low radial immersion milling. *Journal of Manufacturing Science and Engineering*, 2002, **124**, 217-225.

29   **Sims, N.D., Mann, B. and Huyanan, S.** Analytical prediction of chatter stability for variable pitch and variable helix milling tools. *Journal of Sound and Vibration*, 2008, **317**(3-5), 664-686.

30   **Patel, B.R., Mann, B.P. and Young, K.A.** Uncharted islands of chatter instability in milling. *International Journal of Machine Tools and Manufacture*, 2008, **48**(1), 124-134.

31   **Tobias, S.A.** Machine tool vibration research. *International Journal of Machine Tool Design and Research*, 1961, **1**(1-2), 1-14.

32   **Liu, K.J. and Rouch, K.E.** Optimal passive vibration control of cutting process stability in milling. *Journal of Materials Processing Technology*, 1991, **28**(1-2), 285-294.

33   **Sims, N.D.** Vibration absorbers for chatter suppression: A new analytical tuning methodology. *Journal of Sound and Vibration*, 2007, **301**(3-5), 592-607.

34   **Ema, S. and Marui, E.** Suppression of chatter vibration of boring tools using impact dampers. *International Journal of Machine Tools and Manufacture*, 2000, **40**(8), 1141-1156.

35   **Semercigil, S.E. and Chen, L.A.** Preliminary computations for chatter control in end milling. *Journal of Sound and Vibration*, 2002, **249**(3), 622-633.

36   **Tewani, S.G., Rouch, K.E. and Walcott, B.L.** A study of cutting process stability of a boring bar with active dynamic absorber. *International Journal of Machine Tools and Manufacture*, 1995, **35**(1), 91-108.

37   **Tarng, Y.S., Kao, J.Y. and Lee, E.C.** Chatter suppression in turning operations with a tuned vibration absorber. *Journal of Materials Processing Technology*, 2000, **105**(1-2), 55-60.

38   **Huyanan, S. and Sims, N.D.** Active vibration absorbers for chatter mitigation during milling. *Ninth International Conference on Vibrations in Rotating Machinery 2008.* Exeter, 2008. pp. 125-140.

39   **Pratt, J.R. and Nayfeh, A.H.** Chatter control and stability analysis of a cantilever boring bar under regenerative cutting conditions. *Philosophical Trans. of the Royal Society A: Mathematical, Physical and Engineering Sciences*, 2001, **359**(1781), 759-792.

40   **Chung, B., Smith, S. and Tlusty, J.** Active damping of structural modes in high-speed machine tools. *Journal of Vibration and Control*, 1997, **3**(3), 279-295.

41   **Ganguli, A., Deraemaeker, A. and Preumont, A.** Regenerative chatter reduction by active damping control. *Journal of Sound and Vibration*, 2007, **300**(3-5), 847-862.

42   **Zhang, Y. and Sims, N.D.** Milling workpiece chatter avoidance usingpiezoelectric active damping: A feasibility study. *Smart Materials and Structures*, 2005, **14**, 65-70.

43   **Dohner, J.L., Lauffer, J.P., Hinnerichs, T.D., Shankar, N., Regelbrugge, M., Kwan, C.-M., Xu, R., Winterbauer, B. and Bridger, K.** Mitigation of chatter instabilities in milling by active structural control. *Journal of Sound and Vibration*, 2004, **269**(1-2), 197-211.

44   **Glaser, D.J. and Nachtigal, C.L.** Development of a hydraulic chambered, actively controlled boring bar. *J Eng Ind Trans ASME*, 1979, **101**, 362-368.

45   **Wang, M. and Fei, R.** On-line chatter detection and control in boring based on an electrorheological fluid. *Mechatronics*, 2001, **11**(7), 779-792.

46   **Segalman, D.J. and Butcher, E.A.** Suppression of regenerative chatter via impedance modulation. *Journal of Vibration and Control*, 2000, **6**(2), 243-256.

47   **Nigm, M.M.** A method for the analysis of machine tool chatter. *International Journal of Machine Tool Design and Research*, 1981, **21**(3-4), 251-261.

48   **Wang, J.H. and Lee, K.N.** Suppression of chatter vibration of a cnc machine centre-an example. *Mechanical Systems and Signal Processing*, 1996, **10**(5), 551-560.

49   **Chiou, C.-H., Hong, M.-S. and Ehmann, K.F.** The feasibility of eigenstructure assignment for machining chatter control. *International Journal of Machine Tools and Manufacture*, 2003, **43**(15), 1603-1620.

50   **Tlusty, J.** Dynamics of high speed milling. *Transaction ASME Journal of Engineering Industry*, 1985, **108**, 59-67.

51   **Kurdi, M.H., Schmitz, T.L., Haftka, R.T. and Mann, B.P.** Simultaneous optimization of material removal rate and part accuracy in high speed milling. *ASME International mechanical engineering congress and exposition (IMECE),* Anaheim, 2004.

52   **Tarng, Y.S. and Lee, E.C.** A critical investigation of the phase shift between the inner and outer modulation for the control of machine tool chatter. *International Journal of Machine Tools and Manufacture*, 1997, **37**(12), 1661-1672.

53   **Delio, T., Tlusty, J. and Smith, S.** Use of audio signals for chatter detection and control. *J Eng Ind Trans ASME*, 1992, **114**, 146-157.

54   **Sim, W., Dewes, R. and Aspinwall, D.** An integrated approach to the high-speed machining of moulds and dies involving both a knowledge-based system and a chatter detection and control system. *Proceedings of the Institution of*

Mechanical Engineers, Part B: Journal of Engineering Manufacture, 2002, **216**(12), 1635-1646.

55   **Lin, S.C., DeVor, R.E. and Kapoor, S.G.** The effects of variable speed cutting on vibration control in face milling. *J Eng Ind Trans ASME*, 1990, **112**, 1-11.

56   **Altintas, Y. and Chan, P.K.** In-process detection and suppression of chatter in milling. *International Journal of Machine Tools and Manufacture*, 1992, **32**(3), 329-347.

57   **Liao, Y.S. and Young, Y.C.** A new on-line spindle speed regulation strategy for chatter control. *International Journal of Machine Tools and Manufacture*, 1996, **36**(5), 651-660.

58   **Sridhar, S., Shiv, G.K., Richard, E.D. and Geir, E.D.** Chatter stability analysis of the variable speed face-milling process. *Journal of Manufacturing Science and Engineering*, 2001, **123**(4), 753-756.

59   **Tsao, T.-C., McCarthy, M.W. and Kapoor, S.G.** A new approach to stability analysis of variable speed machining systems. *International Journal of Machine Tools and Manufacture*, 1993, **33**(6), 791-808.

60   **Hashimoto, M., Marui, E. and Kato, S.** Experimental research on cutting force variation during regenerative chatter vibration in a plain milling operation. *International Journal of Machine Tools and Manufacture*, 1996, **36**(10), 1073-1092.

61   **Xiao, M., Wang, Q.M., Sato, K., Karube, S., Soutome, T. and Xu, H.** The effect of tool geometry on regenerative instability in ultrasonic vibration cutting. *International Journal of Machine Tools and Manufacture*, 2006, **46**(5), 492-499.

62   **Mei, Z., Yang, S., Shi, H., Chang, S. and Ehmann, K.F.** Active chatter suppression by on-line variation of the rake and clearance angles in turning-principles and experimental investigations. *International Journal of Machine Tools and Manufacture*, 1994, **34**(7), 981-990.

63   **Liu, C.R. and Liu, T.M.** Automated chatter suppression by tool geometry control. *J Eng Ind Trans ASME*, 1985, **107**, 95-98.

64   **Zatarain, M., Munoa, J., Peigne, G. and Insperger, T.** Analysis of the influence of mill helix angle on chatter stability. *CIRP Annals - Manufacturing Technology*, 2006, **55**(1), 365-368.

65   **Varterasian, J.H.** White noise: Tools to reduce chatter. *Manufacturing Engineering and Management*, 1971, **67**(4), 26-28.

66   **Tlusty, J.** Analysis of the state of research in cutting dynamics. *CIRP Annals*, 1978, **27**(2), 583-589.

67   **Elbestawi, M.A., Ismail, F., Du, R. and Ullagaddi, B.C.** Modelling machining dynamics including damping in the tool-workpiece interface. *Transaction ASME Journal of Engineering Industry*, 1994, **116**(4), 435-439.

68   **Turner, S., Merdol, D., Altintas, Y. and Ridgway, K.** Modelling of the stability of variable helix end mills. *International Journal of Machine Tools and Manufacture*, 2007, **47**(9), 1410-1416.

69   **Weck, M., Altintas, Y. and Beer, C.** Cad assisted chatter-free nc tool path generation in milling. *International Journal of Machine Tools and Manufacture*, 1994, **34**(6), 879-891.

70   **Ariffin M K A, S.N.D., Worden K**. Genetic optimisation of machine tool paths. *6 th International Conference on Adaptive Computing In Design And Manufacture In 'Adaptive Computing in Design and Manufacture VI,* Bristol., 2004. pp. 125-136.

71   **Smith, S. and Dvorak, D.** Tool path strategies for high speed milling aluminum workpieces with thin webs. *Mechatronics*, 1998, **8**(4), 291-300.

72   **Fletcher, R.** *Practical methods of optimization*. (John Wilet & Sons, West Sussex, 1987).

73   **Saravanan, R.** *Manufacturing optimization through intelligent techniques*. (Taylor & Francis Group, Boca Raton, 2006).

74   **Merdol, D. and Altintas, Y.** Virtual cutting and optimization of three-axis milling processes. *International Journal of Machine Tools and Manufacture*, 2008, **48**, 1063-1071.

75   **Merdol, D. and Altintas, Y.** Virtual cutting and optimization of milling operations-part 1: Process simulation part 2:Optimization and feedrate scheduling. *Journal of Manufacturing Science and Engineering*, 2008, **130**, DOI 10.1115/1111.2927434-2927435.

76   **Abuelnaga, A.M. and El-Dardiry, M.A.** Optimization methods for metal cutting. *International Journal of Machine Tool Design and Research*, 1984, **24**(1), 11-18.

77   **Aggarwal, A. and Singh, H.** Optmization of machining technique-a retrospective and literature review. *Sadhand*, 2005, **30**(6), 699-711.

78   **Mukherjee, I. and Ray, P.K.** A review of optimization techniques in metal cutting processes. *Computers & Industrial Engineering*, 2006, **50**(1), 15-34.

79   **Tusar, T., Korosec, P., Papa, G., Kilipic, B. and Silc, J.** A comparative study of stochastic optimization methods in electrical motor design. *Artificial Intelligence*, 2007, **27**(2), 101-111.

80   **Mayer, D.G., Kinghorn, B.P. and Archer, A.A.** Differential evolution - an easy and effiecient evolutionary algorithm for model optimisation. *Agricultural Systems*, 2005, **83**, 315-328.

81   **Pener, K. and Littlefair, G.** Free search - a comparative analysis. *Information Science*, 2005, **172**, 173-193.

82   **Price, K.V., Storn, R.M. and Lampinen, J.A.** *Differential evolution a practical approach to global optimization*. (Springer, Berlin Heidelberg, 2005).

83   **Saikumar, S. and Shunmugan, M.S.** Parameter selection based on surface finish in high speed finish in high speed end milling using differential evolution. *Materials and Manufacturing Processes*, 2008, **21**(4), 341-347.

84   **Krishna, A.** Selection of optimal conditions in the surface grinding process using a differential evolution approach. *Proceedings of the Institution of Mechanical Engineers, Part B: Journal of Engineering Manufacture*, 2007, **221**(7), 1185-1192.

85   **Maeda, O., Cao, Y. and Altintas, Y.** Expert spindle design system. *International Journal of Machine Tools and Manufacture*, 2005, **45**(4-5), 537-548.

86   **Tekeli, A. and Budak, E.** Maximization of chatter free material removal rate in end milling using analytical methods. *Machining Science and Technology*, 2007, **9**(2), 147-167.

87   **Shirase, K. and Altintas, Y.** Cutting force and dimensional surface error generation in peripheral milling with variable pitch helical end mills. *International Journal of Machine Tools and Manufacture*, 1996, **36**(5), 567-584.

88   **Nejat, O. and Rifat, S.** A unique methodology for chatter stability mapping in simultaneous machining. *Journal of Manufacturing Science and Engineering*, 2005, **127**(4), 791-800.

89   **Baskar, N., Asokan, P., Saravanan, R. and Prabhaharan, G.** Selection of optimal machining parameters for multi-tool milling operations using a memetic algorithm. *Journal of Materials Processing Tech.*, 2006, **174**(1), 239-249.

90 **Parent, L., Songmene, V. and Kenne, J.-P.** A generalised model for optimising and end milling operation. *Production Planning & Control*, 2007, **18**(4), 319-337.

91 **Yajun, J., Zhenliang, L. and Minghui, L.** Application of fuzzy and rough sets theory in the optimization of machining parameters for mold milling operations. *The International Journal of Advanced Manufacturing Technology*, 2006, **28**(11), 1071-1077.

92 **Juan, H., Yu, S.F. and Lee, B.Y.** The optimal cutting-parameter selection of production cost in hsm for skd61 tool steels. *International Journal of Machine Tools and Manufacture*, 2003, **43**(7), 679-686.

93 **Chua, M.S., Loh, H.T., Wong, Y.S. and Rahman, M.** Optimization of cutting conditions for multi-pass turning operations using sequential quadratic programming. *Journal of Materials Processing Technology*, 1991, **28**(1-2), 253-262.

94 **Stori, J.A. and Wright, P.K.** Parameter space decomposition for selection of the axial and radial depth of cut in endmilling. *Journal of Manufacturing Science and Engineering*, 2001, **123**(4), 654-664.

95 **Armarego, E.J.A., Smith, A.J.R. and Wang, J.** Constrained optimization strategies and cam software for single-pass peripheral milling. *International Journal of Production Research*, 1993, **31**(9), 2139-2160.

96 **Sonmez, A.I., Baykasoglu, A., Dereli, T. and Filiz, I.H.** Dynamic optimization of multipass milling operations via geometric programming. *International Journal of Machine Tools and Manufacture*, 1999, **39**(2), 297-320.

97 **El-Mounayri, H., Kishawy, H. and Briceno, J.** Optimization of cnc ball end milling: A neural network-based model. *Journal of Materials Processing Tech.*, 2005, **166**(1), 50-62.

98 **Stori, J.A., Wright, P.K. and King, C.** Integration of process simulation in machining parameter optimization. *Journal of Manufacturing Science and Engineering*, 1999, **121**(1), 134-143.

99 **Walvekar, A.G. and Lambert, B.K.** An application of geometric programming to machining variable selection. *International Journal of Production Research*, 1970, **8**(3), 241-245.

100 **By Chen, J.S., Huang, Y.K. and Chen, M.S.** Feedrate optimization and tool profile modification for the high-efficiency ball-end milling process. *International Journal of Machine Tools and Manufacture*, 2005, **45**(9), 1070-1076.

101 **Stoic, A., Kopac, J. and Cukor, G.** Testing of machinability of mould steel 40crmnmo7 using genetic algorithm. *Journal of Materials Processing Technology*, 2005, **164-165**, 1624-1630.

102 **Oktem, H., Erzurumlu, T. and Kurtaran, H.** Application of response surface methodology in the optimization of cutting conditions for surface roughness. *Journal of Materials Processing Technology*, 2005, **170**(1-2), 11-16.

103 **Savas, V. and Ozay, C.** The optimization of the surface roughness in the process of tangential turn-milling using genetic algorithm. *The International Journal of Advanced Manufacturing Technology*, 2007, doi:10.1007/s00170-00984-00171.

104 **Chang, C.-K. and Lu, H.** Design optimization of cutting parameters for side milling operations with multiple performance characteristics. *The International Journal of Advanced Manufacturing Technology*, 2007, **32**(1), 18-26.

105 **Vivancos, J., Luis, C.J., Costa, L. and Ortiz, J.A.** Optimal machining parameters selection in high speed milling of hardened steels for injection

moulds. *Journal of Materials Processing Technology*, 2004, **155-156**, 1505-1512.

106   **Baek, D.K., Ko, T.J. and Kim, H.S.** Optimization of feedrate in a face milling operation using a surface roughness model. *International Journal of Machine Tools and Manufacture*, 2001, **41**(3), 451-462.

107   **Balakrishnan, P. and DeVries, M.F.** Sequential estimation of machinibility parameters for adaptive optimization of machinibility data base systems. *Journal of Engineering for Industry*, 1985, **107**, 159-166.

108   **Budak, E.** Improving productivity and part quality in milling of titanium based impellers by chatter suppression and force control. *CIRP Annals - Manufacturing Technology*, 2000, **49**(1), 31-36.

109   **Fazelinia, H. and Olgac, N.** Optimum consitions for variable pitch milling. *2006 ASME International Mechanical Engineering Congress and Exposition,* Illlinois, 2006.

110   **Budak, E. and Tekeli, A.** Maximizing chatter free material removal rate in milling through optimal selection of axial and radial depth of cut. *CIRP Annals - Manufacturing Technology*, 2005, **54**(1), 353-356.

111   **Kurdi, M.H.** Robust multicriteria optimization of surface location error and material removal rate in high speed milling under uncertainty. *PhD Thesis.* Department of Mechanical and aerospace engineering, University of florida, 2005.

112   **Yeo, S.H., Rahman, M. and Wong, Y.S.** A tandem approach to selection of machinability data. *The International Journal of Advanced Manufacturing Technology*, 1995, **10**(2), 79-86.

113   **Abburi, N. and Dixit, U.** Multi-objective optimization of multipass turning processes. *The International Journal of Advanced Manufacturing Technology*, 2007, **32**(9), 902-910.

114   **Wang, Z.G., Rahman, M., Wong, Y.S. and Sun, J.** Optimization of multi-pass milling using parallel genetic algorithm and parallel genetic simulated annealing. *International Journal of Machine Tools and Manufacture*, 2005, **45**(15), 1726-1734.

115   **Baskar, N., Asokan, P., Prabhaharan, G. and Saravanan, R.** Optimization of machining parameters for milling operations using non-conventional methods. *The International Journal of Advanced Manufacturing Technology*, 2005, **25**(11), 1078-1088.

116   **Onwubolu, G.** Optimization of milling operations for the selection of cutting conditions using tribes. *Proceedings of the Institution of Mechanical Engineers, Part B: Journal of Engineering Manufacture*, 2005, **219**(10), 761-771.

117   **Cus, F. and Balic, J.** Optimization of cutting process by ga approach. *Robotics and Computer-Integrated Manufacturing*, 2003, **19**(1-2), 113-121.

118   **Wang, J.** Computer-aided economic optimization of end-milling operations. *International Journal of Production Economics*, 1998, **54**(3), 307-320.

119   **Tolouei-Rad, M. and Bidhendi, I.M.** On the optimization of machining parameters for milling operations. *International Journal of Machine Tools and Manufacture*, 1997, **37**(1), 1-16.

120   **Sorby, K., Tonnessen, K., Torjusen, J.E. and Rasch, F.O.** Improving high speed flank milling operations in multi-axis machines. *CIRP Annals - Manufacturing Technology*, 2000, **49**(1), 371-374.

121   **Kim, K.K., Kang, M.C., Kim, J.S., Jung, Y.H. and Kim, N.K.** A study on the precision machinability of ball end milling by cutting speed optimization. *Journal of Materials Processing Technology*, 2002, **130**, 357-362.

122   **Agapiou, J.S.** Optimization of multistage machining systems, part 1:Mathematical solution. *Journal of engineering for industry*, 1992, **114**, 524-531.

123   **Ghani, J.A., Choudhury, I.A. and Hassan, H.H.** Application of taguchi method in the optimization of end milling parameters. *Journal of Materials Processing Technology*, 2004, **145**(1), 84-92.

124   **Lin, T.R.** Optimisation technique for face milling stainless steel with multiple performance characteristics. *The International Journal of Advanced Manufacturing Technology*, 2002, **19**(5), 330-335.

125   **Koulamas, C.** Simultaneous determination of optimal machining conditions and tool replacement policies in constrained machining economics problems by geometric programming. *International Journal of Production Research*, 1991, **29**(12), 2407-2421.

126   **Jha, N.K.** A discrete data base multiple objective optimization of milling operation through geometric programming. *Journal of Engineering for Industry*, 1990, **112**, 368-374.

127   **Tandon, V., El-Mounayri, H. and Kishawy, H.** Nc end milling optimization using evolutionary computation. *International Journal of Machine Tools and Manufacture*, 2002, **42**(5), 595-605.

128   **Tobias, S.A., Sridhar, R., Hohn, R.E. and Long, G.W.** A stability algorithm for the general milling process. *Machine Tool Vibration*, 1965, **90**, 330-334.

129   **Altintas, Y.** *Manufacturing automation: Metal cutting mechanics, machine tools vibration and cnc design*. (Cambridge University Press, Cambrige, MA, 2000).

130   **Franklin, G.F., Powell, J.D. and Workma, M.** *Digital control of dynamic systems*. (Addison-Wesley, Monle Park, 1997).

131   **Gabor, S., Robert, S., Brian, P.M., Philip, V.B., Tamas, I., Janez, G. and Edvard, G.** Nonlinear dynamics of high-speed milling---analyses, numerics, and experiments. *Journal of Vibration and Acoustics*, 2005, **127**(2), 197-203.

132   **Huang, C.Y.** Analysis of process damping and system dynamics in milling. *PhD Thesis*. Department of Mechanical Engineering, National Cheng Kung University, 2007.

133   **Markus, B.** *Differential evolution*. 2008 [cited 2008 15th June]; Available from:http://www.mathworks.com/matlabcentral/fileexchange/loadFile.do?objectId=18593&objectType=file.

134   **Storn, R. and Price, K.** Differential evolution – a simple and efficient heuristic for global optimization over continuous spaces. *Journal of Global Optimization*, 1997, **11**(4), 341-359.

135   *Optimization toolbox user's guide: For use with matlab*. (The Math Works, Natick, 2001).

136   **Ewins, D.J.** *Modal testing: Theory, practice and application*. (Research Studies Press, Hertfordshire, 1999).

137   **Snyder, J.P., Davies, M.A., Pratt, J. and Smith, S.** A new stable speed test apparatus for milling. *Transactions of NAMRI/SME*, 2001, **24**, pp.153-157.

138   **Kiefer, A.J.** Integrating electromechanical actuator hardware with receptance coupling substructure analysis for chatter prediction on high speed machining centers. *Master of Science*. Mechanical and Aerospace Engineering, North Caroline State University, 2004.

139   **Tatar, K., Rantatalo, M. and Gren, P.** Laser vibrometry measurements of an optically smooth rotating spindle. *Mechanical Systems and Signal Processing*, 2007, **21**, 1739-1745.

140 **Rantatalo, M., Aidanpaa, J.-O., Goransson, B. and Norman, P.** Milling machine spindle analysis using fem and non-contact spindle excitation and response measurement. *International Journal of Machine Tools and Manufacture*, 2007, **47**(7-8), 1034-1045.

141 **Sodano, H.A.** Non-contact eddy current exciation method for vibration testing. *Experimental Mechanics*, 2006, **46**, 627-635.

142 **Esterling, D., Caufield, F.D., Keifer, A., Buckner, G. and Jaju, P.** Non-contact device for measuring frequency response functions of cnc machine tools. *Proc. of 2003 ASME International Mechanical Engineering Congress (IMECE),* Washington DC, 2003.

143 **Feoktistov, V.** *Differential evolution: In search of solutions*. (Springer, New York, 2006).

144 **Kurdi, M.H., Schmitz, T.L., Haftka, R.T. and Mann, B.P.** Simultaneous optimization of material removal rate and part accuracy in high speed milling. *ASME International mechanical engineering congress and exposition (IMECE)*. Anaheim, 2004. pp.

145 **Hock, W. and Schittkowski, K.** A comparative performance evaluation of 27 nonlinear programming codes *Computing*, 1983, **30**, 335-358.

146 **Deb, K.** *Multi-objective optimization using evolutionary algorithms*. (John Wiley & Sons, New York, 2001).

147 **Quiza Sardiñas, R., Rivas Santana, M. and Alfonso Brindis, E.** Genetic algorithm-based multi-objective optimization of cutting parameters in turning processes. *Engineering Applications of Artificial Intelligence*, 2006, **19**(2), 127-133.

148 **Karpat, Y. and Özel, T.** Multi-objective optimization for turning processes using neural network modeling and dynamic-neighborhood particle swarm optimization. *The International Journal of Advanced Manufacturing Technology*, 2007, **35**(3), 234-247.

149 **Wang, J.** Multiple-objective optimisation of machining operations based on neural networks. *The International Journal of Advanced Manufacturing Technology*, 1993, **8**(4), 235-243.

150 **Haimes, Y.Y., Lasdon, L.S. and Wismer, D.A.** On a bicriterion formulation of the problems of integrated system identification and system optimization. *IEEE Transactions on Systems, Man, And Cybernetics*, 1971, **SMC-1**, 296-297.

151 **Yusoff, A.R. and Sims, N.D.** Optimisation of variable helix end millings tools by minimising self excited vibration. *Journal of Physics: Conference Series*, 2009, **181**(1), 012026.

152 **Flynn, C.M.** Variable helix cutting tools. In Patent, U.S., ed. *US 2003/0118411 A1*United States of America, 2006).

153 **Babu, B.V. and Angira, R.** Modified differential evolution (mde) for optimization of non-linear chemical processes. *Computers & Chemical Engineering*, 2006, **30**(6-7), 989-1002.

154 **Nearchou, A.** Balancing large assembly lines by a new heuristic based on differential evolution method. *The International Journal of Advanced Manufacturing Technology*, 2007, **34**(9), 1016-1029.

155 **Zhang, J.Z. and Xu, J.** A new differential evolution for discontinuous optimization problems. *Third International Conference on Natural Computation (ICNC 2007),* 0-7695-2875-9/07, 2007.

156 **Hendershot, Z.V.** A differential evolution algorithm for automatically discovering multiple global optima in multidimensional, discontinuous spaces.

Proceedings of the Fifteenth Midwest Artificial Intelligence and Cognitive Science Conference (MAICS 2004), Illinois, 2004.

157   **Chiou, J.-P. and Wang, F.-S.** Hybrid method of evolutionary algorithms for static and dynamic optimization problems with application to a fed-batch fermentation process. *Computers & Chemical Engineering*, 1999, **23**(9), 1277-1291.

158   **Pedchote, C. and Purdy, D.** Parameter estimation of a single wheel station using hybrid differential evolution. *Proceedings of the Institution of Mechanical Engineers, Part D: Journal of Automobile Engineering*, 2003, **217**(6), 431-447.

159   **Hendtlass, T.** A combined swarm differential evolution algorithm for optimization problems. *Engineering of intelligent systems*, pp. 11-18 (Springer-Berlin, Heidelberg, 2001).

160   **Tasoulis, D.K., Pavlidis, N.G., Plagianakos, V.P. and Vrahatis, M.N.** Parallel differential evolution. *International Symposium Parallel Computing in Electrical Engineering (PAR ELEC 2006)*. 2006. pp. 319-329.

161   **Chiou, J.-P., Chang, C.-F. and Su, C.-T.** Ant direction hybrid differential evolution for solving large capacitor placement problems *IEEE Transactions on Power Systems*, 2004, **19**(4), 1794-1800.

162   **Yusoff, A.R., Sims, N.D. and Turner, S.** Experimental validation of chatter stability for variable helix milling tools. *Trends in Aerospace Manufacturing 2009 International Conference (TRAM '09),* Sheffield, 2009.

163   **Huyanan, S. and Sims, N.D.** Vibration control strategies for proof-mass actuators. *Journal of Vibration and Control*, 2007, **13**(12), 1785-1806.

164   **Virgin, L.N.** *Introduction to experimental nonlinear dynamics: A case study in mechanical vibration*. (Cambridge University Press, New York, 2000).

165   **Insperger, T., Mann, B.P., Surmann, T. and Stepan, G.** On the chatter frequencies of milling processes with runout. *International Journal of Machine Tools and Manufacture*, 2008, **48**, 1081-1089.

166   **Altintas, Y. and Weck, M.** Chatter stability of metal cutting and grinding. *CIRP Annals - Manufacturing Technology*, 2004, **53**(2), 619-642.

167   **Budak, E. and Tunc, L.T.** A new method for identification and modeling of process damping in machining. *Journal of Manufacturing Science and Engineering*, 2009, **131**(5), 051019.

168   **Altintas, Y., Eynian, M. and Onozuka, H.** Identification of dynamic cutting force coefficients and chatter stability with process damping. *CIRP Annals - Manufacturing Technology*, 2008, **57**(1), 371-374.

169   **Montgomery, D. and Altintas, Y.** Mechanism of cutting force and surface generation in dynamic milling. *Transaction ASME Journal of Engineering Industry*, 1991, **113**, 160-168.

170   **Delio, T., Smith, S., Tlusty, J. and Zamudio, C.** Stiffness, stability, and loss of process damping in high speed machining : Fundamental issues in machining. *Precision Engineering*, 1991, **43**(3), 171-191.

171   **Ranganath, S., Narayanan, K. and Sutherland, J.W.** The role of flank face interference in improving the accuracy of dynamic force predictions in peripheral milling. *Journal of Manufacturing Science and Engineering*, 1999, **121**, 593-599.

172   **Huang, C.Y. and Wang, J.J.J.** Mechanistic modeling of process damping in peripheral milling. *Journal of Manufacturing Science and Engineering*, 2007, **129**(1), 12-20.

173   **Turner, S.** Process damping parameters. *Trends in Aerospace Manufacturing 2009 International Conference (TRAM '09),* Sheffield, 2009.

174 **Sisson, T.R. and Kegg, R.L.** An explaination of low speed chatter effects. *Transaction ASME Journal of Engineering Industry*, 1969, **91**(4), 951-956.

175 **Sims, N.D.** The self-excitation damping ratio: A chatter criterion for time-domain milling simulations. *Journal of Manufacturing Science and Engineering*, 2005, **127**(3), 433-445.

APPENDIX A: ABSTRACTS OF CONFERENCE AND JOURNAL

PUBLICATIONS

Non-contacting electromagnetic actuators for chatter stability analysis of milling tools

Ahmad R Yusoff[1], Neil D Sims[1], and Richard E Clark[2]

[1]Dept of Mechanical Engineering, University of Sheffield, Mappin Street, S1 3JD, UK.

[2]Dept of Electrical and Electronic Engineering, University of Sheffield, Mappin Street,

S1 3JD, UK.

ABSTRACT

This paper explores the use of non-contact electromagnetic actuators to measure the frequency response of milling tools. Milling is one of the most common manufacturing processes, but its productivity is limited by the onset of regenerative chatter. This is a form of unstable self-excited vibration that occurs when the volume of material removed is too large for a particular spindle speed. This form of chatter is undesirable because it results in premature tool wear, poor surface finish on the machined component and the possibility of serious damage to the machine itself.

The chatter stability of a milling process can be determined using well-established theory, provided that the frequency response of the flexible structure can be determined. In practice, this usually involves excitation of a stationary (non-rotating) milling tool with a modal hammer, and measurement of the response of the tool with a co-located accelerometer. However, this measurement is not necessarily accurate due to amplitude dependency factor consideration.   There is anecdotal evidence that structural nonlinearity can have a significant effect on the chatter stability of some milling machines.

The present study investigates the use of non-contacting electromagnetic actuators to excite the milling tool. Although this approach is well documented for general rotating machinery problems, there are relatively few reports that focus on metal machining problems. In principle, this approach enables frequency response measurements whilst the tool is rotating and proper setting of both amplitude and output offset effects can be appropriately determined.   The article describes the practical application of this approach and discusses its amplitude dependency and output offset dependency for both current and force excitation during FRF measurement using magnetic force generation.

Optimisation of variables helix end millings tools by minimising self excited vibration

Ahmad R Yusoff and Neil D Sims

Dept of Mechanical Engineering, University of Sheffield, Mappin Street, S1 3JD, UK

E-mail[1]: n.sims@sheffield.ac.uk

ABSTRACT

During machining, self-excited vibrations known as regenerative chatter can occur. This instability can be avoided by modifying the tool geometry, thereby influencing the time delay terms that arise in the governing equations. The present study uses Differential Evolution (DE) to optimise the tool helix geometry, so as to avoid chatter. The results are compared to those from Sequential Quadratic Programming (SQP). It is shown that the DE approach can significantly increase the chatter stability, and substantially out-performs the SQP algorithm. The performance of the DE approach is due to its ability to perform global optimisation in the presence of significant nonlinearities.

Experimental validation of chatter stability for variable helix milling tools

Ahmad R Yusoff[1], Neil D Sims[2] and Sam Turner[3]

[1,2]Dept of Mechanical Engineering, The University of Sheffield,

Mapping Street S1 3JD, UK

[3]Factory of the Future, Advanced Manufacturing Research Centre with Boeing, The

University of Sheffield, Advanced Manufacturing Park, Wallis Way, Catcliffe,

Rotherham S10 1GZ, UK

ABSTRACT

The occurrence of self-excited vibrations during machining is known as regenerative chatter, and this phenomenon can severely limit the machining productivity. By modifying and optimising the tool's pitch and helix geometry, this regenerative chatter can be suppressed to increase material removal rate. In this paper, experimental verification of an optimised variable helix and variable pitch tools is presented. The geometry was optimised using a Differential Evolution (DE) algorithm. Based on stability diagrams of original and optimised milling tools, the experiment was conducted and the results were compared when chatter occurred. The optimised cutter significantly outperformed the original cutter in term of chatter suppression.

Period-one instability of variable pitch milling tools

Ahmad R Yusoff and Neil D Sims

Department of Mechanical Engineering, University of Sheffield, Mappin Street,

Sheffield, S1 3JD United Kingdom

ABSTRACT

The onset of regenerative chatter limits machining productivity when machining with a larger materials removal rate. This unstable self-excited vibration should be avoided as it can accelerate tool wear, cause poor machined surfaces and reduce the spindle lifetime. Several studies have discovered regions (or 'islands') of unstable period-doubling island chatter when the helix angle of a tool is properly considered This paper contribution concerns the experimental occurrence of period-one chatter instability for a special class of milling tool that has a variable helix angle. This builds upon earlier work which focused on theoretical modeling of such tools

A four-flute variable helix (37°, 40°, 37°, 40°) and variable pitch (78.4°, 80.4°, 78.4°, 80.4°) commercially available milling tool was used in the present study. This was used to down-mill (at 5 per cent radial immersion) an aluminium 7075-T6 block mounted on a flexible that could be modeled as a single-degree-of-freedom systems. The cutting stiffness of the tool/workpiece was estimated to be K_n= 283 MN/m^2 and K_t= 143 MN/m^2 and the flexure dynamic properties were obtained from impact test as m=1.41 kg, f_n=200 Hz and ζ = 0.0024.

The experimental configuration is shown in Figure 1. An eddy-current displacement sensor signal was used to measure the onset of chatter vibrations. A pulse signal produced from a hall-effect probe monitoring the milling spindle was to produce once-per-revolution samples of the eddy-current measurement. The response of the system could be then analysed in terms of the frequency domain, the once/rev vibration samples, and the Poincaré section in delayed coordinates.

Figure 2a illustrates the predicted chatter stability using the approach described in. There is a large region that is associated with hopf-bifurcation, as found in classical machining chatter. However, in addition, there are isolated regions of period doubling and period-one instability. Previous works on regular helix milling tools has identified regions of period doubling instability, but the existence of period-one bifurcations has previously only been associated with tool runout. The present contribution predicts that period-one bifurcation can also arise for variable helix tools.

In Figure 2b, experimental results are summarised, and the theoretical prediction is superimposed as a solid black line. The theoretical prediction is also repeated for a tool with regular helix and variable pitch (dashed black line). This differs from the variable pitch tool because there is no isolated region of period-one instability at 1975 rev/min.

Experimental measurements are shown on Figure 2b as markers. For each experimental test, chatter stability was evaluated using the analysis procedure illustrated in Figure 3. Hopf-bifurcations were associated with pseudo-periodic motion on the Poincaré section, and high variance of the once per revolution samples. Period-one bifurcations were associated with significantly higher vibration levels than the stable cuts within the immediate neighborhood. The example shown in Figure 3 corresponds to a period-one bifurcation. Note that the tool was engaged in the workpiece between time 5 s and 9 s, corresponding to revolution 150 and revolution 300 of the tool. The Poincaré section is misleading at first sight, because it contains data when the tool was not cutting.

To summarise, this contribution has confirmed experimentally that period-one bifurcations can occur for variable helix milling tools. However, the identification of this behavior is not straightforward, since the vibration characteristics are similar to those for stable forced vibrations.
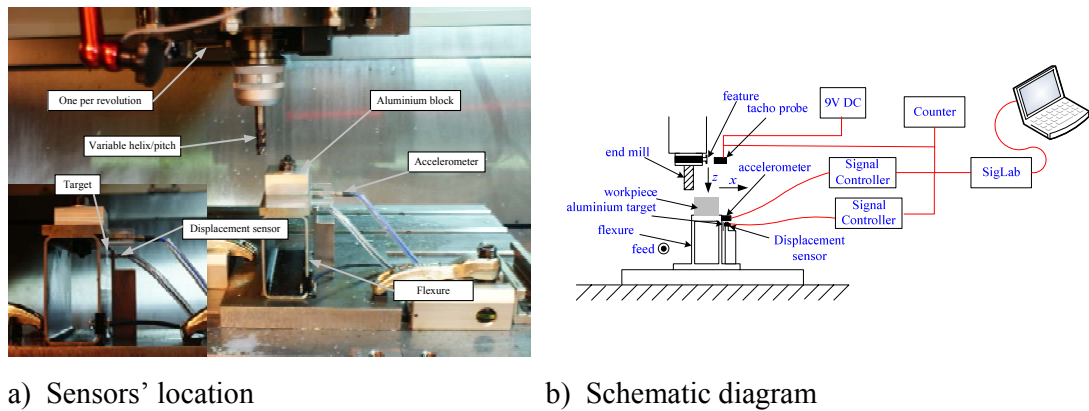

a) Sensors' location   b) Schematic diagram

Figure 1 Experimental arrangement

a) Theoretical prediction   b) Experimental validation
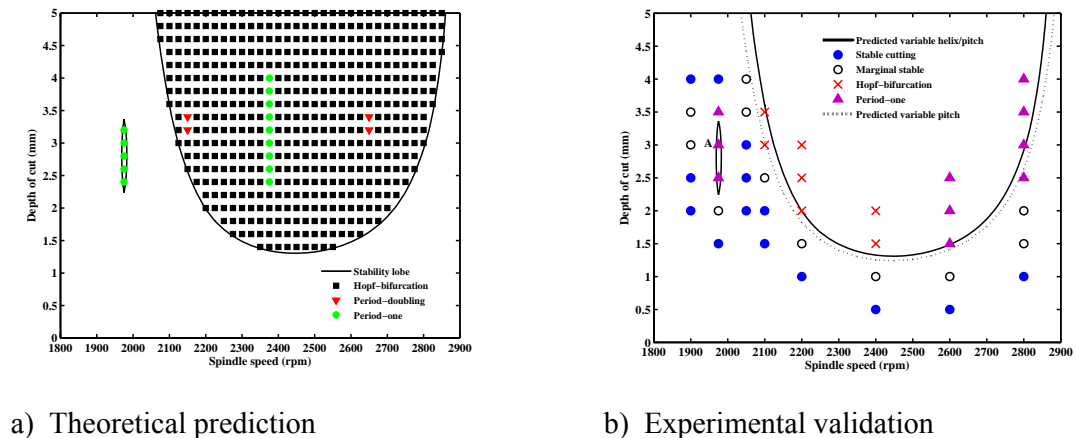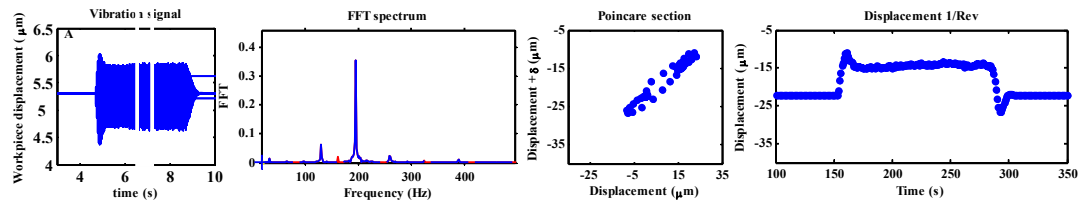
Figure 2 Chatter stability for variable helix and variable pitch

Figure 3 Vibration signal, 1/Rev, Poincare sections and FFT-spectrums for unstable period one at case A in Figure 2b

The role of tool geometry in process damped milling

Ahmad R Yusoff[1], Sam Turner[2] Chris M Taylor[1], and Neil D Sims[1]

[1]Dept of Mechanical Engineering, University of Sheffield,

Mappin Street, S1 3JD, UK

[2]Factory of the Future,

Advanced Manufacturing Research Centre with Boeing,

The University of Sheffield, Advanced Manufacturing Park,

Wallis Way, Catcliffe, Rotherham S10 1GZ, UK

ABSTRACT

The complex interaction between machining structural systems and the cutting process results in machining instability, so-called chatter. In some milling scenarios, process damping is a useful phenomenon that can be exploited to improve the limited productivity due to chatter. In the present study, experiments are performed to evaluate the performance of process damped milling under different tool geometries (edge radius, rake and relief angles and variable helix/pitch). The results clearly indicate that variable helix/pitch angles most significantly increase process damping performance. Additionally, increased cutting edge radius moderately improves process damping performance, while rake and relief angles have a smaller and closely coupled effect.